



Universidade Federal do Paraná – UFPR

**Departamento de Física
Programa de Pós-Graduação em Física**

Mini-curso: “Fundamentals and new directions in photoelectron spectroscopy”

Prof. Charles Fadley

Lawrence Berkeley National Laboratory / Advanced Light Source

Período: 04 – 08 de abril de 2016 (13:30 – 17:00 hs)

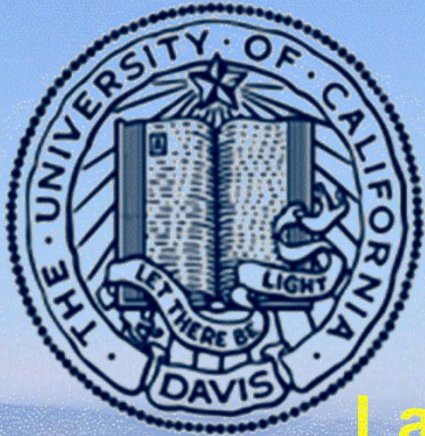
Local: Departamento de Física – UFPR, Curitiba (PR)

Inscrições: 14 – 24 de março (gislaine@fisica.ufpr.br)



Prof. Dr. Ismael Graff – Muito muito obrigado!!!

Fundamentals and New Directions in Photoelectron Spectroscopy (Photoemission)



Chuck Fadley
Dept. of Physics, UC Davis
and
Materials Sciences Division
Lawrence Berkeley National Laboratory



Supported by:

U.S. Dept. of Energy: LBNL Materials Sciences Division
Army Research Office-Multi-University Initiative:
“Emergent Phenomena at Mott Interfaces”
Jülich Research Center (Germany)
APTCOM Project, Labex Program (France)

Lectures at
Federal University of Parana State, Curitiba, Brazil
04-08 April, 2016



**Bem
Vindo a
Berkeley**

Class statistics:

Total no. of students: 23

Physics? 15

Chemistry? 3

Other?: 5

Used photoelectron spectroscopy before?

Laboratory XPS? 6

Synchrotron radiation XPS? 5

Laboratory low-energy ARPES? 1

Synchrotron radiation ARPES? 1

Done other synchrotron radiation experiments?

X-ray absorption, XMCD? 5

EXAFS? 3

Other? 1

LNLS: 6



Prof. Ismael Graff





Ismael
Graff

Some key references:

"Basic Concepts of X-ray Photoelectron Spectroscopy", C. S. Fadley, invited chapter for Electron Spectroscopy: Theory, Techniques, and Applications, C. R. Brundle and A. D. Baker, Eds. (Academic Press, London, 1978) Vol. II, Chap. 1, 145 pp., 53 figs, available at:

<http://www.physics.ucdavis.edu/Classes/Physics243A/BasicConceptsofXPS.Fadley.pdf>

"X-ray Photoelectron Spectroscopy : Progress and Perspectives", C.S. Fadley, invited review, Journal of Electron Spectroscopy and Related Phenomena 178–179, 2 (2010), 30 pp., 35 figs., available at:

<http://www.physics.ucdavis.edu/Classes/Physics243A/XPS.Present&Future.JESRP.Fadley.pdf>

And others downloadable from two websites:

<http://www.physics.ucdavis.edu/fadleygroup/> Lecture slides from this course will be posted there

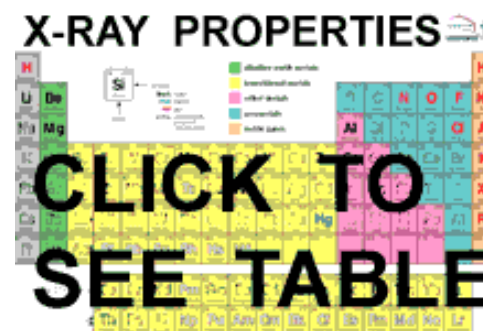
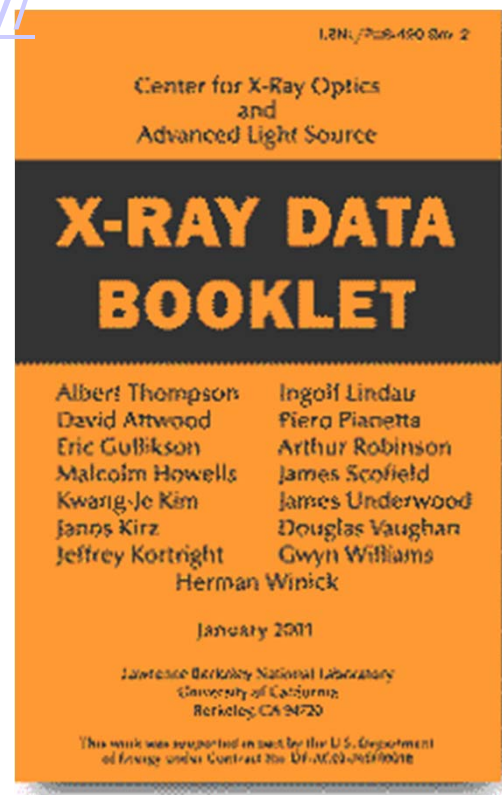
<http://www.physics.ucdavis.edu/Classes/Physics243A/> A ten-week course of 20 lectures, with slides and videos posted

X-RAY DATA BOOKLET

Center for X-ray Optics and Advanced Light Source
Lawrence Berkeley National Laboratory

<http://xdb.lbl.gov/>

- [Introduction](#)
- [X-Ray Properties of Elements](#)
- [Electron Binding Energies](#)
- [X-Ray Energy Emission Energies](#)
- [Fluorescence Yields for K and L Shells](#)
- [Principal Auger Electron Energies](#)
- [Subshell Photoionization Cross-Sections](#)
- [Mass Absorption Coefficients](#)
- [Atomic Scattering Factors](#)
- [Energy Levels of Few Electron Ions](#)
- [Periodic Table of X-Ray Properties](#)
- [Synchrotron Radiation](#)
- [Characteristics of Synchrotron Radiation](#)
- [History of X-rays and Synchrotron Radiation](#)
- [Synchrotron Facilities](#)
- [Scattering Processes](#)
- [Scattering of X-rays from Electrons and Atoms](#)
- [Low-Energy Electron Ranges in Matter](#)
- [Optics and Detectors](#)
- [Crystal and Multilayer Elements](#)
- [Specular Reflectivities for Grazing-Incidence Mirrors](#)
- [Gratings and Monochromators](#)
- [Zone Plates](#)
- [X-Ray Detectors](#)
- [Miscellaneous](#)
- [Physical Constants](#)
- [Physical Properties of the Elements](#)
- [Electromagnetic Relations](#)
- [Radioactivity and Radiation Protection](#)
- [Useful Formulas](#)



Basic Concepts:



A Little Electronic Structure

The X-Ray-Based Experiments

X-Ray Sources, Synchrotron Radiation, Free Electron Lasers

Core-Level Photoemission

Intensities and Quantitative Analysis, the 3-Step Model

Varying Surface and Bulk Sensitivity

Chemical Shifts

Multiplet Splittings

Electron Screening and Satellite Structure

Magnetic and Non-Magnetic Dichroism

Resonant Photoemission

Photoelectron Diffraction and Holography

Valence-Level Photoemission

Band-Mapping in the Ultraviolet Photoemission Limit

Densities of States in the X-Ray Photoemission Limit

Some New Directions

Photoemission with Hard X-Rays (throughout lectures)

Photoemission with Standing Wave Excitation

Photoemission with: Higher Pressures → multi-Torr → Atmosphere?

Spatial Resolution-Photoelectron Microscopy

Temporal Resolution

OBSERVED (+ CALCULATED) ORDER OF FILLING ATOMIC LEVELS:

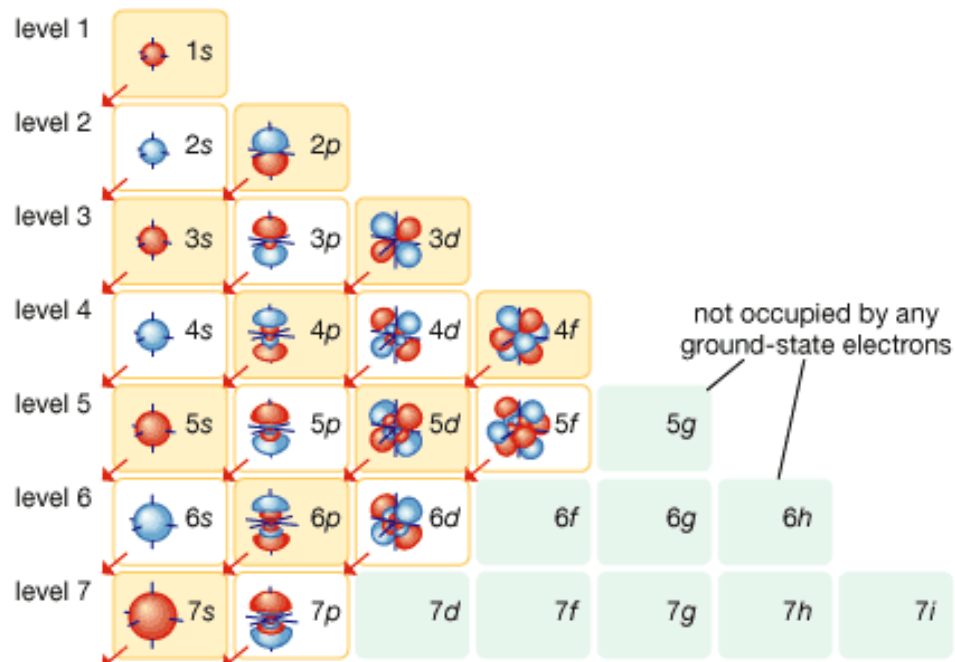
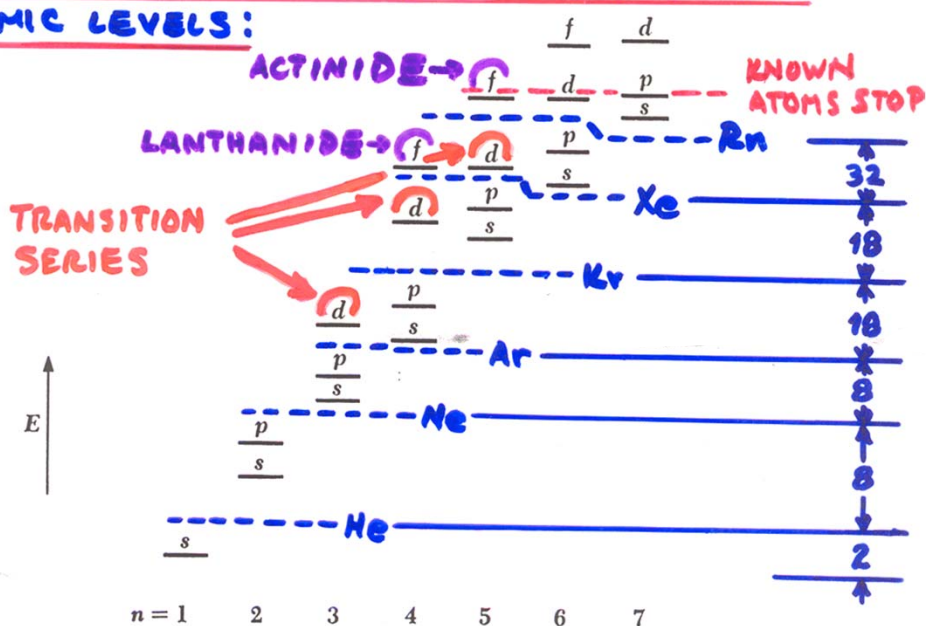


FIGURE 7.13 The sequence of quantum states in an atom. Not to scale.

EXAMPLE CONFIGURATIONS:

Z ATOM CONFIG.

8 O $1s^2 2s^2 2p^4$

GROUND-STATE OPEN SHELL COUPLING?

$\uparrow\downarrow$ \uparrow \uparrow
 $2p_{-1}$ $2p_0$ $2p_{+1}$

26 Fe $1s^2 2s^2 2p^6 3s^2 3p^6$
 $3d^6 4s^2$

$\uparrow\downarrow$ \uparrow \uparrow \uparrow \uparrow
 $3d_{-2}$ $3d_{-1}$ $3d_0$ $3d_{+1}$ $3d_{+2}$

⇒ LARGE μ_{3d} + MAGNETISM

63 Eu $1s^2 2s^2 2p^6 3s^2 3p^6$
 $3d^{10} 4s^2 4p^6 4d^{10}$
 $4f^7 6s^2$

ALSO MAGNETIC! \uparrow \uparrow \uparrow \uparrow \uparrow \uparrow \uparrow
 $4f_{-3}$ $4f_{-2}$ $4f_{-1}$ $4f_0$ $4f_{+1}$ $4f_{+2}$ $4f_{+3}$

Exchange interaction.
 Hund's First Rule:
 highest total spin
 angular momentum

s¹

TRANSITION METALS

Periodic Table, with the Outer Electron Configurations of Neutral Atoms in Their Ground States

The notation used to describe the electronic configuration of atoms and ions is discussed in all textbooks of introductory atomic physics. The letters *s*, *p*, *d*, ... signify electrons having orbital angular momentum 0, 1, 2, ... in units \hbar ; the number to the left of the letter denotes the principal quantum number of one orbit, and the superscript to the right denotes the number of electrons in the orbit.

p¹ p² p³ p⁴ p⁵ p⁶

H ¹																	He ²				
1s																	1s ²				
Li ³	Be ⁴															B ⁵	C ⁶	N ⁷	O ⁸	F ⁹	Ne ¹⁰
2s	2s ²															2s ² 2p	2s ² 2p ²	2s ² 2p ³	2s ² 2p ⁴	2s ² 2p ⁵	2s ² 2p ⁶
Na ¹¹	Mg ¹²															Al ¹³	Si ¹⁴	P ¹⁵	S ¹⁶	Cl ¹⁷	Ar ¹⁸
3s	3s ²															3s ² 3p	3s ² 3p ²	3s ² 3p ³	3s ² 3p ⁴	3s ² 3p ⁵	3s ² 3p ⁶
K ¹⁹	Ca ²⁰	Sc ²¹	Ti ²²	V ²³	Cr ²⁴	Mn ²⁵	Fe ²⁶	Co ²⁷	Ni ²⁸	Cu ²⁹	Zn ³⁰	Ga ³¹	Ge ³²	As ³³	Se ³⁴	Br ³⁵	Kr ³⁶				
4s	4s ²	3d	3d ²	3d ³	3d ⁵	3d ⁵	3d ⁶	3d ⁷	3d ⁸	3d ¹⁰	3d ¹⁰	4s ² 4p	4s ² 4p ²	4s ² 4p ³	4s ² 4p ⁴	4s ² 4p ⁵	4s ² 4p ⁶				
Rb ³⁷	Sr ³⁸	Y ³⁹	Zr ⁴⁰	Nb ⁴¹	Mo ⁴²	Tc ⁴³	Ru ⁴⁴	Rh ⁴⁵	Pd ⁴⁶	Ag ⁴⁷	Cd ⁴⁸	In ⁴⁹	Sn ⁵⁰	Sb ⁵¹	Te ⁵²	I ⁵³	Xe ⁵⁴				
5s	5s ²	4d	4d ²	4d ⁴	4d ⁵	4d ⁶	4d ⁷	4d ⁸	4d ¹⁰	4d ¹⁰	4d ¹⁰	5s ² 5p	5s ² 5p ²	5s ² 5p ³	5s ² 5p ⁴	5s ² 5p ⁵	5s ² 5p ⁶				
Cs ⁵⁵	Ba ⁵⁶	La ⁵⁷	Hf ⁷²	Ta ⁷³	W ⁷⁴	Re ⁷⁵	Os ⁷⁶	Ir ⁷⁷	Pt ⁷⁸	Au ⁷⁹	Hg ⁸⁰	Tl ⁸¹	Pb ⁸²	Bi ⁸³	Po ⁸⁴	At ⁸⁵	Rn ⁸⁶				
6s	6s ²	5d	4f ¹⁴	5d ²	5d ³	5d ⁴	5d ⁵	5d ⁶	5d ⁹	5d ⁹	5d ¹⁰	5d ¹⁰	6s ² 6p	6s ² 6p ²	6s ² 6p ³	6s ² 6p ⁴	6s ² 6p ⁶				
Fr ⁸⁷	Ra ⁸⁸	Ac ⁸⁹	... 4f(5d) FILLING ...																		
7s	7s ²	6d	Ce ⁵⁸	Pr ⁵⁹	Nd ⁶⁰	Pm ⁶¹	Sm ⁶²	Eu ⁶³	Gd ⁶⁴	Tb ⁶⁵	Dy ⁶⁶	Ho ⁶⁷	Er ⁶⁸	Tm ⁶⁹	Yb ⁷⁰	Lu ⁷¹	RARE EARTHS				
			4f ²	4f ³	4f ⁴	4f ⁵	4f ⁶	4f ⁷	4f ⁷	4f ⁸	4f ¹⁰	4f ¹¹	4f ¹²	4f ¹³	4f ¹⁴	5d					
			6s ²	6s ²	6s ²	6s ²	6s ²	6s ²	6s ²	6s ²	6s ²	6s ²	6s ²	6s ²	6s ²	6s ²					
			Th ⁹⁰	Pa ⁹¹	U ⁹²	Np ⁹³	Pu ⁹⁴	Am ⁹⁵	Cm ⁹⁶	Bk ⁹⁷	Cf ⁹⁸	Es ⁹⁹	Fm ¹⁰⁰	Md ¹⁰¹	No ¹⁰²	Lr ¹⁰³	ACTINIDES				
			-	5f ²	5f ³	5f ⁵	5f ⁶	5f ⁷	5f ⁷	5f ⁷	5f ⁷	5f ⁷									
			6d ²	6d	6d	6d	6d	6d													
			7s ²	7s ²	7s ²	7s ²	7s ²	7s ²	7s ²	7s ²	7s ²	7s ²	7s ²	7s ²	7s ²	7s ²					

☐ = EXCEPTIONS

◻ = EXCEPTIONS

→ d⁵ + d¹⁰ : 1/2 FILLED / FILLED MORE STABLE

Assume N-electron, P nucleus wave function to be:

$\Psi \approx \Phi = \text{Slater determinant}$

$$= \frac{1}{\sqrt{N!}} \begin{pmatrix} \phi_1(\vec{r}_1)\chi_1(\sigma_1) & \dots & \phi_N(\vec{r}_1)\chi_N(\sigma_1) \\ \vdots & \ddots & \vdots \\ \phi_1(\vec{r}_N)\chi_1(\sigma_N) & \dots & \phi_N(\vec{r}_N)\chi_N(\sigma_N) \end{pmatrix} \quad (35a)$$

space: like 1s, 2s, ...
spin: $\alpha(\uparrow)$ or $\beta(\downarrow)$

and also require orthonormality of one-electron orbitals

$$\int \phi_i^*(\vec{r})\phi_j(\vec{r})dV = \delta_{ij}$$

Minimize total energy \rightarrow Hartree-Fock equations

$$\hat{H}(\vec{r}_1)\phi_i(\vec{r}_1) = \varepsilon_i\phi_i(\vec{r}_1); i = 1, 2, \dots, N \quad (42)$$

with:

$$\varepsilon_i = \varepsilon_i^0 + \sum_{j=1}^N J_{ij} - \delta_{m_{s_i}, m_{s_j}} K_{ij} \quad (47)$$

One-electron integral:

$$\varepsilon_i^0 = \left\langle \phi_i(\vec{r}_1) \left| -\frac{1}{2}\nabla_1^2 - \sum_{\ell=1}^P \frac{Z_\ell}{r_{1\ell}} \right| \phi_i(\vec{r}_1) \right\rangle \quad (48)$$

Two-electron coulomb integral:

$$J_{ij} \equiv \left\langle \phi_i(\vec{r}_1) \left| \hat{K}_j \right| \phi_i(\vec{r}_1) \right\rangle = \iint \phi_i^*(\vec{r}_1)\phi_j^*(\vec{r}_2) \frac{1}{r_{12}} \phi_i(\vec{r}_1)\phi_j(\vec{r}_2)dV_1dV_2 \quad (45)$$

Two-electron exchange integral:

$$K_{ij} \equiv \left\langle \phi_i(\vec{r}_1) \left| \hat{J}_j \right| \phi_i(\vec{r}_1) \right\rangle = \iint \phi_i^*(\vec{r}_1)\phi_j^*(\vec{r}_2) \frac{1}{r_{12}} \phi_j(\vec{r}_1)\phi_i(\vec{r}_2)dV_1dV_2 \quad (46)$$

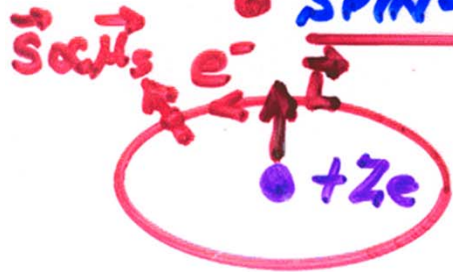
Lowers energy—"attractive"

If ϕ_j ($j \neq i$) don't relax around a ϕ_i hole \rightarrow
Koopmans' Theorem:
- One-electron energies (eigenvalues) =
- $\varepsilon_i \approx E_{\text{Binding}}$

Note— $K_{ij} \leftrightarrow J_{ij}$ in solid state

Spin-orbit: Final important relativistic interaction

• SPIN-ORBIT SPLITTING OF LEVELS:



⇒ EFFECTIVE \vec{B} (NUCLEUS AROUND e^-) $\propto \vec{L}$

$$\hat{H}_{s-o} = \xi(r) \vec{L} \cdot \vec{S}$$

• SPLITS ALL nl LEVELS $2(2l+1)$

$\nearrow nl_j = l + 1/2 \text{ — } 2l+2$
 $\searrow nl_j = l - 1/2 \text{ — } 2l$

• MIXES SPIN & ORBITAL ANGULAR MOM.:

$$\psi_{nljm_j} = C_1 \psi_{nl, m_j - 1/2} \begin{pmatrix} 1 \\ 0 \end{pmatrix} + C_2 \psi_{nl, m_j + 1/2} \begin{pmatrix} 0 \\ 1 \end{pmatrix}$$

\parallel
 $m_s = +1/2$
 \parallel
 \uparrow

\parallel
 $m_s = -1/2$
 \parallel
 \downarrow

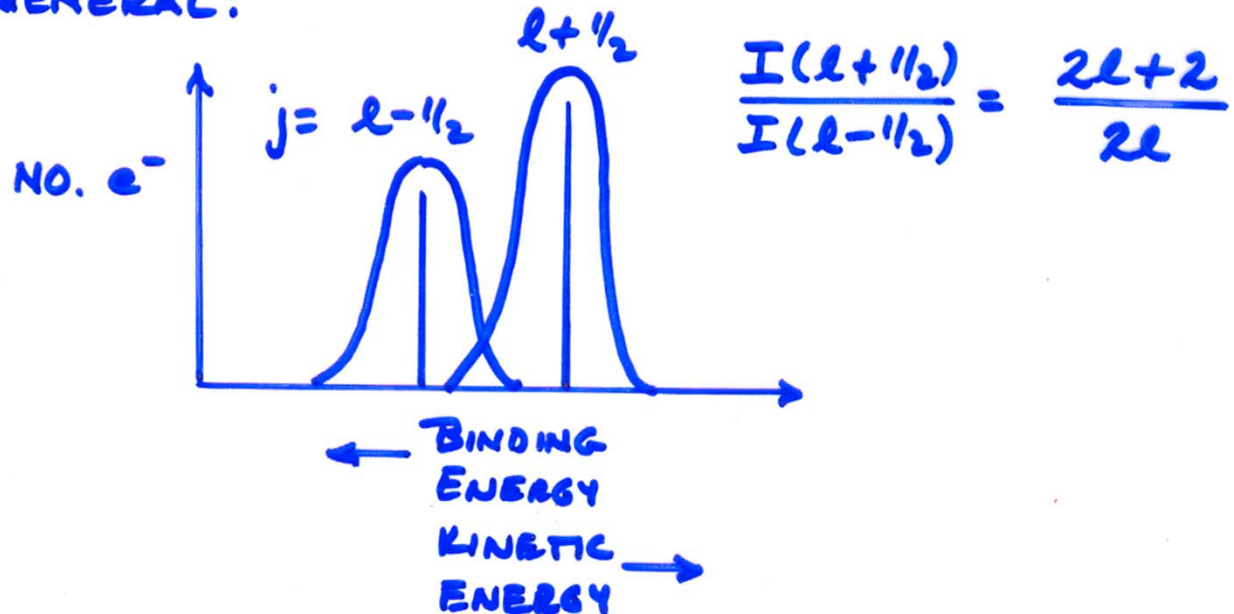
WITH C_1 AND C_2 TABULATED CLEBSCH-GORDAN OR WIGNER $3j$ SYMBOLS

SOME SPIN-ORBIT SPLITTINGS: (IN eV)

$2p^6$ $\swarrow \searrow$ $2p_{1/2}^2 \quad 2p_{3/2}^4$	$Z = 13$ (Al) 0.4	28 (Ni) 17.8	46 (Pd) 157.0
$3d^{10}$ $\swarrow \searrow$ $3d_{3/2}^4 \quad 3d_{5/2}^6$	$Z = 30$ (Zn) 0.1	48 (Cd) 6.7	64 (Gd) 32.3
$4f^{14}$ $\swarrow \searrow$ $4f_{5/2}^6 \quad 4f_{7/2}^8$	$Z = 74$ (W) 2.2	84 (Pb) 7.0	92 (U) 64

INCREASE WITH Z FOR A GIVEN LEVEL.

IN GENERAL:



X-Ray Data Booklet--Section 1.1 ELECTRON BINDING ENERGIES

The energies are given in eV relative to the vacuum level for the rare gases and for H₂, N₂, O₂, F₂, and Cl₂; relative to the Fermi level for the metals; and relative to the top of the valence bands for semiconductors (and insulators).

Electronic configuration	Element	K 1s	L ₁ 2s	L ₂ 2p _{1/2}	L ₃ 2p _{3/2}	M ₁ 3s	M ₂ 3p _{1/2}	M ₃ 3p _{3/2}
1s	1 H	13.6						
1s ²	2 He	24.6*						
1s ² 2s	3 Li	54.7*						
1s ² 2s ²	4 Be	111.5*						
1s ² 2s ² 2p	5 B	188*						
1s ² 2s ² 2p ²	6 C	284.2*						
1s ² 2s ² 2p ³	7 N	409.9*	37.3*	~ 9	~ 9			
1s ² 2s ² 2p ⁴	8 O	543.1*	41.6*	~ 13	~ 13			
1s ² 2s ² 2p ⁵	9 F	696.7*	~ 45	~ 17	~ 17			
1s ² 2s ² 2p ⁶	10 Ne	870.2*	48.5*	21.7*	21.6*			
[Ne] 3s	11 Na	1070.8†	63.5†	30.65	30.81			
[Ne] 3s ²	12 Mg	1303.0†	88.7	49.78	49.50			
[Ne] 3s ² 3p	13 Al	1559.6	117.8	72.95	72.55			
[Ne] 3s ² 3p ²	14 Si	1839	149.7*b	99.82	99.42			
[Ne] 3s ² 3p ³	15 P	2145.5	189*	136*	135*			
[Ne] 3s ² 3p ⁴	16 S	2472	230.9	163.6*	162.5*			
[Ne] 3s ² 3p ⁵	17 Cl	2822.4	270*	202*	200*			
[Ne] 3s ² 3p ⁶	18 Ar	3205.9*	326.3*	250.6†	248.4*	29.3*	15.9*	15.7*
[Ar] 4s	19 K	3608.4*	378.6*	297.3*	294.6*	34.8*	18.3*	18.3*
[Ar] 4s ²	20 Ca	4038.5*	438.4†	349.7†	346.2†	44.3 †	25.4†	25.4†
	21 Sc	4492	498.0*	403.6*	398.7*	51.1*	28.3*	28.3*
	22 Ti	4966	560.9†	460.2†	453.8†	58.7†	32.6†	32.6†



Interpolated, extrapolated

Missing valence B.E.s



X-Ray Data Booklet--Section 1.1 ELECTRON BINDING ENERGIES

Element	K 1s	L ₁ 2s	L ₂ 2p _{1/2}	L ₃ 2p _{3/2}	M ₁ 3s	M ₂ 3p _{1/2}	M ₃ 3p _{3/2}	M ₄ 3d _{3/2}	M ₅ 3d _{5/2}	N ₁ 4s	N ₂ 4p _{1/2}	N ₃ 4p _{3/2}			
23 V	5465	626.7†	519.8†	512.1†	66.3†	37.2†	37.2†	Valence levels							
24 Cr	5989	696.0†	583.8†	574.1†	74.1†	42.2†	42.2†								
25 Mn	6539	769.1†	649.9†	638.7†	82.3†	47.2†	47.2†								
26 Fe	7112	844.6†	719.9†	706.8†	91.3†	52.7†	52.7†								
27 Co	7709	925.1†	793.2†	778.1†	101.0†	58.9†	59.9†								
28 Ni	8333	1008.6†	870.0†	852.7†	110.8†	68.0†	66.2†								
29 Cu	8979	1096.7†	952.3†	932.7	122.5†	77.3†	75.1†								
30 Zn	9659	1196.2*	1044.9*	1021.8*	139.8*	91.4*	88.6*						10.2*	10.1*	Valence levels
31 Ga	10367	1299.0*b	1143.2†	1116.4†	159.5†	103.5†	100.0†	18.7†	18.7†						
32 Ge	11103	1414.6*b	1248.1*b	1217.0*b	180.1*	124.9*	120.8*	29.8	29.2						
33 As	11867	1527.0*b	1359.1*b	1323.6*b	204.7*	146.2*	141.2*	41.7*	41.7*						
34 Se	12658	1652.0*b	1474.3*b	1433.9*b	229.6*	166.5*	160.7*	55.5*	54.6*						
35 Br	13474	1782*	1596*	1550*	257*	189*	182*	70*	69*						
36 Kr	14326	1921	1730.9*	1678.4*	292.8*	222.2*	214.4	95.0*	93.8*	27.5*	14.1*	14.1*			
37 Rb	15200	2065	1864	1804	326.7*	248.7*	239.1*	113.0*	112*	30.5*	16.3*	15.3*			
38 Sr	16105	2216	2007	1940	358.7†	280.3†	270.0†	136.0†	134.2†	38.9†	21.3	20.1†			
39 Y	17038	2373	2156	2080	392.0*b	310.6*	298.8*	157.7†	155.8†	43.8*	24.4*	23.1*			
40 Zr	17998	2532	2307	2223	430.3†	343.5†	329.8†	181.1†	178.8†	50.6†	28.5†	27.1†			
41 Nb	18986	2698	2465	2371	466.6†	376.1†	360.6†	205.0†	202.3†	56.4†	32.6†	30.8†			
42 Mo	20000	2866	2625	2520	506.3†	411.6†	394.0†	231.1†	227.9†	63.2†	37.6†	35.5†			
43 Tc	21044	3043	2793	2677	544*	447.6	417.7	257.6	253.9*	69.5*	42.3*	39.9*			
44 Ru	22117	3224	2967	2838	586.1*	483.5†	461.4†	284.2†	280.0†	75.0†	46.3†	43.2†			
45 Rh	23220	3412	3146	3004	628.1†	521.3†	496.5†	311.9†	307.2†	81.4*b	50.5†	47.3†			
46 Pd	24350	3604	3330	3173	671.6†	559.9†	532.3†	340.5†	335.2†	87.1*b	55.7†a	50.9†			
47 Ag	25514	3806	3524	3351	719.0†	603.8†	573.0†	374.0†	368.3	97.0†	63.7†	58.3†			

Basic Concepts:

A Little Electronic Structure



The X-Ray-Based Experiments

X-Ray Sources, Synchrotron Radiation, Free Electron Lasers

Core-Level Photoemission

Intensities and Quantitative Analysis, the 3-Step Model

Varying Surface and Bulk Sensitivity

Chemical Shifts

Multiplet Splittings

Electron Screening and Satellite Structure

Magnetic and Non-Magnetic Dichroism

Resonant Photoemission

Photoelectron Diffraction and Holography

Valence-Level Photoemission

Band-Mapping in the Ultraviolet Photoemission Limit

Densities of States in the X-Ray Photoemission Limit

Some New Directions

Photoemission with Hard X-Rays (throughout lectures)

Photoemission with Standing Wave Excitation

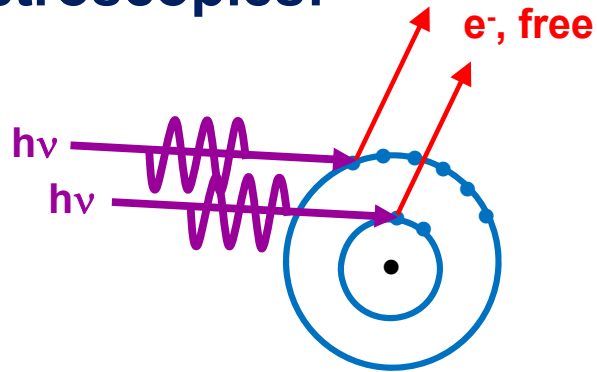
Photoemission with: Higher Pressures → multi-Torr → Atmosphere?

Spatial Resolution-Photoelectron Microscopy

Temporal Resolution

The vacuum ultraviolet, soft x-ray, hard x-ray measurements:

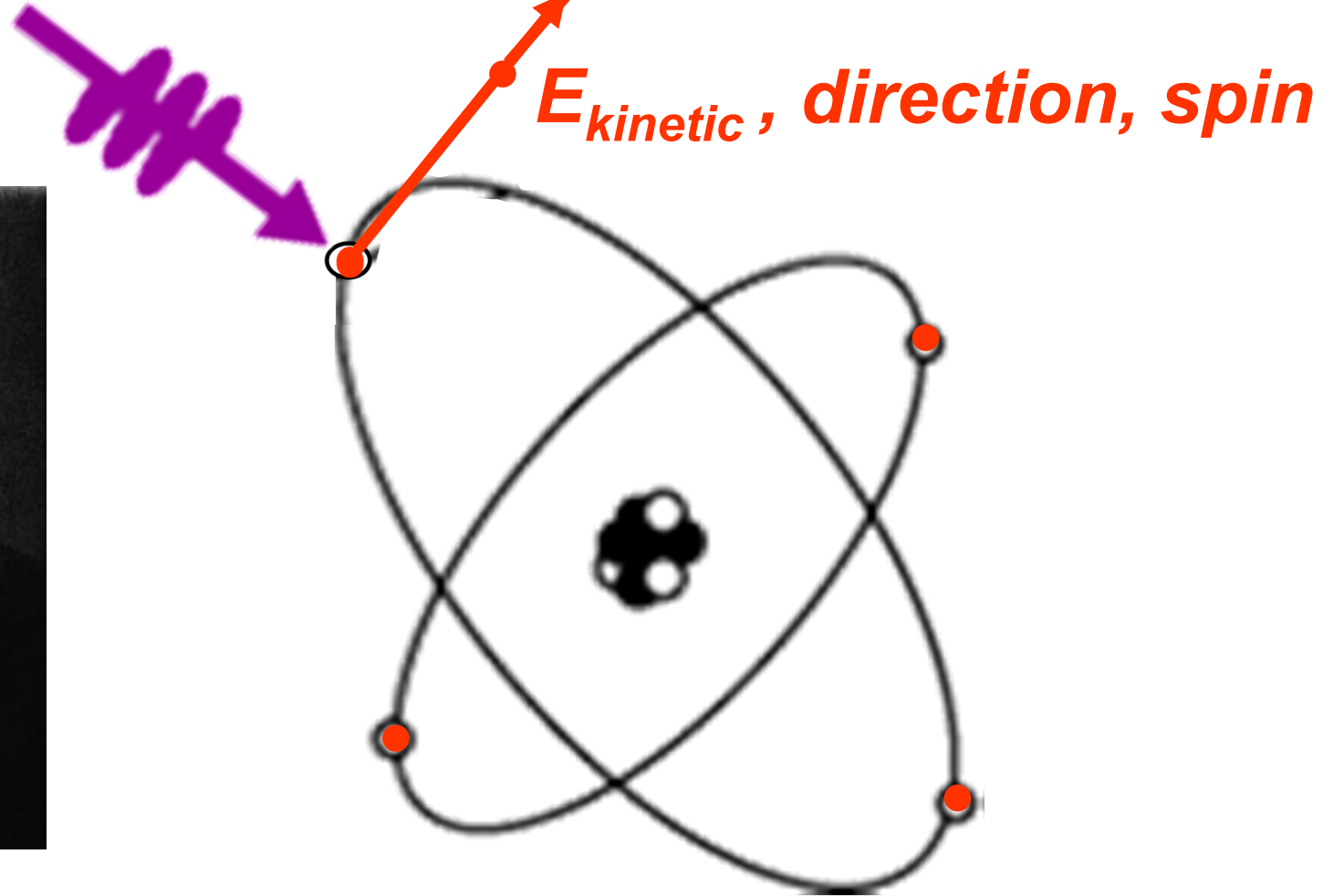
The spectroscopies:



PHOTOELECTRON SPECTROSCOPY=
PHOTOEMISSION – PS, PES, UPS, XPS
+ DIFFRACTION-XPD, PhD
+ HOLOGRAPHY-PH
+ MICROSCOPY-PEEM

The Photoelectric Effect, Einstein, 1905

Light can behave like a Particle!



$$h\nu = E_{initial} - E_{final} = E_{binding} + E_{kinetic}$$

But not everybody liked this idea to start with!



“I would like to tell you how pleased I am that you have given up your light-quantum theory”

von Laue to Einstein, 1907 letter

...and even Planck



In his 1913 letter nominating Einstein for the membership of Prussian Academy of Science, Max Planck et al. wrote:

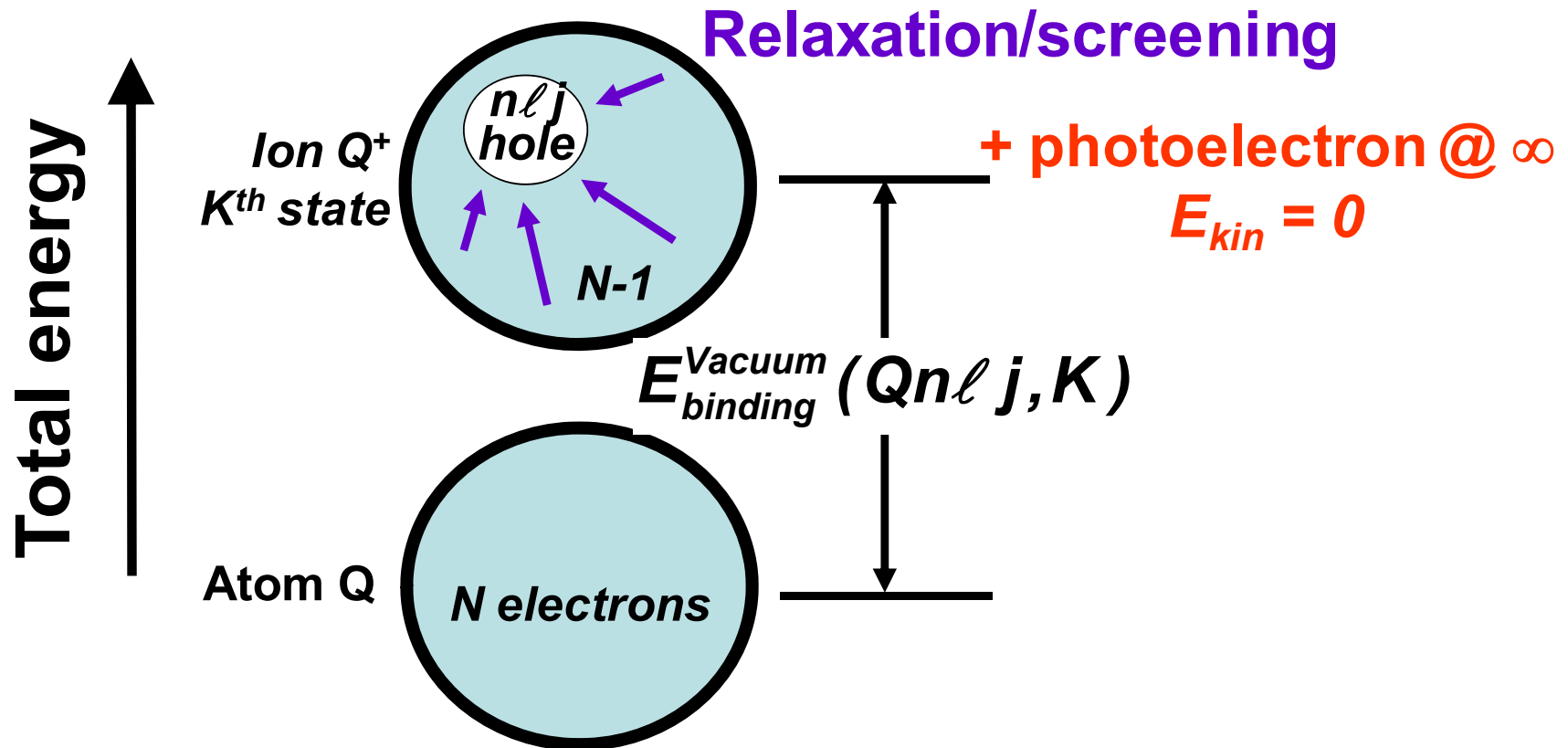
“In sum, one can say there is hardly one among the great problems in which modern physics is so rich to which Einstein has not made a remarkable contribution. That he may sometimes have missed the target in his speculations, as, for example, in his hypothesis of light quanta, cannot really be held too much against him, for it is not possible to introduce really new ideas even in the most exact sciences without sometimes taking a risk.”

Basic energetics—Many e⁻ picture

$$h\nu = E_{\text{binding}}^{\text{Vacuum}} + E_{\text{kinetic}} = E_{\text{binding}}^{\text{Fermi}} + \varphi_{\text{spectrometer}} + E_{\text{kinetic}}$$

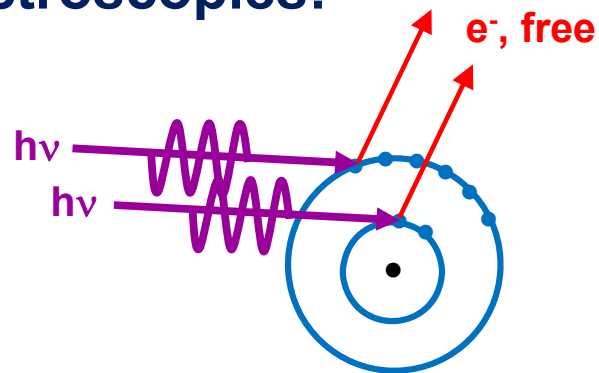
Many states, many values

$$E_{\text{binding}}^{\text{Vacuum}}(Qn\ell j, K) = E_{\text{final}}(N-1, Qn\ell j \text{ hole}, K) - E_{\text{initial}}(N)$$

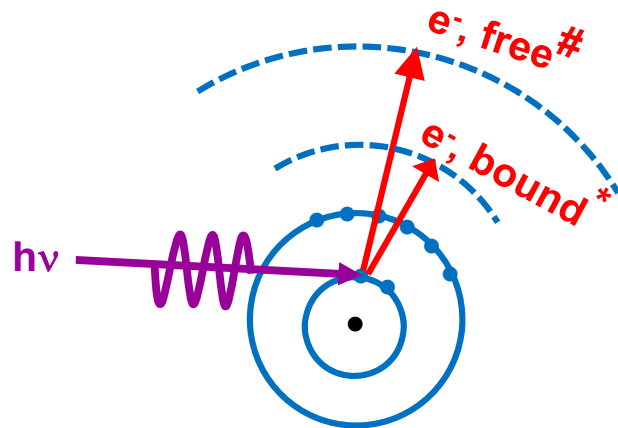


The vacuum ultraviolet, soft x-ray, hard x-ray measurements:

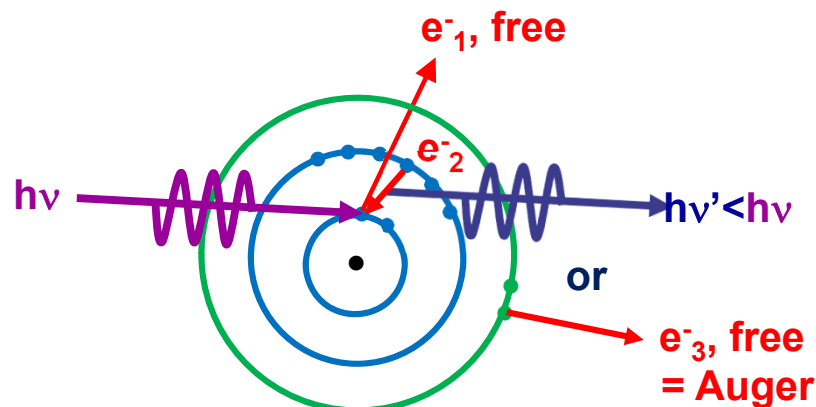
The spectroscopies:



PHOTOELECTRON SPECTROSCOPY=
PHOTOEMISSION – PS, PES, UPS, XPS
+ DIFFRACTION-XPD, PhD
+ HOLOGRAPHY-PH
+ MICROSCOPY-PEEM



X-RAY ABSORPTION SPECTROSCOPY- XAS
* NEAR-EDGE – NEXAFS, XANES
EXTENDED- EXAFS, XAFS
+ X-RAY MAGNETIC CIRCULAR/LINEAR
DICHROISM- XMCD, XMLD

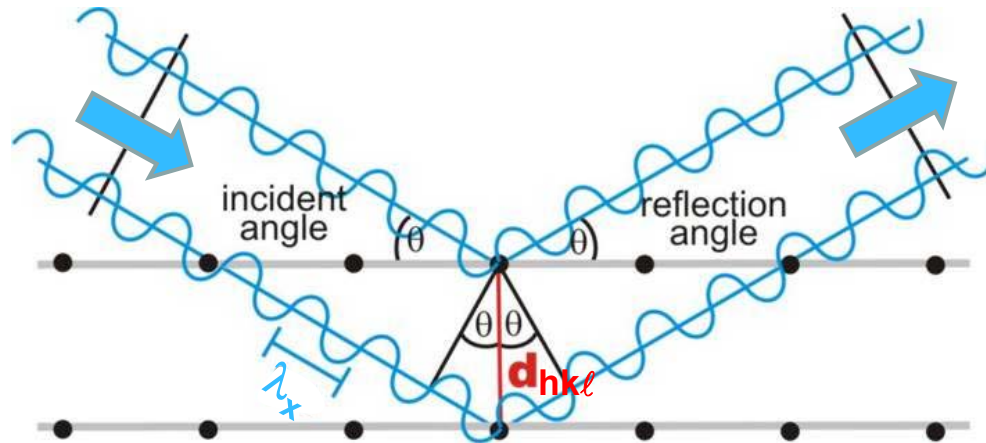


X-RAY EMISSION (FLUORESCENCE)
SPECTROSCOPY

+ AUGER ELECTRON SPECTROSCOPY

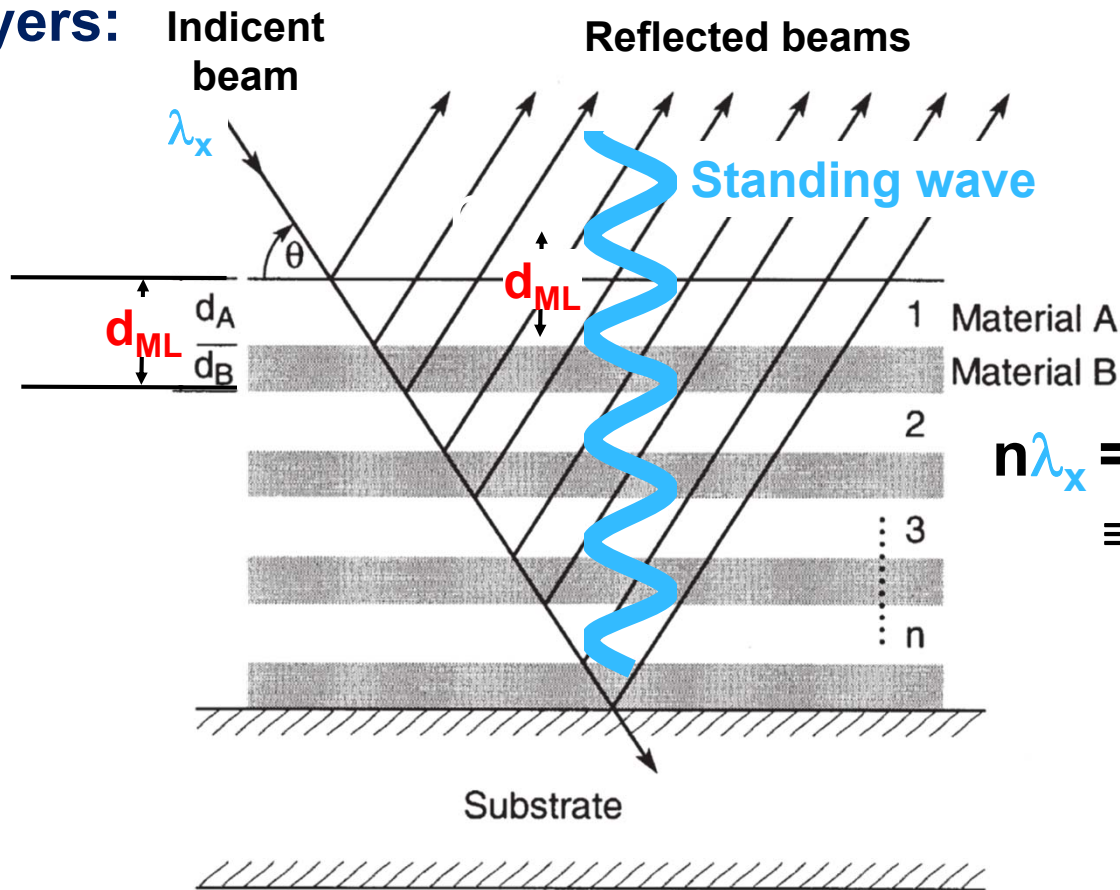
The vacuum ultraviolet, soft x-ray, hard x-ray measurements:

Plus diffraction and scattering:
From crystals:



$$n\lambda_x = 2d_{hkl} \sin\theta$$

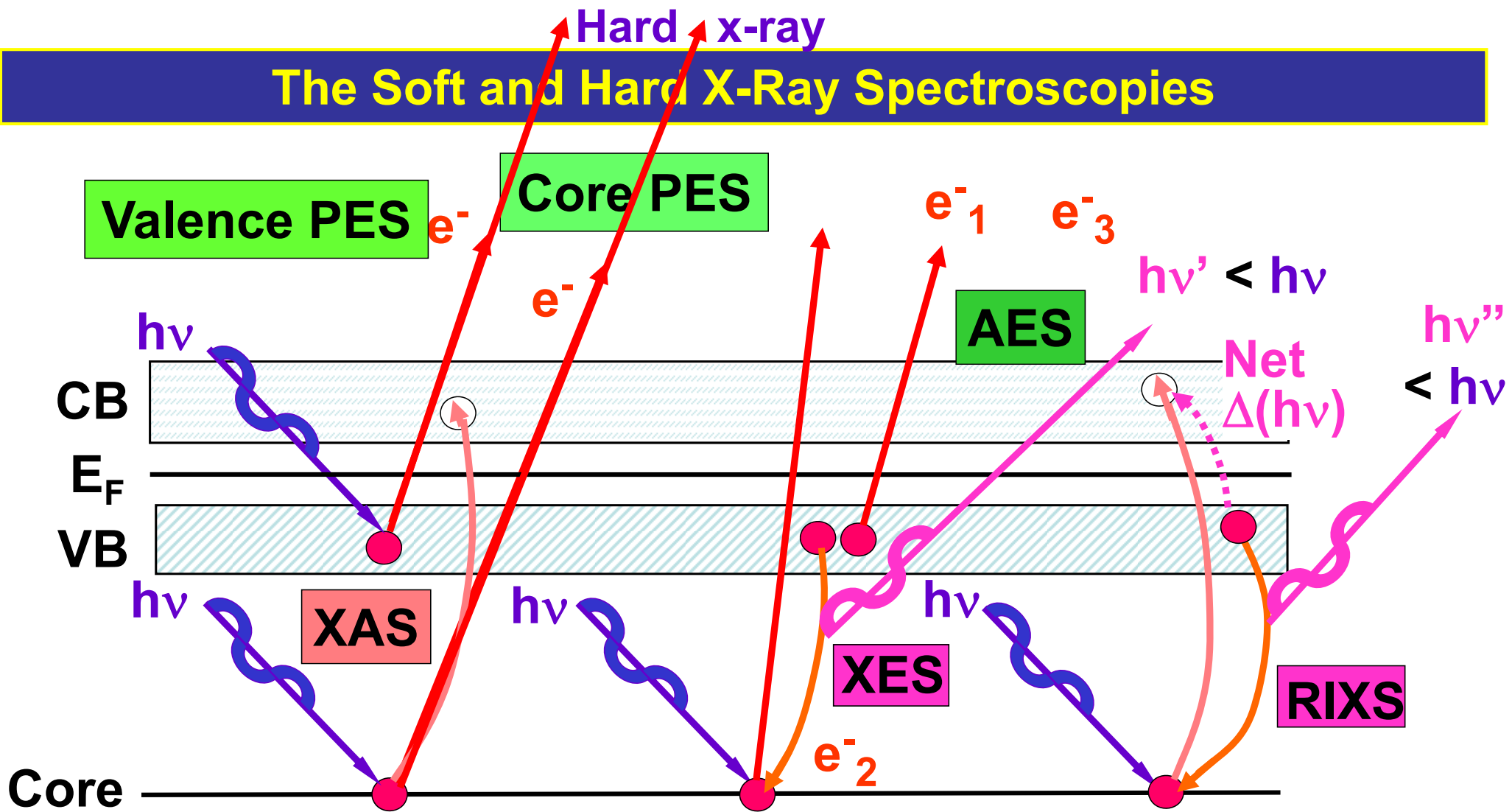
From multilayers:



$$n\lambda_x = 2(d_A + d_B) \sin\theta$$

$$\equiv 2d_{ML} \sin\theta$$

The Soft and Hard X-Ray Spectroscopies



PES = photoemission = photoelectron spectroscopy

XAS = x-ray absorption spectroscopy

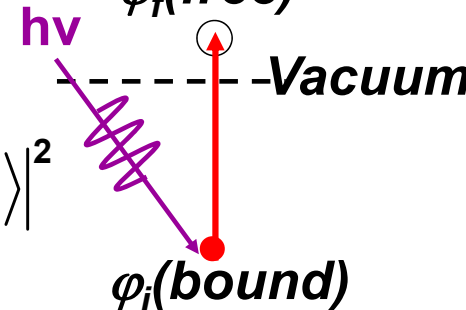
AES = Auger electron spectroscopy

XES = x-ray emission spectroscopy

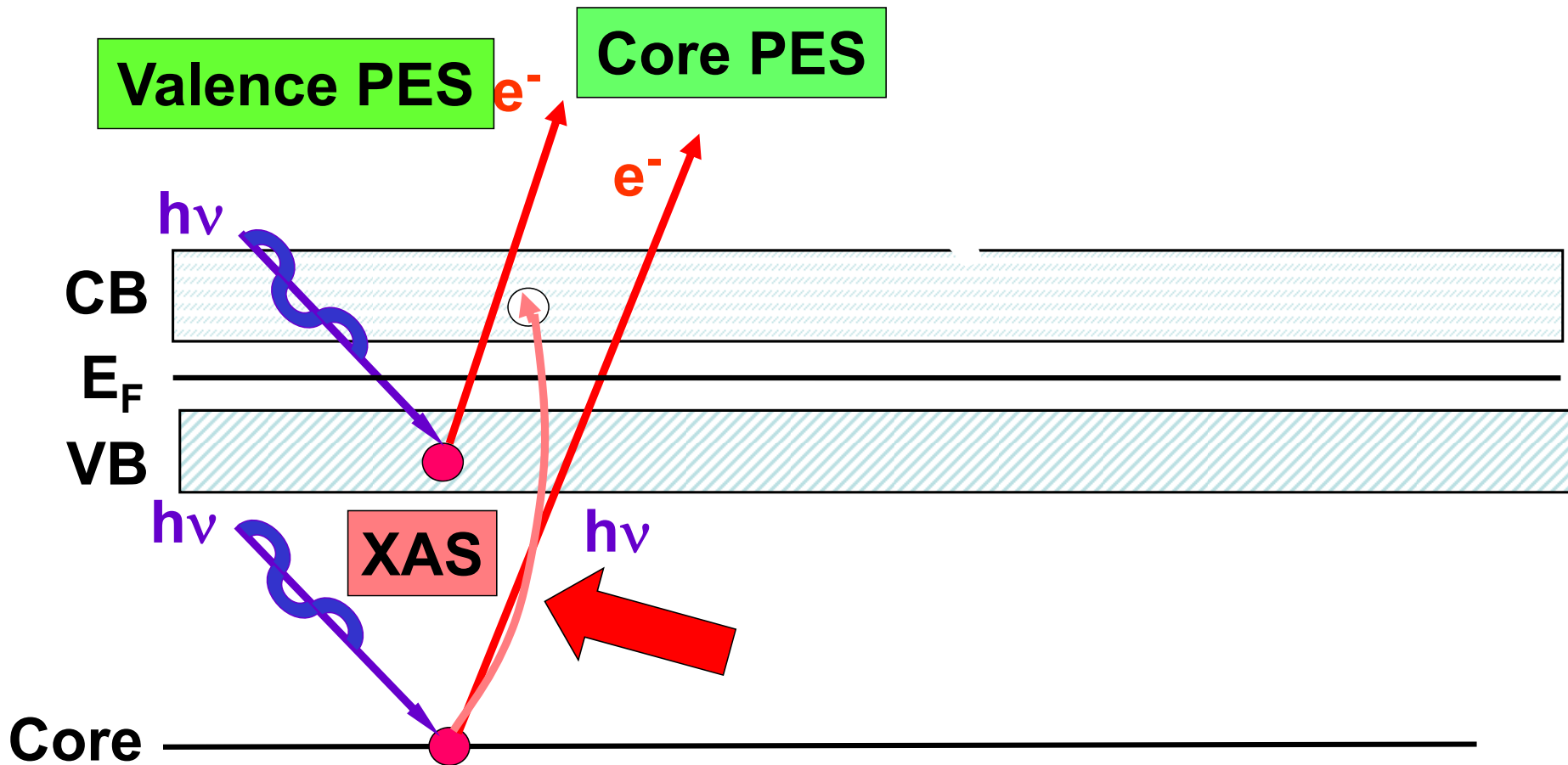
RIXS = resonant inelastic x-ray scattering / x-ray Raman scatt.

MATRIX ELEMENTS IN The Soft and Hard X-Ray Spectroscopies: DIPOLE LIMIT

- Photoelectron spectroscopy/photoemission: $\varphi_f(\text{free})$

$$I \propto \left| \hat{\mathbf{e}} \cdot \langle \varphi_f(\mathbf{1}) | \vec{r} | \varphi_i(\mathbf{1}) \rangle \right|^2$$


The Soft and Hard X-Ray Spectroscopies



PES = photoemission = photoelectron spectroscopy

XAS = x-ray absorption spectroscopy

AES = Auger electron spectroscopy

XES = x-ray emission spectroscopy

REXS/RIXS = resonant elastic/inelastic x-ray scattering

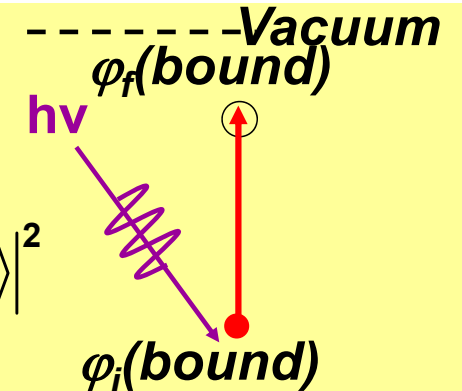
MATRIX ELEMENTS IN The Soft and Hard X-Ray Spectroscopies: DIPOLE LIMIT

- Photoelectron spectroscopy/photoemission:

$$I \propto \left| \hat{\mathbf{e}} \cdot \langle \varphi_f(\mathbf{1}) | \vec{r} | \varphi_i(\mathbf{1}) \rangle \right|^2$$

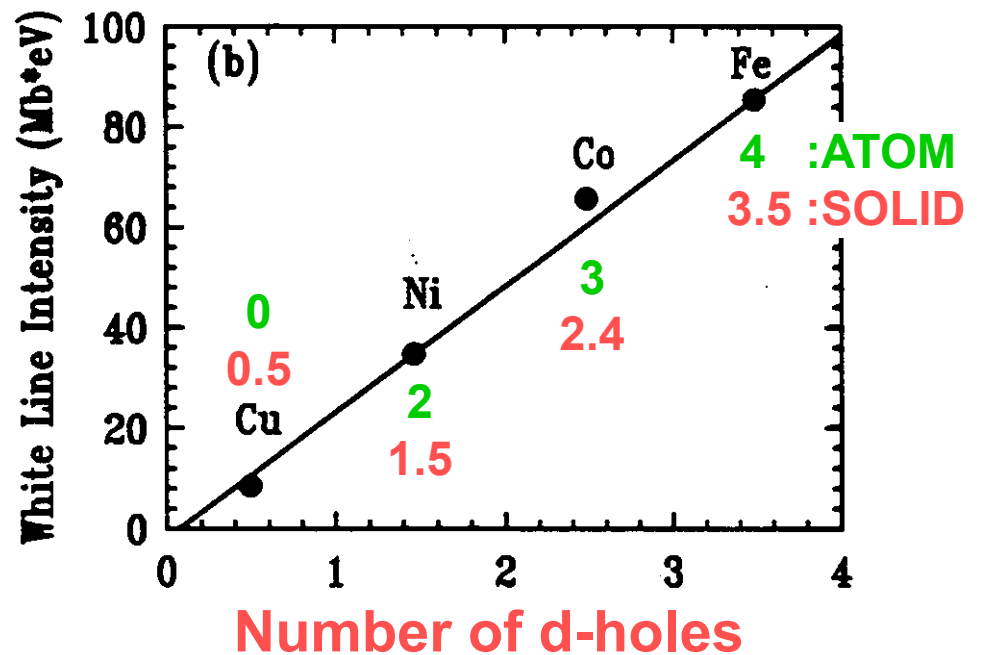
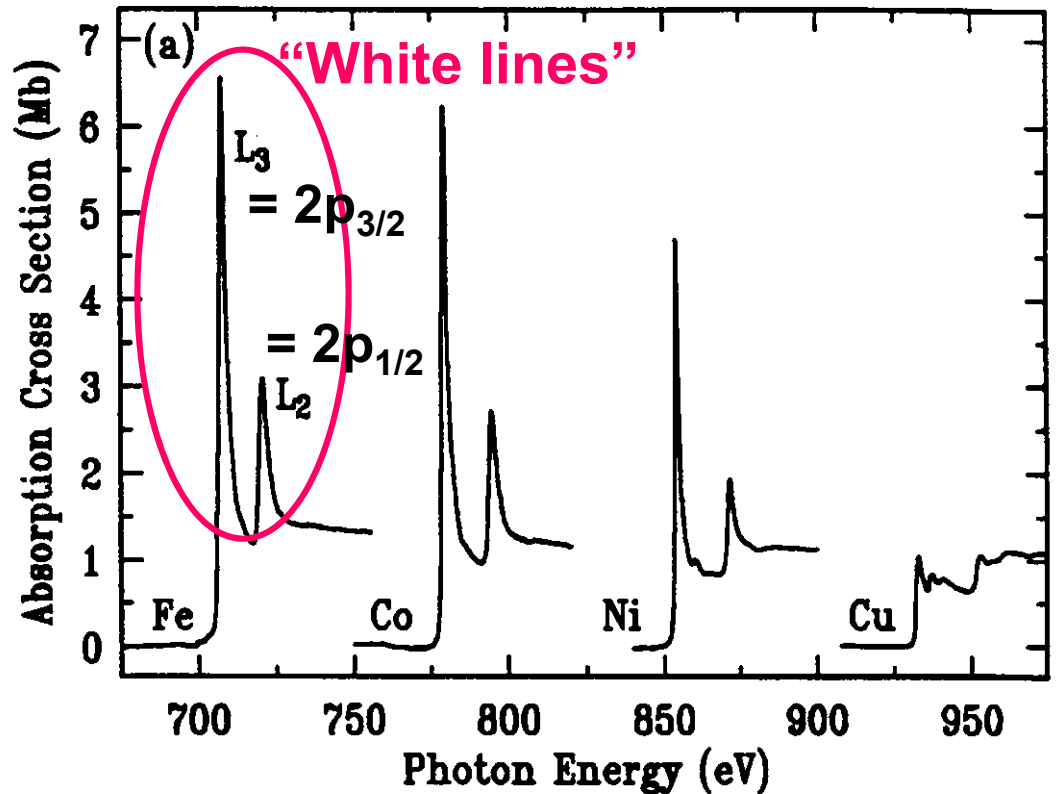
- Near-edge x-ray absorption:

$$I \propto \left| \hat{\mathbf{e}} \cdot \langle \varphi_f(\mathbf{1}) | \vec{r} | \varphi_i(\mathbf{1}) \rangle \right|^2$$

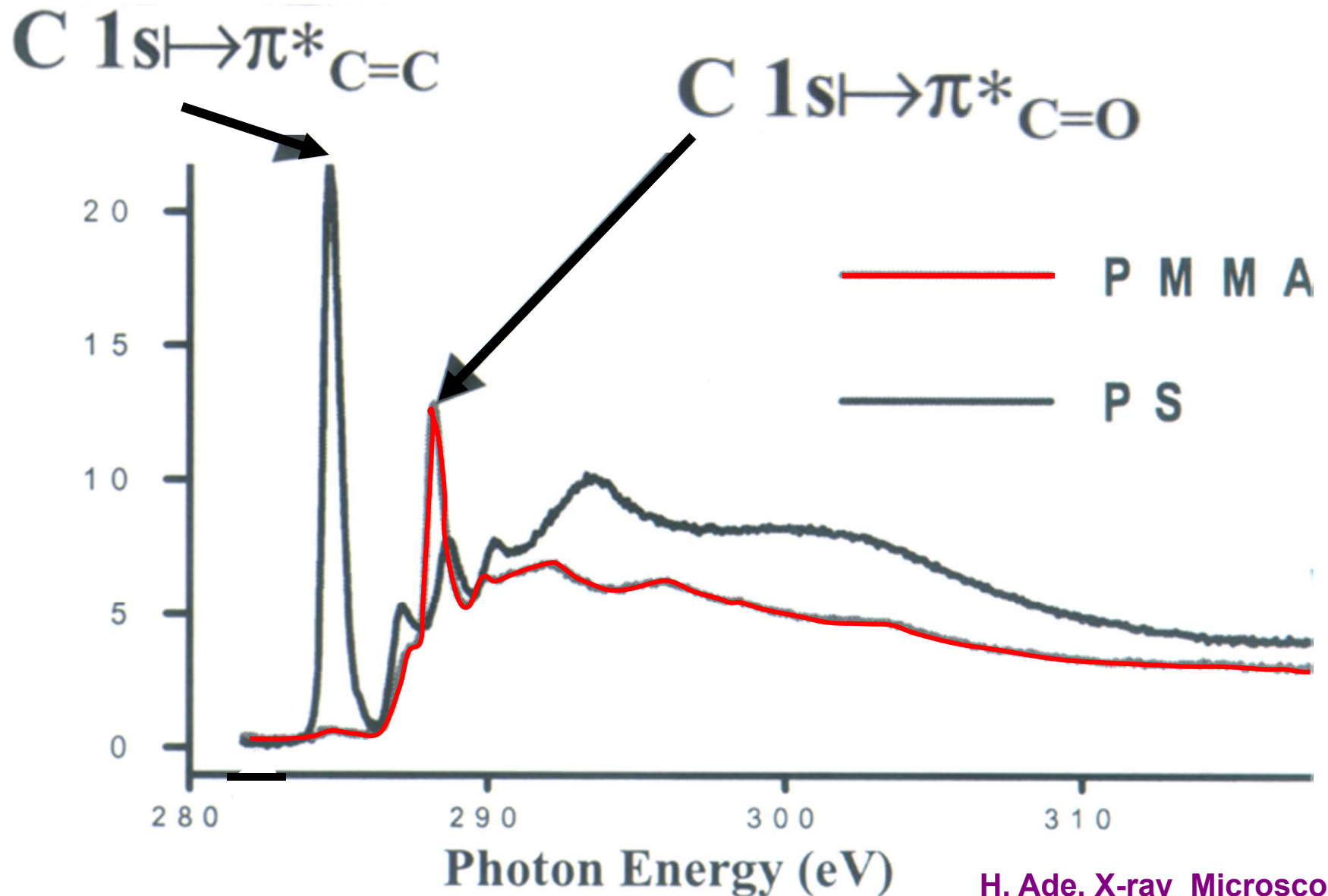


Variation of Near-Edge X-Ray Absorption Fine Structure (NEXAFS) with Atomic No. for Some 3d Transition Metals

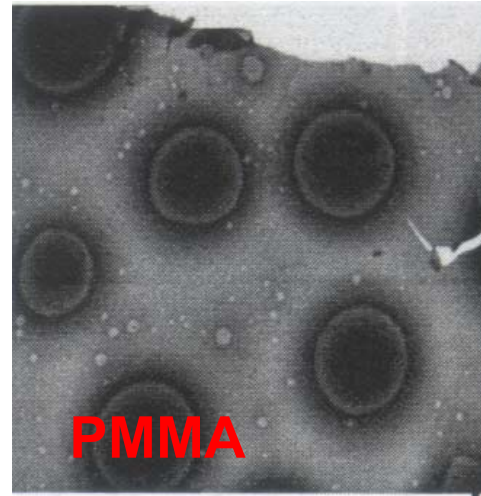
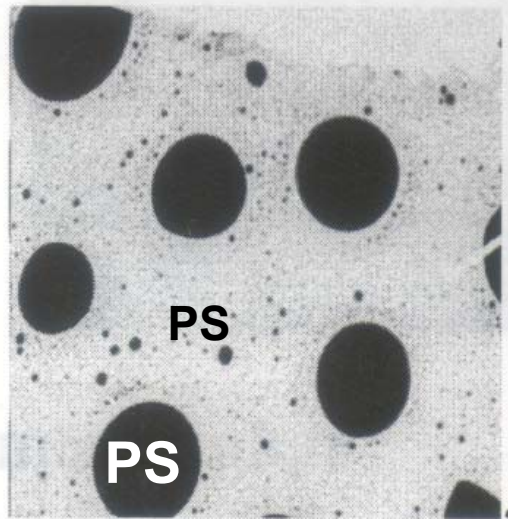
J. Stohr, "NEXAFS Spectroscopy" (Spring, 1992),
 Stohr and Siegmann, "Magnetism: From Fundamentals to Nanoscale Dynamics" (Springer Series in Solid-State Sciences, 2006),
 Chapter 9
 Download from 243A website:
<http://physics.ucdavis.edu/Classes/Physics243A/XMCD.stohr.siegmann.abridged-for-emailing.pdf>



Variation of Near-Edge X-Ray Absorption Fine Structure (NEXAFS) for Different Polymers

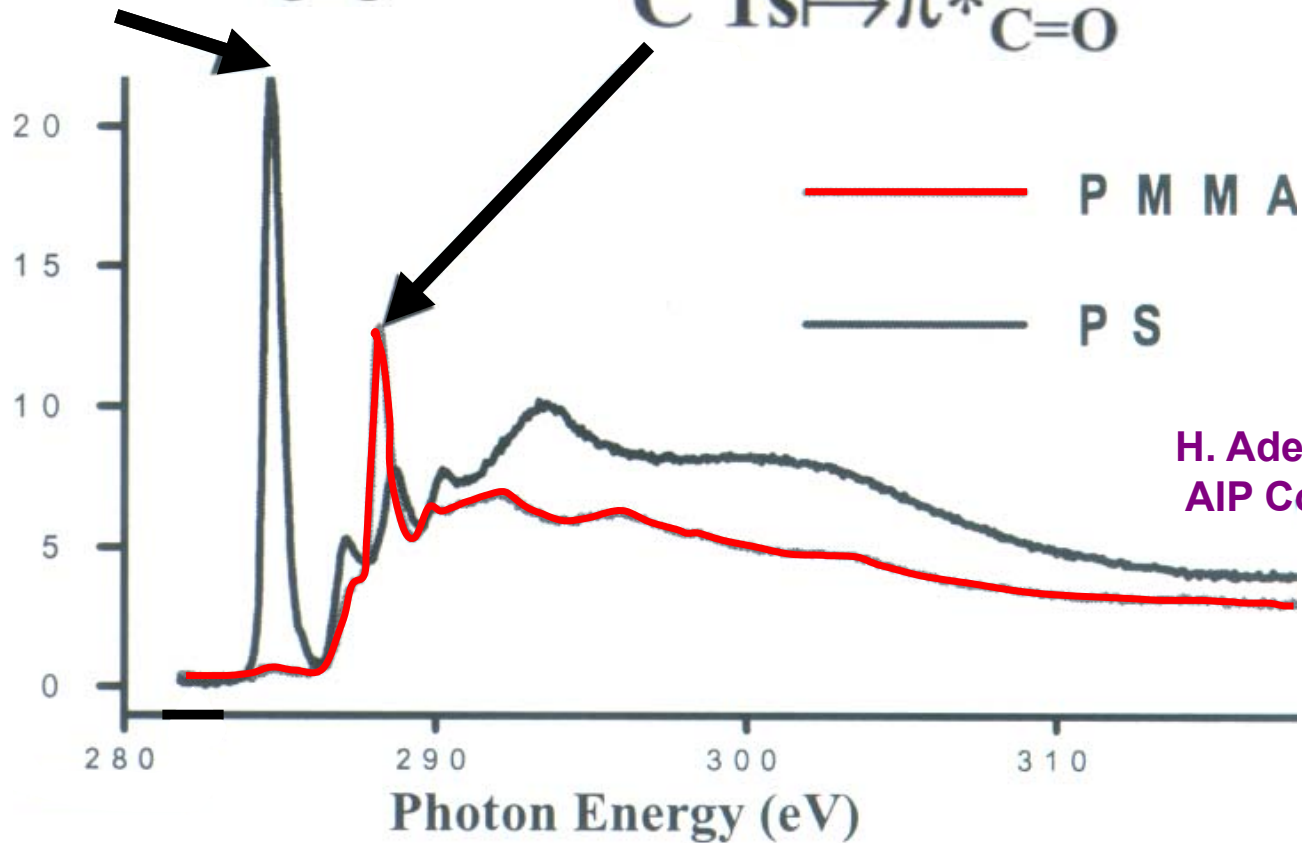


SCANNING TRANSMISSION X-RAY MICROSCOPY OF POLYMER BLEND



$C\ 1s \rightarrow \pi^*_{C=C}$

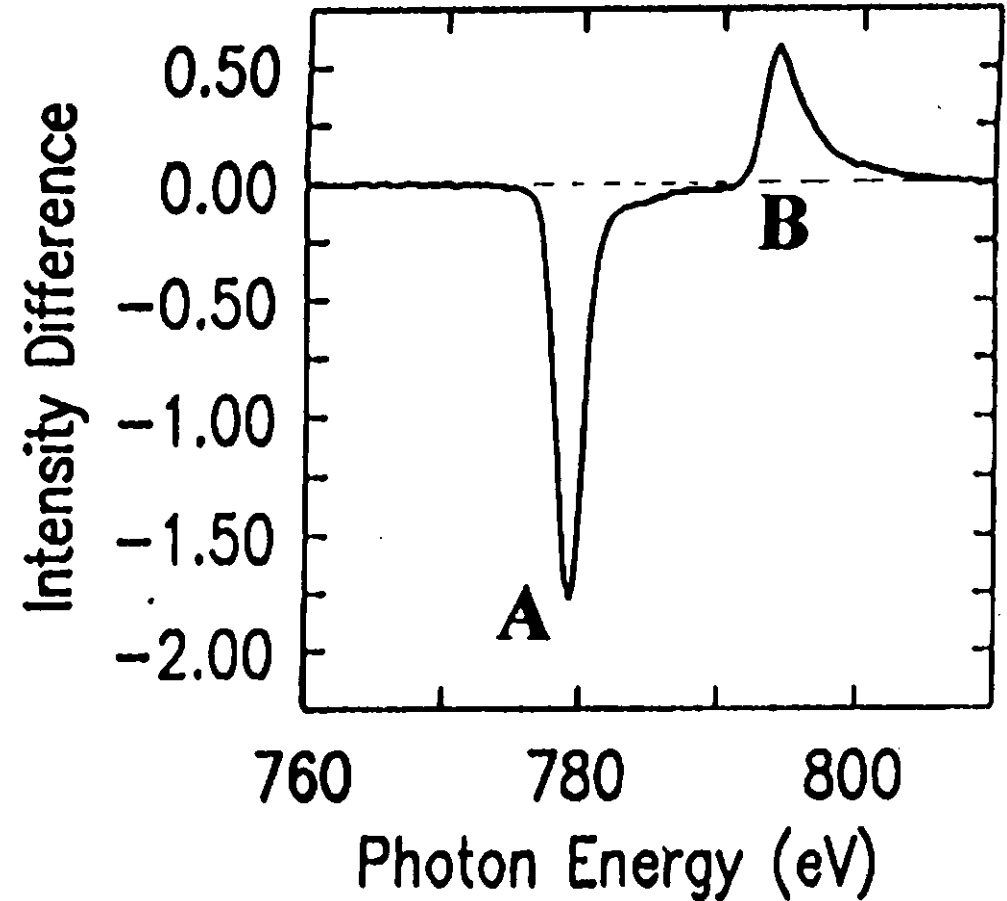
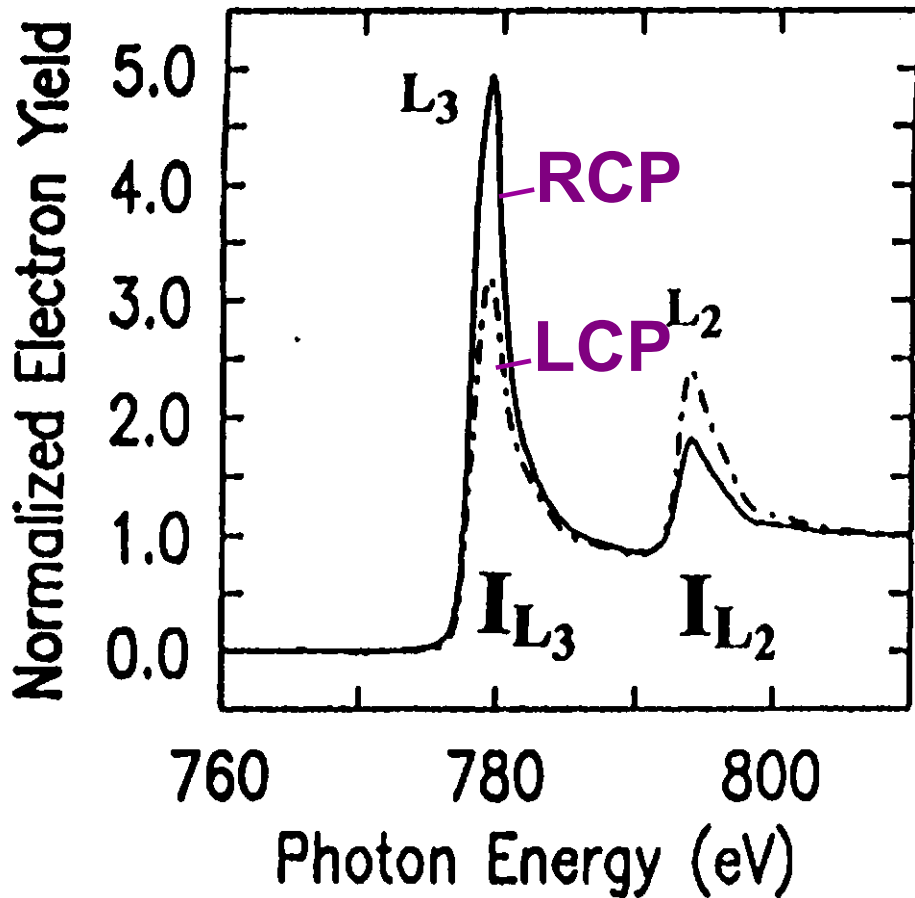
$C\ 1s \rightarrow \pi^*_{C=O}$



H. Ade, X-ray Microscopy 99,
AIP Conf. Proc. 507, p.197

Magnetic Circular Dichroism in X-Ray Absorption (XMCD)

Ferromagnetic cobalt with magnetization along incident light direction



Very useful sum rules: Spin magnetic moment—

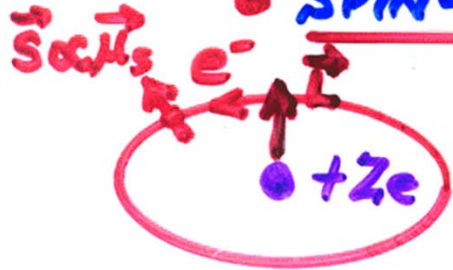
$$[A - 2B]_{\alpha} = -\frac{C}{\mu_B} (m_{spin})$$

Orbital magnetic moment—
($\alpha \rightarrow$ component along magnetic field)

$$[A + B]_{\alpha} = -\frac{3C}{2\mu_B} m_{orbital}^{\alpha}$$

Magnetic Circular Dichroism in X-Ray Absorption (XMCD): Only happens because of the spin-orbit effect

• SPIN-ORBIT SPLITTING OF LEVELS:



⇒ EFFECTIVE \vec{B} (NUCLEUS AROUND e^-) $\propto \vec{L}$

$$\hat{H}_{s-o} = \xi(r) \vec{L} \cdot \vec{S}$$

- SPLITS ALL nl LEVELS $2(2l+1)$
 - $nl_j = l + 1/2$ — $2l+2$
 - $nl_j = l - 1/2$ — $2l$

• MIXES SPIN & ORBITAL ANGULAR MOM.:

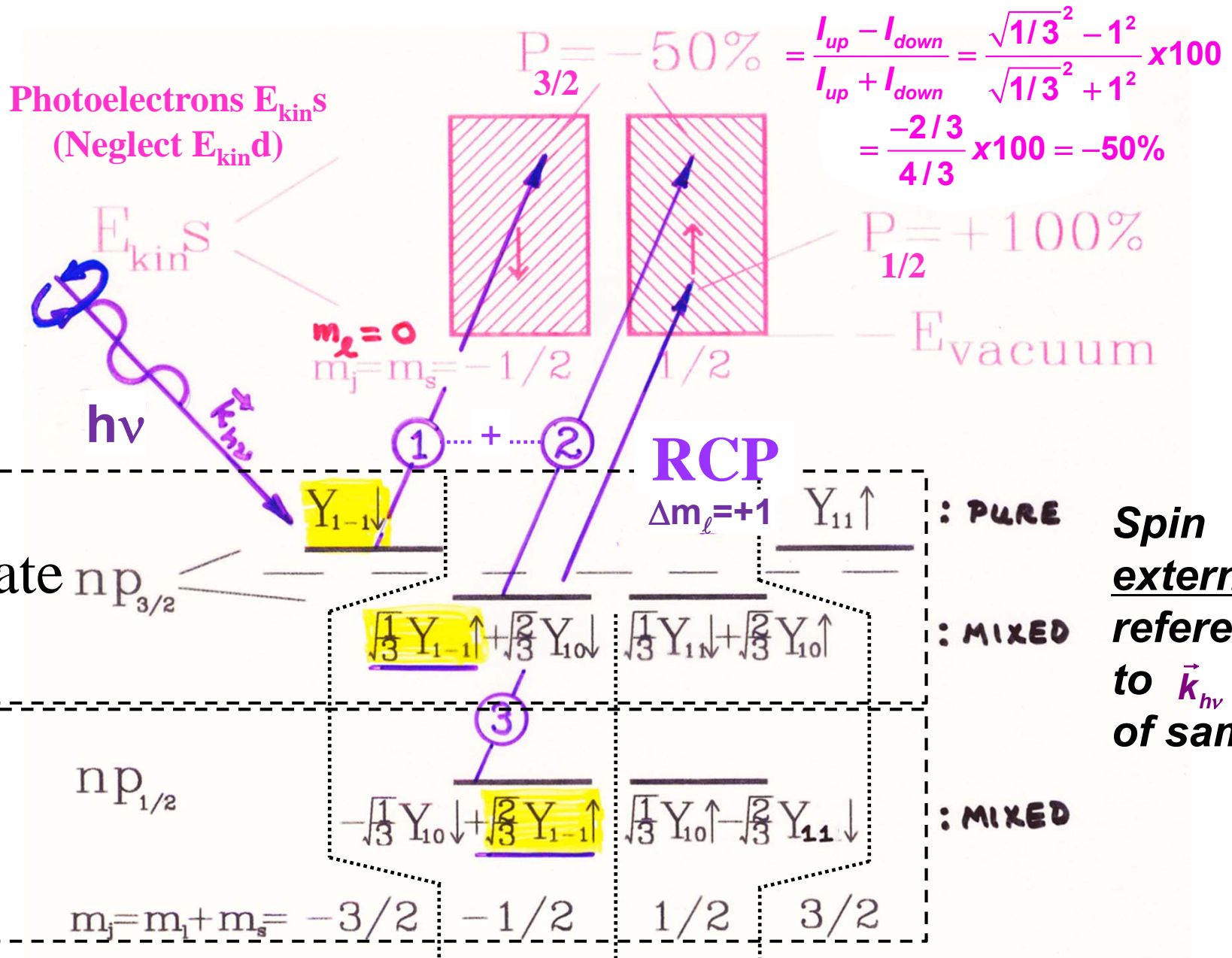
$$\psi_{nljm_j} = C_1 \psi_{nl, m_j - 1/2} \begin{pmatrix} 1 \\ 0 \end{pmatrix} + C_2 \psi_{nl, m_j + 1/2} \begin{pmatrix} 0 \\ 1 \end{pmatrix}$$

\parallel
 $m_s = +1/2$
 \parallel
 \uparrow

\parallel
 $m_s = -1/2$
 \parallel
 \downarrow

WITH C1 AND C2 TABULATED CLEBSCH-GORDAN
OR WIGNER 3j SYMBOLS

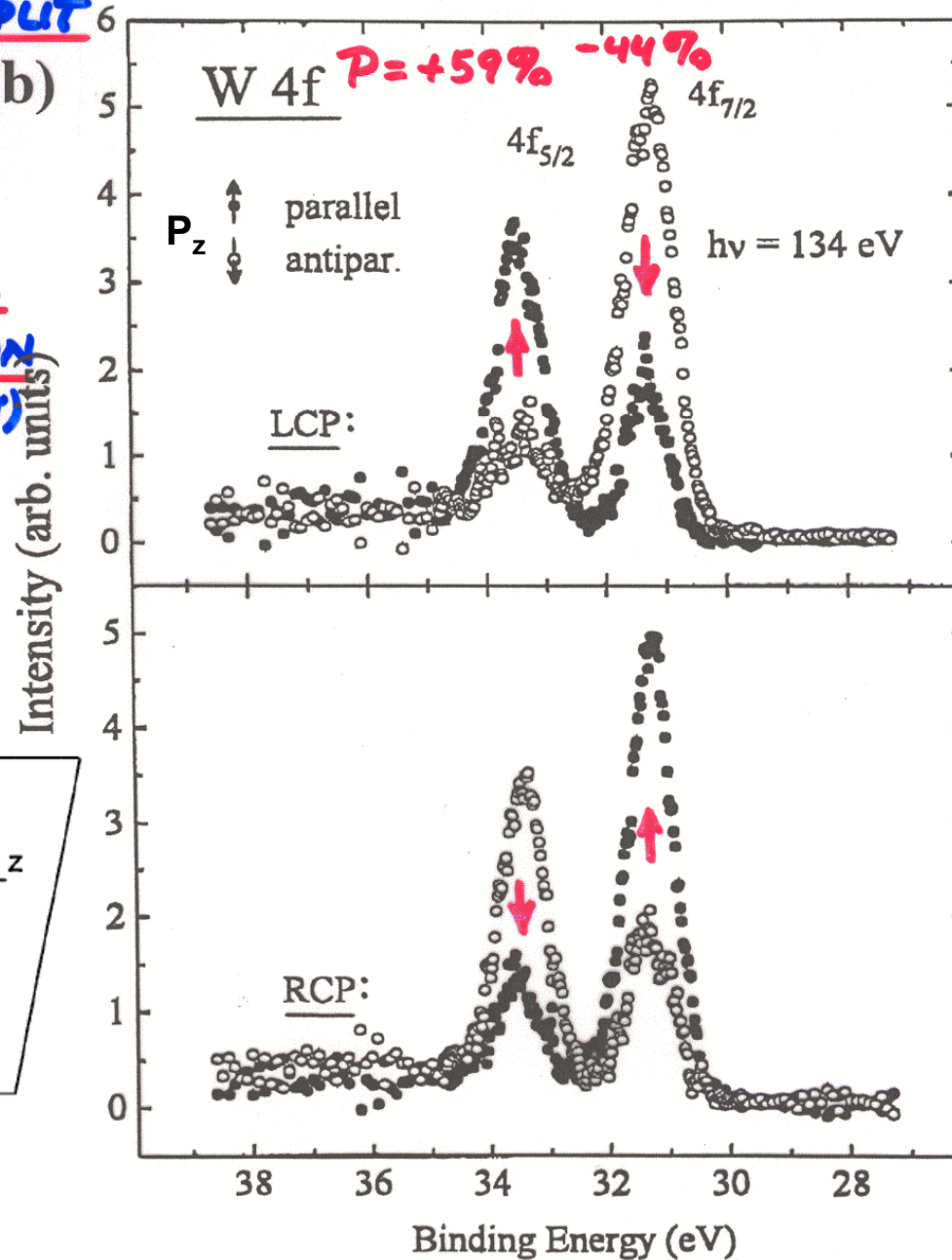
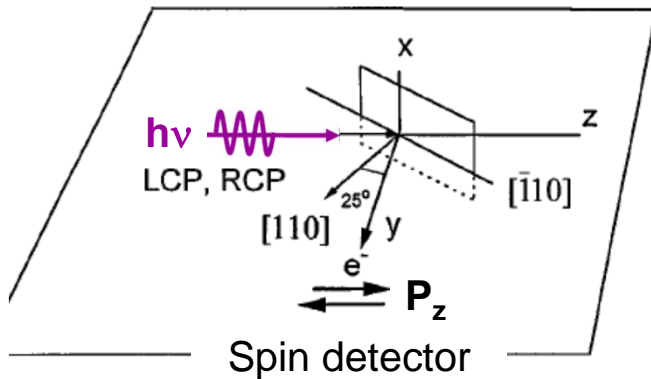
Example: Photoelectron spin polarization from spin-orbit coupling and circularly-polarized radiation—The Fano Effect



Spin externally referenced to \vec{k}_{hv} and \vec{M} of sample

Fano effect and spin polarization (SP) in core photoelectron spectra—expt.

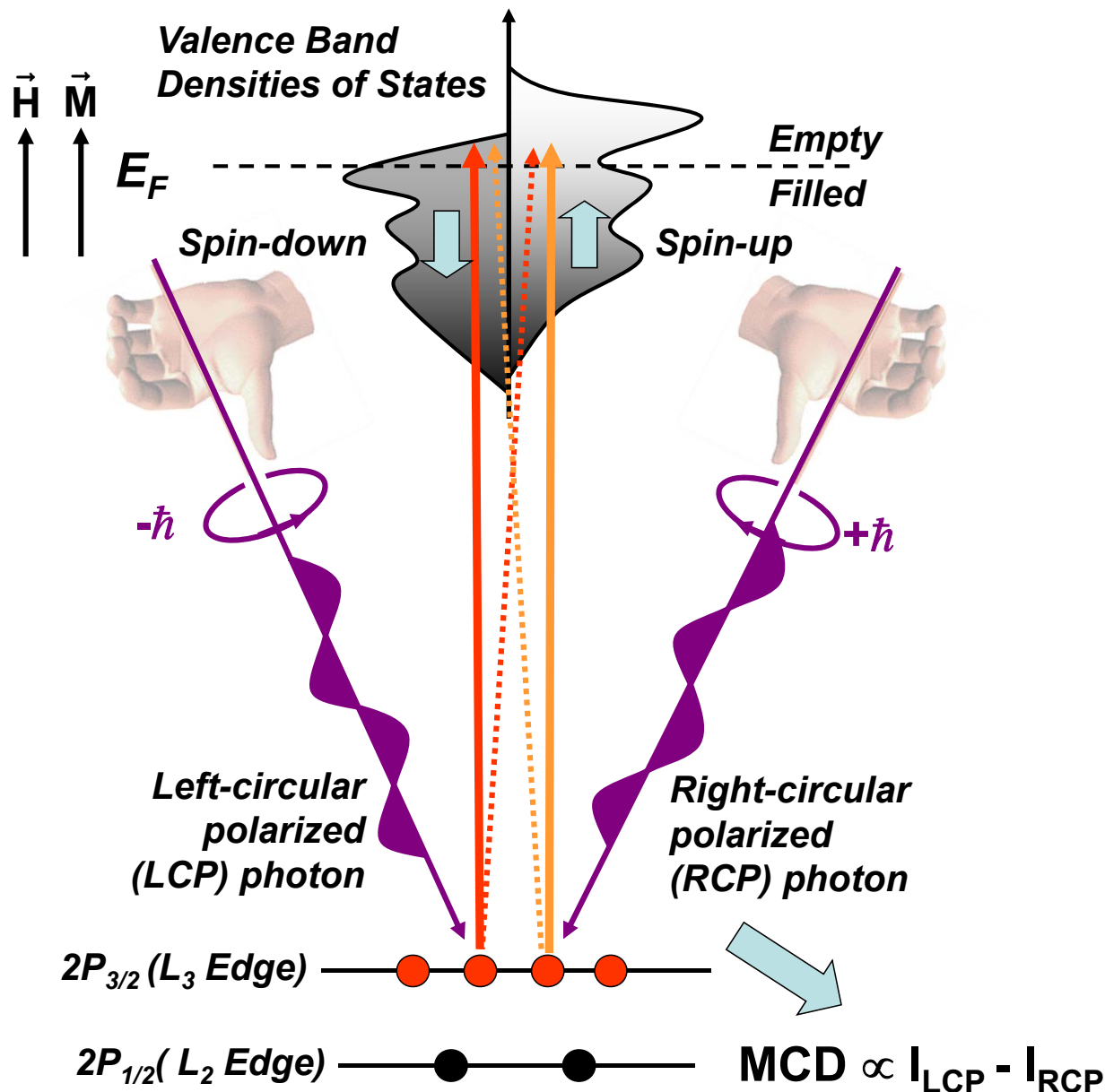
SPIN-ORBIT SPLIT
LEVEL (b)
EXCITED
WITH
CIRCULAR
POLARIZATION
(FANO EFFECT)



EXPT. - STARKE ET AL.
 PRB 53, 210544
 (1996)

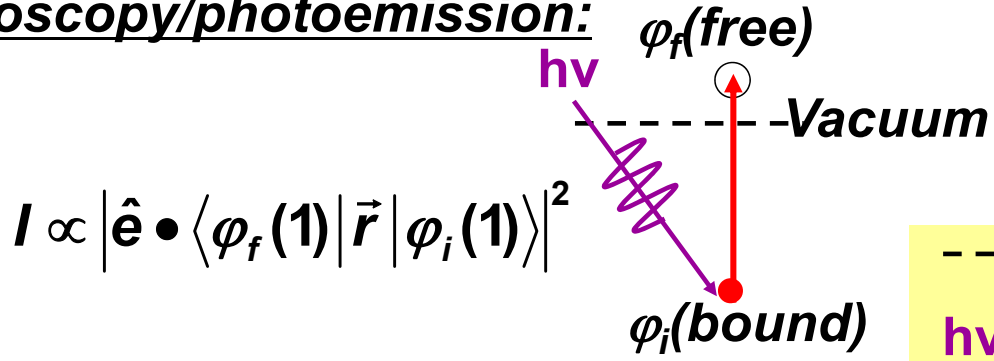
Magnetic Circular Dichroism in X-Ray Absorption (XMCD)

J. Stohr, *Journal of Magnetism and Magnetic Materials* 200 (1999) 470–497



MATRIX ELEMENTS IN The Soft and Hard X-Ray Spectroscopies: DIPOLE LIMIT

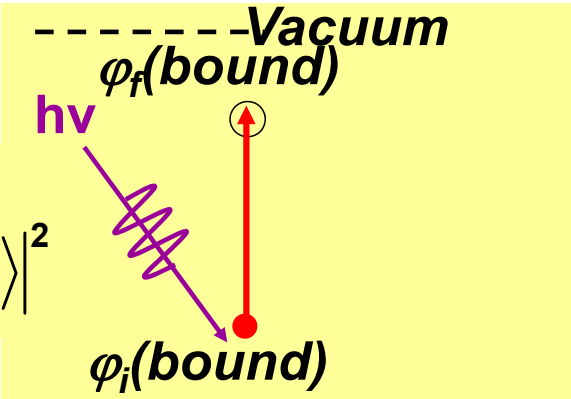
- Photoelectron spectroscopy/photoemission:



$$I \propto \left| \hat{\mathbf{e}} \cdot \langle \varphi_f(\mathbf{1}) | \vec{r} | \varphi_i(\mathbf{1}) \rangle \right|^2$$

- Near-edge x-ray absorption:

$$I \propto \left| \hat{\mathbf{e}} \cdot \langle \varphi_f(\mathbf{1}) | \vec{r} | \varphi_i(\mathbf{1}) \rangle \right|^2$$



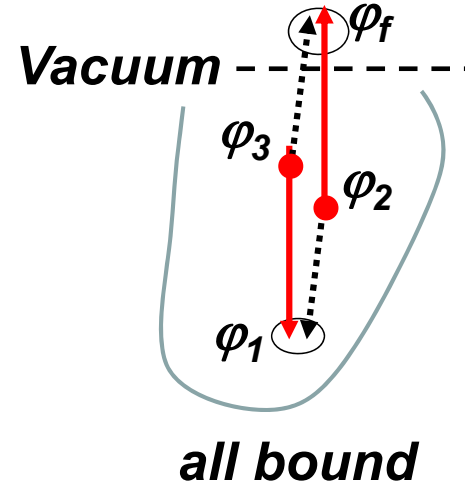
- Auger electron emission:

$$I \propto \left| \langle \varphi_f(\mathbf{1})\varphi_1(\mathbf{2}) | \frac{e^2}{r_{12}} | \varphi_3(\mathbf{1})\varphi_2(\mathbf{2}) \rangle - \langle \varphi_1(\mathbf{1})\varphi_f(\mathbf{2}) | \frac{e^2}{r_{12}} | \varphi_3(\mathbf{1})\varphi_2(\mathbf{2}) \rangle \right|^2$$

Exchange

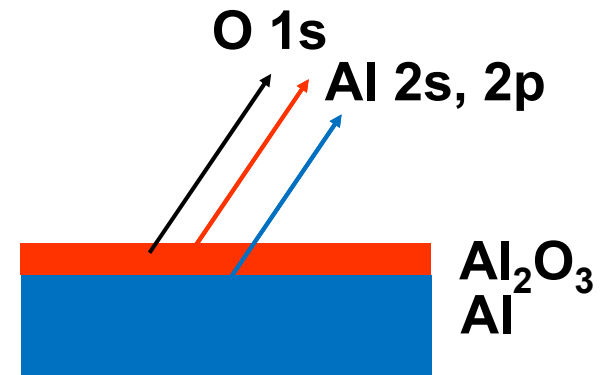
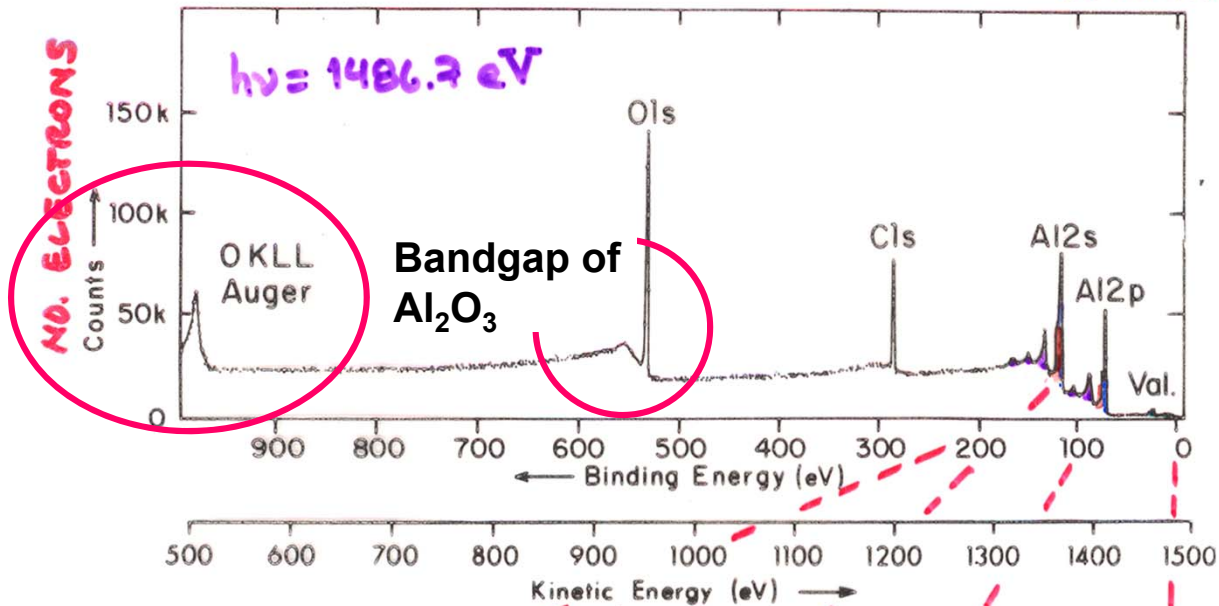
with $r_{12} = |\vec{r}_1 - \vec{r}_2|$, and

$$\frac{e^2}{|\vec{r}_1 - \vec{r}_2|} = 4\pi e^2 \sum_{l=0}^{\infty} \sum_{m_l=-l}^l \frac{1}{2l+1} \frac{r_{<}^l}{r_{>}^{l+1}} Y_l^{m_l}(\theta_1, \phi_1) [Y_l^{m_l}(\theta_2, \phi_2)]^*$$



a complex operator, no simple selection rules

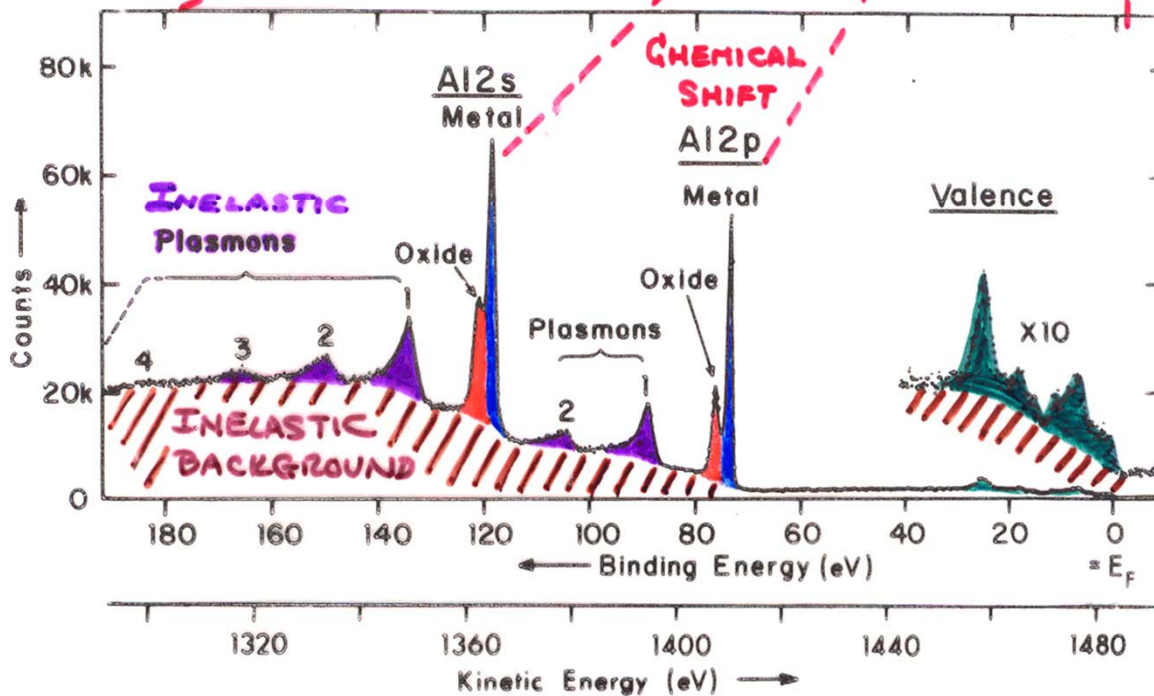
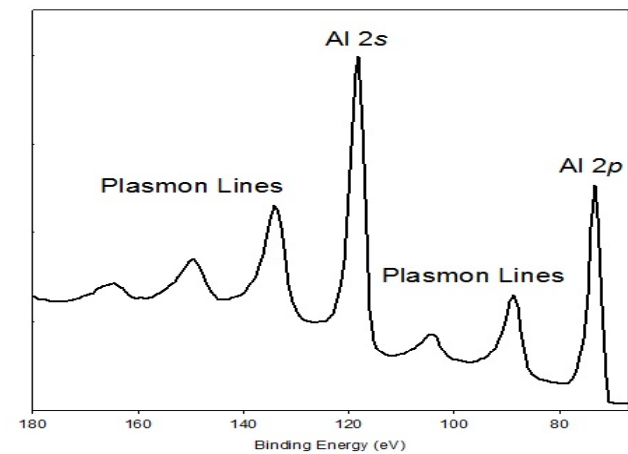
TYPICAL PHOTOELECTRON SPECTRA: OXIDIZED ALUMINUM



Plasmons:

$$E_{\text{plasmon}} = \hbar\omega_p = \hbar(n_{\text{valence}} e^2 / m_e \epsilon_0)^{1/2}$$

CLEAN ALUMINUM



"Basic Concepts of XPS"
 Figure 1

THE AUGER PROCESS

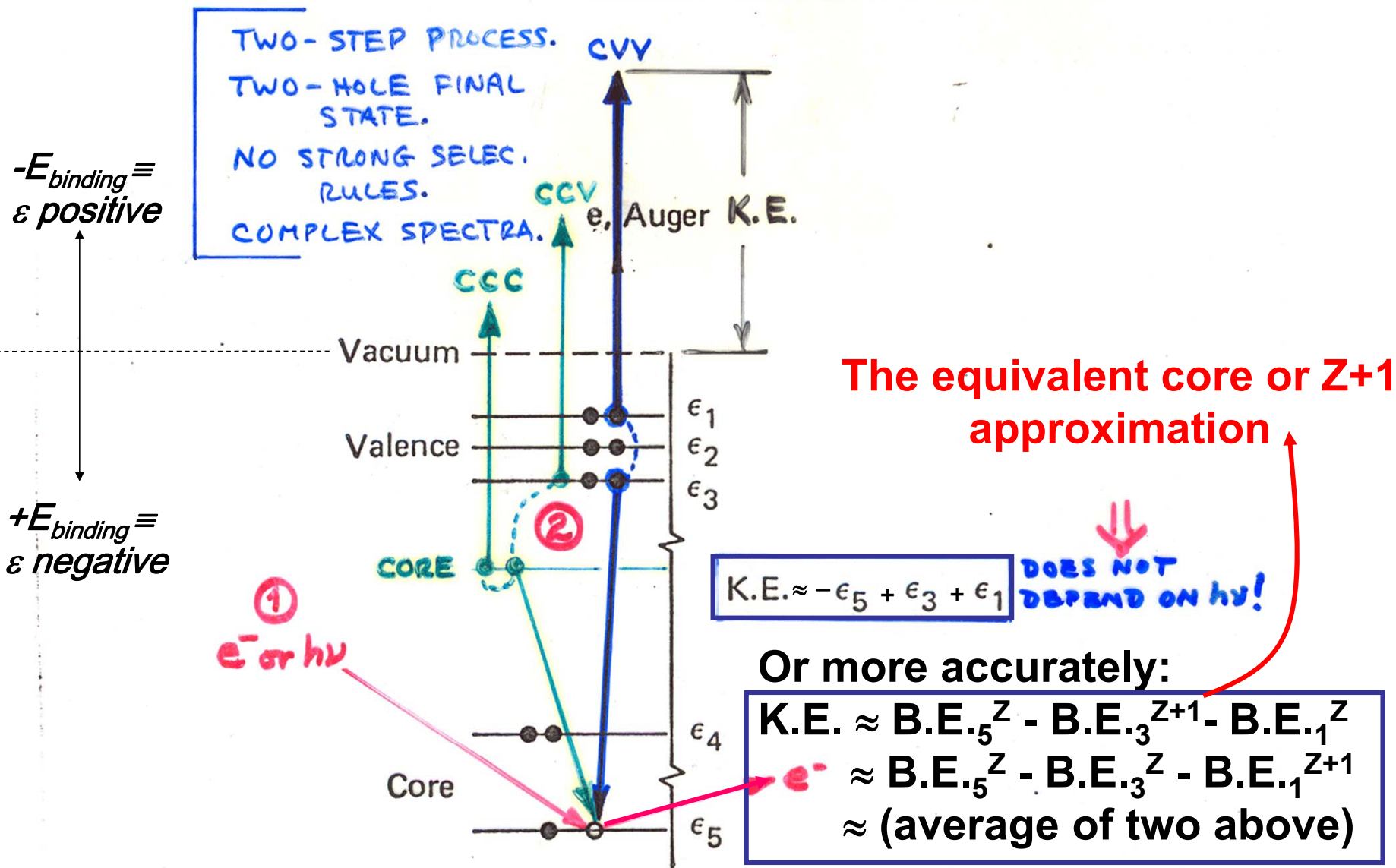
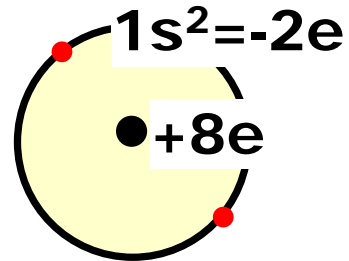


Figure 2. Scheme of the Auger process. A valence-level involved Auger emission is illustrated here, but the two electrons involved also could have come from core level, ϵ_4 , provided $\epsilon_5 - 2\epsilon_4 > 0$.

The equivalent core or Z+1 approximation

O: $Z = 8$

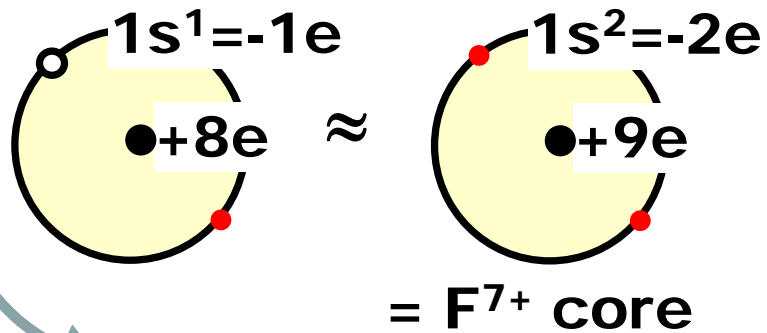
O core = O $1s^2 = O^{6+}$



Assume:

O^{6+} core with

$1s$ hole = $O^{7+} =$

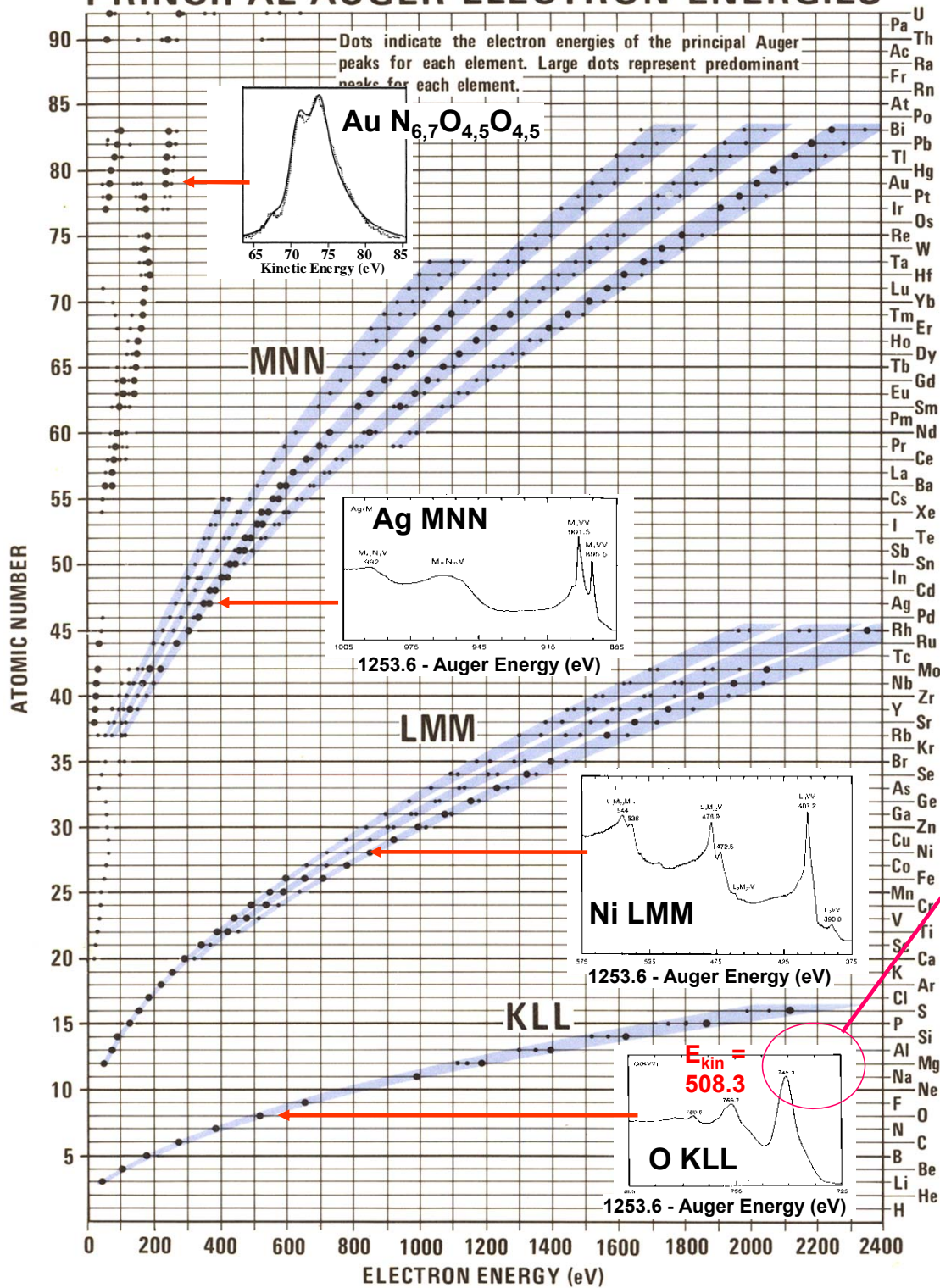


= F^{7+} core

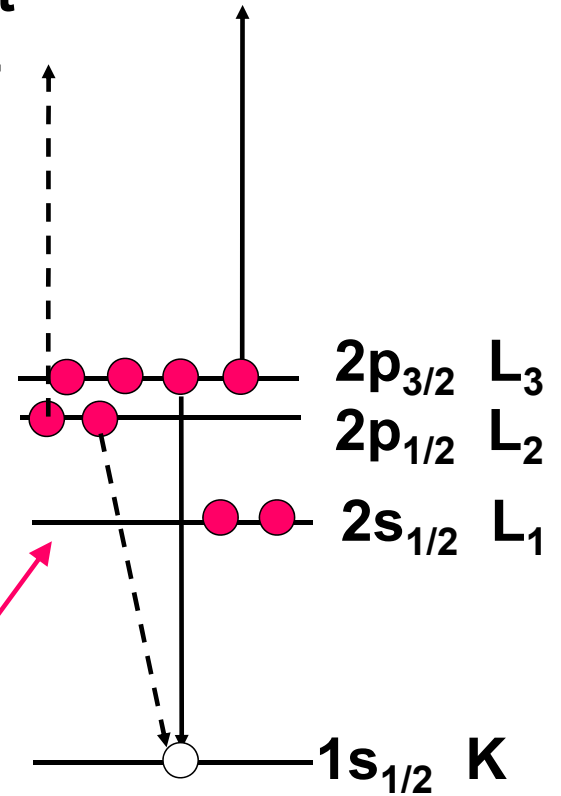
F: $Z = 9$

Plus see pp. 92-93 in
"Basic Concepts of XPS"

PRINCIPAL AUGER ELECTRON ENERGIES



X-Ray Data Booklet Fig. 1.4



$$\begin{aligned}
 \text{K.E.} &\approx \text{B.E.}_{1s}^{Z=8} - \text{B.E.}_{2p}^9 - \text{B.E.}_{2p}^8 \\
 &\approx \text{B.E.}_{1s}^8 + \text{B.E.}_{2p}^8 - \text{B.E.}_{2p}^9 \\
 &\approx 543.1 - 17 - 13 \approx \mathbf{513 \text{ eV}}
 \end{aligned}$$

X-Ray Data Booklet--Section 1.1 ELECTRON BINDING ENERGIES

The energies are given in eV relative to the vacuum level for the rare gases and for H₂, N₂, O₂, F₂, and Cl₂; relative to the Fermi level for the metals; and relative to the top of the valence bands for semiconductors (and insulators).

Electronic configuration	Element	K 1s	L ₁ 2s	L ₂ 2p _{1/2}	L ₃ 2p _{3/2}	M ₁ 3s	M ₂ 3p _{1/2}	M ₃ 3p _{3/2}
1s	1 H	13.6						
1s²	2 He	24.6*						
1s² 2s	3 Li	54.7*						
1s² 2s²	4 Be	111.5*						
1s² 2s² 2p	5 B	188*						
1s² 2s² 2p²	6 C	284.2*						
1s² 2s² 2p³	7 N	409.9*	37.3*	~ 9	~ 9			
1s² 2s² 2p⁴	8 O	543.1*	41.6*	~ 13	~ 13			
1s² 2s² 2p⁵	9 F	696.7*	~ 45	~ 17	~ 17			
1s² 2s² 2p⁶	10 Ne	870.2*	48.5*	21.7*	21.6*			
[Ne] 3s	11 Na	1070.8†	63.5†	30.65	30.81			
[Ne] 3s²	12 Mg	1303.0†	88.7	49.78	49.50			
[Ne] 3s² 3p	13 Al	1559.6	117.8	72.95	72.55			
[Ne] 3s² 3p²	14 Si	1839	149.7*b	99.82	99.42			
[Ne] 3s² 3p³	15 P	2145.5	189*	136*	135*			
[Ne] 3s² 3p⁴	16 S	2472	230.9	163.6*	162.5*			
[Ne] 3s² 3p⁵	17 Cl	2822.4	270*	202*	200*			
[Ne] 3s² 3p⁶	18 Ar	3205.9*	326.3*	250.6†	248.4*	29.3*	15.9*	15.7*
[Ar] 4s	19 K	3608.4*	378.6*	297.3*	294.6*	34.8*	18.3*	18.3*
[Ar] 4s²	20 Ca	4038.5*	438.4†	349.7†	346.2†	44.3 †	25.4†	25.4†
	21 Sc	4492	498.0*	403.6*	398.7*	51.1*	28.3*	28.3*
	22 Ti	4966	560.9†	460.2†	453.8†	58.7†	32.6†	32.6†

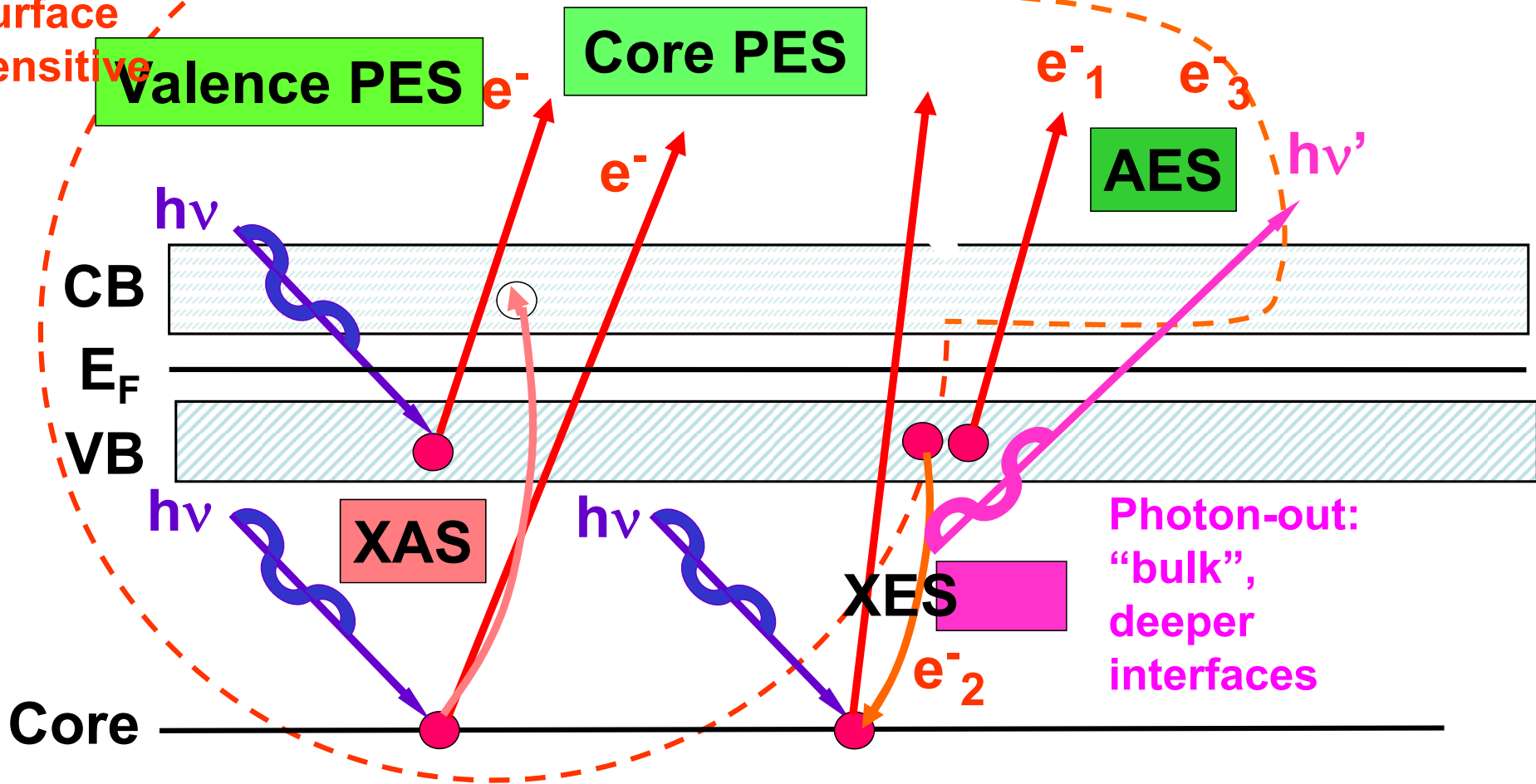


Interpolated, extrapolated

Missing valence B.E.s



The Soft and Hard X-Ray Spectroscopies



PES = photoemission = photoelectron spectroscopy

XAS = x-ray absorption spectroscopy

AES = Auger electron spectroscopy

XES = x-ray emission spectroscopy

REXS/RIXS = resonant elastic/inelastic x-ray scattering

THE AUGER PROCESS

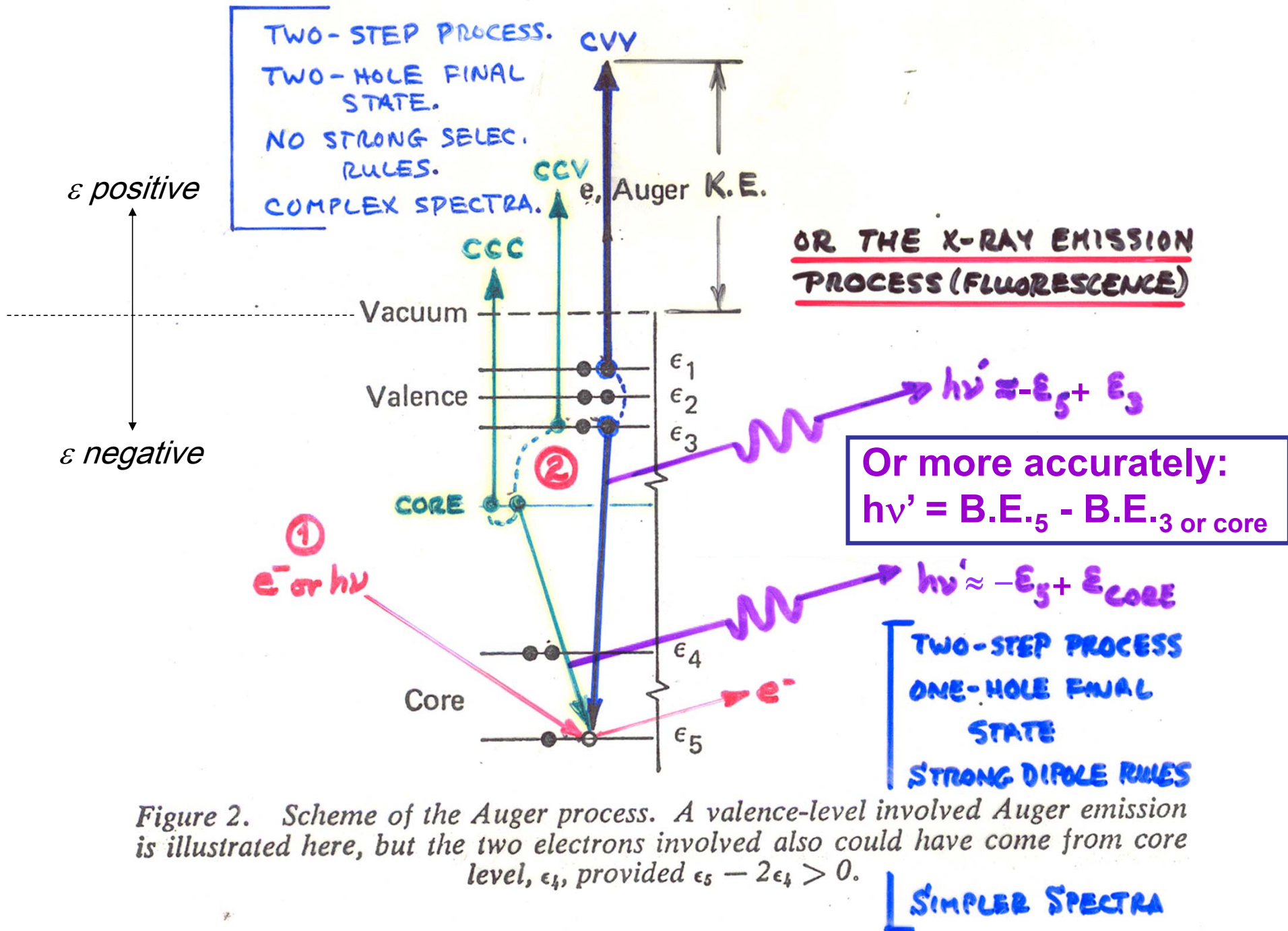
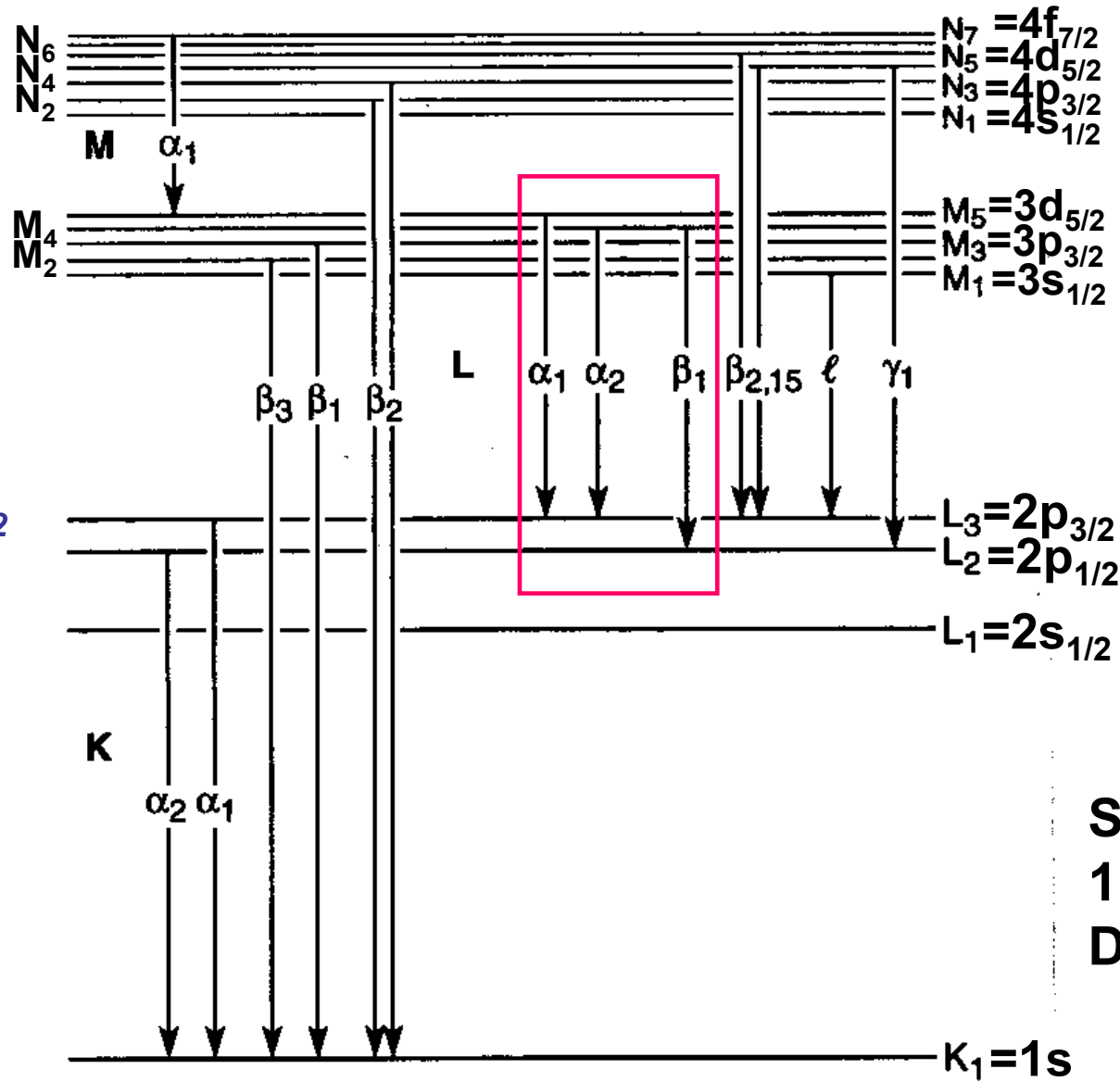


Figure 2. Scheme of the Auger process. A valence-level involved Auger emission is illustrated here, but the two electrons involved also could have come from core level, ϵ_4 , provided $\epsilon_5 - 2\epsilon_4 > 0$.

X-Ray Nomenclature (from "X-Ray Data Booklet")

In general:

$$nl \begin{cases} \text{Spin-}nl_{j=l+1/2} \\ \text{orbit } nl_{j=l-1/2} \end{cases}$$



$$\Delta j = 0, \pm 1$$

See Section 1.2 in "X-Ray Data Booklet"

Fig. 1-1. Transitions that give rise to the emission lines in Table 1-3.

Electron binding energies

Element	K 1s	L ₁ 2s	L ₂ 2p _{1/2}	L ₃ 2p _{3/2}	M ₁ 3s	M ₂ 3p _{1/2}	M ₃ 3p _{3/2}	M ₄ 3d _{3/2}	M ₅ 3d _{5/2}
23 V	5465	626.7†	519.8†	512.1†	66.3†	37.2†	37.2†		
24 Cr	5989	696.0†	583.8†	574.1†	74.1†	42.2†	42.2†		
25 Mn	6539	769.1†	649.9†	638.7†	82.3†	47.2†	47.2†		
26 Fe	7112	844.6†	719.9†	706.8†	91.3†	52.7†	52.7†		
27 Co	7709	925.1†	793.2†	778.1†	101.0†	58.9†	59.9†		
28 Ni	8333	1008.6†	870.0†	852.7†	110.8†	68.0†	66.2†		
29 Cu	8979	1096.7†	952.3†	932.7	122.5†	77.3†	75.1†		
30 Zn	9659	1196.2*	1044.9*	1021.8*	139.8*	91.4*	88.6*	10.2*	10.1*

Diff. = 11.2

Table 1-2. Energies of x-ray emission lines (continued).

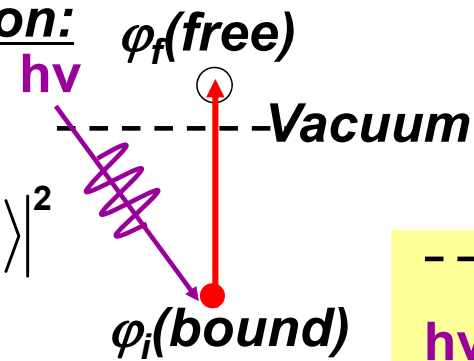
Element	Kα ₁	Kα ₂	Kβ ₁	Lα ₁	Lα ₂	Lβ ₁	Lβ ₂	Lγ ₁	Mα ₁
22 Ti	4,510.84	4,504.86	4,931.81	452.2	452.2	458.4			
23 V	4,952.20	4,944.64	5,427.29	511.3	511.3	519.2			
24 Cr	5,414.72	5,405.509	5,946.71	572.8	572.8	582.8			
25 Mn	5,898.75	5,887.65	6,490.45	637.4	637.4	648.8			
26 Fe	6,403.84	6,390.84	7,057.98	705.0	705.0	718.5			
27 Co	6,930.32	6,915.30	7,649.43	776.2	776.2	791.4			
28 Ni	7,478.15	7,460.89	8,264.66	851.5	851.5	868.8			
29 Cu	8,047.78	8,027.83	8,905.29	929.7	929.7	949.8			
30 Zn	8,638.86	8,615.78	9,572.0	1,011.7	1,011.7	1,034.7			

Diff. = 11.4

See Tables 1.1
and 1.2 in X-Ray
Data Booklet

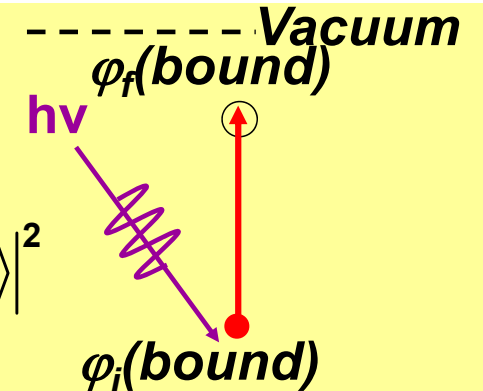
MATRIX ELEMENTS IN The Soft and Hard X-Ray Spectroscopies: DIPOLE LIMIT

- Photoelectron spectroscopy/photoemission:

$$I \propto \left| \hat{\mathbf{e}} \cdot \langle \varphi_f(\mathbf{1}) | \vec{r} | \varphi_i(\mathbf{1}) \rangle \right|^2$$


- Near-edge x-ray absorption:

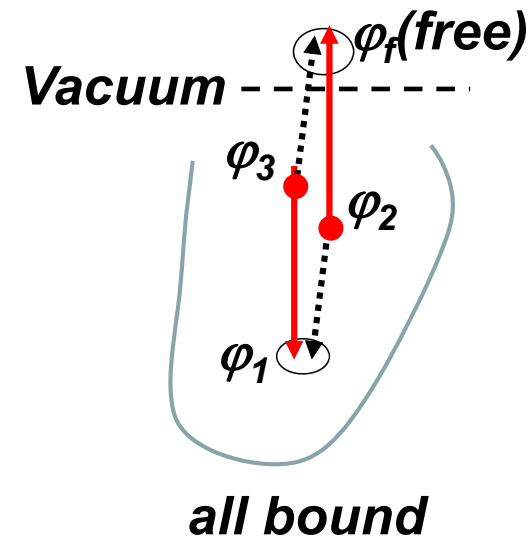
$$I \propto \left| \hat{\mathbf{e}} \cdot \langle \varphi_f(\mathbf{1}) | \vec{r} | \varphi_i(\mathbf{1}) \rangle \right|^2$$



- Auger electron emission:

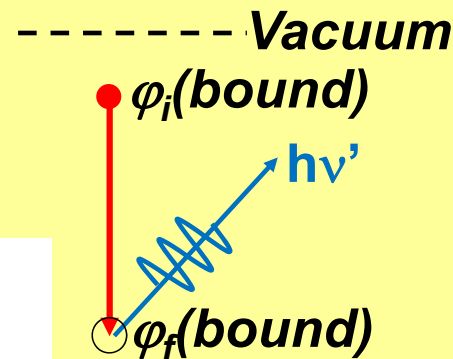
$$I \propto \left| \langle \varphi_f(\mathbf{1})\varphi_1(\mathbf{2}) | \frac{e^2}{r_{12}} | \varphi_3(\mathbf{1})\varphi_2(\mathbf{2}) \rangle - \langle \varphi_1(\mathbf{1})\varphi_f(\mathbf{2}) | \frac{e^2}{r_{12}} | \varphi_3(\mathbf{1})\varphi_2(\mathbf{2}) \rangle \right|^2$$

Direct Exchange



- X-ray emission:

$$I \propto \left| \hat{\mathbf{e}} \cdot \langle \varphi_f(\mathbf{1}) | \vec{r} | \varphi_i(\mathbf{1}) \rangle \right|^2$$



1.3 FLUORESCENCE YIELDS FOR K AND L SHELLS

Jeffrey B. Kortright

Fluorescence yields for the *K* and *L* shells for the elements $5 \leq Z \leq 110$ are plotted in Fig. 1-2; the data are based on Ref. 1. These yields represent the probability of a core hole in the *K* or *L* shells being filled by a radiative process, in competition with nonradiative processes. Auger processes are the only nonradiative processes competing with fluorescence for the *K* shell and

Fluorescence yield \equiv FY

FY = probability of radiative decay \rightarrow x-ray emission)

1 - FY = probability of non-radiative decay \rightarrow Auger electron emission

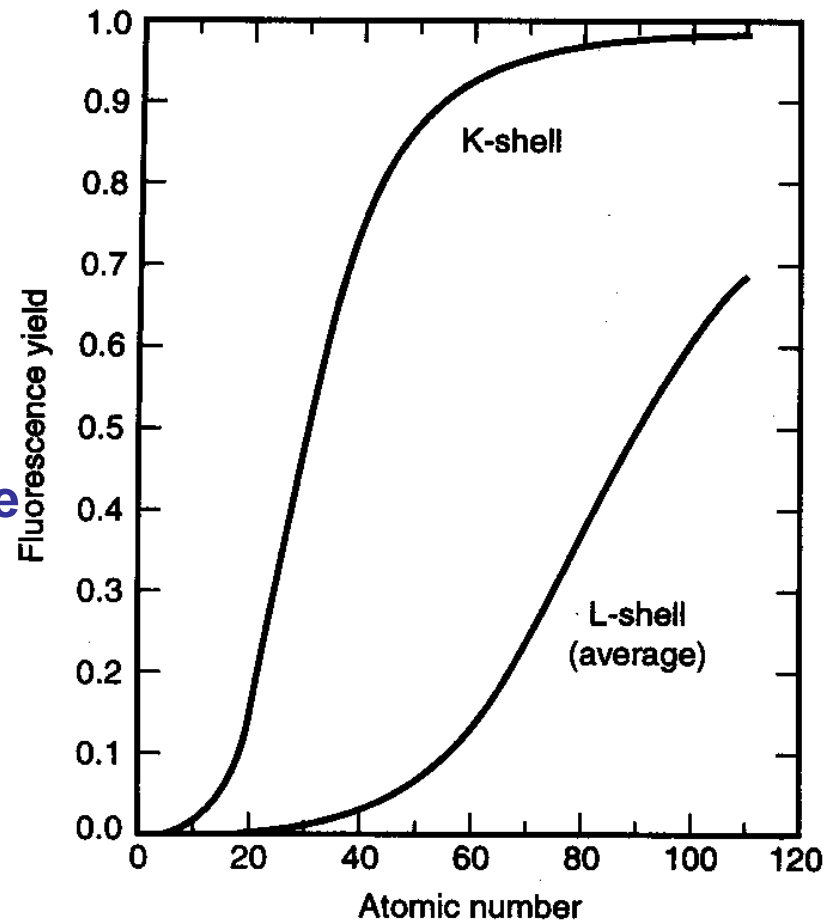
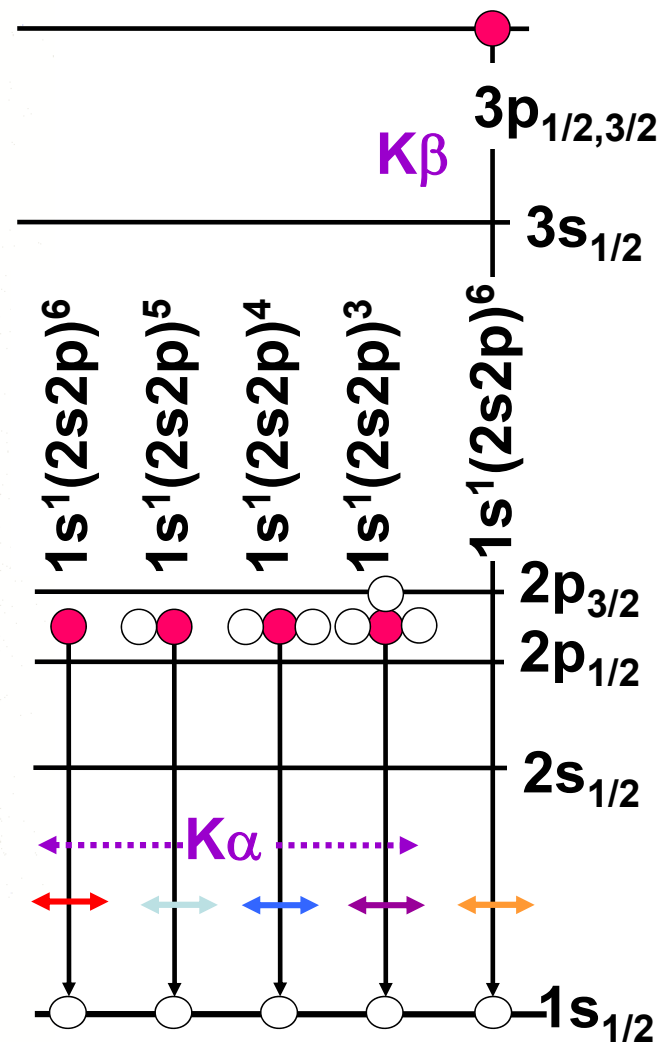
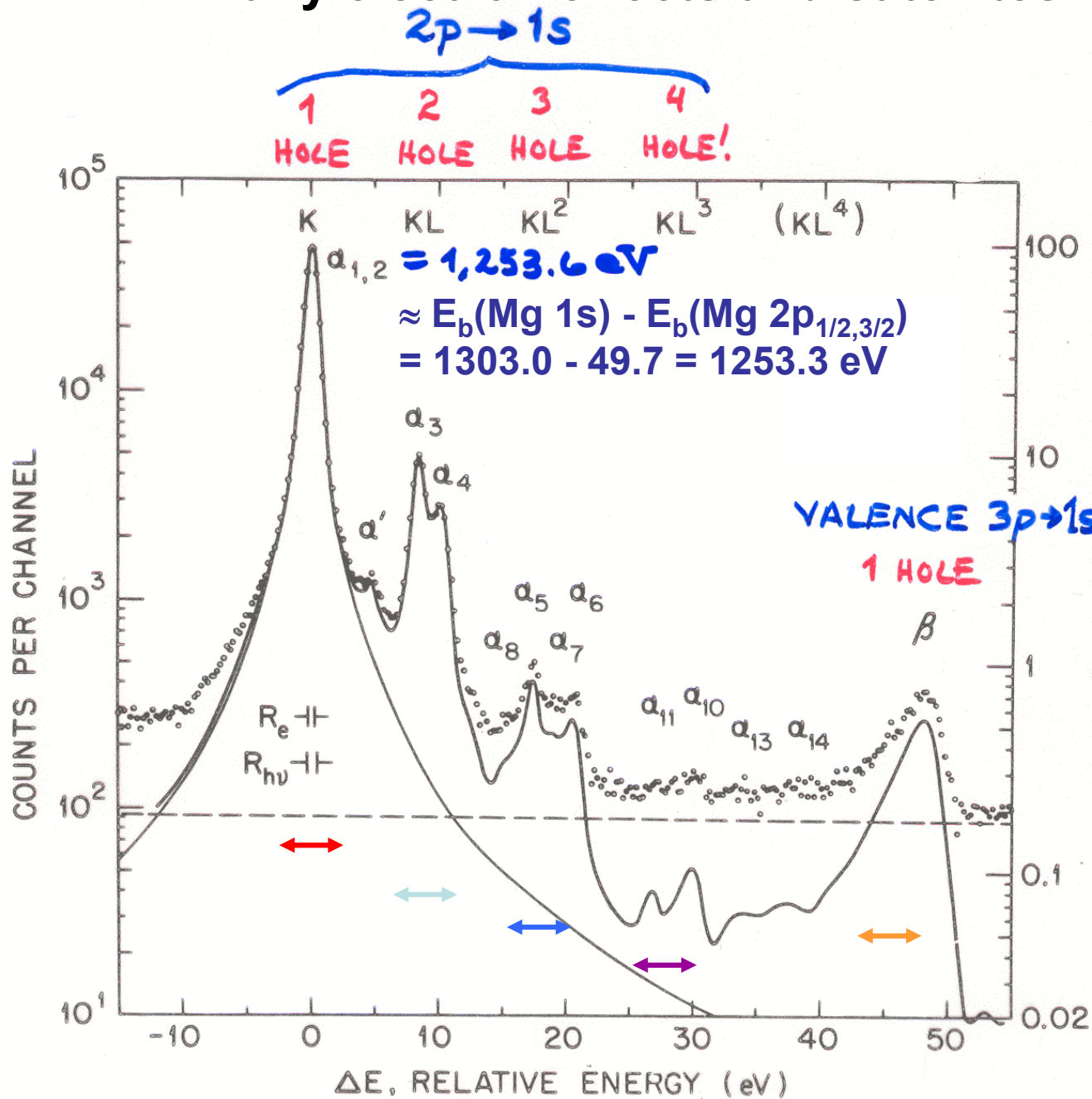


Fig. 1-2. Fluorescence yields for *K* and *L* shells for 110. The plotted curve for the *L* shell represents average of *L*₁, *L*₂, and *L*₃ effective yields

Many electron effects and satellites in x-ray emission



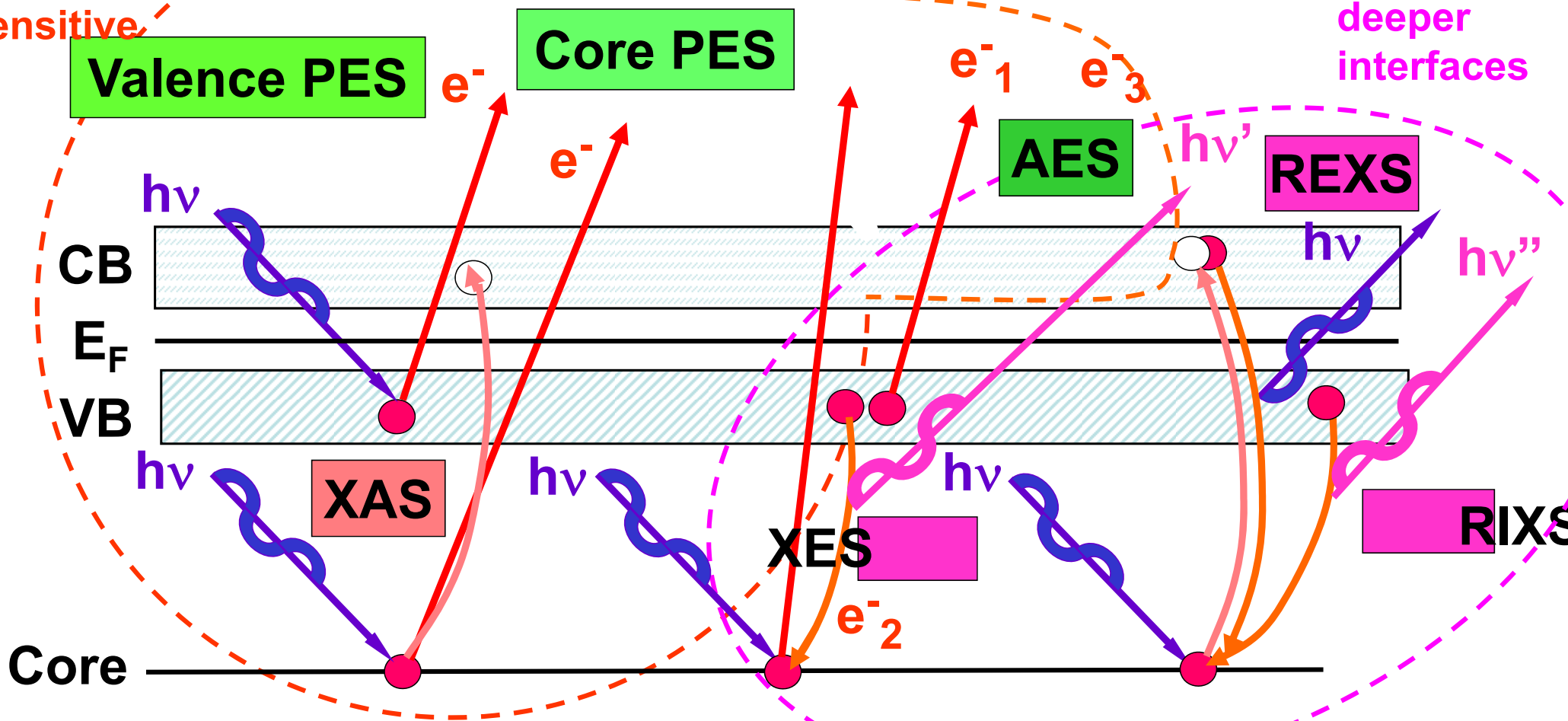
Mg K series of x-rays:
 atomic no. = 12
 Fluorescence Yield ≈ 0.03

A STANDARD LABORATORY X-RAY SOURCE

The Soft and Hard X-Ray Spectroscopies

Electron-out:
surface sensitive

Photon-out:
"bulk",
deeper
interfaces



PES = photoemission = photoelectron spectroscopy

XAS = x-ray absorption spectroscopy

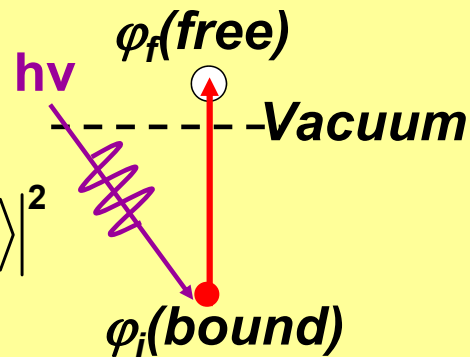
AES = Auger electron spectroscopy

XES = x-ray emission spectroscopy

REXS/RIXS = resonant elastic/inelastic x-ray scattering

MATRIX ELEMENTS IN The Soft and Hard X-Ray Spectroscopies: RESONANT EFFECTS

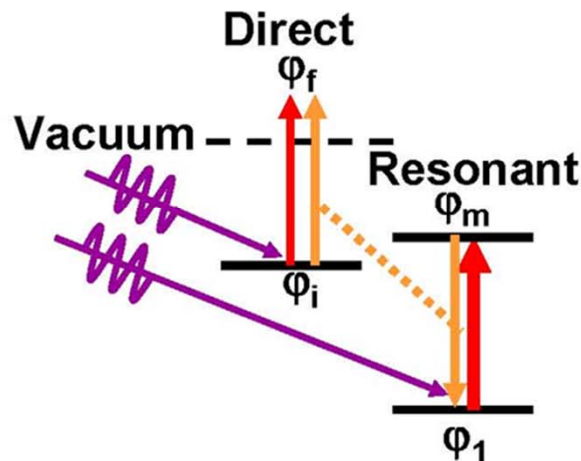
- **Non-resonant photoemission:**

$$I \propto \left| \hat{\mathbf{e}} \cdot \langle \varphi_f(\mathbf{1}) | \vec{r} | \varphi_i(\mathbf{1}) \rangle \right|^2$$


- **Resonant photoemission:**

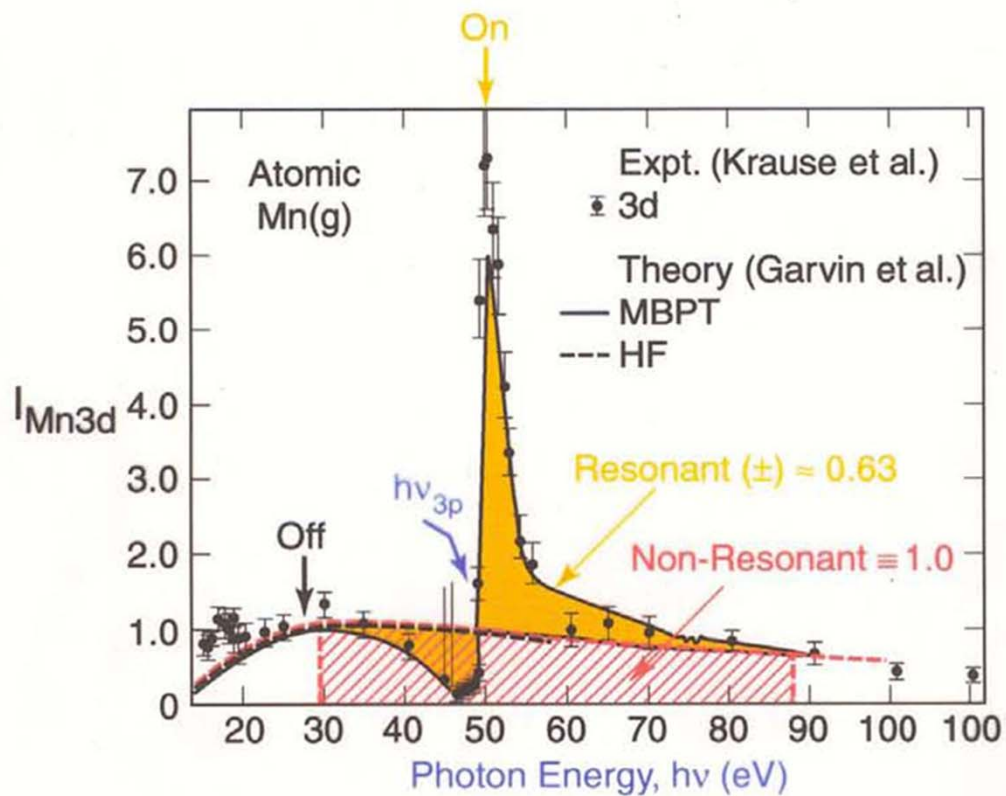
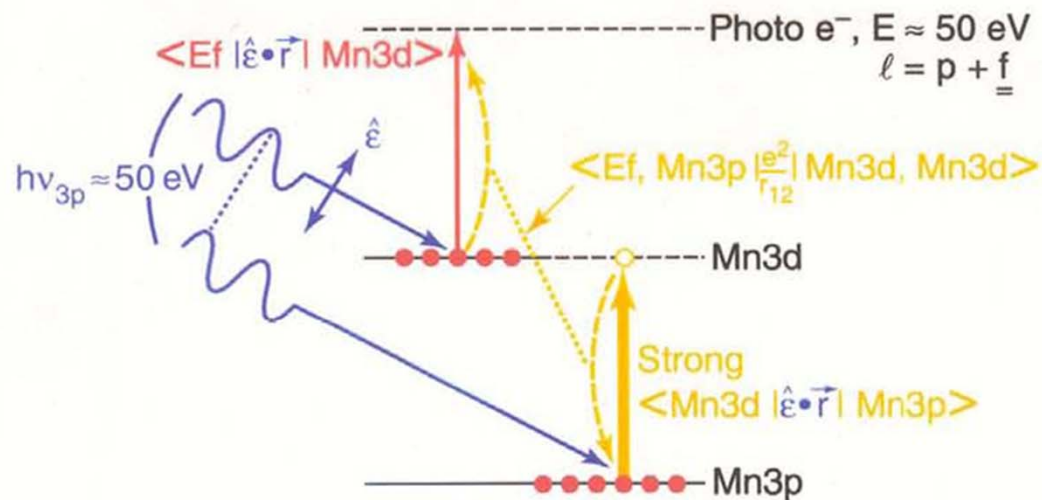
$$I \propto \left| \langle \varphi_f(\mathbf{1}) | \hat{\mathbf{e}} \cdot \vec{r} | \varphi_i(\mathbf{1}) \rangle + \sum_m \langle \varphi_f(\mathbf{1}) \varphi_1(\mathbf{2}) | \frac{e^2}{r_{12}} | \varphi_i(\mathbf{1}) \varphi_m(\mathbf{2}) \rangle \langle \varphi_m(\mathbf{1}) | \hat{\mathbf{e}} \cdot \vec{r} | \varphi_1(\mathbf{1}) \rangle \right|^2$$

$$\times \delta(h\nu - (E_m - E_1))$$



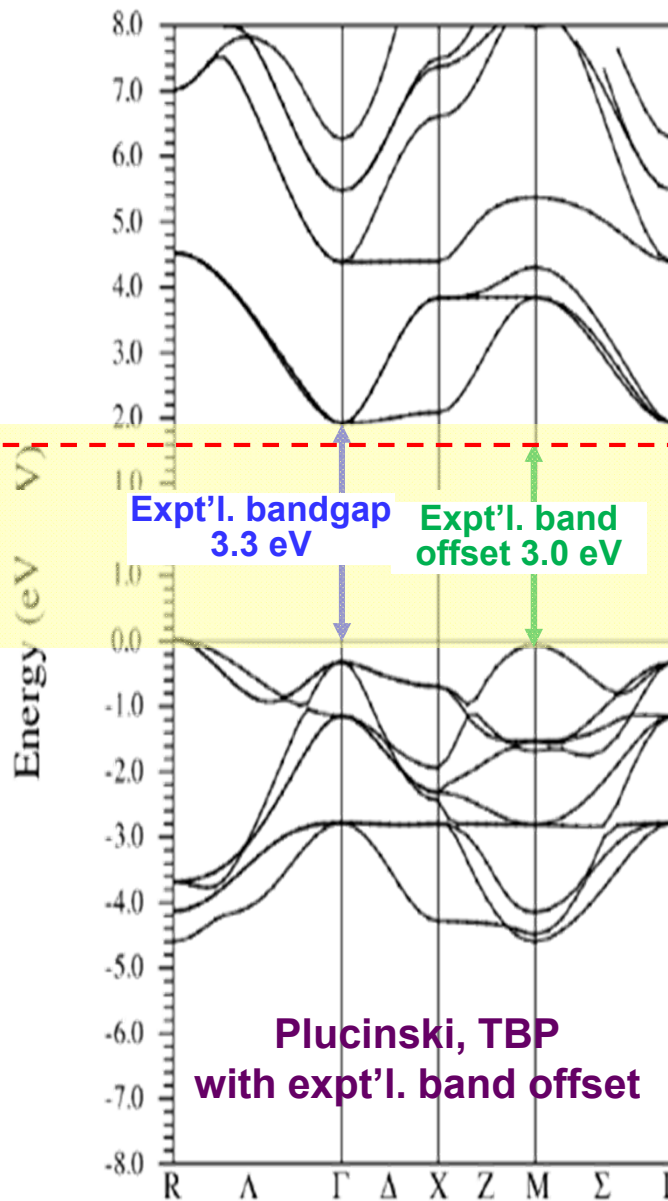
Single-atom resonant photoemission:

Ex. – Mn atom: Mn3d emission, resonance with Mn3p

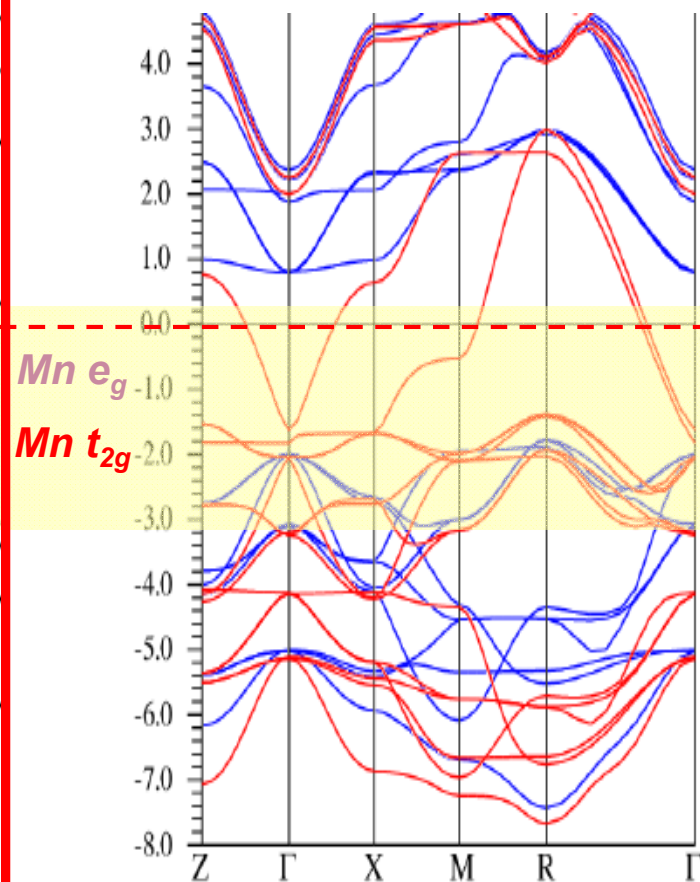


SrTiO₃ and La_{0.67}Sr_{0.33}MnO₃ band structures and DOS

SrTiO₃-band insulator



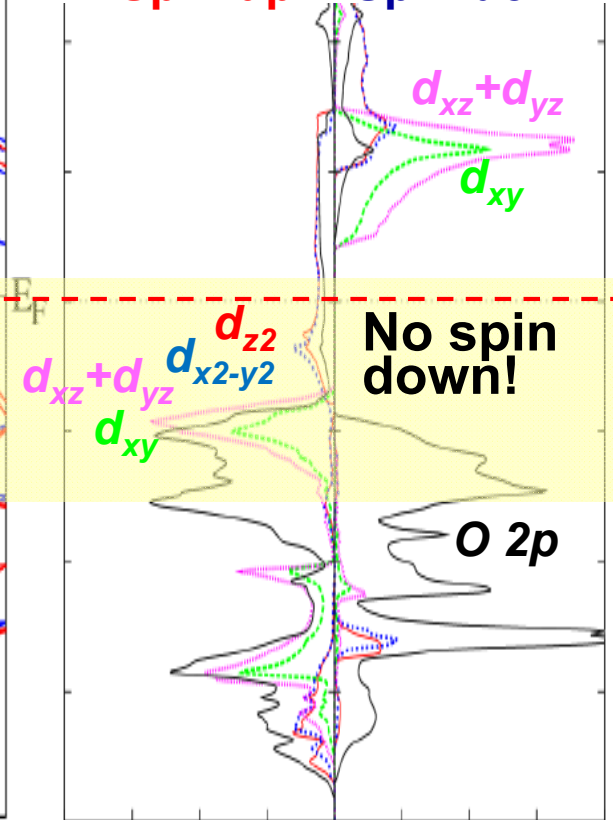
La_{0.67}Sr_{0.33}MnO₃- Half-Metallic Ferromagnet



Chikamatsu et al.,
PRB 73, 195105 (2006);
Plucinski, TBP

Projected DOSs

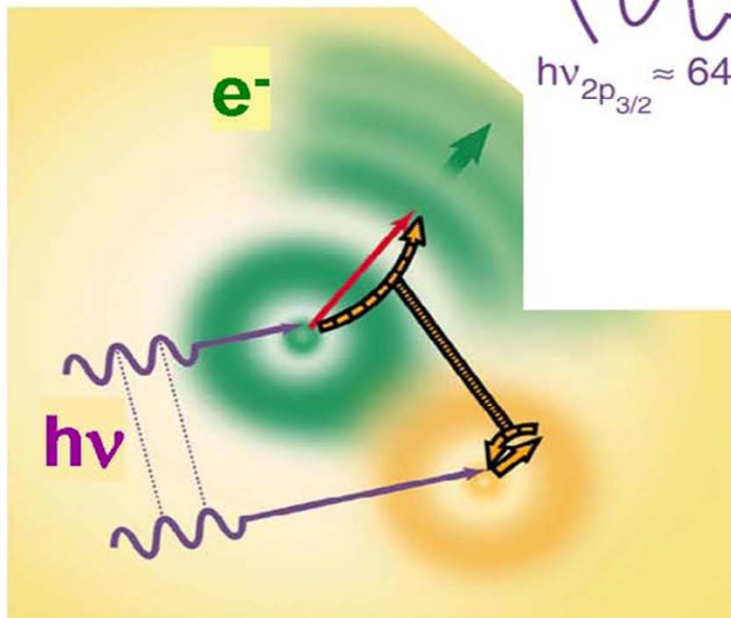
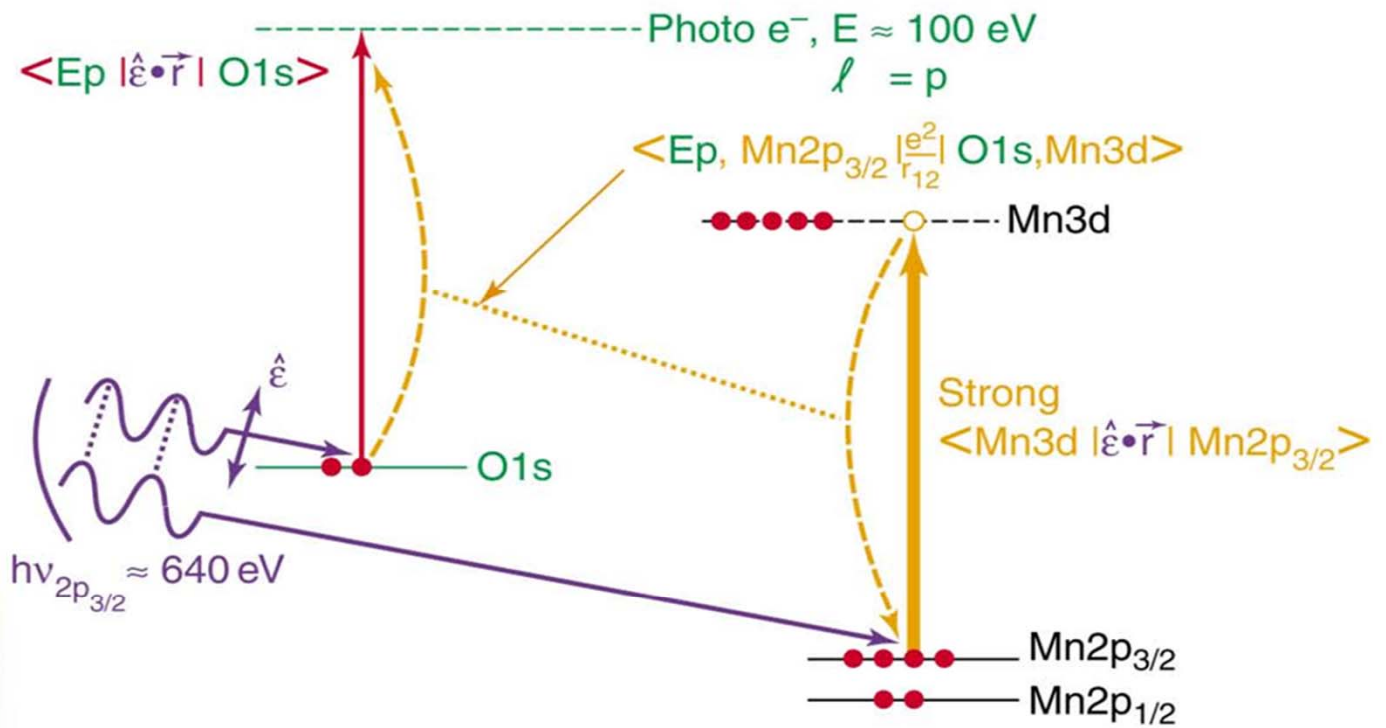
Spin-up Spin-down



Zheng, Binggeli, J. Phys.
Cond. Matt. 21, 115602 (2009)
Plucinski, TBP

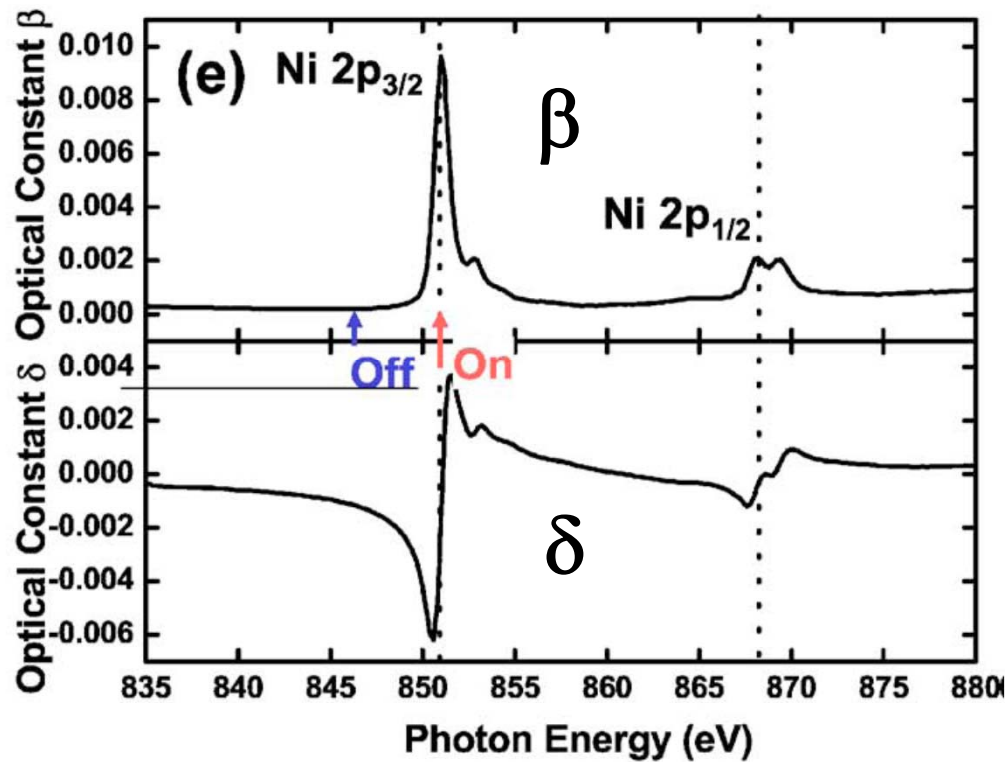
Multi-Atom Resonant Photoemission

Ex. – MnO(001): O1s emission, resonance with Mn2p_{3/2}

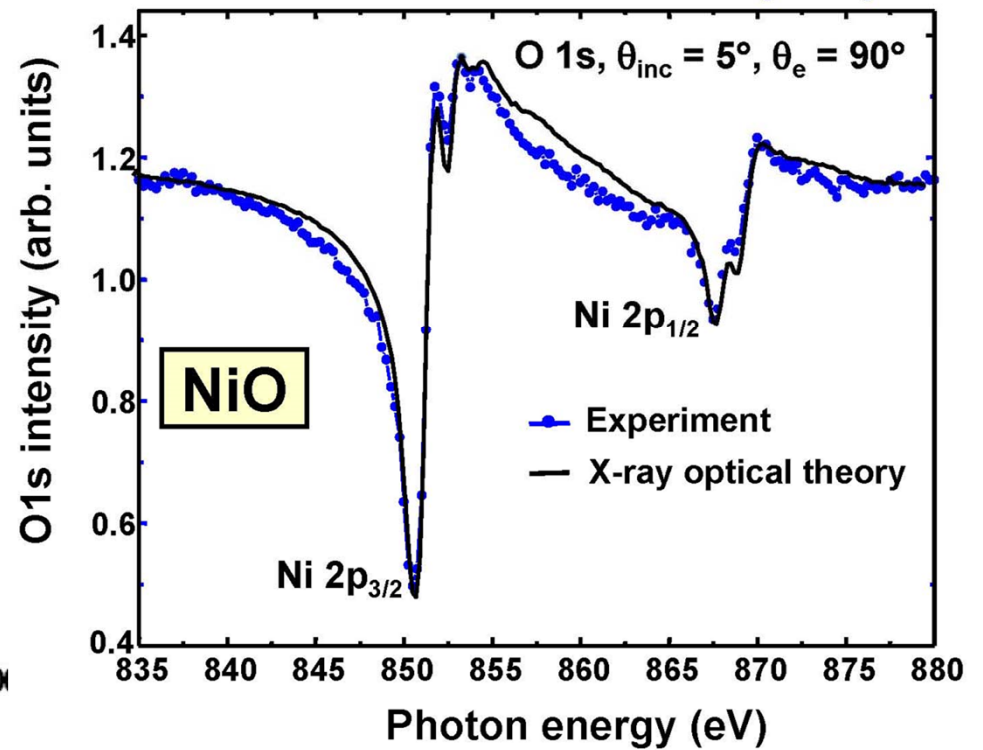


Kay et al.,
Science 281, 679 ('98);
Corrected picture in
PRB 61, 5119 ('01)←

Index of refraction over
Ni 2p resonances in NiO



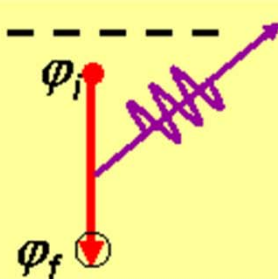
Multi-Atom Resonant Photoemission—
O 1s emission from NiO(001)



MATRIX ELEMENTS IN The Soft and Hard X-Ray Spectroscopies: RESONANT EFFECTS

- X-ray emission:

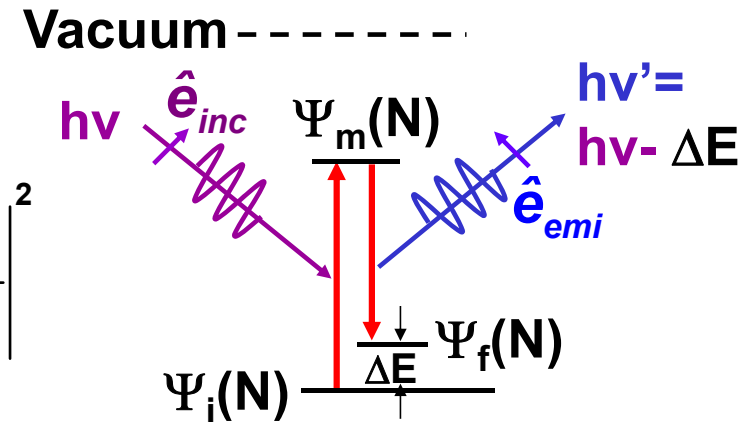
$$I \propto |\hat{\mathbf{e}} \cdot \langle \varphi_f(\mathbf{1}) | \vec{r} | \varphi_i(\mathbf{1}) \rangle|^2$$



- Resonant inelastic x-ray scattering:

$$I \propto \sum_f \left| \sum_m \frac{\langle \Psi_f(N) | \hat{\mathbf{e}}_{emi} \cdot \vec{r} | \Psi_m(N) \rangle \langle \Psi_m(N) | \hat{\mathbf{e}}_{inc} \cdot \vec{r} | \Psi_i(N) \rangle}{h\nu + E_i(N) - E_m(N) - i\Gamma_m} \right|^2$$

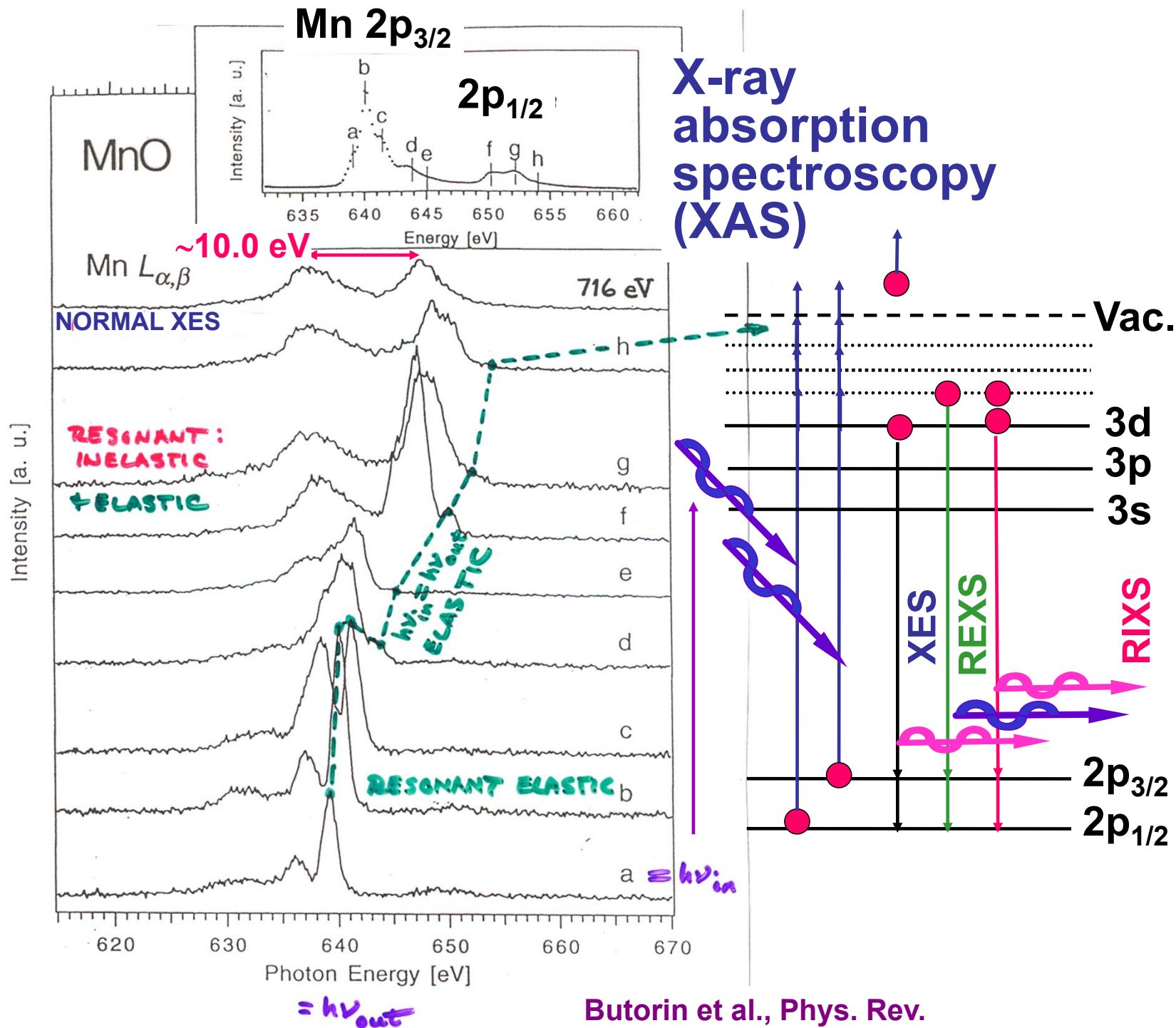
$$\times \delta(h\nu - (E_m(N) - E_i(N)))$$



$$N_m(t) = N_m(0) e^{-\frac{2\Gamma_m t}{\hbar}} = N_m(0) e^{-\frac{t}{T_{lifetime}}}$$

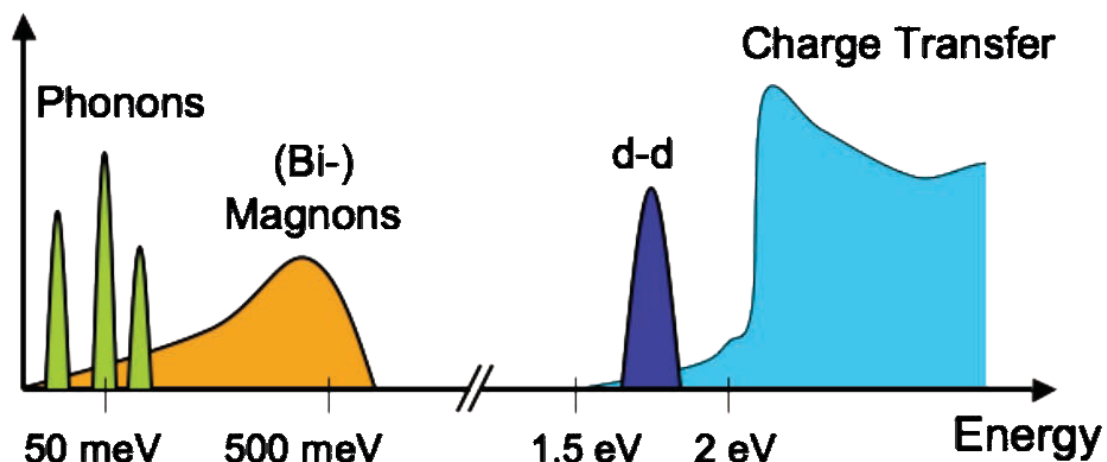
X-ray fluorescence spectroscopy = X-ray emission spectroscopy (XES) and Resonant inelastic x-ray scattering (RIXS)

Resonant inelastic x-ray scattering (RIXS) and Resonant elastic x-ray scattering (REXS)

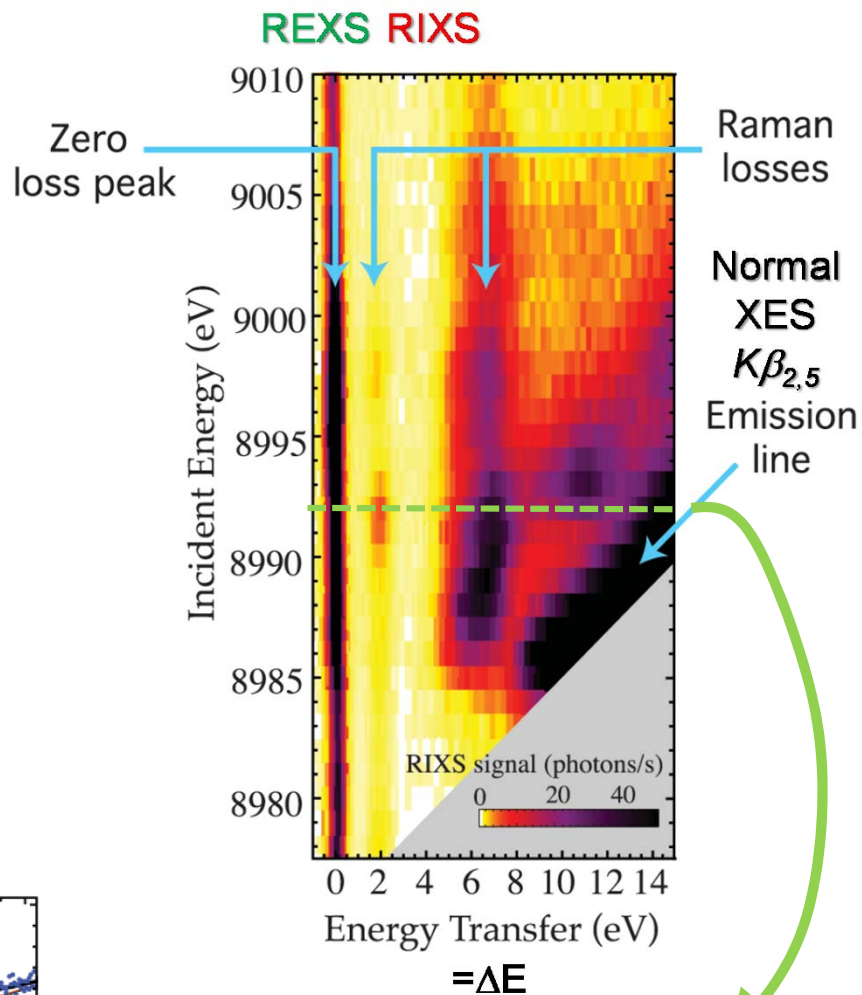


Butorin et al., Phys. Rev. B 54, 4405 ('96)

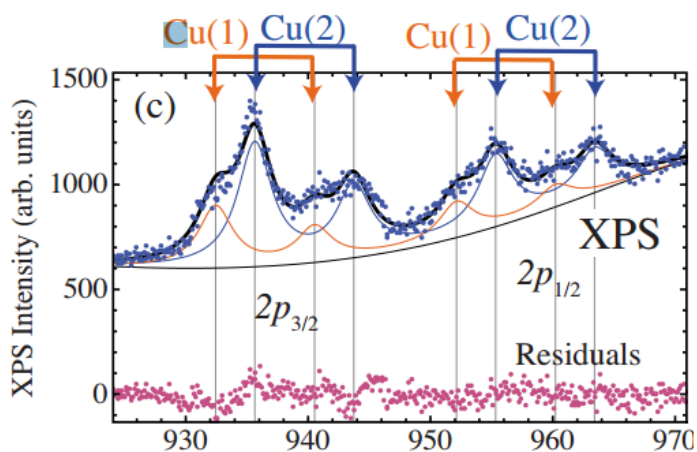
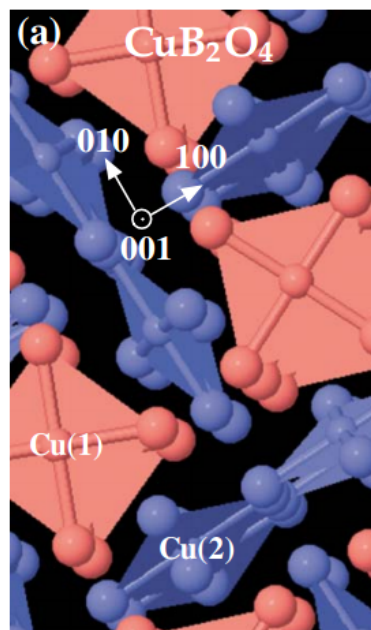
Excitations probed by RIXS



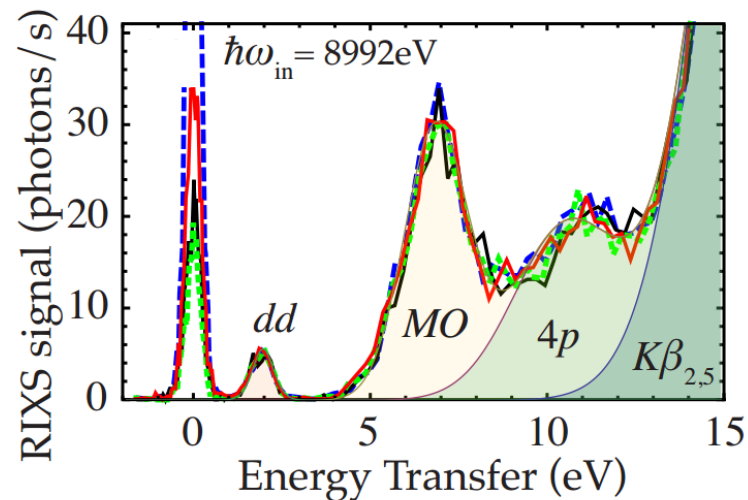
Aments et al., Rev. Mod. Phys. 83, 705 (2011)



Example: CuB_2O_4 plaquettes



Hancock et al., Phys. Rev. B 80, 092509 (2009)



The Soft and Hard X-Ray Spectroscopies

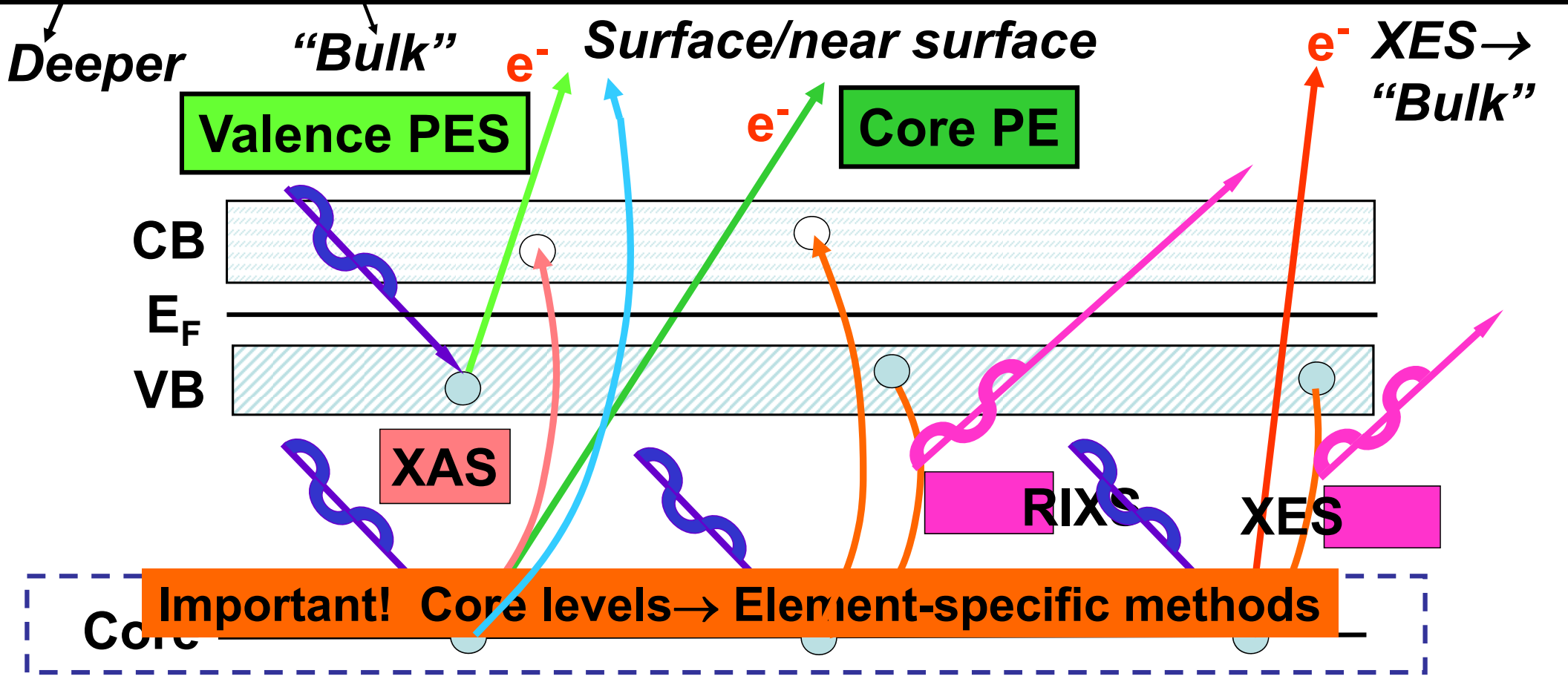
EXAFS
Atomic structure

XAS
unoccupied DOS
(2° e- and hv
Detection)

Valence PES -
band struct.,
quasipart. exc.,
DOS, spin pol.

Core PES -
stoichiometry
BE shifts
splittings, MCD
spin polarization
diffraction

XES, RIXS -
band structure,
partial DOS,
d-d/other
excitations



The five ways in which x-rays interact with matter:

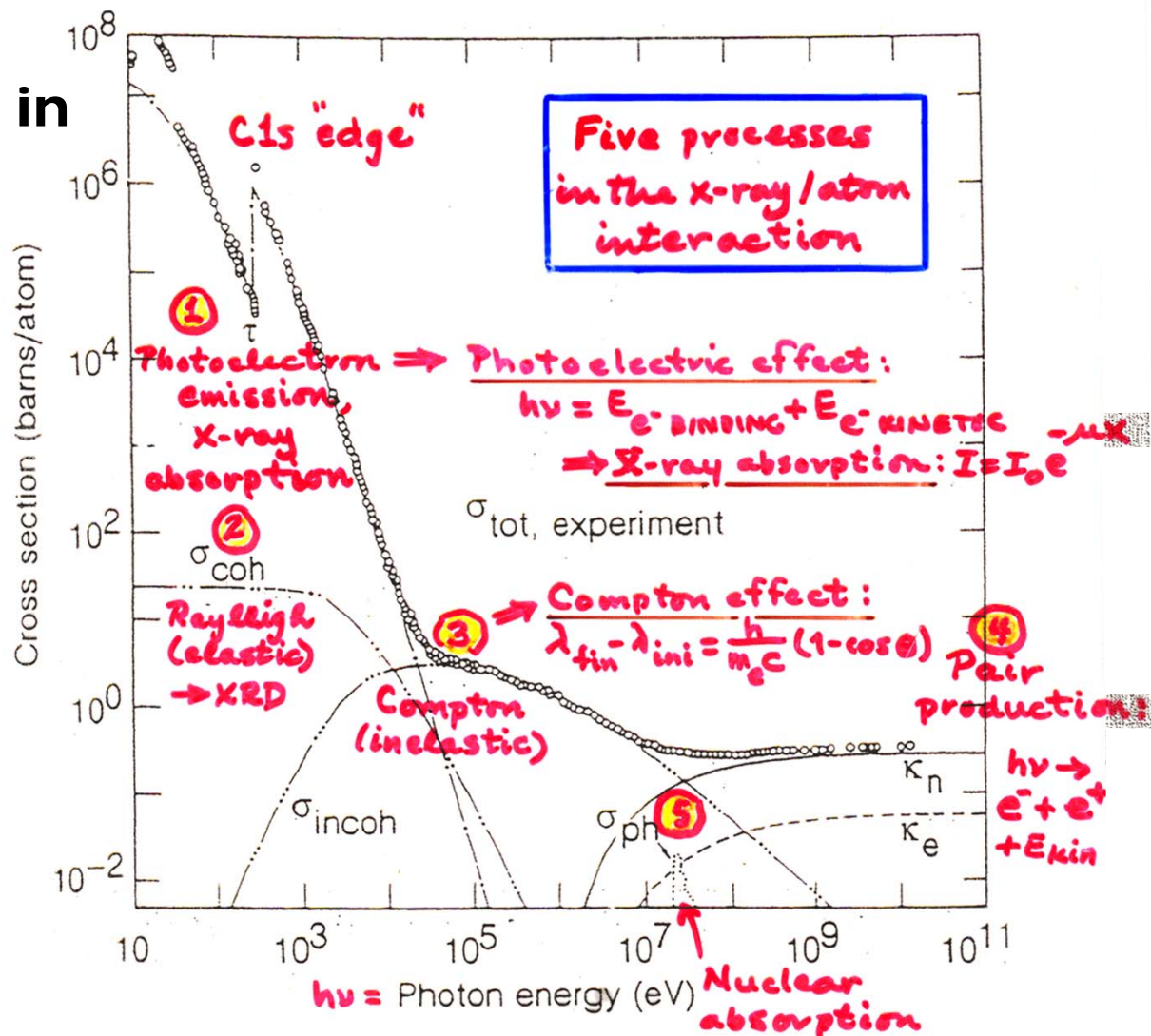


Fig. 3-1. Total photon cross section σ_{tot} in carbon, as a function of energy, showing the contributions of different processes: τ , atomic photo-effect (electron ejection, photon absorption); σ_{coh} , coherent scattering (Rayleigh scattering—atom neither ionized nor excited); σ_{incoh} , incoherent scattering (Compton scattering off an electron); κ_n , pair production, nuclear field; κ_e , pair production, electron field; σ_{ph} , photonuclear absorption (nuclear absorption usually followed by emission of a neutron or other particle). (From Ref. 3; figure courtesy of J. H. Hubbell.)

LBNL Center for X-Ray Optics
 "X-Ray Data Booklet"
 Section 3.1
<http://cxro.lbl.gov/x-ray-data-booklet>

A LITTLE X-RAY OPTICS

Index of refraction = $n = 1 - \delta - i\beta$

(Sometimes with + signs on δ and/or β)

$\delta = +$ no. = refractive decrement $\ll 1$

(Sometimes changes sign through absorption resonances)

$\beta = +$ no. = absorptive decrement $\ll 1$

δ and β linked by Kramers-Kronig transform

(See next page)

n also = $1 - (r_e/2\pi)\lambda_{hv}^{-2}\sum n_i f_i$ (0=fwd. scatt.)

r_e = classical electron radius

= $e^2/4\pi\epsilon_0 m_e e^2 = 2.817 \times 10^{-15}$ m

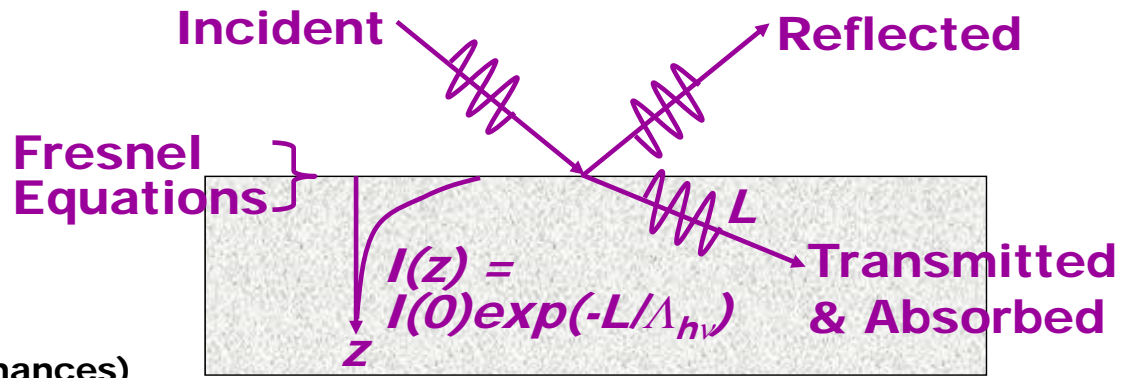
λ_{hv} = x-ray wavelength

n_i = no. i atoms per unit volume

f_i = x-ray scattering factor for i th type of atom, in forward direction

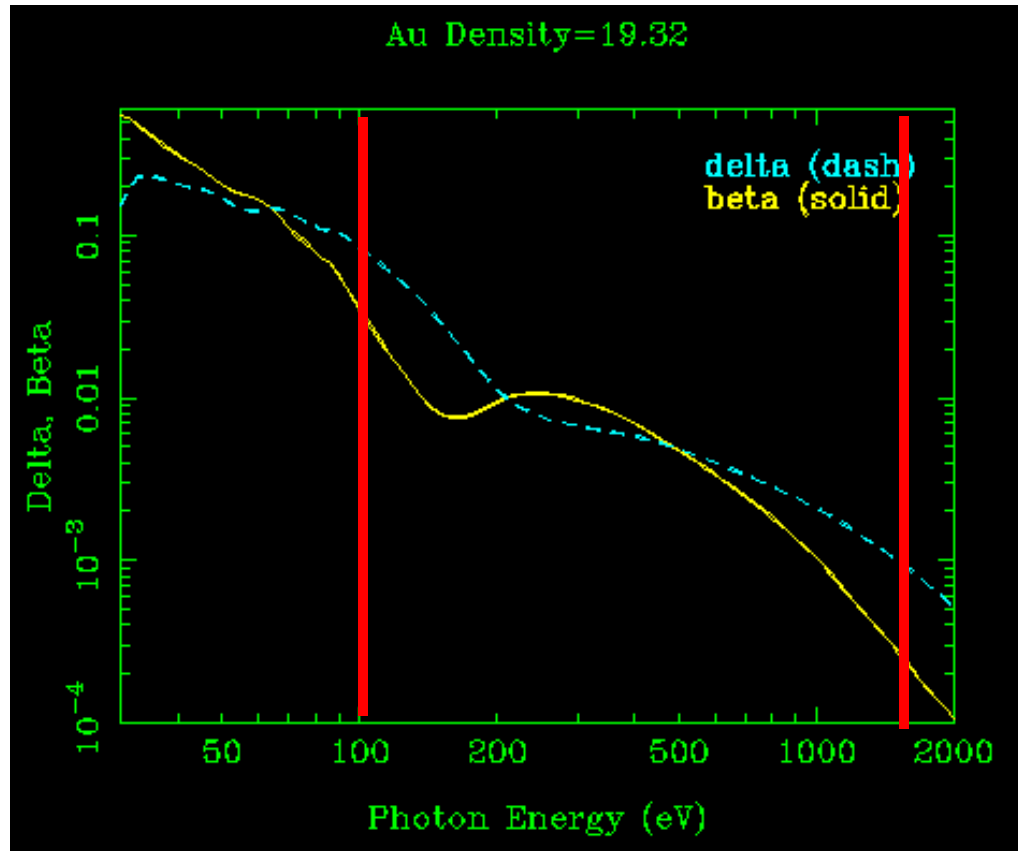
Exponential absorption length = $l_{abs} = \lambda_{hv}/(4\pi\beta) = \Lambda_{hv}$

θ_{CRIT} = critical grazing angle at which reflectivity begins ($R \approx 0.20$) = $[2\delta]^{0.5}$



Online data and calculations excluding resonant behavior at:

http://henke.lbl.gov/optical_constants/getdb2.html



Sections 1.6 and 1.7 of X-Ray Data Booklet

1.7 ATOMIC SCATTERING FACTORS

Eric M. Gullikson

The optical properties of materials in the photon energy range above about 30 eV can be described by the atomic scattering factors. The index of refraction of a material is related to the scattering factors of the individual atoms by

$$n = 1 - \delta - i\beta = 1 - \frac{r_e}{2\pi} \lambda^2 \sum_i n_i f_i(0) \quad (1)$$

where r_e is the classical electron radius, λ is the wavelength, and n_i is the number of atoms per unit volume. The parameters δ and β are called the refractive index decrement and the absorption index, respectively. The complex atomic scattering factor for the forward scattering direction is

$$f(0) = f_1 + if_2 \quad (2)$$

The imaginary part is derived from the atomic photoabsorption cross section:

$$f_2 = \frac{\sigma_a}{2r_e\lambda} \quad (3)$$

The real part of the atomic scattering factor is related to the imaginary part by the Kramers-Kronig dispersion relation:

$$f_1 = Z^* + \frac{1}{\pi r_e h c} \int_0^\infty \frac{\varepsilon^2 \sigma_a(\varepsilon)}{E^2 - \varepsilon^2} d\varepsilon \quad (4)$$

In the high-photon-energy limit, f_1 approaches Z^* , which differs from the atomic number Z by a small relativistic correction:

$$Z^* = Z - (Z/82.5)^{2.37} \quad (5)$$

Sections 1.6 and 1.7 of X-Ray Data Booklet Plus the "Bible" of Soft X-Ray Optics: Henke, Gullikson, Davis, Atomic and Nuclear Data Tables 54, 181-342 (1993)

www.cxro.lbl.gov/optical_constants/]. The mass absorption coefficient μ (cm²/g) is related to the transmitted intensity through a material of density ρ (g/cm³) and thickness d by

$$I = I_0 e^{-\mu \rho d} \quad (1)$$

Thus, the linear absorption coefficient is μ_ℓ (cm⁻¹) = $\mu\rho$. For a pure material, the mass absorption coefficient is directly related to the total atomic absorption cross section σ_a (cm²/atom) by

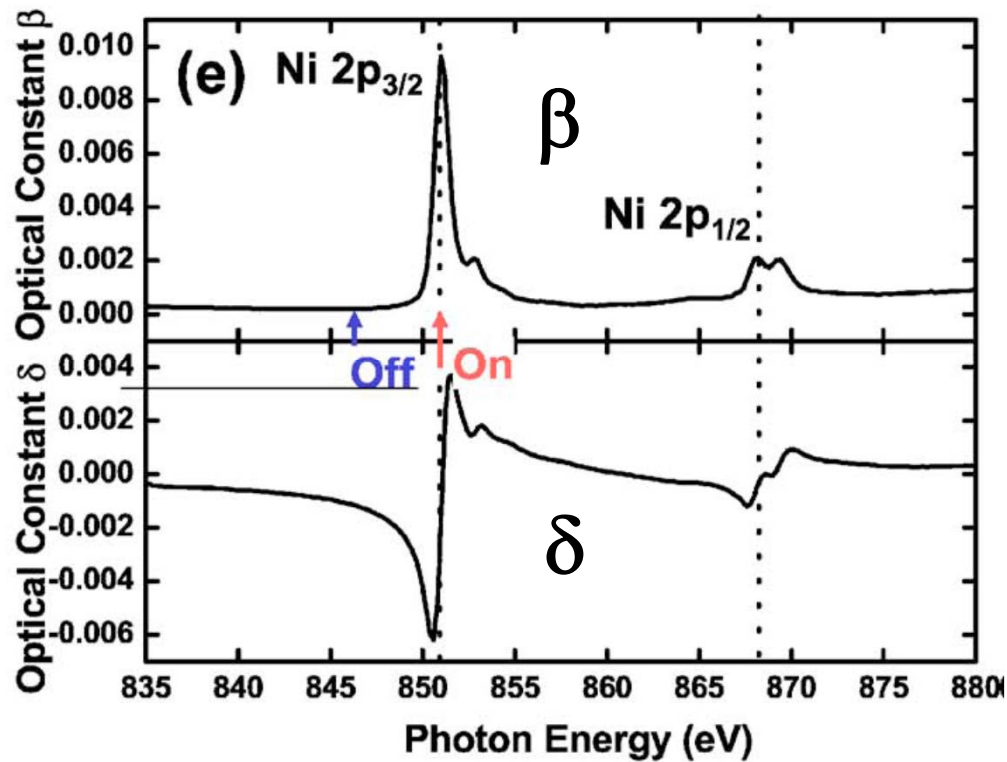
$$\mu = \frac{N_A}{A} \sigma_a \quad (2)$$

where N_A is Avogadro's number and A is the atomic weight. For a compound material, the mass absorption coefficient is obtained from the sum of the absorption cross sections of the constituent atoms by

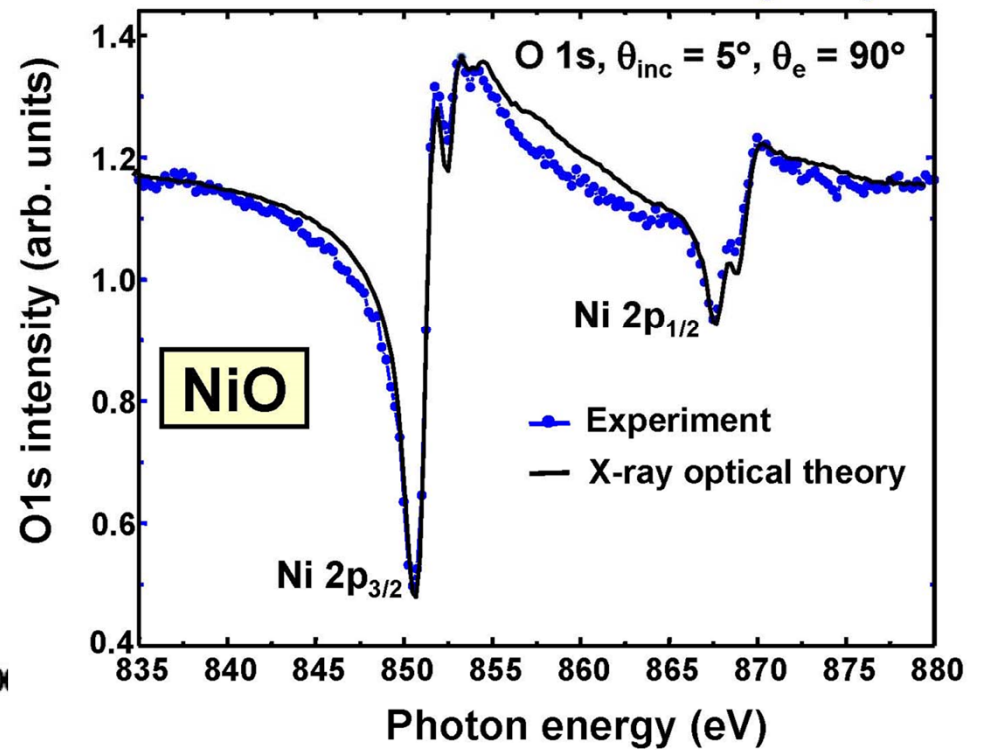
$$\mu = \frac{N_A}{MW} \sum_i x_i \sigma_{ai} \quad (3)$$

where the molecular weight of a compound containing x_i atoms of type i is $MW = \sum_i x_i A_i$. This approximation, which neglects interactions among the atoms in the material, is generally applicable for photon energies above about 30 eV and sufficiently far from absorption edges.

Index of refraction over
Ni 2p resonances in NiO



Multi-Atom Resonant Photoemission—
O 1s emission from NiO(001)



SOME X-RAY OPTICAL EFFECTS: REDUCED PENETRATION DEPTHS AND INCREASED REFLECTIVITY AT GRAZING INCIDENCE ANGLES

θ_{CRIT} = Grazing angle at which reflectivity begins ($R \approx 0.20$)
 $= [2\delta]^{0.5}$

Regardless of energy, in total reflection the mean depth of x-ray penetration shrinks to nm range

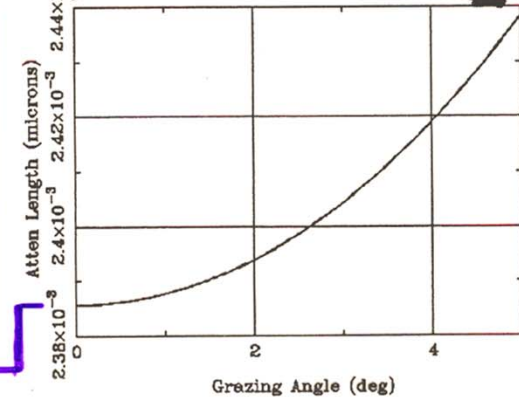
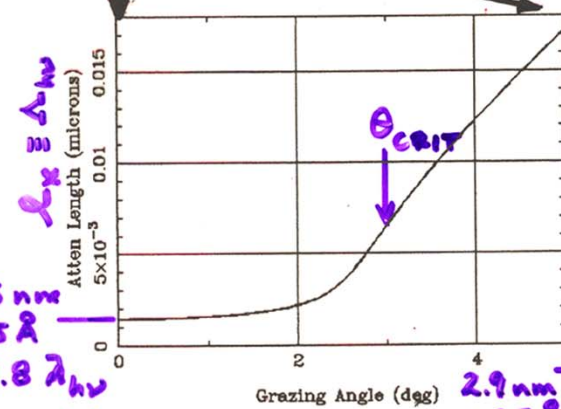
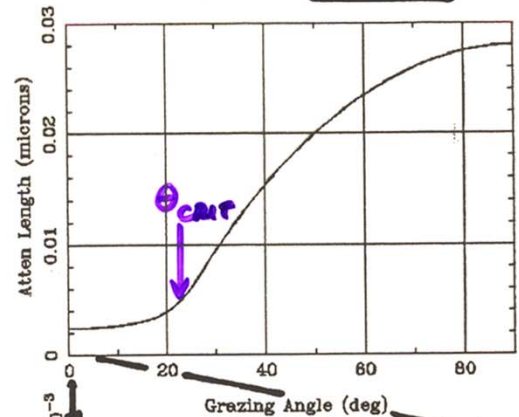
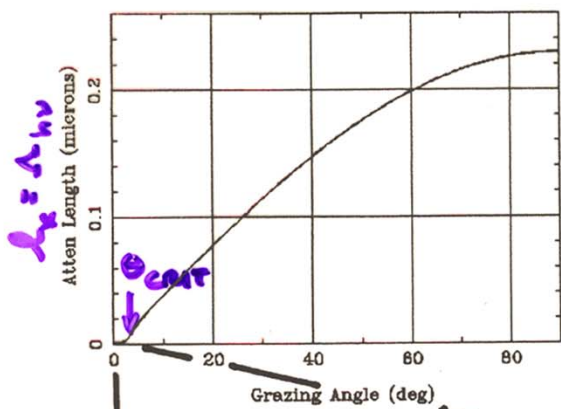
Calculated online from:
http://henke.lbl.gov/optical_constants/atten2.html

ENHANCED SURFACE SENSITIVITY @ GRAZING INCIDENCE



X-Ray Attenuation Length
 Au Density=19.32, Energy=1487.eV

X-Ray Attenuation Length
 Au Density=19.32, Energy=100.eV

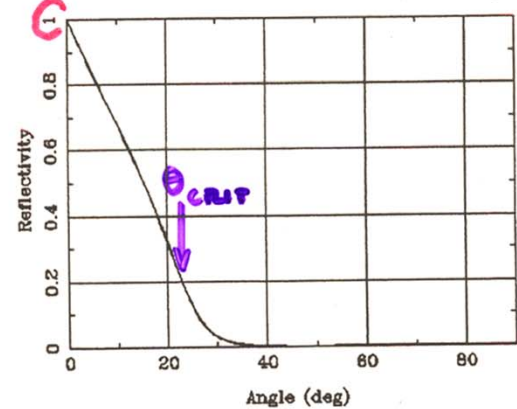
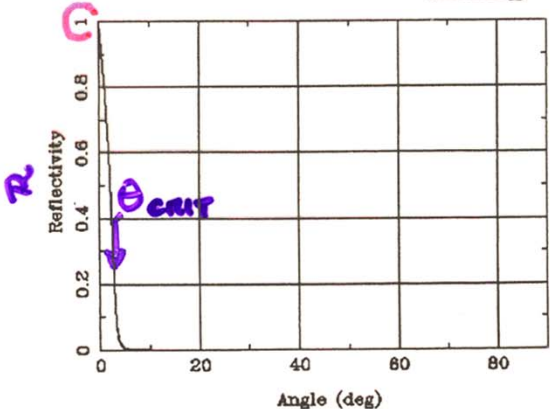


Mirror Reflectivity

Mirror Reflectivity

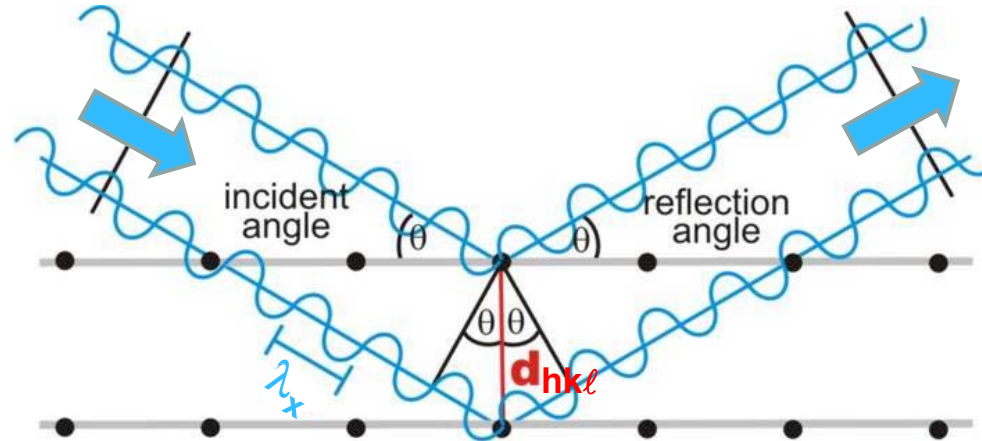
Au Rho=19.32, Sig=0.nm, P=-1., E=1487.eV

Au Rho=19.32, Sig=0.nm, P=-1., E=100.eV



The ultraviolet, soft x-ray, hard x-ray measurements:

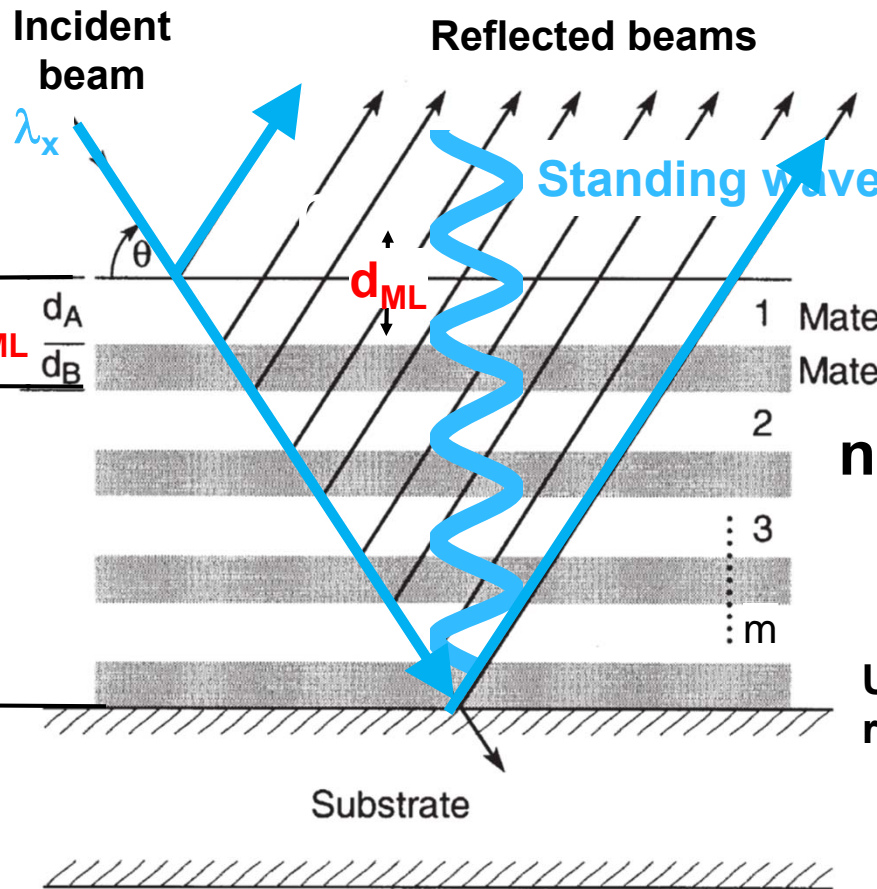
Plus diffraction and scattering:
From crystals:



$$n\lambda_x = 2d_{hkl} \sin\theta$$

Use atomic scattering factors f_i

From multilayers:



Plus Kiessig fringes:

$$p\lambda_x = 2md_{ML} \sin\theta$$

$$\equiv 2D_{ML} \sin\theta$$

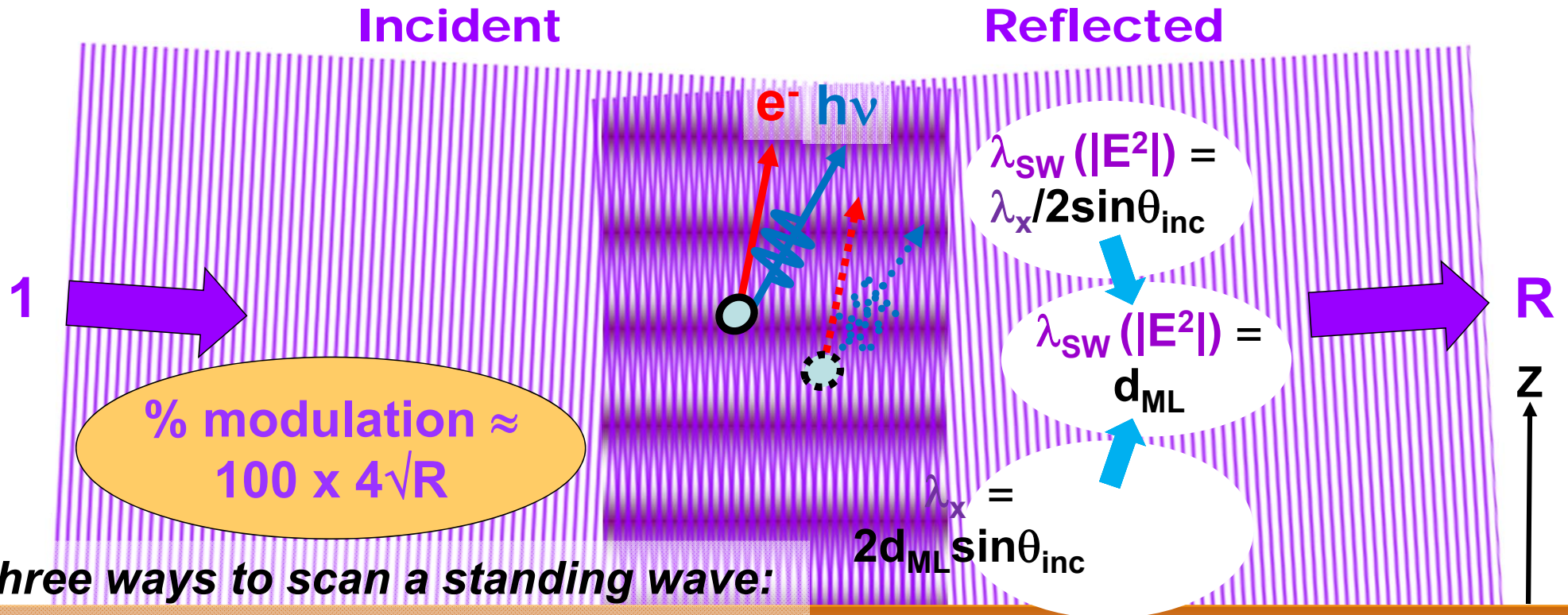
$p = 1, 2, \dots$
unknown no.

$$n\lambda_x = 2(d_A + d_B) \sin\theta$$

$$\equiv 2d_{ML} \sin\theta$$

Use complex index of refraction $n = 1 - \delta - i\beta$
Fresnel Equations

Three ways to scan a standing wave formed in reflection from single-crystal Bragg planes, or a multilayer mirror*



1. Rocking curve:

$$I(\theta_{inc}) \propto 1 + R(\theta_{inc}) + 2\sqrt{R(\theta_{inc})} f \cos[\varphi(\theta_{inc}) - 2\pi(\Delta z / \lambda_{sw})]$$

Multilayer Mirror

2. Photon energy scan:

$$I(h\nu) \propto 1 + R(h\nu) + 2\sqrt{R(h\nu)} f \cos[\varphi(h\nu) - 2\pi(\Delta z / \lambda_{sw})]$$

d_{ML}

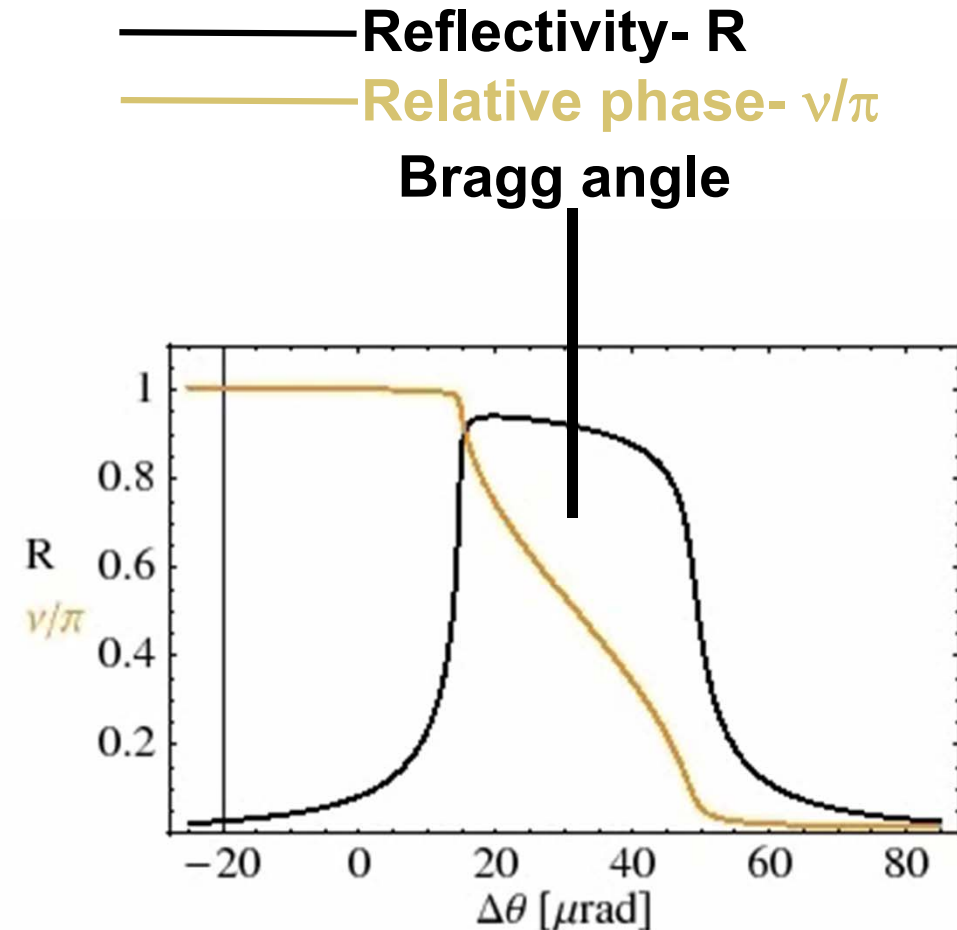
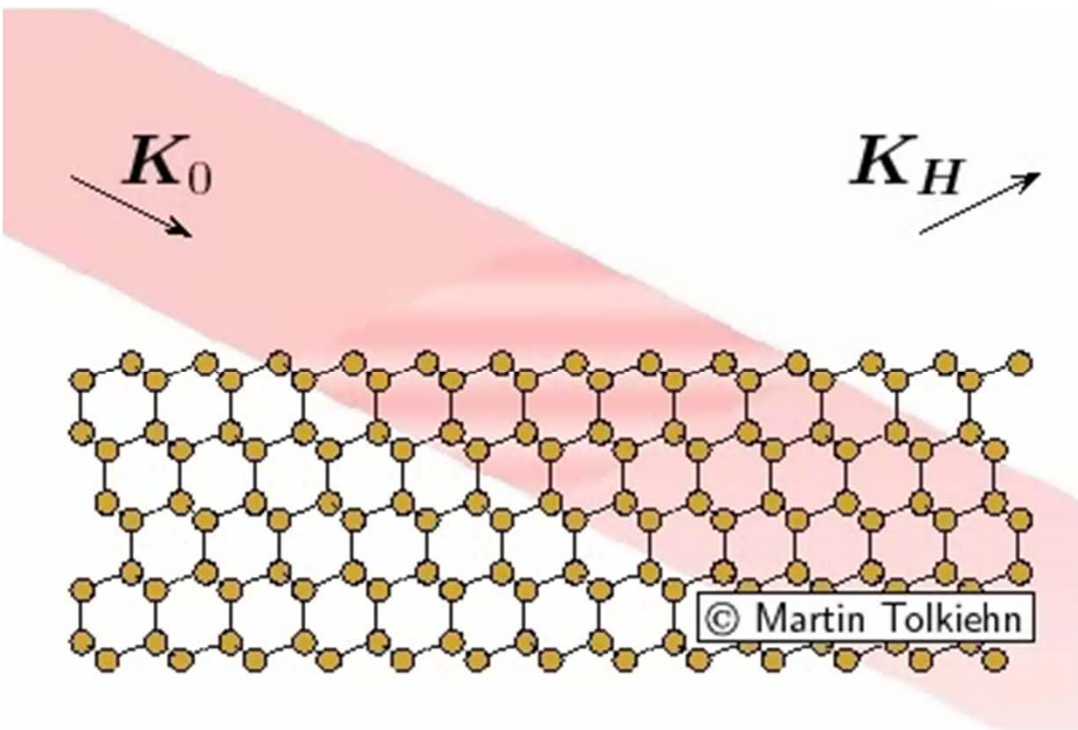
with: f = coherent fraction of atoms, $\Delta z / \lambda_{sw}$ = phase of coherent-atom position

3. Phase scan with wedge-shaped sample ("Swedge" method)

*Standing waves via Bragg reflection of hard x-rays: Batterman, Phys. Rev A 133, 759 (1964)

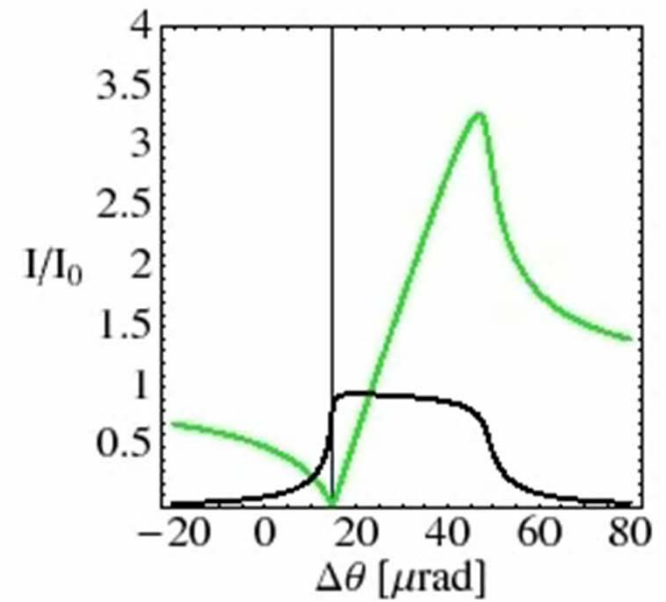
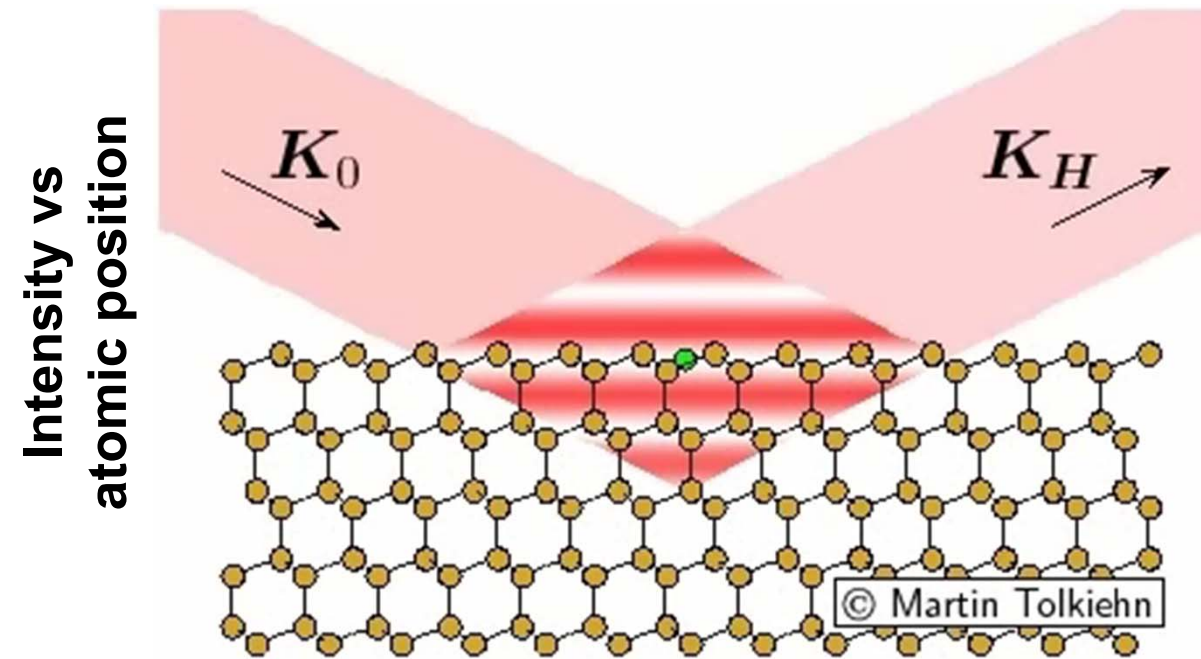
*In x-ray magnetic circular dichroism (XMCD)—Kim, Kortright, PRL 86, 1347(2001)

Standing Wave Behavior During a Rocking Curve or Photon-Energy Scan



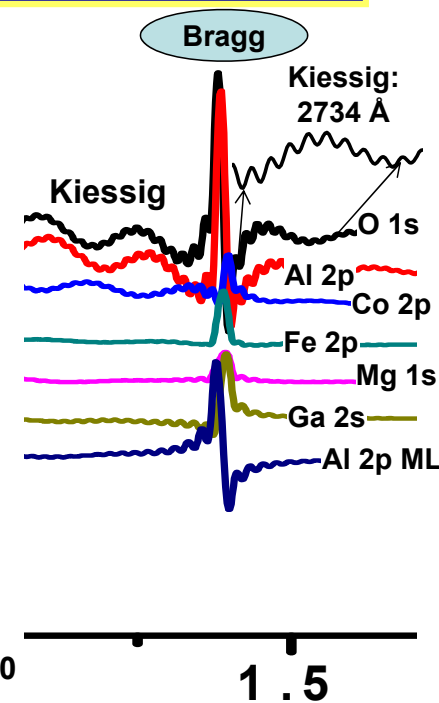
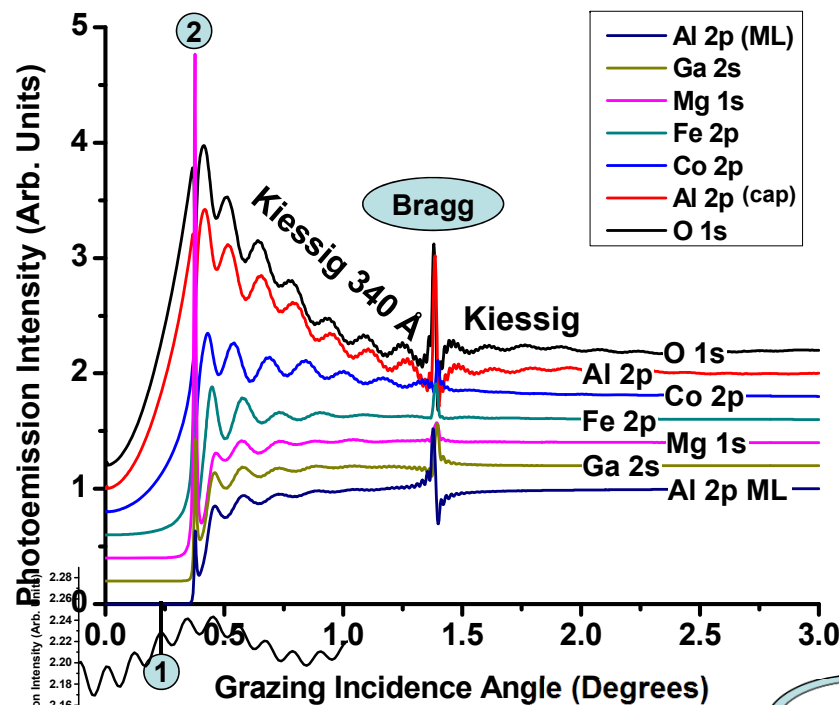
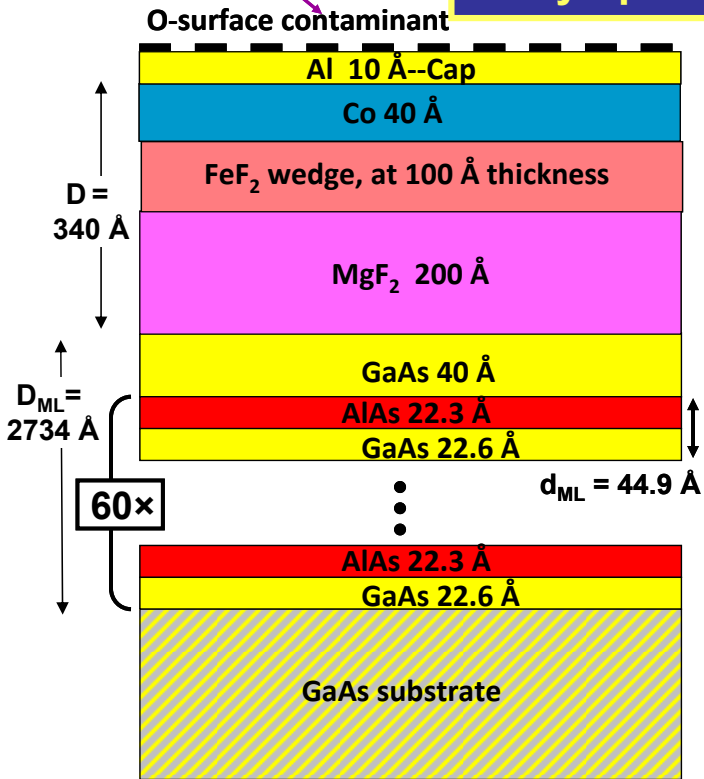
+Same general forms if **photon energy** is scanned

Form of rocking curve is unique to position of emitter

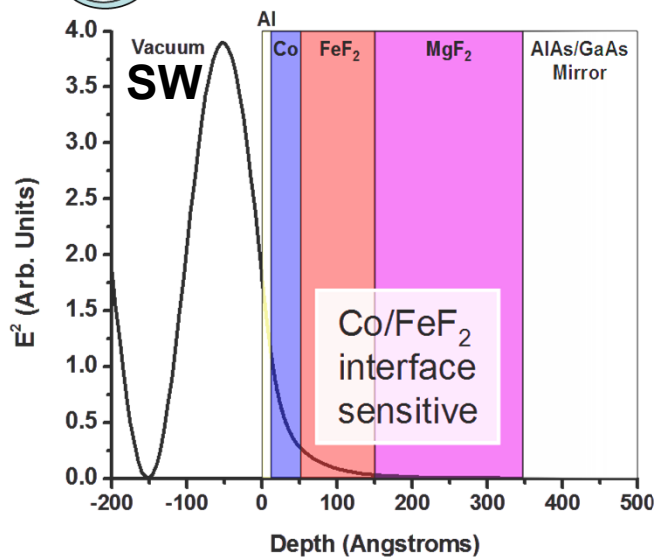


$h\nu = 5.9 \text{ keV}$

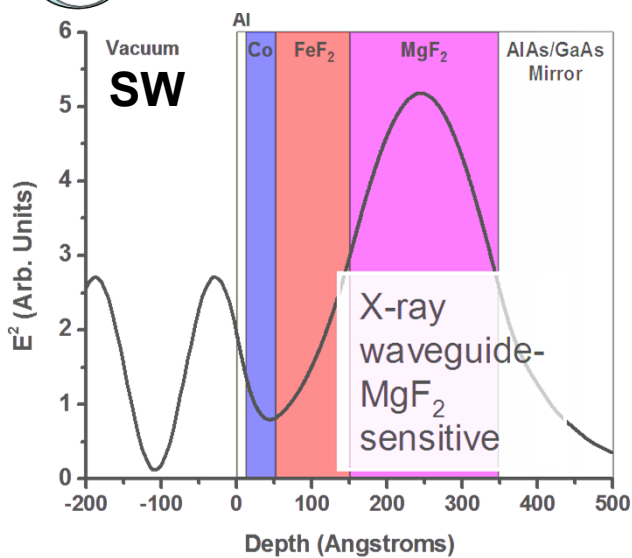
X-ray optical effects in hard x-ray reflectivity from a multilayer structure



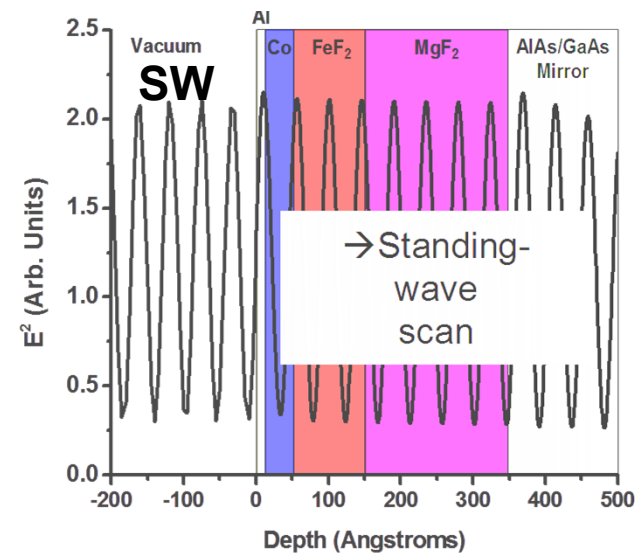
1 [Electric Field]² VS. Depth



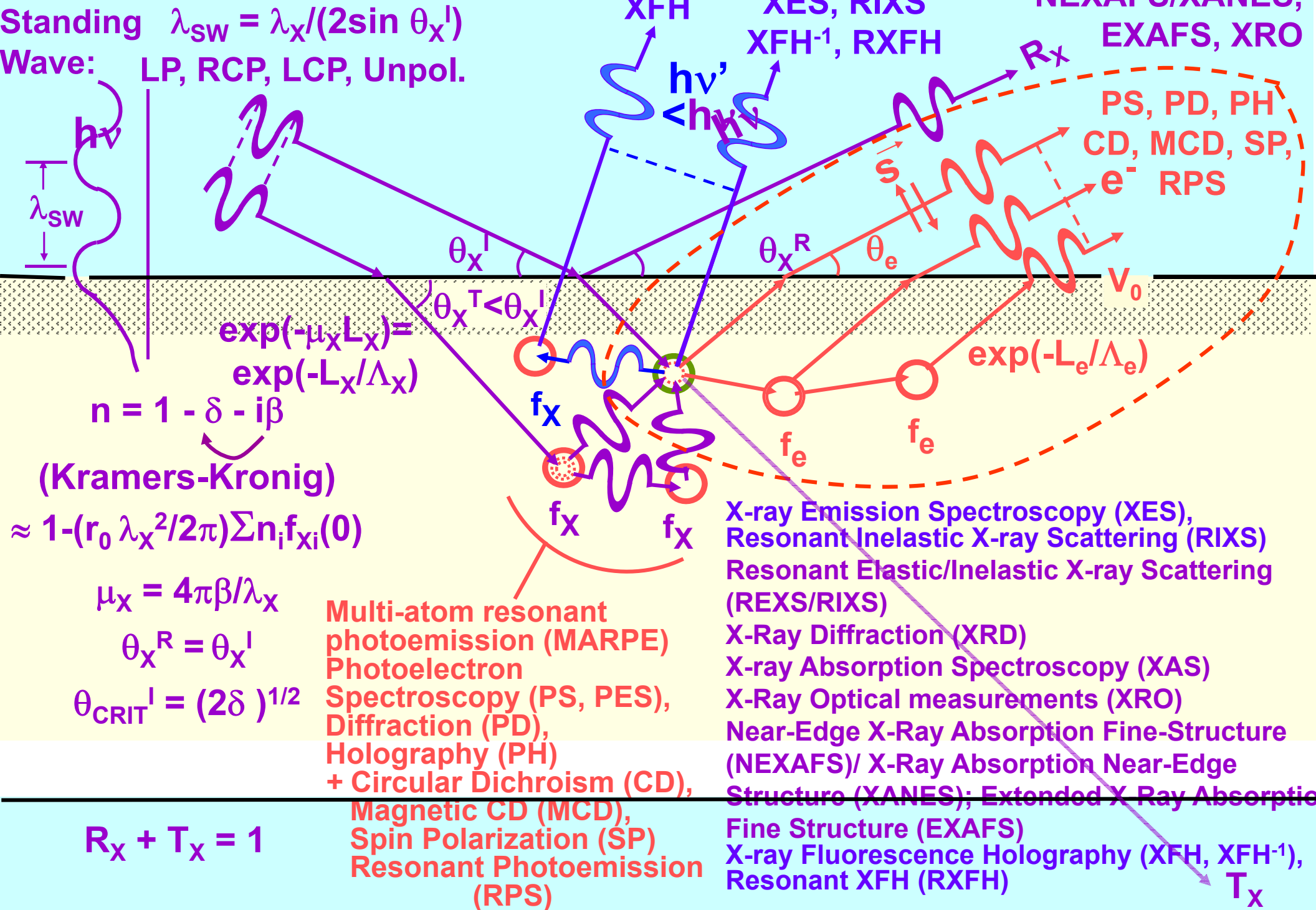
2 [Electric Field]² VS. Depth



[Electric Field]² VS. Depth



Some basic measurements:



Basic Concepts:

A Little Electronic Structure

The X-Ray-Based Experiments

 X-Ray Sources, Synchrotron Radiation, Free Electron Lasers

Core-Level Photoemission

Intensities and Quantitative Analysis, the 3-Step Model

Varying Surface and Bulk Sensitivity

Chemical Shifts

Multiplet Splittings

Electron Screening and Satellite Structure

Magnetic and Non-Magnetic Dichroism

Resonant Photoemission

Photoelectron Diffraction and Holography

Valence-Level Photoemission

Band-Mapping in the Ultraviolet Photoemission Limit

Densities of States in the X-Ray Photoemission Limit

Some New Directions

Photoemission with Hard X-Rays (throughout lectures)

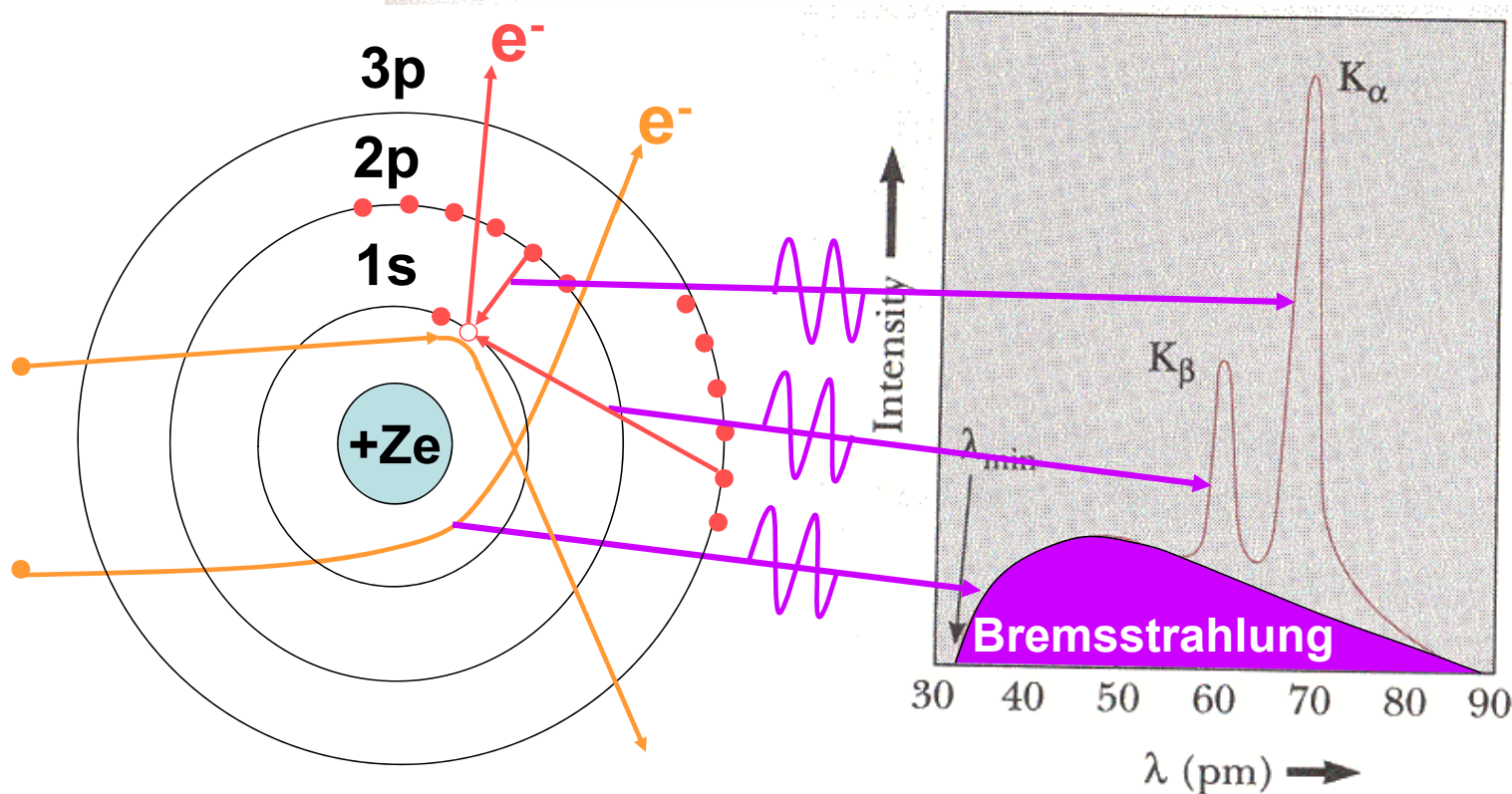
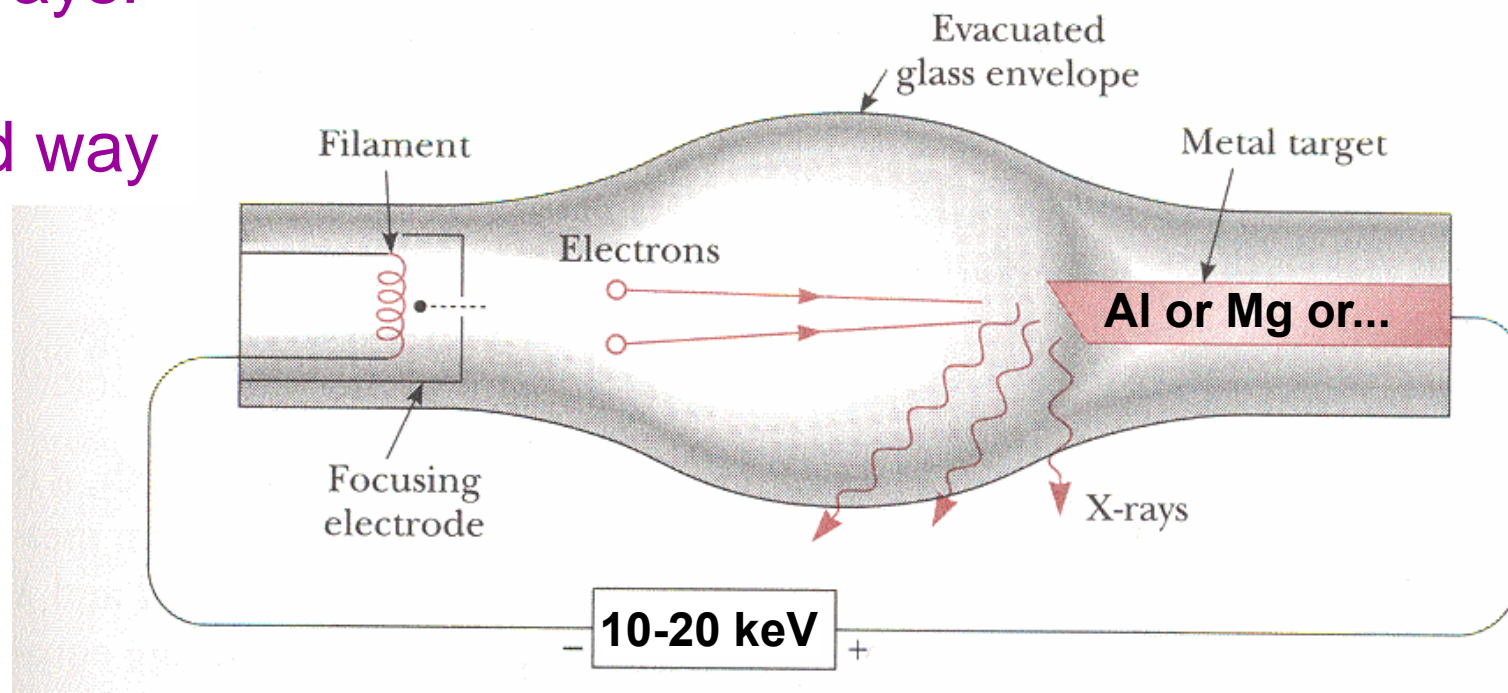
Photoemission with Standing Wave Excitation

Photoemission with: Higher Pressures → multi-Torr → Atmosphere?

Spatial Resolution-Photoelectron Microscopy

Temporal Resolution

Producing x-rays: the good old-fashioned way

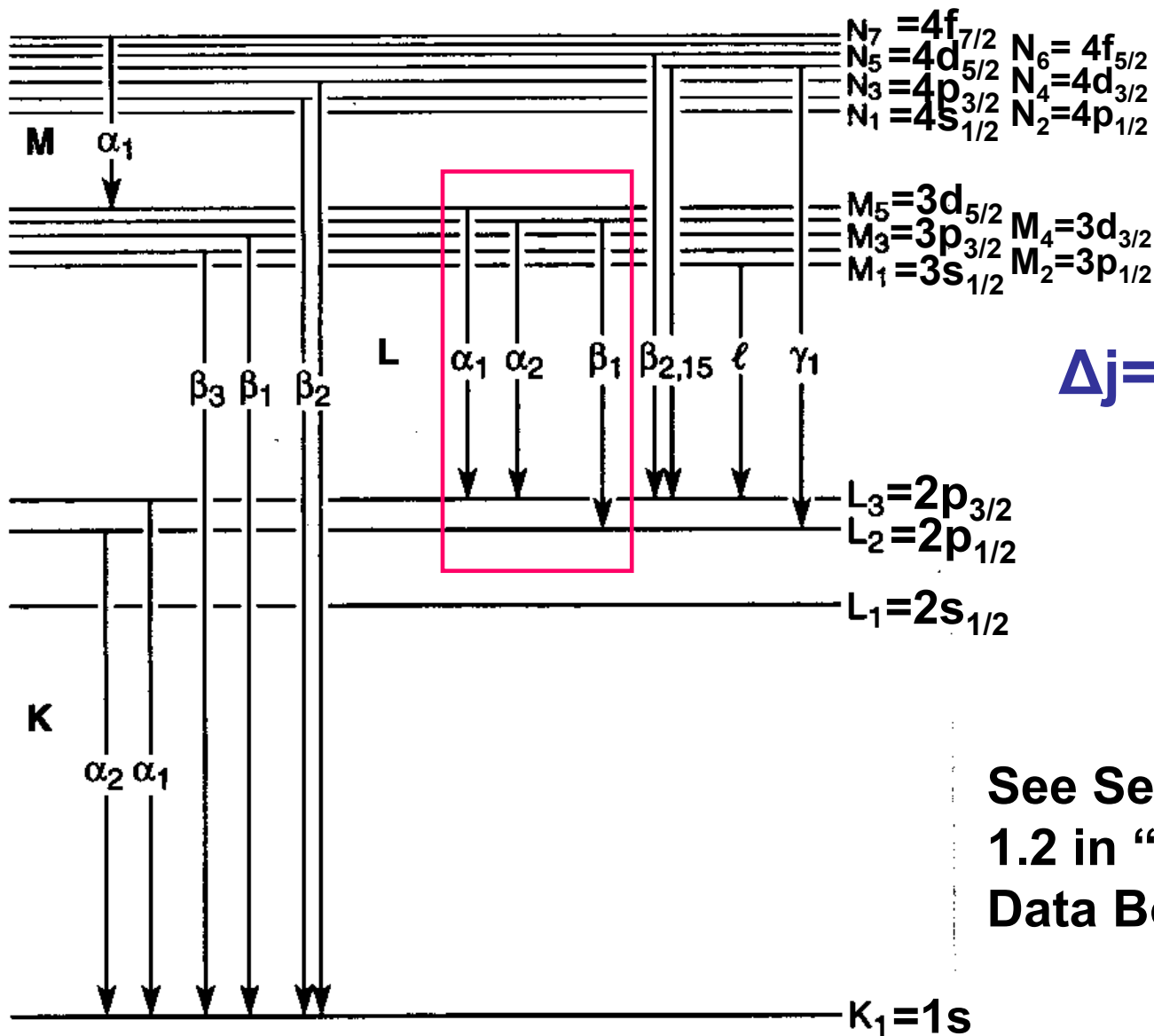


See Section
1.2 in "X-Ray
Data Booklet"

X-Ray Nomenclature (from "X-Ray Data Booklet")

In general:

$$nl \begin{cases} \text{Spin-} nl_{j=l+1/2} \\ \text{orbit } nl_{j=l-1/2} \end{cases}$$



$$\Delta j = 0, \pm 1$$

See Section 1.2 in "X-Ray Data Booklet"

Fig. 1-1. Transitions that give rise to the emission lines in Table 1-3.

X-Ray energies from the “X-Ray Data Booklet”

Table 1-2. Photon energies, in electron volts, of principal K-, L-, and M-shell emission lines.

Element	$K\alpha_1$	$K\alpha_2$	$K\beta_1$	$L\alpha_1$	$L\alpha_2$	$L\beta_1$	$L\beta_2$	$L\gamma$	$M\alpha_1$
3 Li	54.3								
4 Be	108.5								
5 B	183.3								
6 C	277								
7 N	392.4								
8 O	524.9								
9 F	676.8								
10 Ne	848.6	848.6							
11 Na	1,040.98	1,040.98	1,071.1						
12 Mg	1,253.60	1,253.60	1,302.2						
13 Al	1,486.70	1,486.27	1,557.45						
14 Si	1,739.98	1,739.38	1,835.94						
15 P	2,013.7	2,012.7	2,139.1						
16 S	2,307.84	2,306.64	2,464.04						
17 Cl	2,622.39	2,620.78	2,815.6						
18 Ar	2,957.70	2,955.63	3,190.5						
19 K	3,313.8	3,311.1	3,589.6						
20 Ca	3,691.68	3,688.09	4,012.7	341.3	341.3	344.9			
21 Sc	4,090.6	4,086.1	4,460.5	395.4	395.4	399.6			

Popular laboratory sources
for common soft x-ray photoelectron spectroscopy

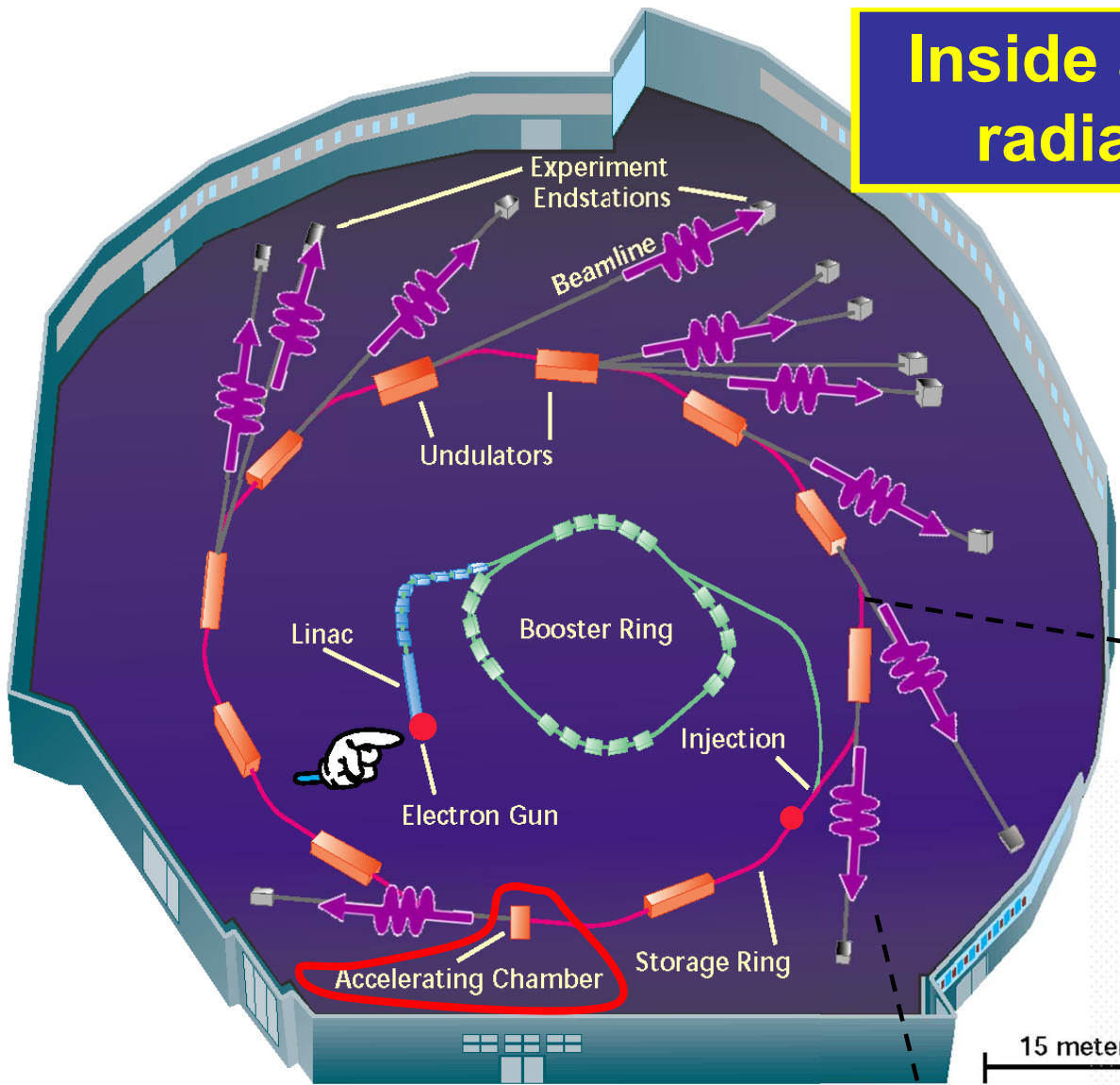
X-Ray energies from the “X-Ray Data Booklet”

Table 1-2. Energies of x-ray emission lines (continued).

Element	$K\alpha_1$	$K\alpha_2$	$K\beta_1$	$L\alpha_1$	$L\alpha_2$	$L\beta_1$	$L\beta_2$	$L\gamma$	$M\alpha_1$
22 Ti	4,510.84	4,504.86	4,931.81	452.2	452.2	458.4			
23 V	4,952.20	4,944.64	5,427.29	511.3	511.3	519.2			
24 Cr	5,414.72	5,405.509	5,946.71	572.8	572.8	582.8			
25 Mn	5,898.75	5,887.65	6,490.45	637.4	637.4	648.8			
26 Fe	6,403.84	6,390.84	7,057.98	705.0	705.0	718.5			
27 Co	6,930.32	6,915.30	7,649.43	776.2	776.2	791.4			
28 Ni	7,478.15	7,460.89	8,264.66	851.5	851.5	868.8			
29 Cu	8,047.78	8,027.83	8,905.29	929.7	929.7	949.8			
30 Zn	8,638.86	8,615.78	9,572.0	1,011.7	1,011.7	1,034.7			
31 Ga	9,251.74	9,224.82	10,264.2	1,097.92	1,097.92	1,124.8			
32 Ge	9,886.42	9,855.32	10,982.1	1,188.00	1,188.00	1,218.5			
33 As	10,543.72	10,507.99	11,726.2	1,282.0	1,282.0	1,317.0			
34 Se	11,222.4	11,181.4	12,495.9	1,379.10	1,379.10	1,419.23			
35 Br	11,924.2	11,877.6	13,291.4	1,480.43	1,480.43	1,525.90			
36 Kr	12,649	12,598	14,112	1,586.0	1,586.0	1,636.6			
37 Rb	13,395.3	13,335.8	14,961.3	1,694.13	1,692.56	1,752.17			
38 Sr	14,165	14,097.9	15,835.7	1,806.56	1,804.74	1,871.72			
39 Y	14,958.4	14,882.9	16,737.8	1,922.56	1,920.47	1,995.84			
40 Zr	15,775.1	15,690.9	17,667.8	2,042.36	2,039.9	2,124.4 ^r	2,219.4	2,302.7	

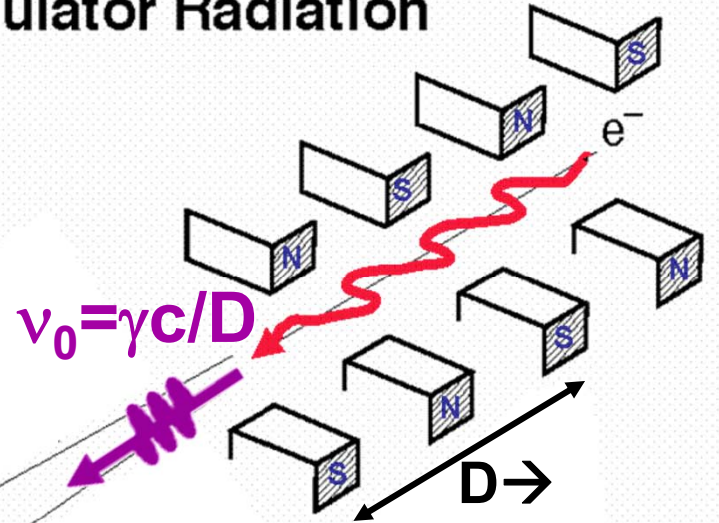
**Popular laboratory
sources
for hard x-ray
photoelectron
spectroscopy**

Inside a synchrotron radiation source



Electron speed near c :
 $0.999999994 c$, $\gamma = 3719$
 Einstein needed again—
 Special Relativity

Undulator Radiation



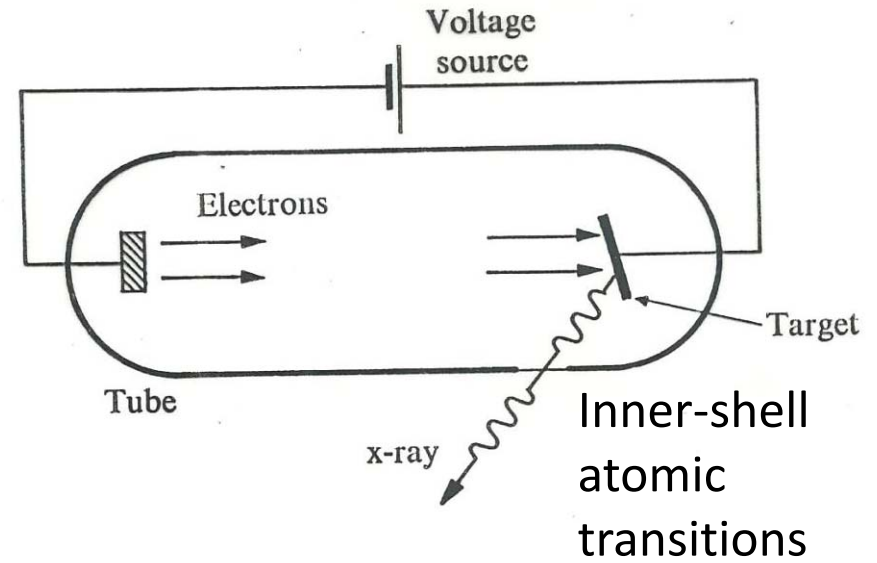
Radiofrequency Cavity

+Doppler
 $v = \gamma^2 c / D$

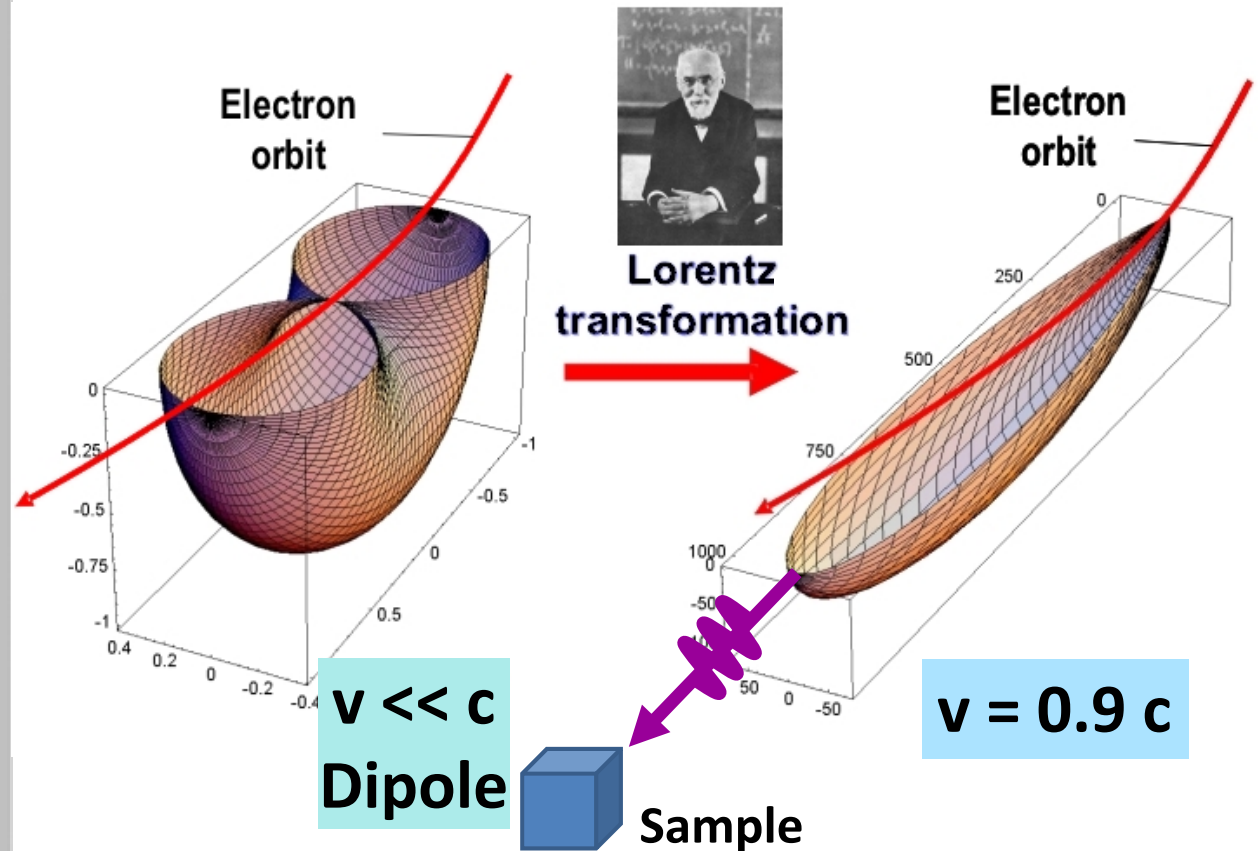
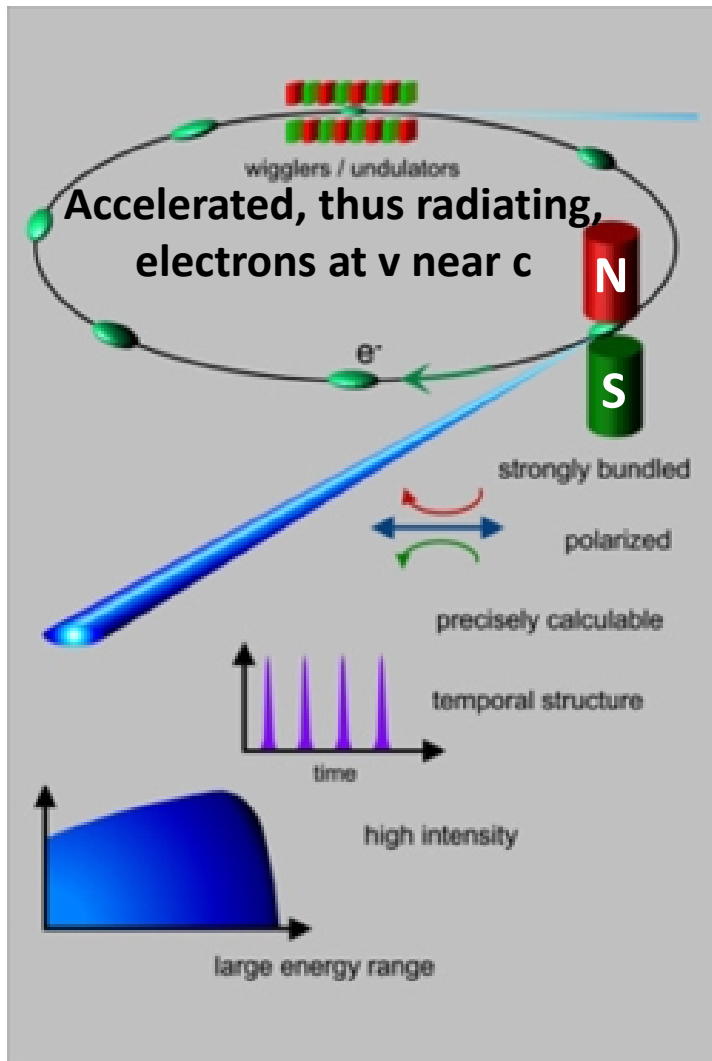
$D \rightarrow$
 D/γ as seen by electrons

The generation of x-rays:

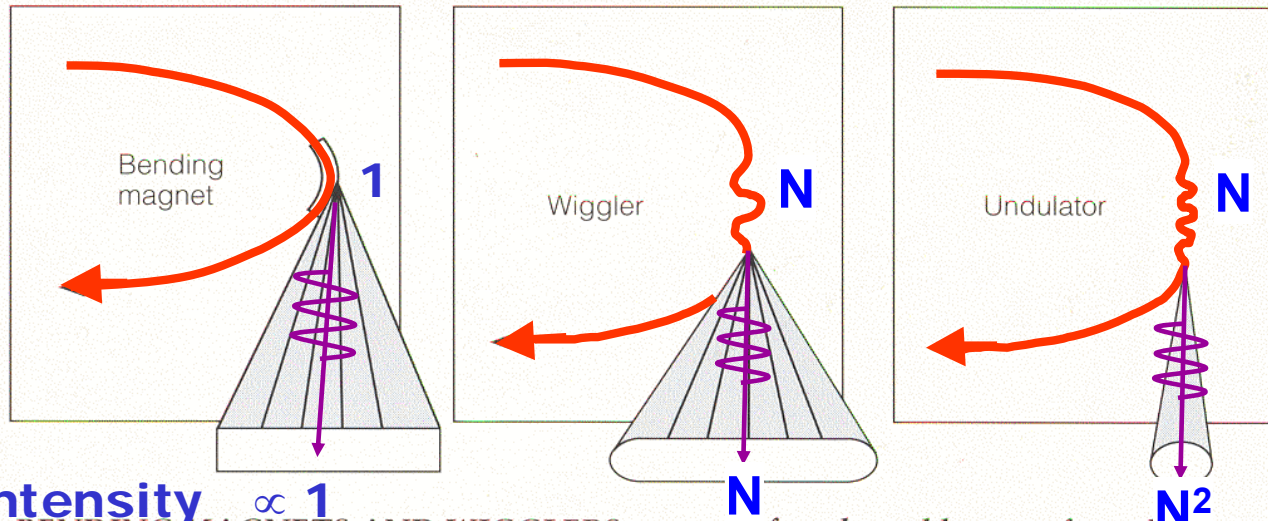
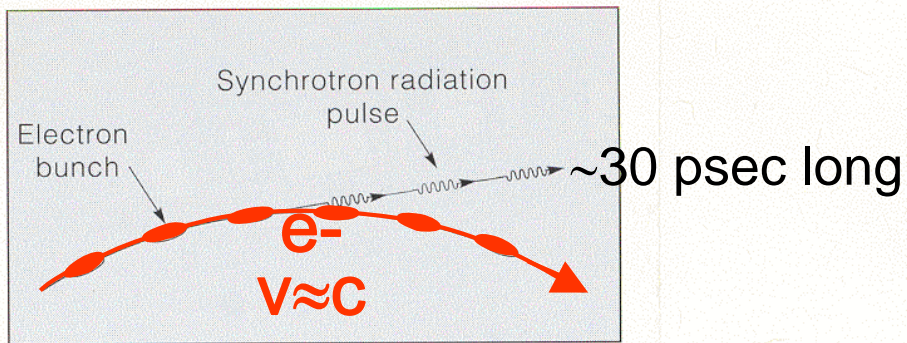
An x-ray tube:



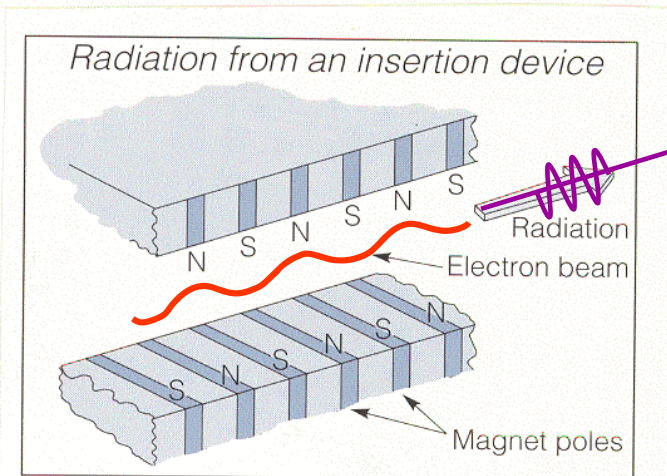
Synchrotron radiation: e.g. the Berkeley Advanced Light Source



Synchrotron Radiation Sources:

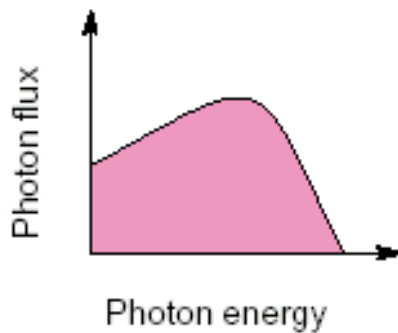
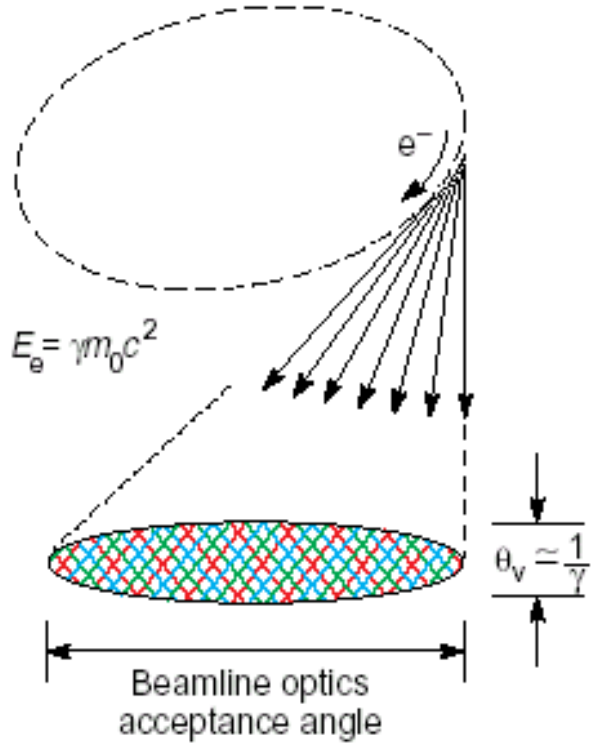


BENDING MAGNETS AND WIGGLERS generate fan-shaped beams of synchrotron radiation, whereas undulators emit pencil-thin beams.

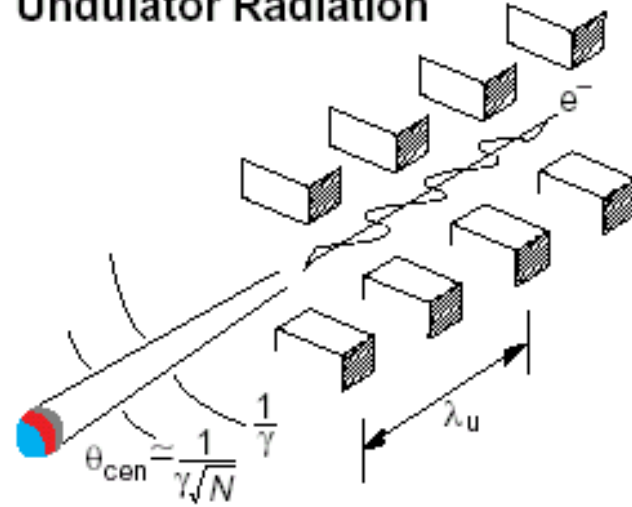


Bend-Magnet Radiation

$$\gamma = \frac{1}{\sqrt{1 - \frac{v^2}{c^2}}}$$



Undulator Radiation



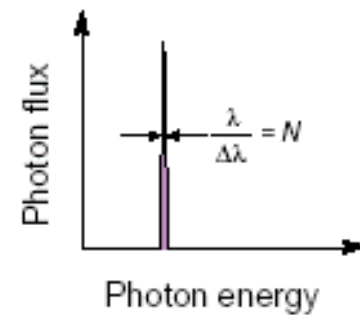
$$\lambda_x = \frac{\lambda_u}{2\gamma^2} \left(1 + \frac{K^2}{2} + \gamma^2 \theta^2 \right) \quad K = \frac{eB_0\lambda_u}{2\pi m_0 c}$$

In the central radiation cone:

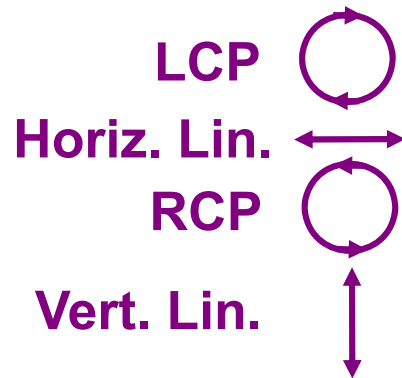
$$\frac{\Delta\omega}{\omega} \approx \frac{1}{N}$$

$$\theta_{cen} \approx \frac{1}{\gamma\sqrt{N}}$$

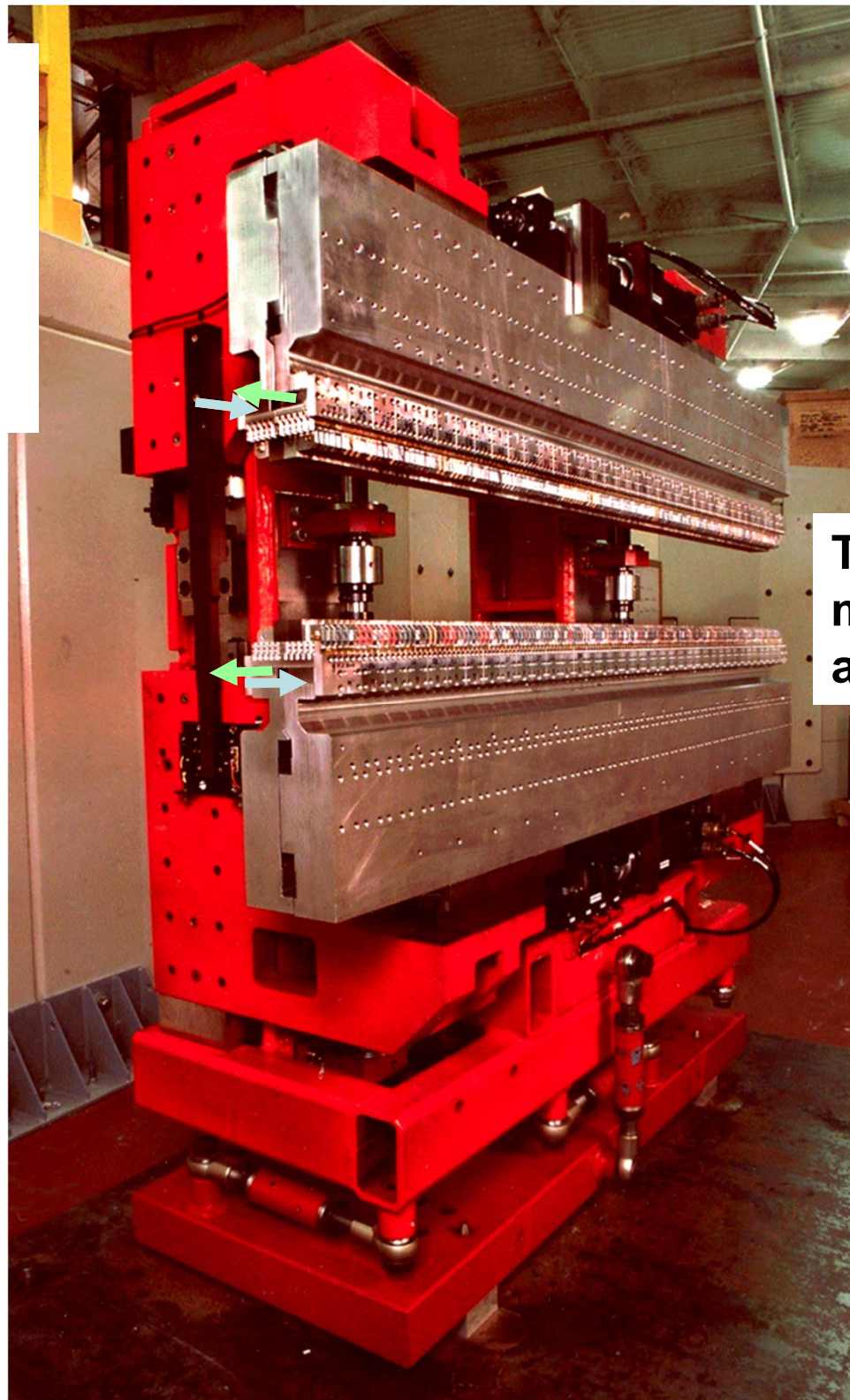
λ_x as observed will increase if the magnetic field B_0 is increased or if viewed away from the axis by an angle θ



Advanced Light Source--
Sasaki-Carr
Elliptically-Polarized
Undulator:
Variable light
polarization

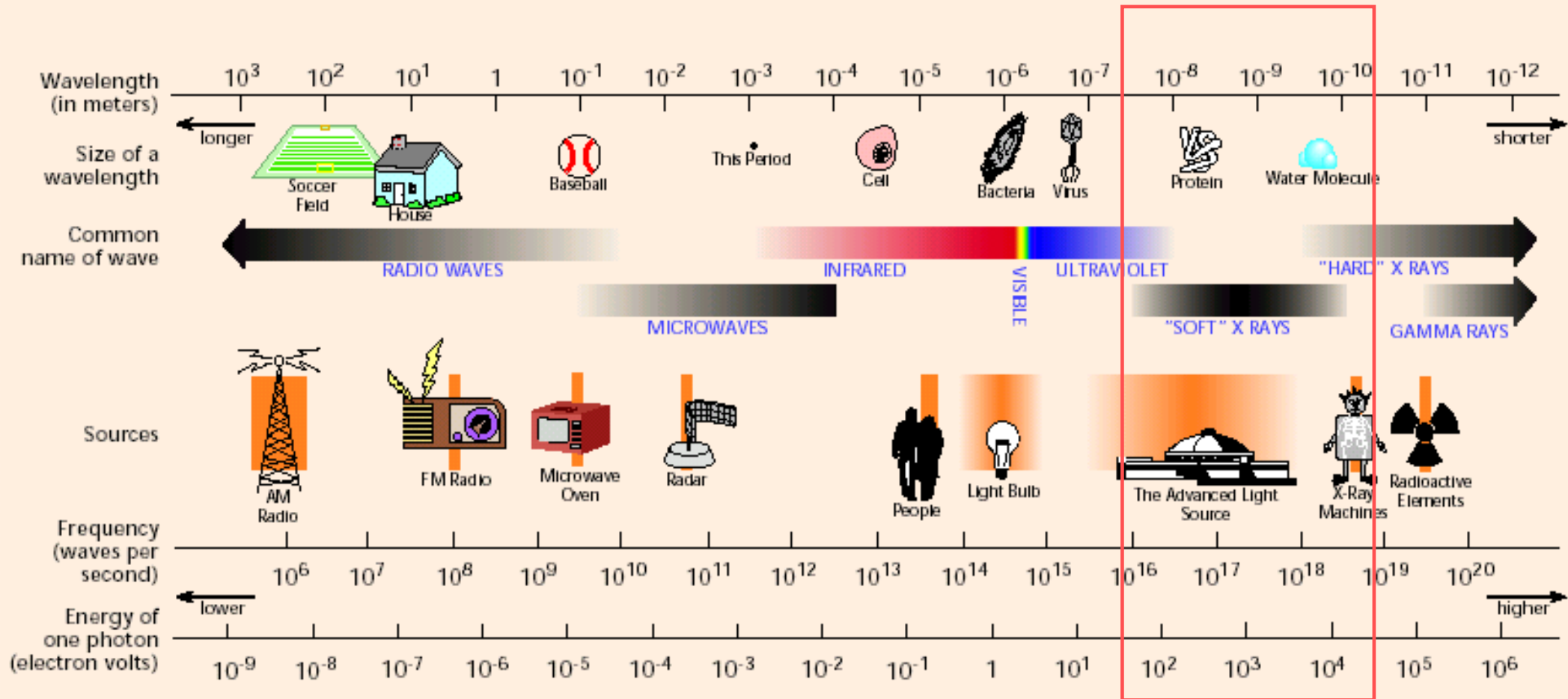


[Can also vary polarization
to LCP, RCP by going
above and below the orbit
plane in a bend magnet]



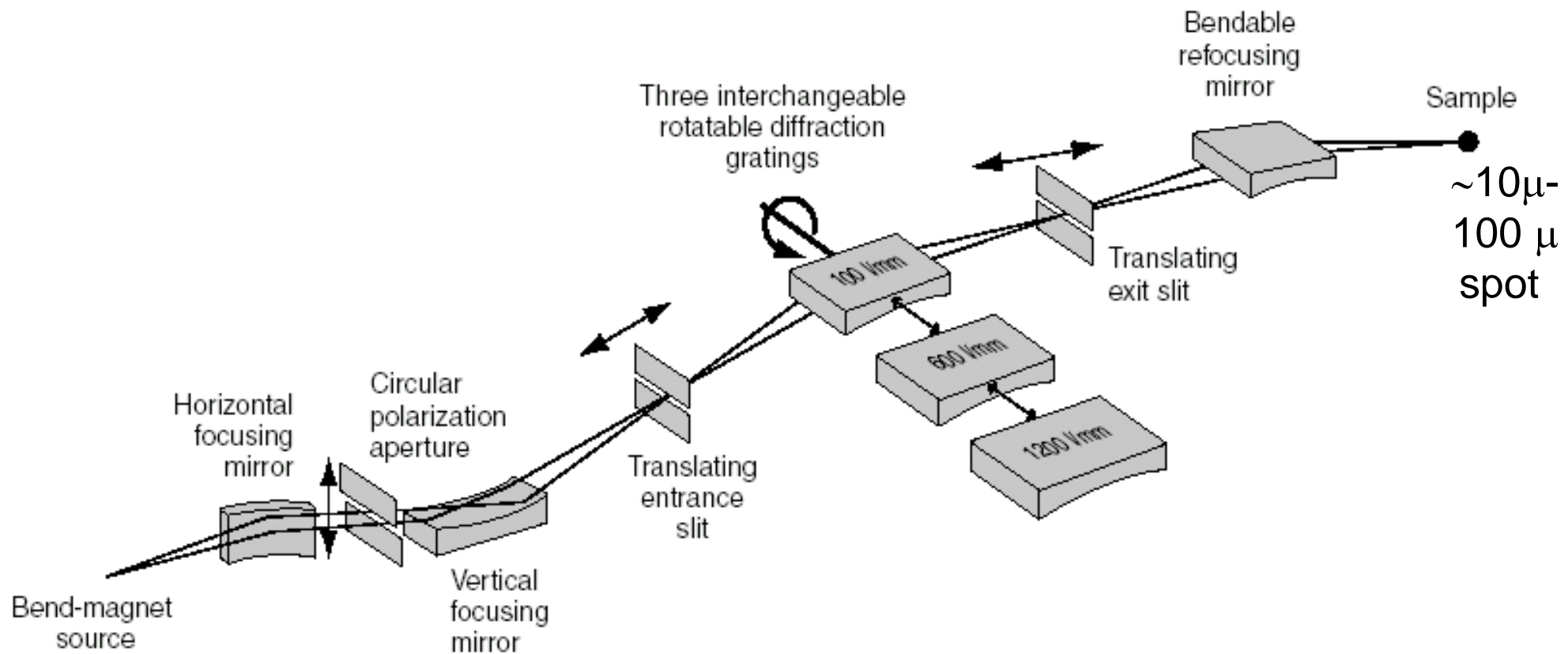
Translating
magnet
arrays

THE ELECTROMAGNETIC SPECTRUM



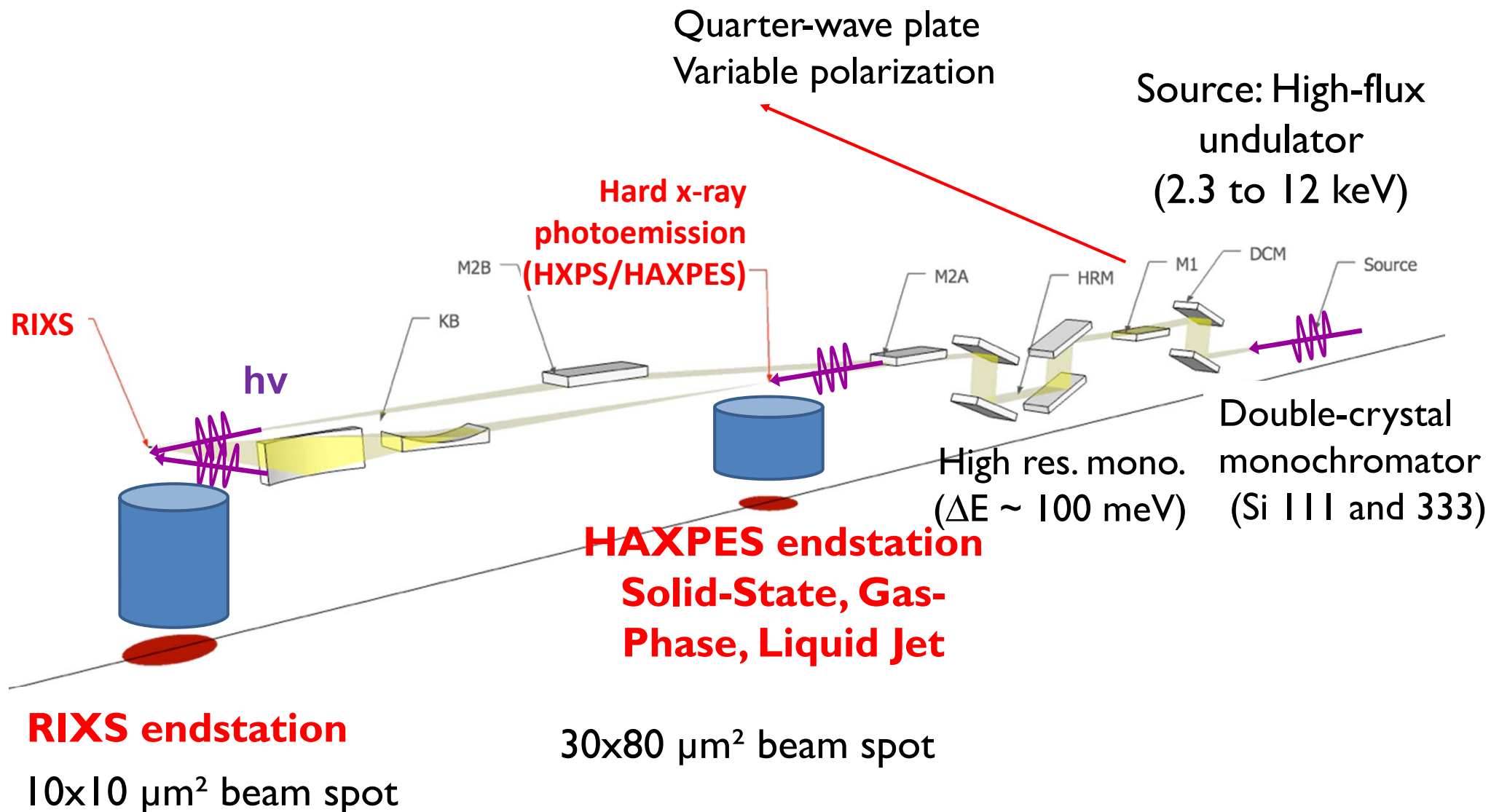
Typical surface/materials science expts.

Advanced Light Source-- Typical Soft X-Ray Spectroscopy Beamline Layout: to ca. 1500 eV



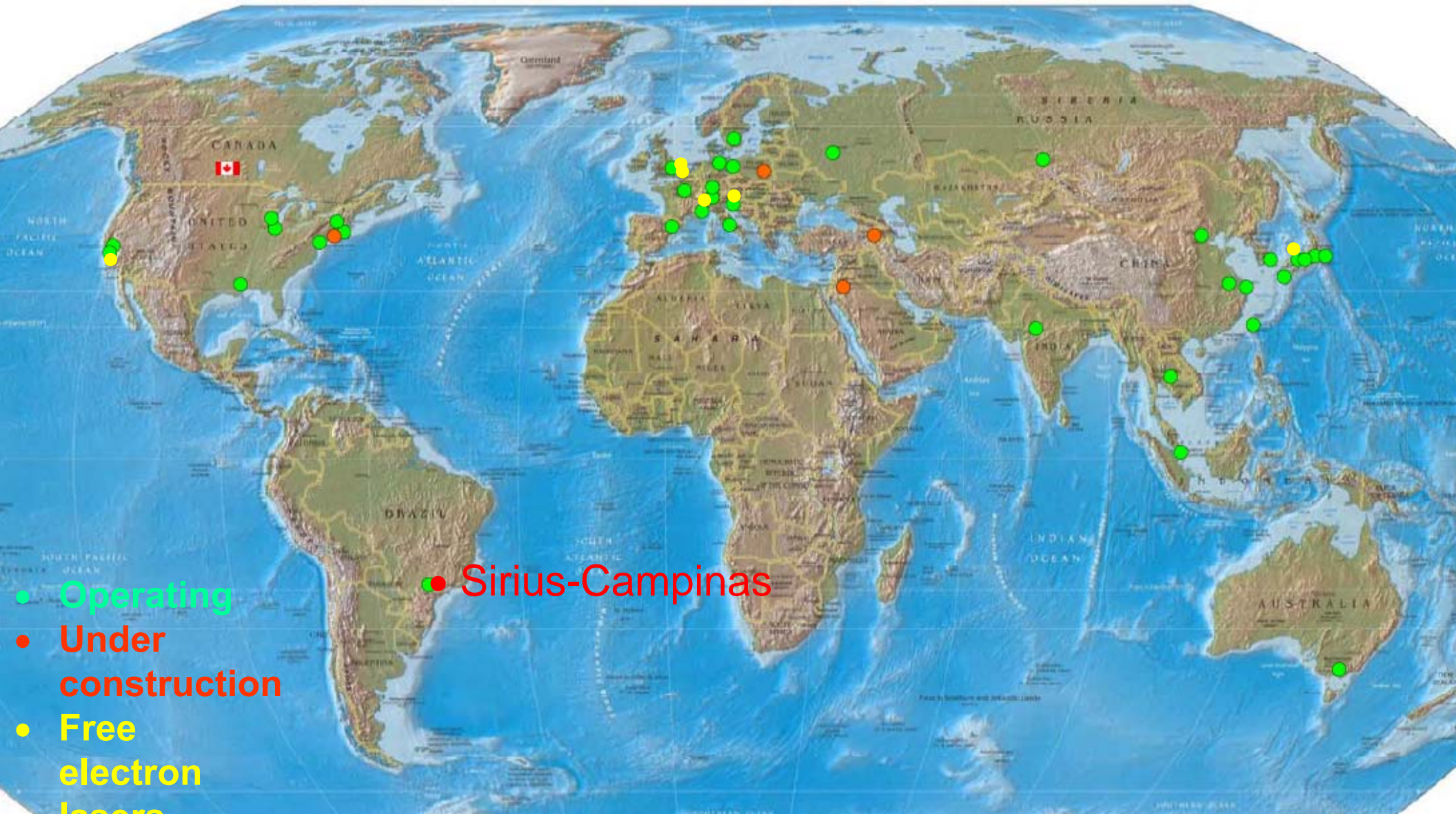
Schematic layout of Beamline 9.3.2.

Soleil (Paris)—Typical hard x-ray spectroscopy beamline



Synchrotron radiation sources of the world- about 41 and growing

Free-electron laser (VUV, X-ray)- about 5 and growing





San Francisco

Marin County

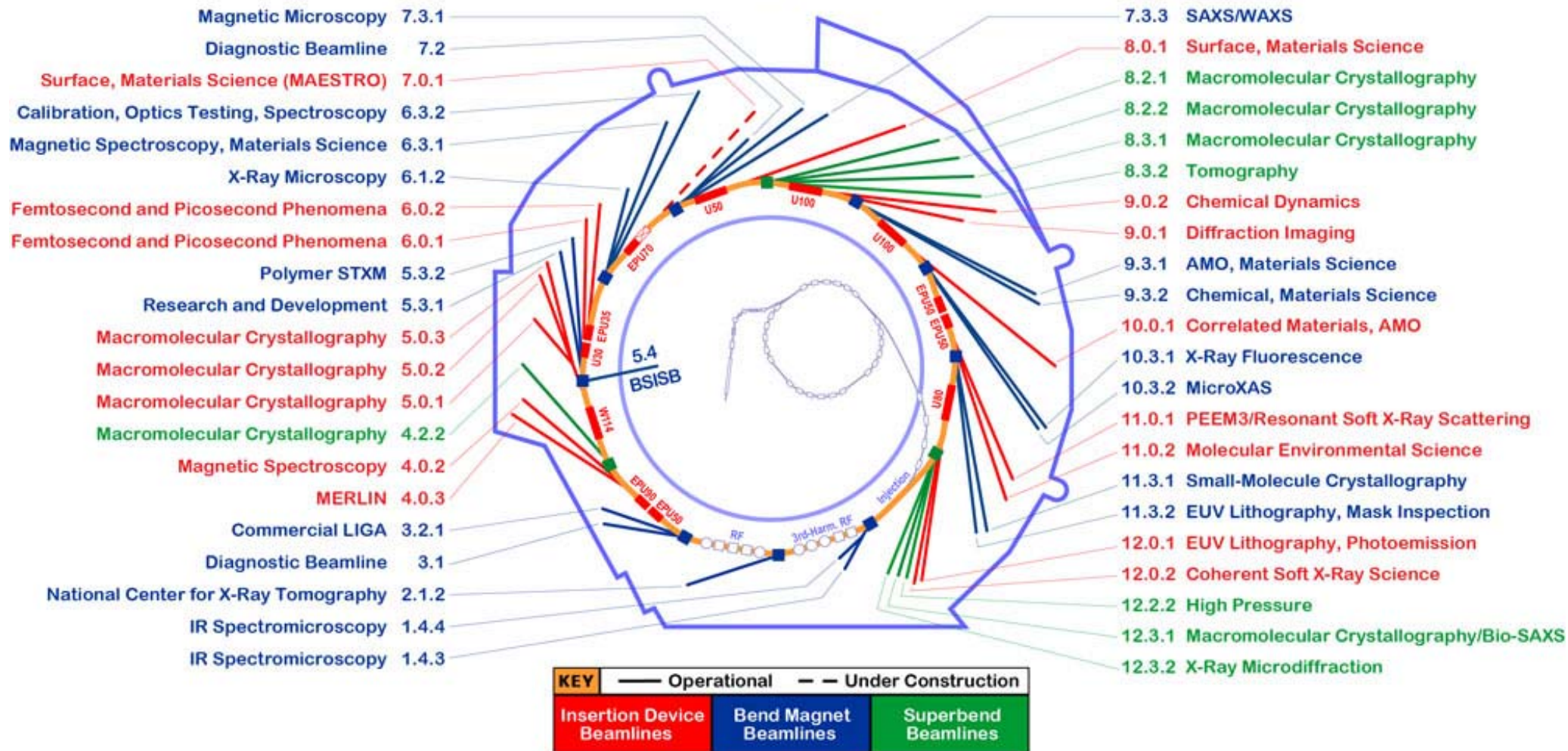
UC Berkeley

Advanced
Light Source

Group offices
& lab.

ALS Beamlines

January 2014

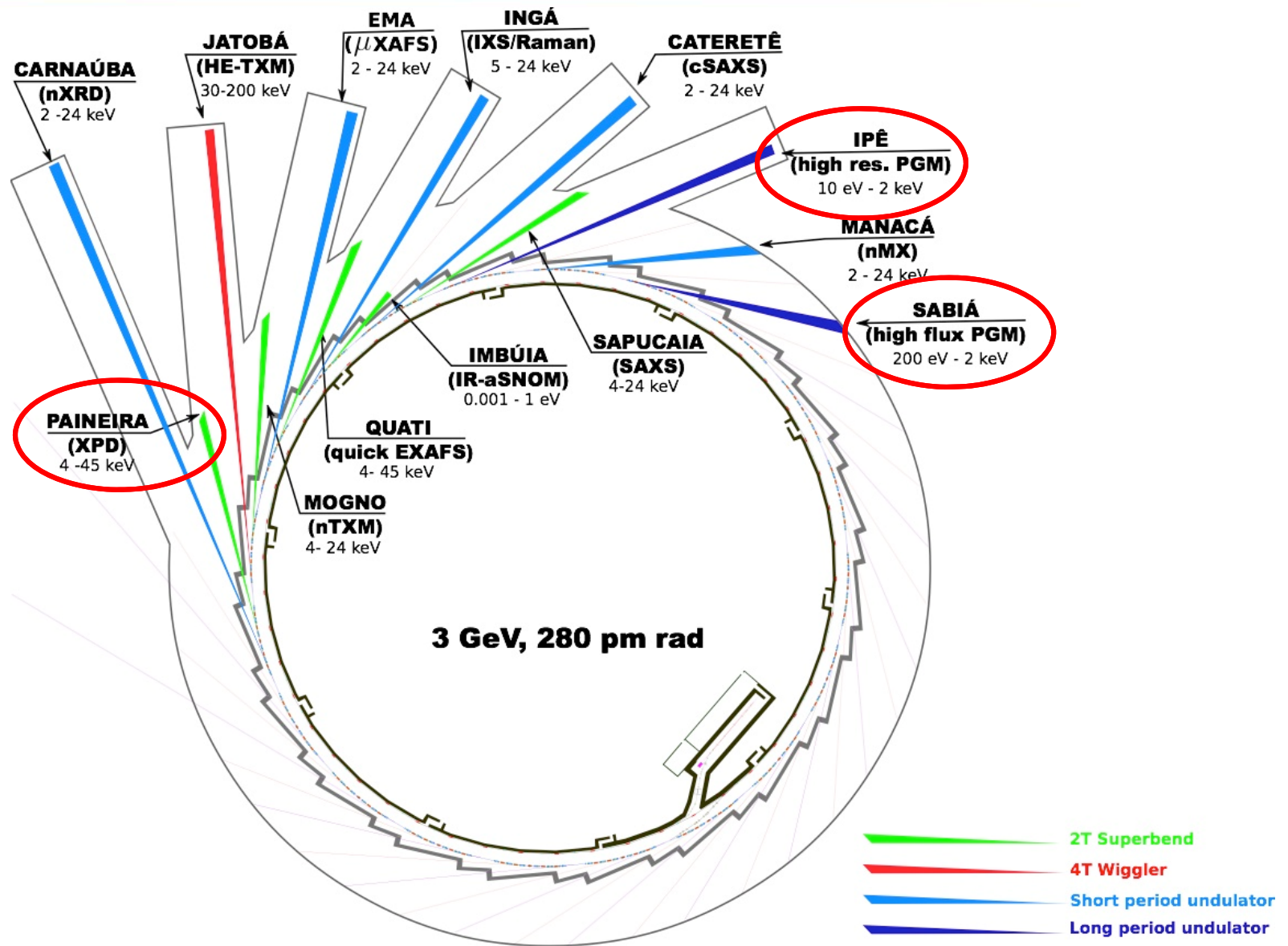


SIRIUS



- 3 GeV
- 13 beam lines in phase 1
- 280 pm electrons emittance
- Open to users in 2018 → 2019?

SIRIUS: initial beam lines



CNPEM

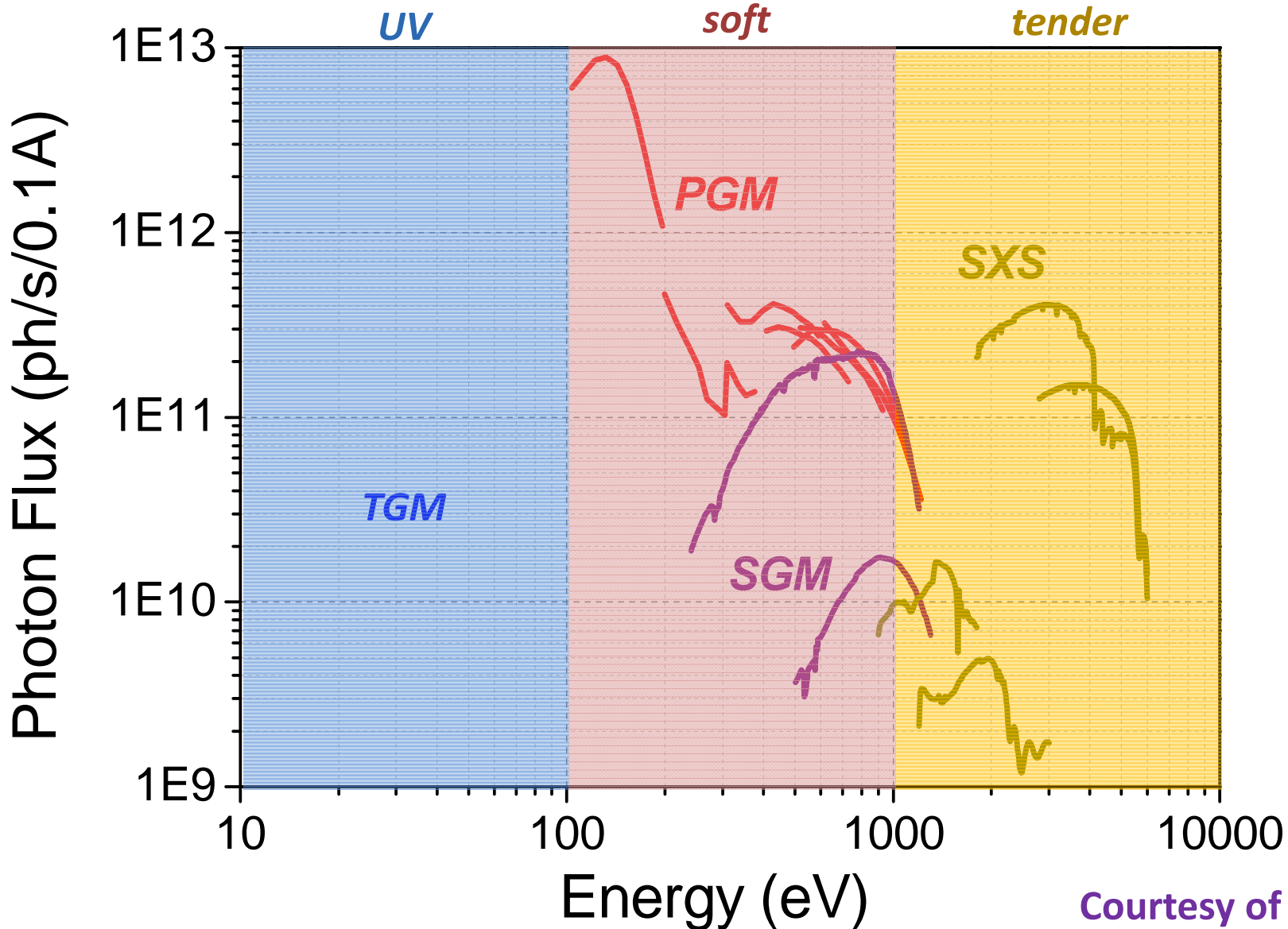


Laboratório Nacional
de Luz Síncrotron

ENFMC 2014

Courtesy of Julio Cesar, LNLS

4 beamlines covering from 3 eV to 6 KeV



Spectroscopy

- ✓ XANES
- ✓ XMCD
- ✓ ARPES
- ✓ XPS
- ✓ XPD
- ✓ PEPICO

Scattering

- ✓ (M)RXRR
- ✓ RSAXS

Imaging

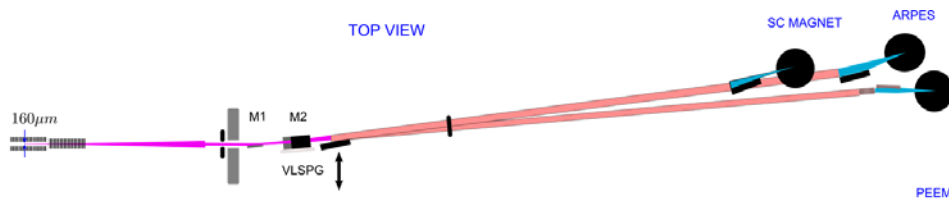
- ✓ PEEM

Courtesy of Tulio Rocha, LNLS

- ✓ EPU with 50mm period
- ✓ Multi-branches
- ✓ VLS PGM monochromator
- ✓ KB focusing

SABIÁ

(Soft X-ray Absorption spectroscopy and Imaging)



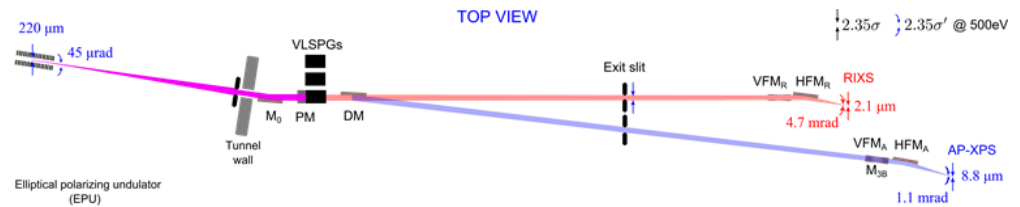
ARPES, PEEM, XMCD/XMLD

UHV condensed matter research

- ✓ *In situ sample preparation*
- ✓ *Magnetism*
- ✓ *Multiferroic materials*
- ✓ *Superconductivity*
- ✓ *Topological insulators*
- ✓ *Surface science*

IPÊ

(Inelastic and Photoelectron Spectroscopy)



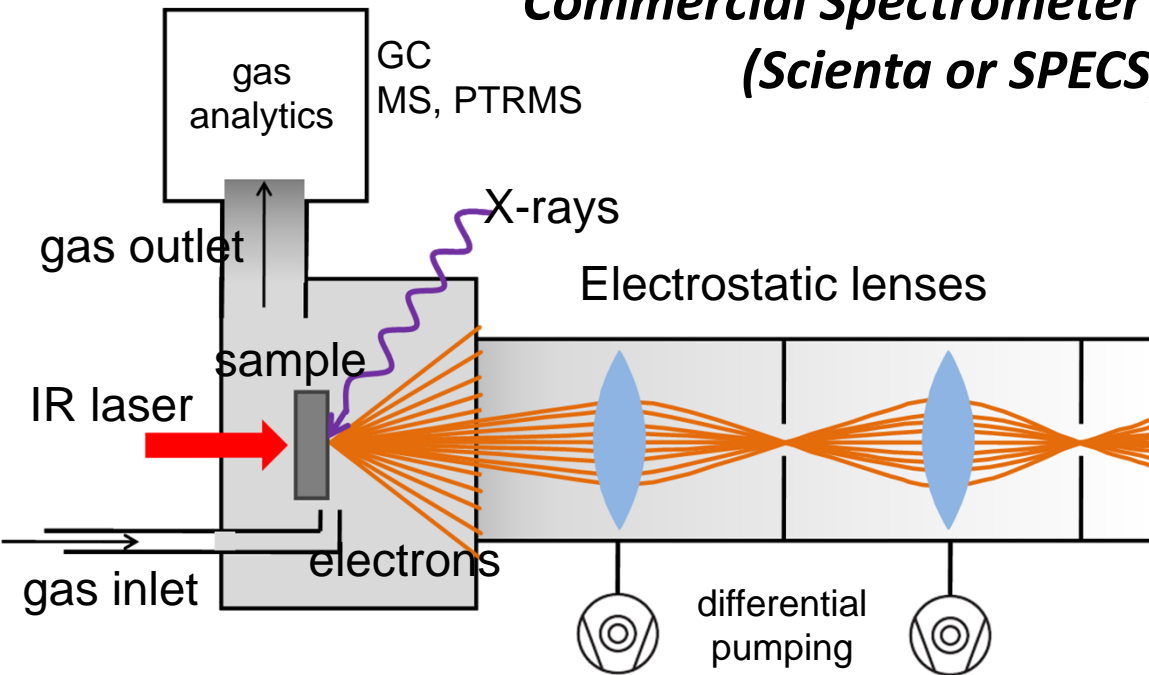
Ambient Pressure XPS (AP-XPS), RIXS

Environmental conditions

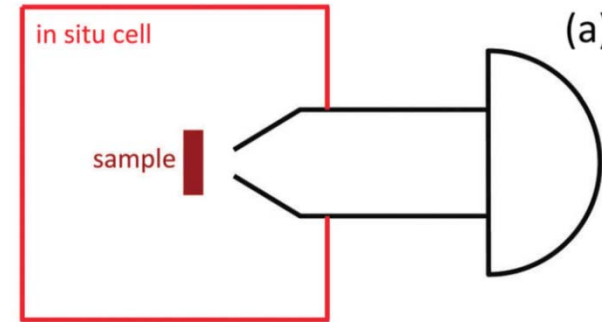
- ✓ *In situ measurements*
- ✓ *Catalysis*
- ✓ *Corrosion*
- ✓ *Hydrated surfaces*
- ✓ *Solvated molecules*
- ✓ *Correlated materials*

APXPS endstation

Commercial Spectrometer ~10 mbar (Scienta or SPECS)

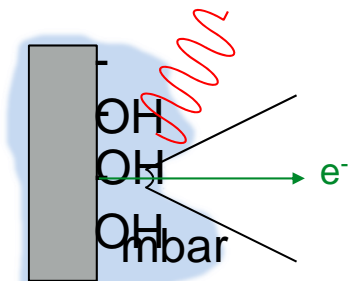


Interchangeable Chambers

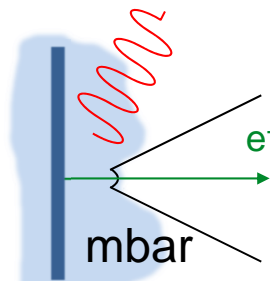


Probing interfaces

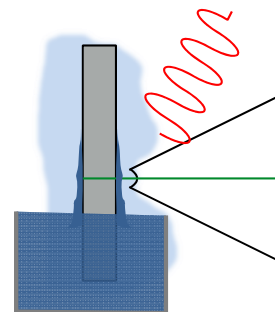
Solid-gas



Liquid-gas



Solid-liquid

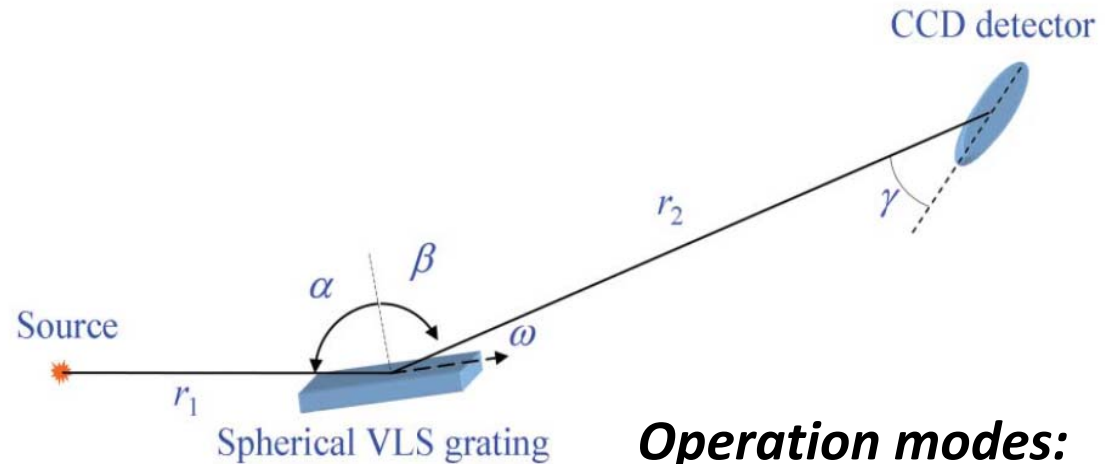


Requirements:

Spot size < 10 μm

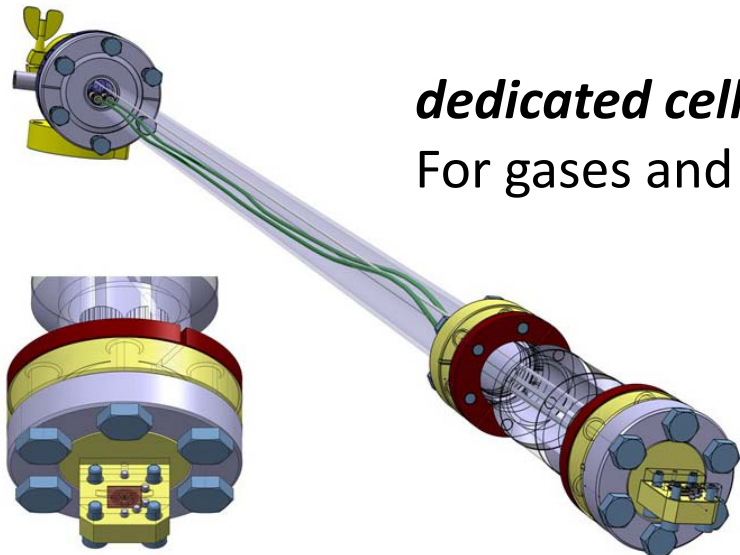
$E/\Delta E \sim 5000$

- ✓ Spherical VLS
- ✓ Electron Multiplying CCD
- ✓ Variable 4-6 m arm



Operation modes:

- ✓ High resolution ~ 50000
- ✓ High transmission



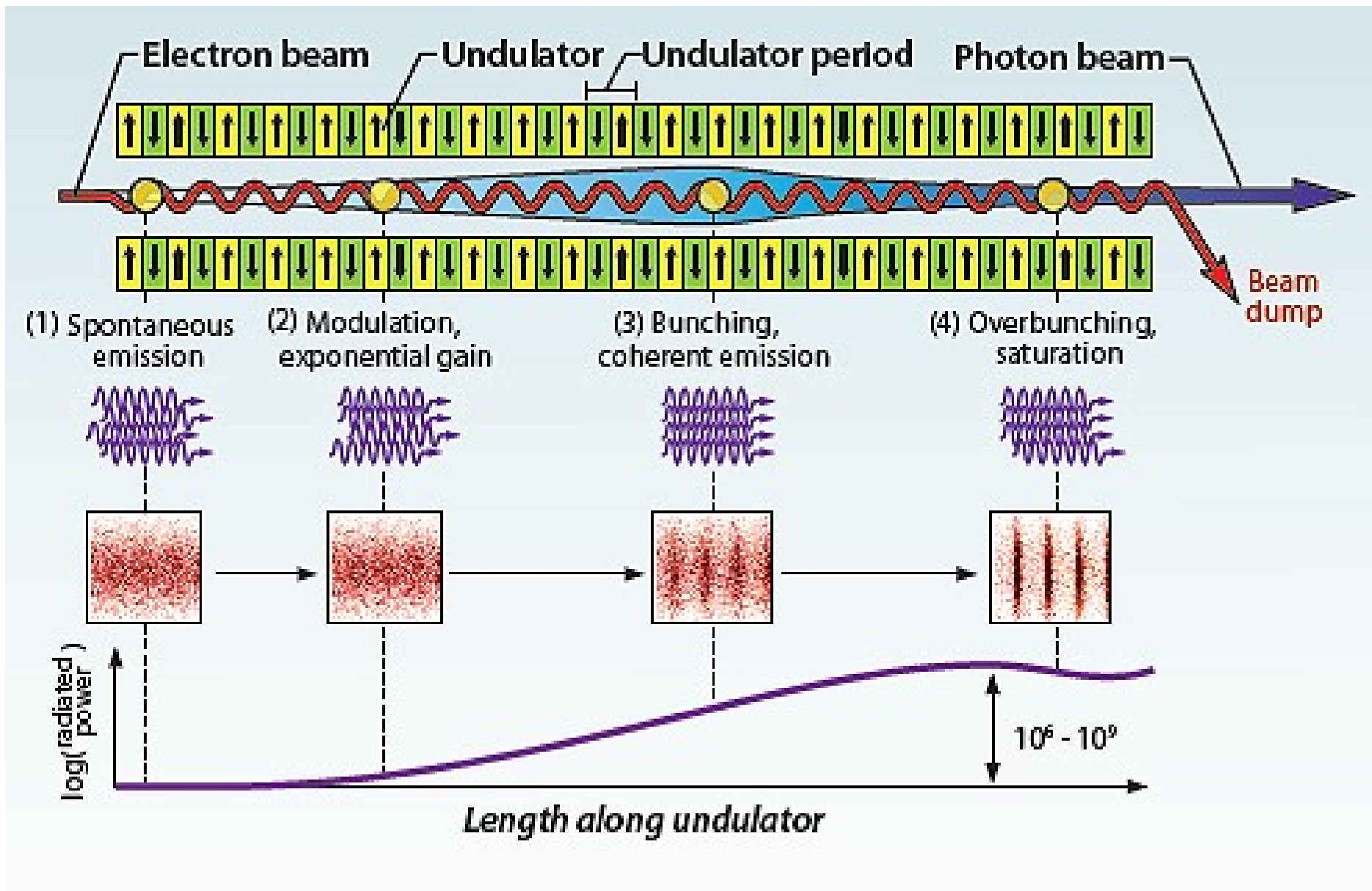
dedicated cells
For gases and liquids

Requirements:

Spot size $< 1 \mu\text{m}$

$E/\Delta E \sim 60000 @ 500\text{eV}$

The Next Generation: The Free-Electron Laser

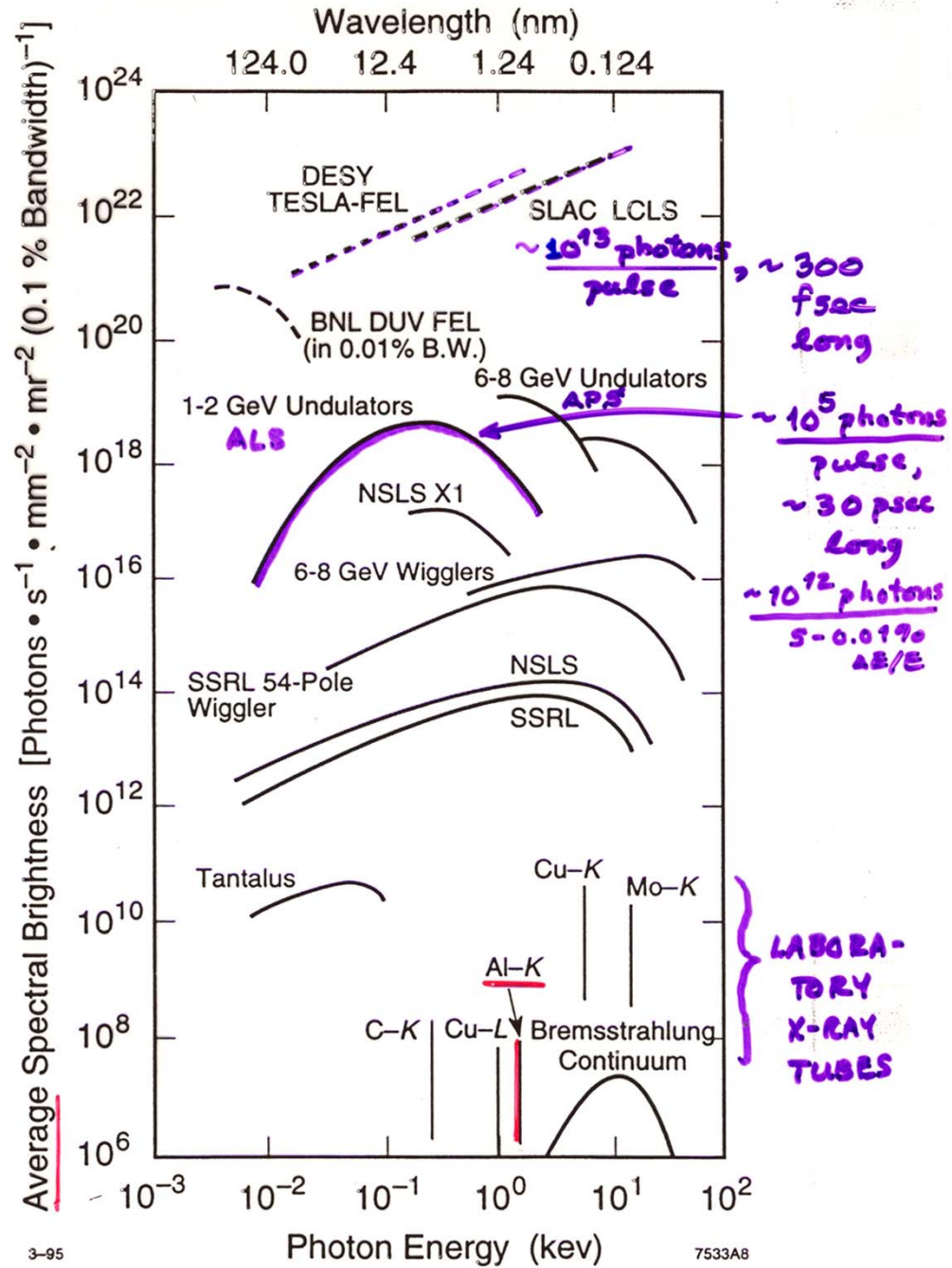


Average brightness

PRESENT
&
FUTURE

PRESENT

PAST



3-95

7533A8

Fig. 2. Average brightness comparisons of the LCLS and other light sources, including proposed FELs at Brookhaven [14] and DESY [15].

Peak brightness

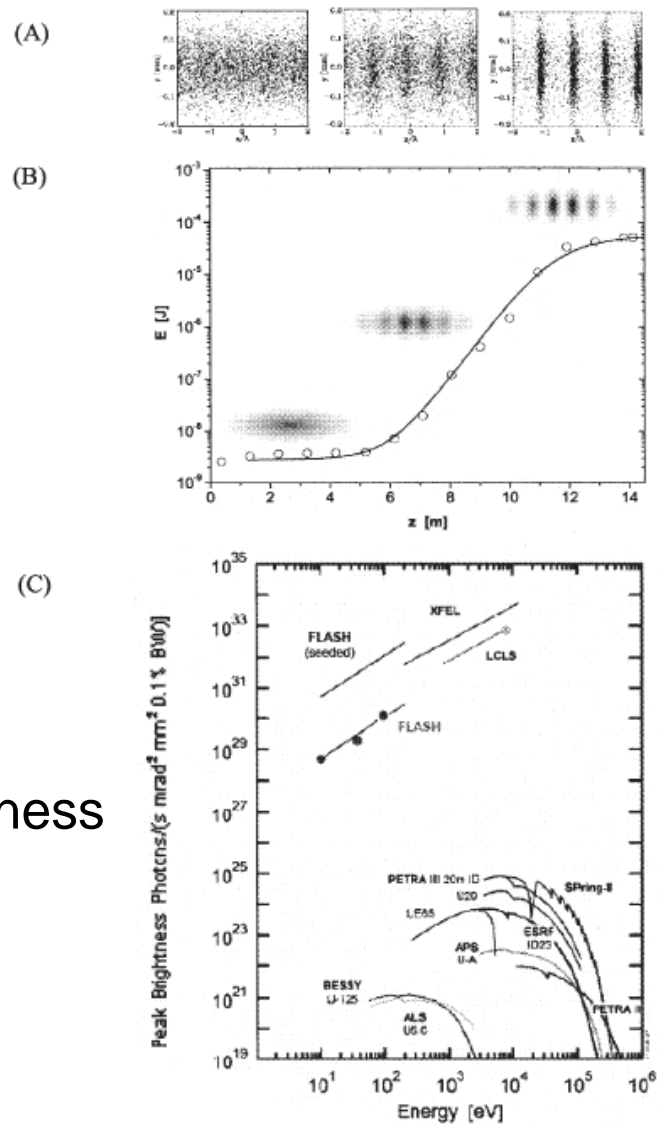
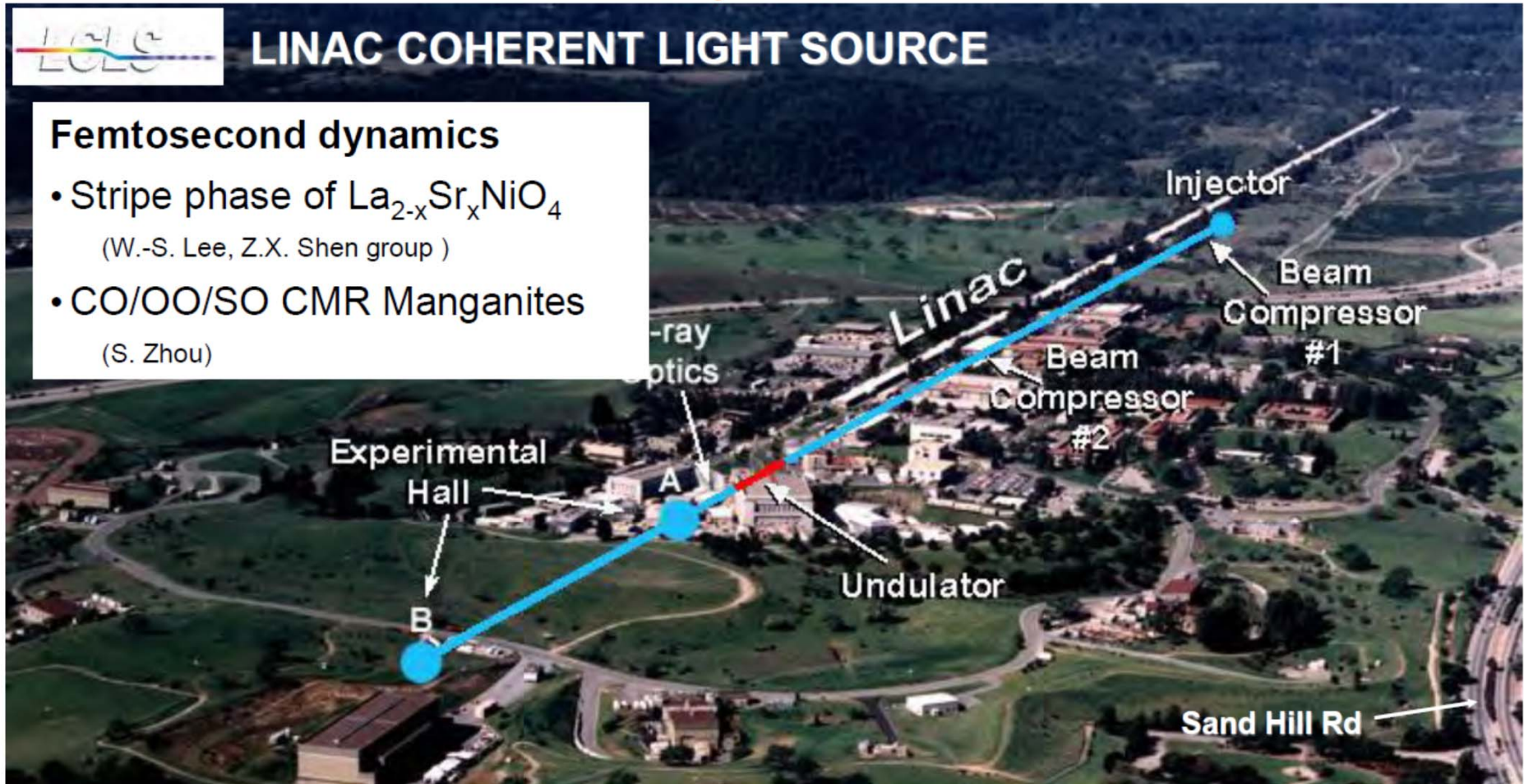


Figure 2-10. (A) Simulation of the electron microbunching process and (B) the exponential growth of FEL output energy due to microbunching (following S. Reiche and K.-J. Kim). (C) FEL beams have very short pulse duration and full spatial coherence, with peak brightness many orders of magnitude higher than 3rd generation synchrotron facilities [4, modified].

An operational vuv/x-ray free-electron laser

SLAC National Accelerator Laboratory



**Plus: FLASH (Hamburg)
Fermi (Trieste)
SACLA (Japan)
XFEL-soon (Hamburg)**

**MULTI-TECHNIQUE
SPECTROMETER/
DIFFRACTOMETER (MTSD)**

**5-axis
sample
manipulator**

**Sample prep.
chamber: LEED,
Knudsen cells,
electromagnet,...**

**Scienta
electron
spectrometer
(hidden)**

**ALS
BL 9.3.1
 $h\nu = 2-5 \text{ keV}$**

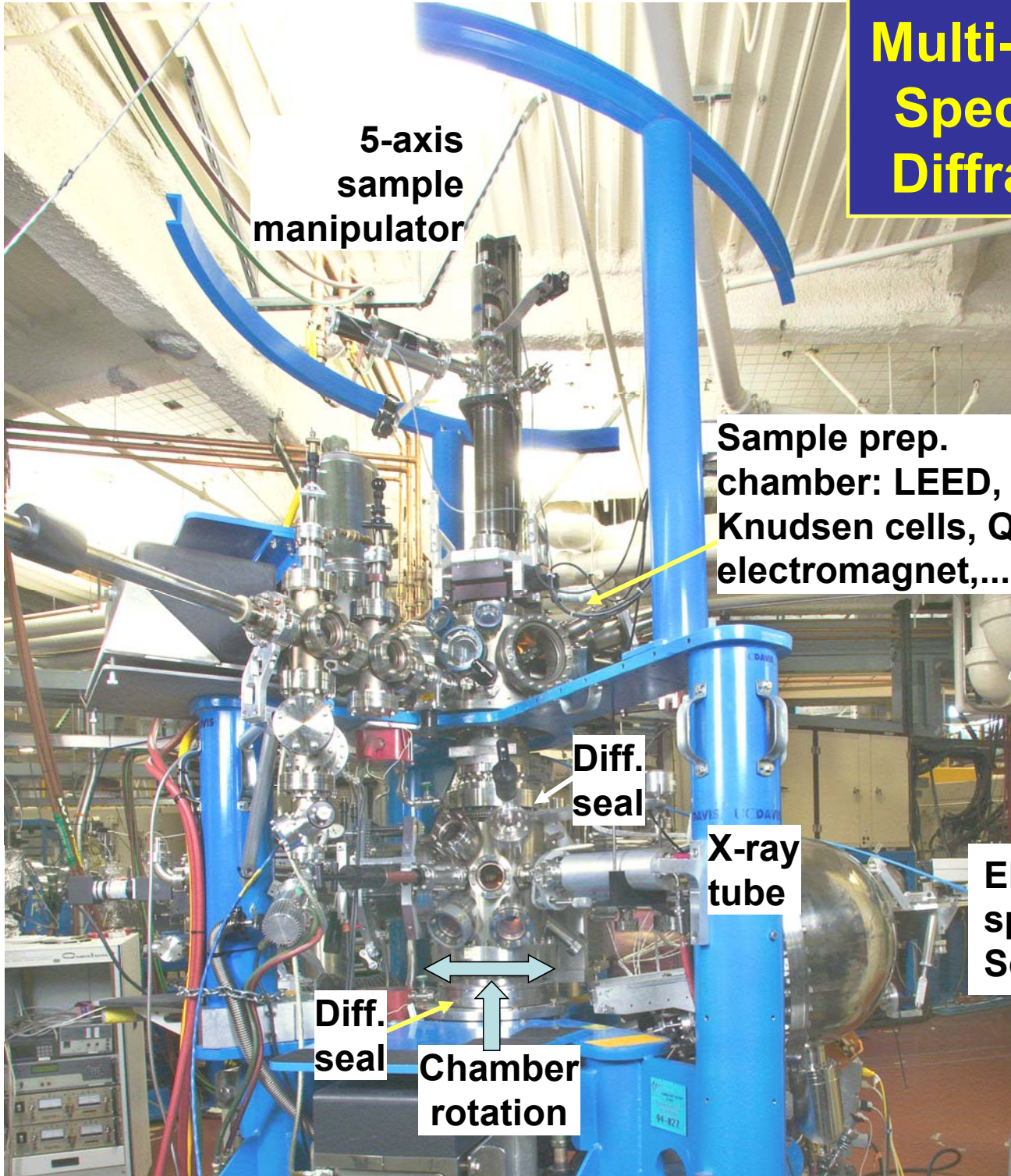


**Chamber
rotation**

**Scienta
soft x-ray
spectrometer**

**Permits using all relevant soft and hard x-ray spectroscopies on a single sample:
PS, PD, PH; XAS (e^- or photon detection), XES/RIXS, with MCD, MLD**

Multi-Technique Spectrometer/ Diffractometer



5-axis
sample
manipulator

Loadlock
for sample
introduction

Sample prep.
chamber: LEED,
Knudsen cells, QCM,
electromagnet,...

Diff.
seal

X-ray
tube

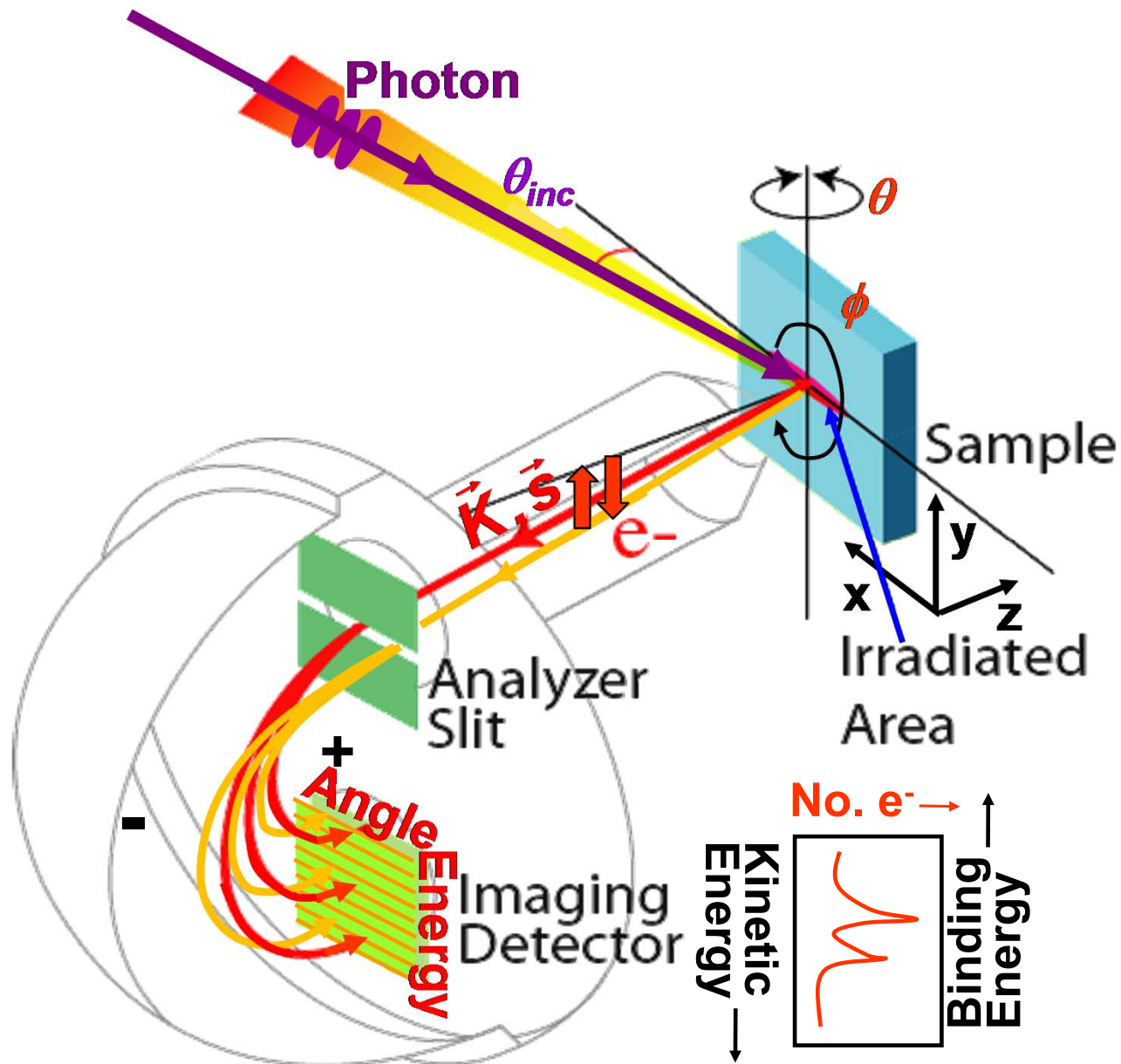
Electron
spectrometer:
Scienta SES 200

Soft x-ray
spectrometer:
Scienta
XES 300

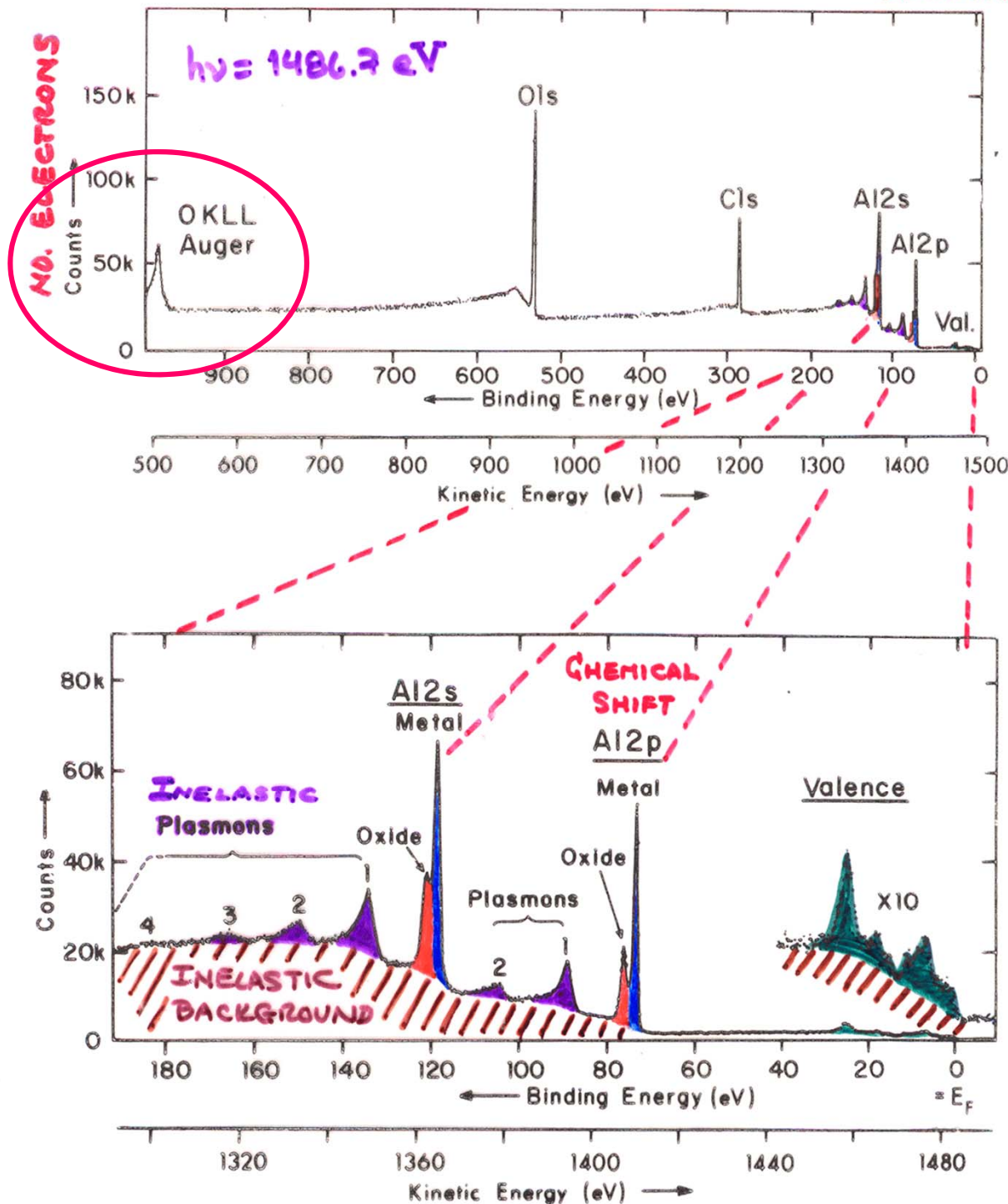
Diff.
seal

Chamber
rotation

Typical experimental geometry for energy- and angle-resolved photoemission measurements



TYPICAL PHOTOELECTRON SPECTRA: OXIDIZED ALUMINUM

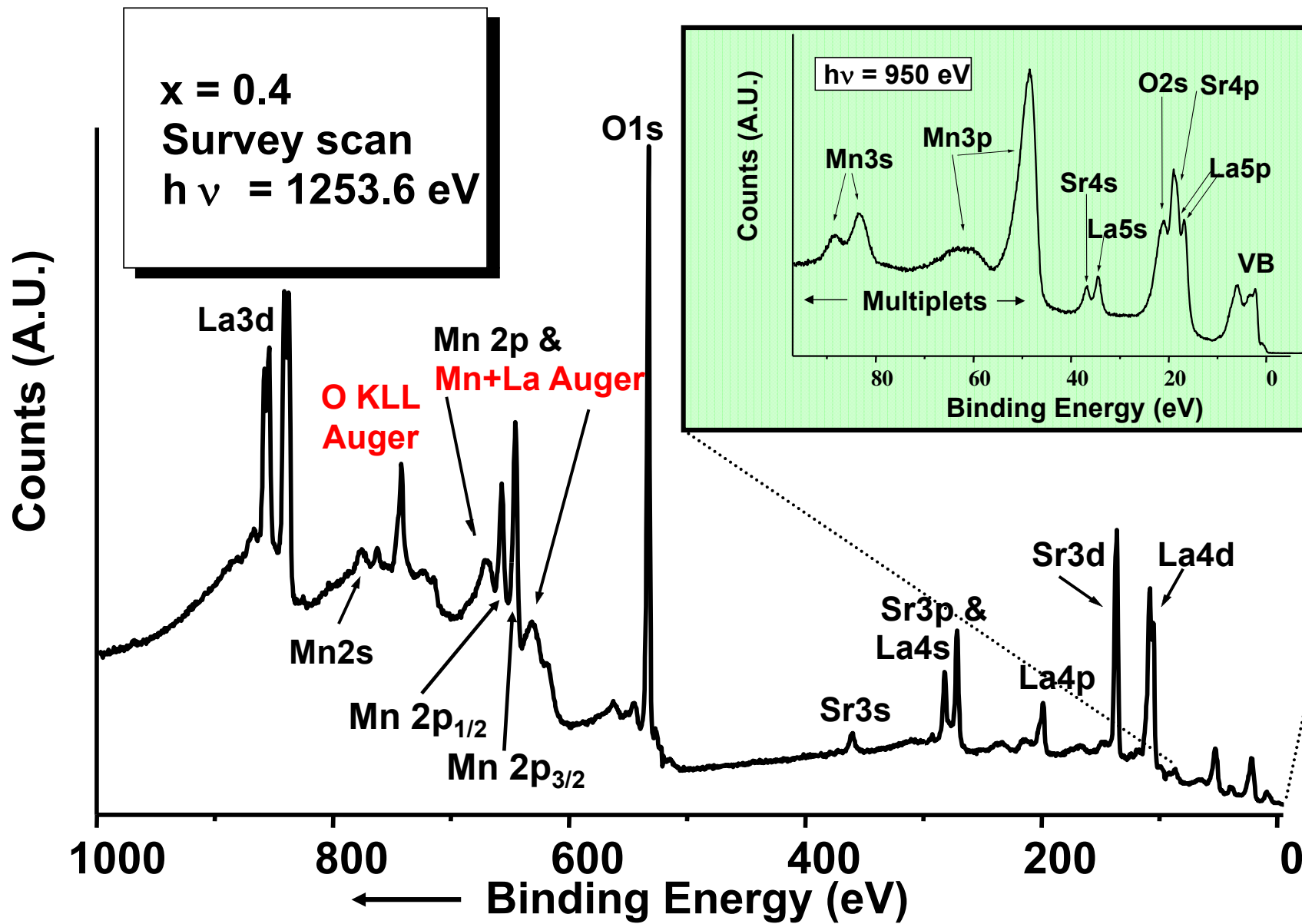


Auger kinetic energies do not change with photon energy

Photoelectron kinetic energies shift linearly with photon energy

“Basic Concepts of XPS”
Figure 1

Core and valence photoemission



Basic Concepts:

A Little Electronic Structure

The X-Ray-Based Experiments

X-Ray Sources, Synchrotron Radiation, Free Electron Lasers

Core-Level Photoemission



Intensities and Quantitative Analysis, the 3-Step Model

Varying Surface and Bulk Sensitivity

Chemical Shifts

Multiplet Splittings

Electron Screening and Satellite Structure

Magnetic and Non-Magnetic Dichroism

Resonant Photoemission

Photoelectron Diffraction and Holography

Valence-Level Photoemission

Band-Mapping in the Ultraviolet Photoemission Limit

Densities of States in the X-Ray Photoemission Limit

Some New Directions

Photoemission with Hard X-Rays (throughout lectures)

Photoemission with Standing Wave Excitation

Photoemission with: Higher Pressures → multi-Torr → Atmosphere?

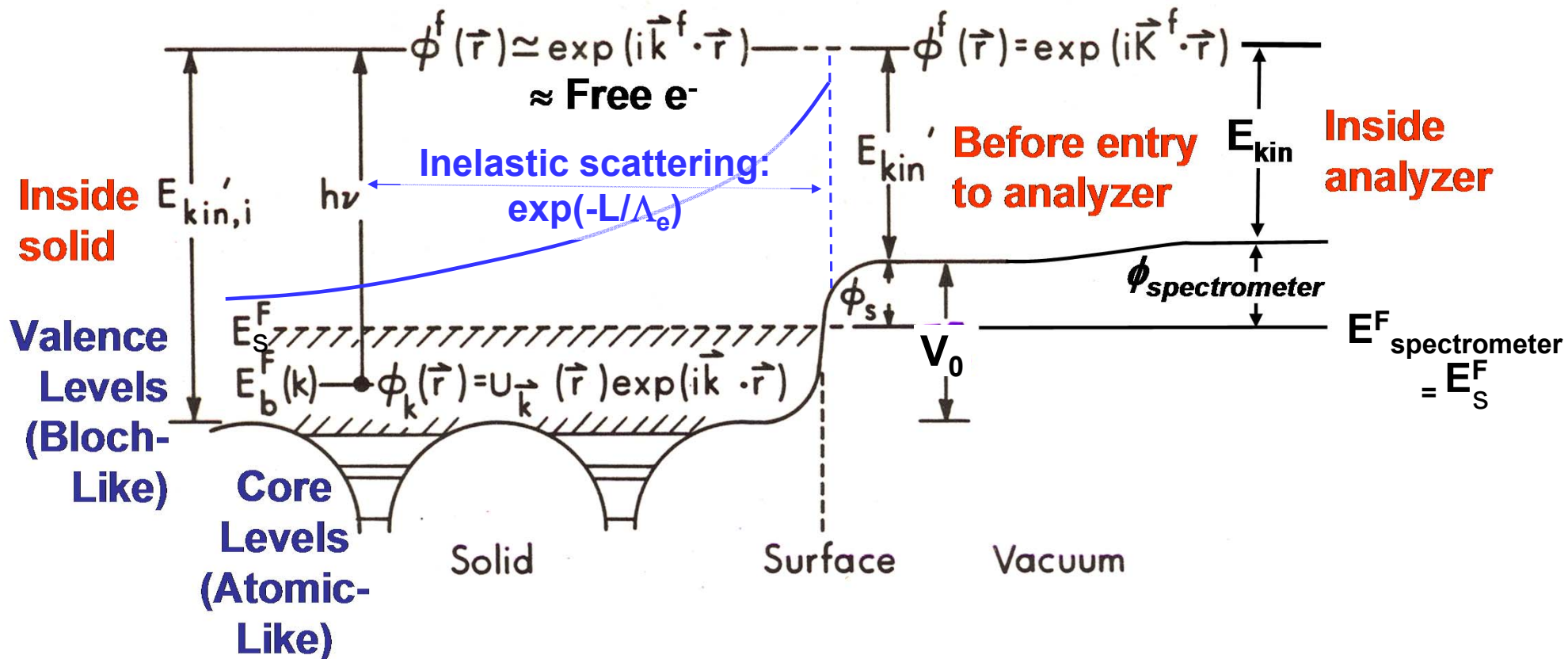
Spatial Resolution-Photoelectron Microscopy

Temporal Resolution

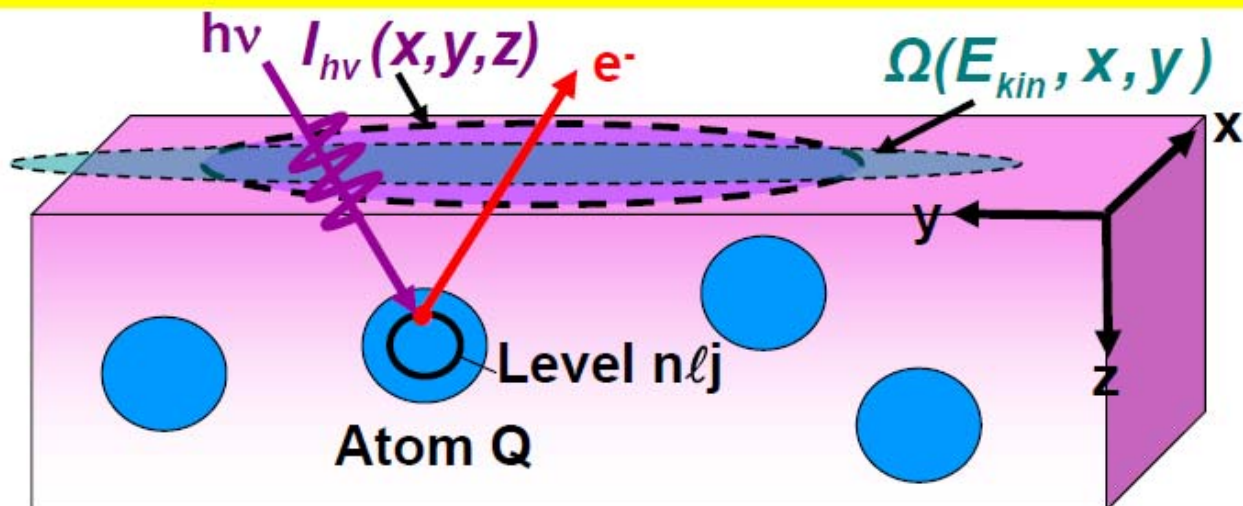
Basic energetics

$$h\nu = E_{\text{binding}}^{\text{Vacuum}} + E_{\text{kinetic}} = E_{\text{binding}}^{\text{Fermi}} + \phi_{\text{spectrometer}} + E_{\text{kinetic}}$$

One-Electron Picture of Photoemission from a Surface



CORE PHOTOELECTRON INTENSITIES AND COMPOSITION



$$I(Qn\ell j) =$$

$$C \int_0^{\infty} I_{hv}(x,y,z) \rho_Q(x,y,z) \frac{d\sigma_{Qn\ell j}(hv)}{d\Omega} \exp\left[-\frac{z}{\Lambda_e(E_{kin}) \sin\theta}\right] \Omega(E_{kin}, x, y) dx dy dz$$

$$I_{hv}(x,y,z) = \text{x-ray flux}$$

$\rho_Q(x,y,z)$ = density of atoms Q → quantitative analysis

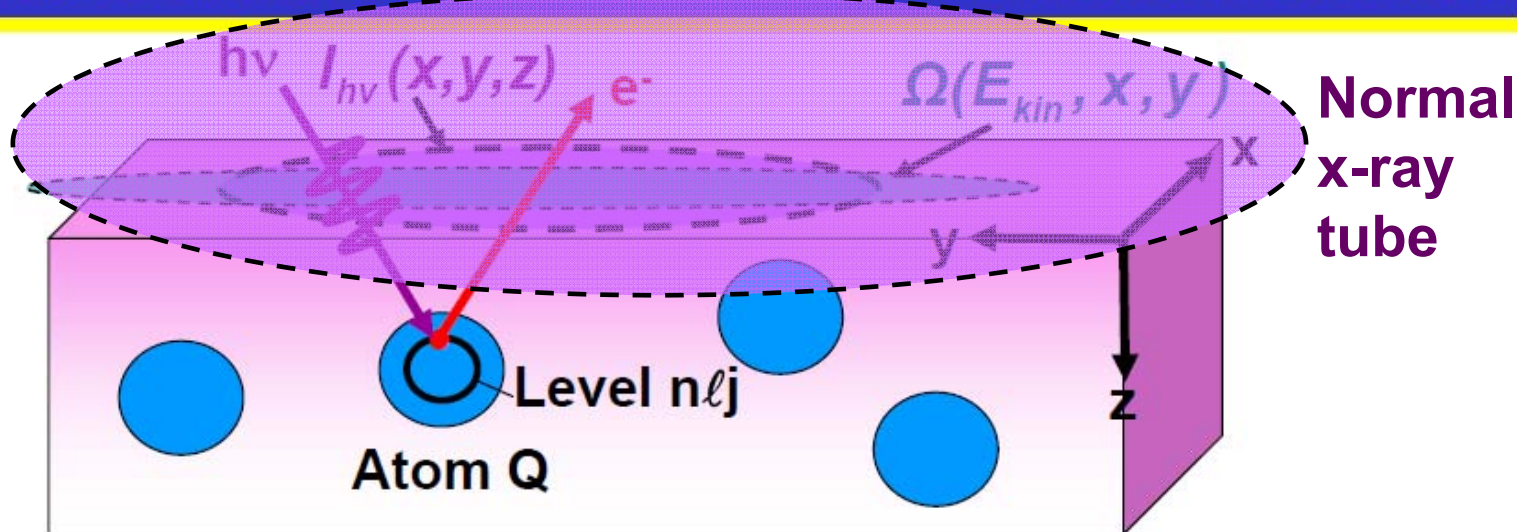
$$\frac{d\sigma_{Qn\ell j}(hv)}{d\Omega} = \text{energy-dependent differential photoelectric cross section for subshell } Qn\ell j$$

$$\Lambda_e(E_{kin}) = \text{energy-dependent inelastic attenuation length}$$

→ Effective Attenuation Length (EAL) → Mean Emission Depth (MED)

$$\Omega(E_{kin}, x, y) = \text{energy-dependent spectrometer acceptance solid angle}$$

CORE PHOTOELECTRON INTENSITIES AND COMPOSITION



$$I(Qn\ell j) =$$

$$C \int_0^{\infty} I_{hv}(x, y, z) \rho_Q(x, y, z) \frac{d\sigma_{Qn\ell j}(hv)}{d\Omega} \exp\left[-\frac{z}{\Lambda_e(E_{kin}) \sin\theta}\right] \Omega(E_{kin}, x, y) dx dy dz$$

$$I_{hv}(x, y, z) = \text{x-ray flux}$$

$\rho_Q(x, y, z)$ = density of atoms Q → quantitative analysis

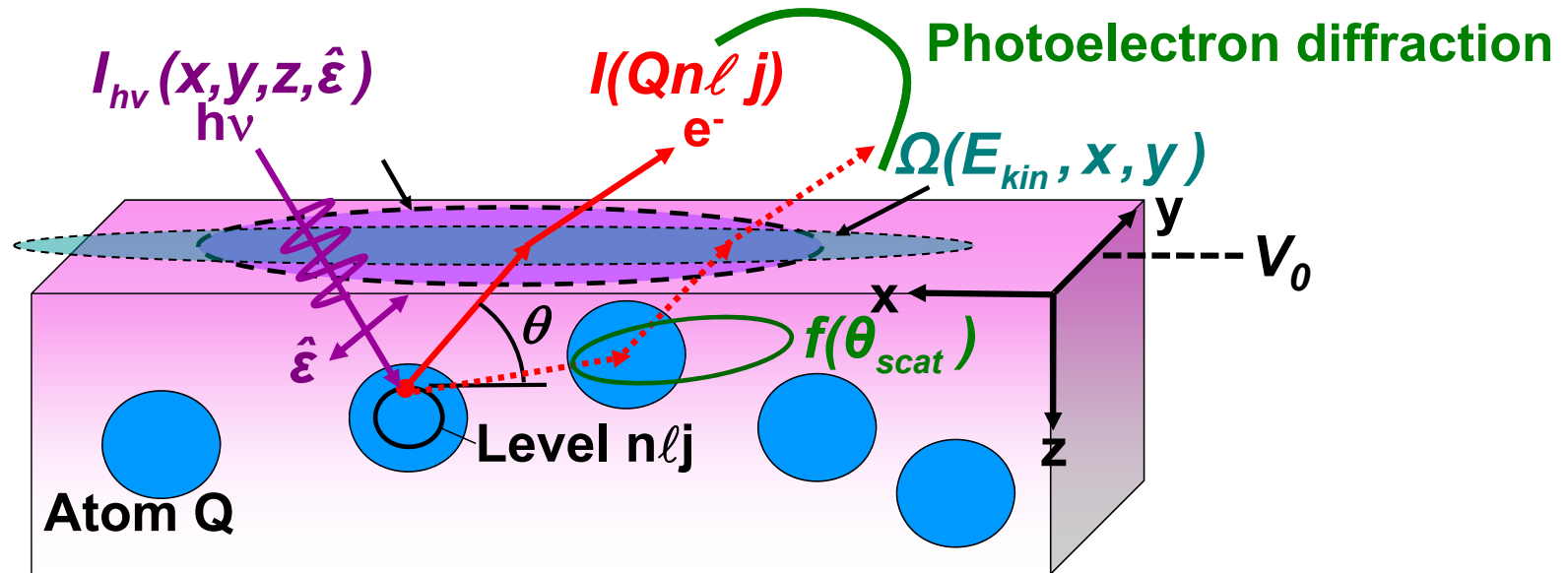
$$\frac{d\sigma_{Qn\ell j}(hv)}{d\Omega} = \text{energy-dependent differential photoelectric cross section for subshell } Qn\ell j$$

$$\Lambda_e(E_{kin}) = \text{energy-dependent inelastic attenuation length}$$

→ Effective Attenuation Length (EAL) → Mean Emission Depth (MED)

$$\Omega(E_{kin}, x, y) = \text{energy-dependent spectrometer acceptance solid angle}$$

ATOMIC (CORE) PHOTOELECTRON INTENSITIES: THE THREE-STEP MODEL



$$I(Qn\ell j) =$$

$$C \int_0^{\infty} I_{hv}(x,y,z,\hat{\epsilon}) \rho_Q(x,y,z) \frac{d\sigma_{Qn\ell j}(hv,\hat{\epsilon})}{d\Omega} \exp\left[-\frac{z}{\Lambda_e(E_{kin}) \sin\theta}\right] \Omega(E_{kin},x,y) dx dy dz$$

$I_{hv}(x,y,z,\hat{\epsilon})$ = x-ray flux, $\hat{\epsilon}$ = polarization

$\rho_Q(x,y,z)$ = density of atoms Q → quantitative analysis

$\frac{d\sigma_{Qn\ell j}(hv,\hat{\epsilon})}{d\Omega}$ = **energy-dependent** differential photoelectric cross section for subshell Qnℓj

$\Lambda_e(E_{kin})$ = **energy-dependent** inelastic attenuation length + **elastic scattering**: $f(\theta_{scatt})$

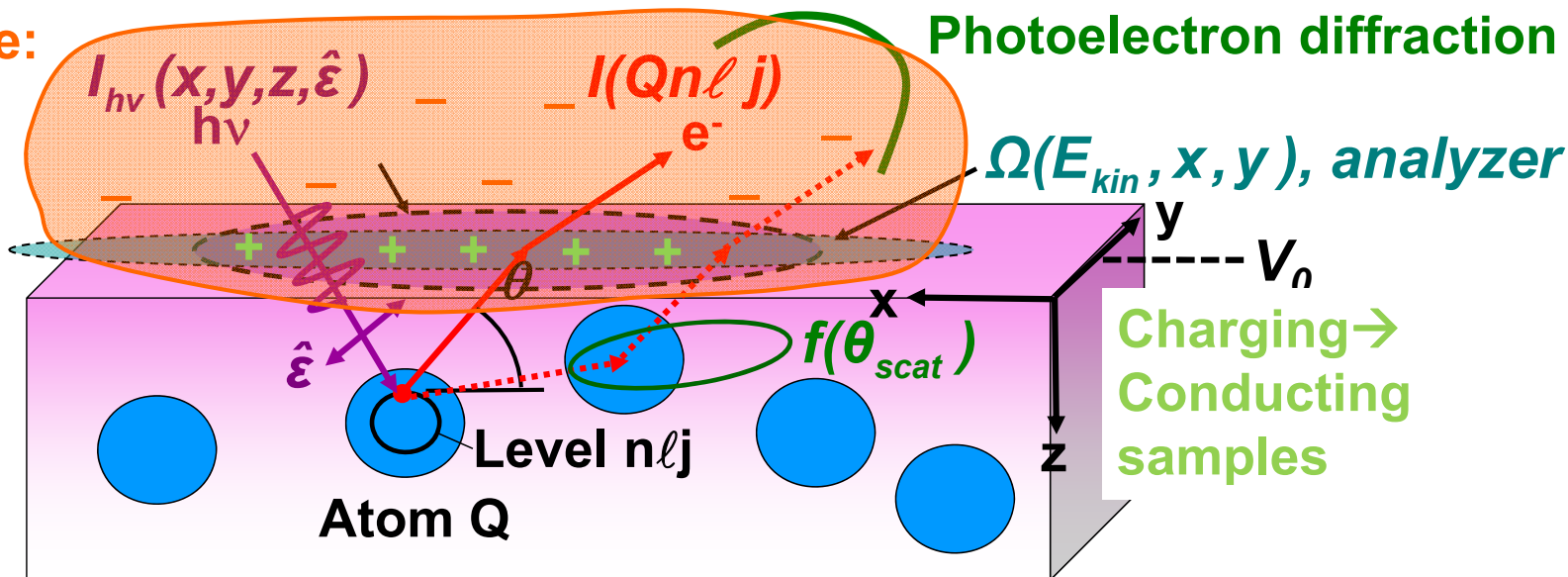
→ Effective Attenuation Length (EAD) → Mean Emission Depth (MED)

$\Omega(E_{kin},x,y)$ = **energy-dependent** spectrometer acceptance solid angle = transmission function

V_0 = inner potential

ATOMIC (CORE) PHOTOELECTRON INTENSITIES: THE "FOUR-STEP" MODEL

e⁻ space charge:
 Hellman et al.
 (FLASH), Phys. Rev.
 B 85, 075109 (2012);
 Oloff et al. (SACLA),
 New J. Phys. 16,
 123045 (2014);
 J.Sync.Rad.Res. 21,
 183 (2014): Turn
 down the light!



$I(Qn\ell j) =$

$$C \int_0^{\infty} I_{h\nu}(x, y, z, \hat{\epsilon}) \rho_Q(x, y, z) \frac{d\sigma_{Qn\ell j}(h\nu, \hat{\epsilon})}{d\Omega} \exp\left[-\frac{z}{\Lambda_e(E_{kin}) \sin\theta}\right] \Omega(E_{kin}, x, y) dx dy dz$$

$I_{h\nu}(x, y, z, \hat{\epsilon}) =$ x-ray flux, $\hat{\epsilon}$ = polarization

$\rho_Q(x, y, z) =$ density of atoms Q \rightarrow quantitative analysis

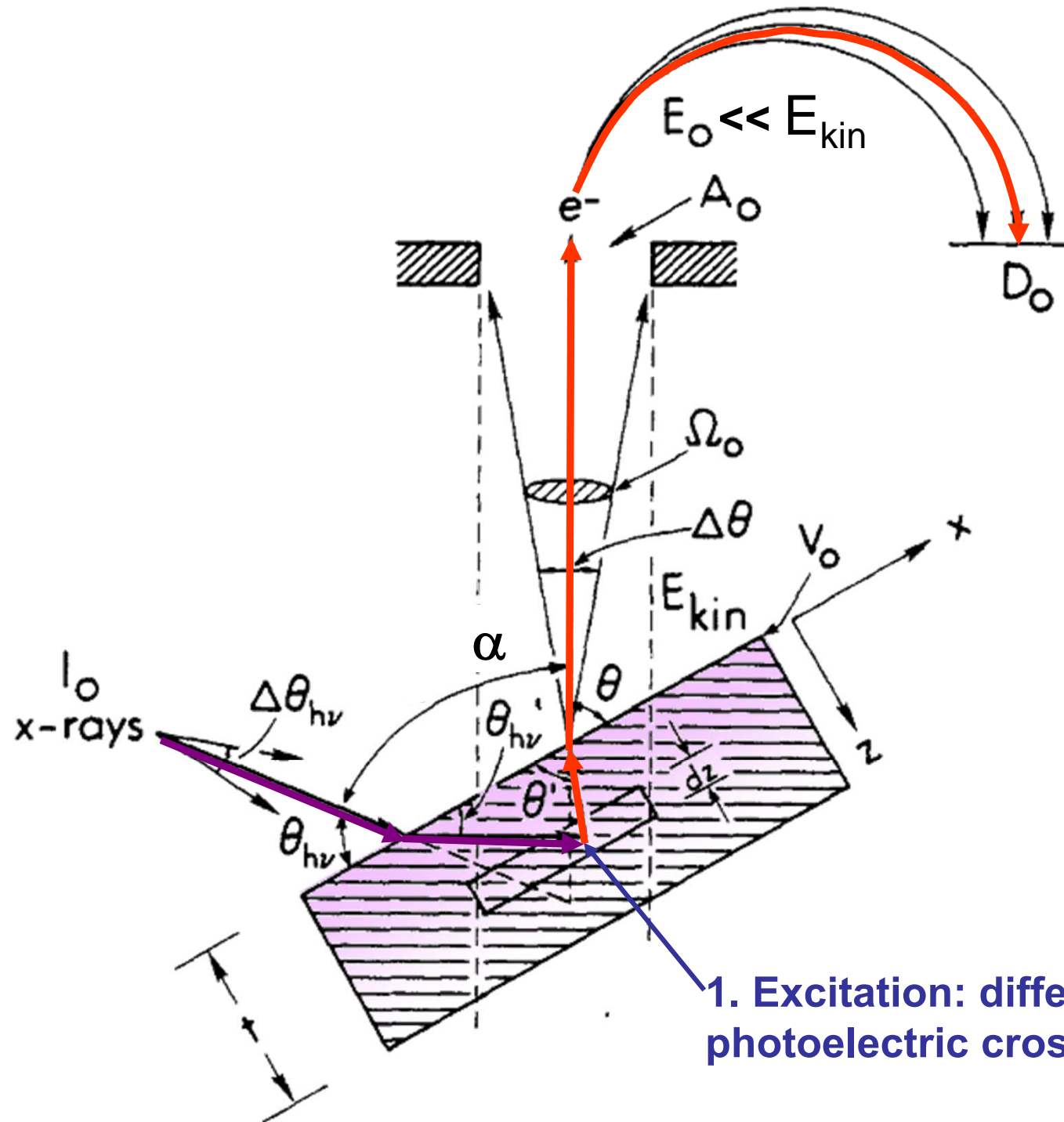
$\frac{d\sigma_{Qn\ell j}(h\nu, \hat{\epsilon})}{d\Omega} =$ energy-dependent differential photoelectric cross section for subshell Qn ℓ j

$\Lambda_e(E_{kin}) =$ energy-dependent inelastic attenuation length + elastic scattering: $f(\theta_{scatt})$
 \rightarrow Effective Attenuation Length (EAD) \rightarrow Mean Emission Depth (MED)

$\Omega(E_{kin}, x, y) =$ energy-dependent analyzer acceptance solid angle = transmission function

$V_0 =$ inner potential

PHOTOELECTRON INTENSITIES—THE 3-STEP MODEL

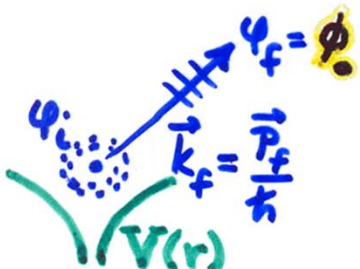


1. Excitation: differential photoelectric cross section ($d\sigma/d\Omega$)

PHOTOELECTRON EMISSION - BASIC MATRIX ELEMENTS + SELECTION RULES:

● ATOMIC-LIKE (LOCALIZED) STATES ⇒ CORE:

$$\psi_i(\vec{r}) = \psi_{n_i, l_i, m_i}(r, \theta, \phi) = R_{n_i, l_i}(r) Y_{l_i, m_i}(\theta, \phi) \begin{cases} \alpha(\sigma) = m_{s_i} = +1/2 = \uparrow \\ \beta(\sigma) = m_{s_i} = -1/2 = \downarrow \end{cases}$$



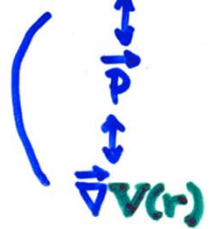
$$\psi_f(\vec{r}, \vec{k}_f) = \psi_{E_f}(\vec{r}, \vec{k}_f) \begin{cases} \alpha(\sigma) \\ \beta(\sigma) \end{cases}$$

$$= 4\pi \sum_{l_f, m_f} i^{l_f} e^{-i\delta_{l_f}} Y_{l_f, m_f}^*(\theta, \phi) Y_{l_f, m_f}(\theta, \phi) R_{E_f, l_f}(r) \begin{cases} \alpha(\sigma) \\ \beta(\sigma) \end{cases}$$

PHASE SHIFT OF l_f WAVE IN $V(r)$

DIPOLE APPROX.: INT. $\propto |\langle \psi_f | \hat{E} \cdot \vec{r} | \psi_i \rangle|^2 = |\hat{E} \langle \psi_f | \vec{r} | \psi_i \rangle|^2 \Rightarrow \left\{ \begin{array}{l} \Delta l = l_f - l_i = \pm 1 \\ \text{TWO CHANNELS} \end{array} \right.$

EQUIVALENT WITHIN CONSTANT FACTOR



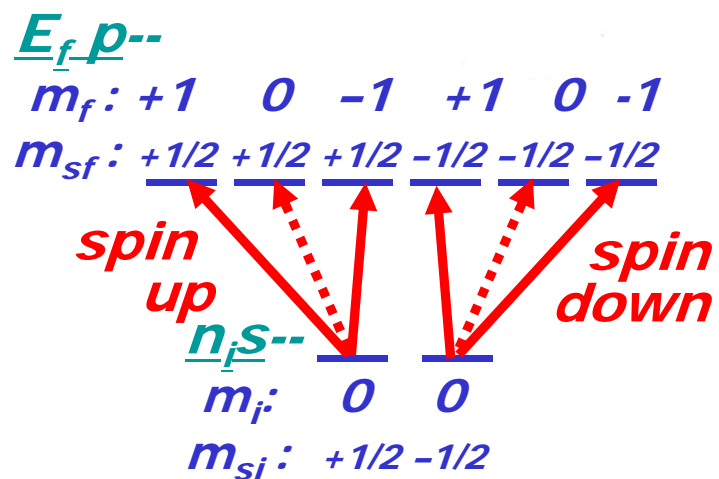
- $\Delta m = m_f - m_i = 0, \pm 1$
LINEAR POLARIZ.
- $\Delta m = \pm 1$, CIRCULAR POLARIZATION

$$\Delta m_s = m_{s_f} - m_{s_i} = 0!$$

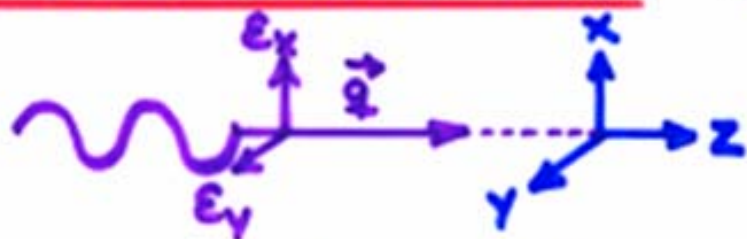
FOR A GIVEN n_i, l_i, m_i, m_{s_i} : SUM OVER DEGENERATE INITIAL STATES m_i, m_{s_i} AND AVERAGE OVER FINAL STATES E_f, l_f, m_f, m_{s_f} ACCESSED FROM EACH m_i TO YIELD DIFFERENTIAL SUBSHELL PHOTOELECTRIC CROSS SECTION:

$$d\sigma_{n_i, l_i} / d\Omega$$

\propto PROBABILITY PER UNIT SOLID ANGLE OF EXCITING ONE ELECTRON FROM SUBSHELL n_i, l_i INTO THE DIRECTION k_f



● RADIATION POLARIZATION: $\hat{\mathbf{E}} \cdot \vec{r} = \hat{\mathbf{E}} \cdot (x\hat{x} + y\hat{y} + z\hat{z})$



LINEARLY POLARIZED -

 x: $\hat{\mathbf{E}} \cdot \vec{r} \Rightarrow x \Rightarrow \text{INT.}_x$
 $\propto Y_{\ell=1, m_\ell=+1}(\theta, \phi) + Y_{\ell=1, m_\ell=-1}(\theta, \phi)$

 y: $\hat{\mathbf{E}} \cdot \vec{r} \Rightarrow y \Rightarrow \text{INT.}_y$
 $\propto Y_{\ell=1, m_\ell=+1}(\theta, \phi) - Y_{\ell=1, m_\ell=-1}(\theta, \phi)$

CIRCULARLY POLARIZED $\propto Y_{\ell=1, m_\ell=1}(\theta, \phi)$

 LEFT \equiv LCP: $\hat{\mathbf{E}} \cdot \vec{r} \Rightarrow x - iy \Rightarrow \text{INT.}_{LCP}$

 RIGHT \equiv RCP: $\hat{\mathbf{E}} \cdot \vec{r} \Rightarrow x + iy \Rightarrow \text{INT.}_{RCP}$
 $\propto Y_{\ell=1, m_\ell=+1}(\theta, \phi)$

UNPOLARIZED -

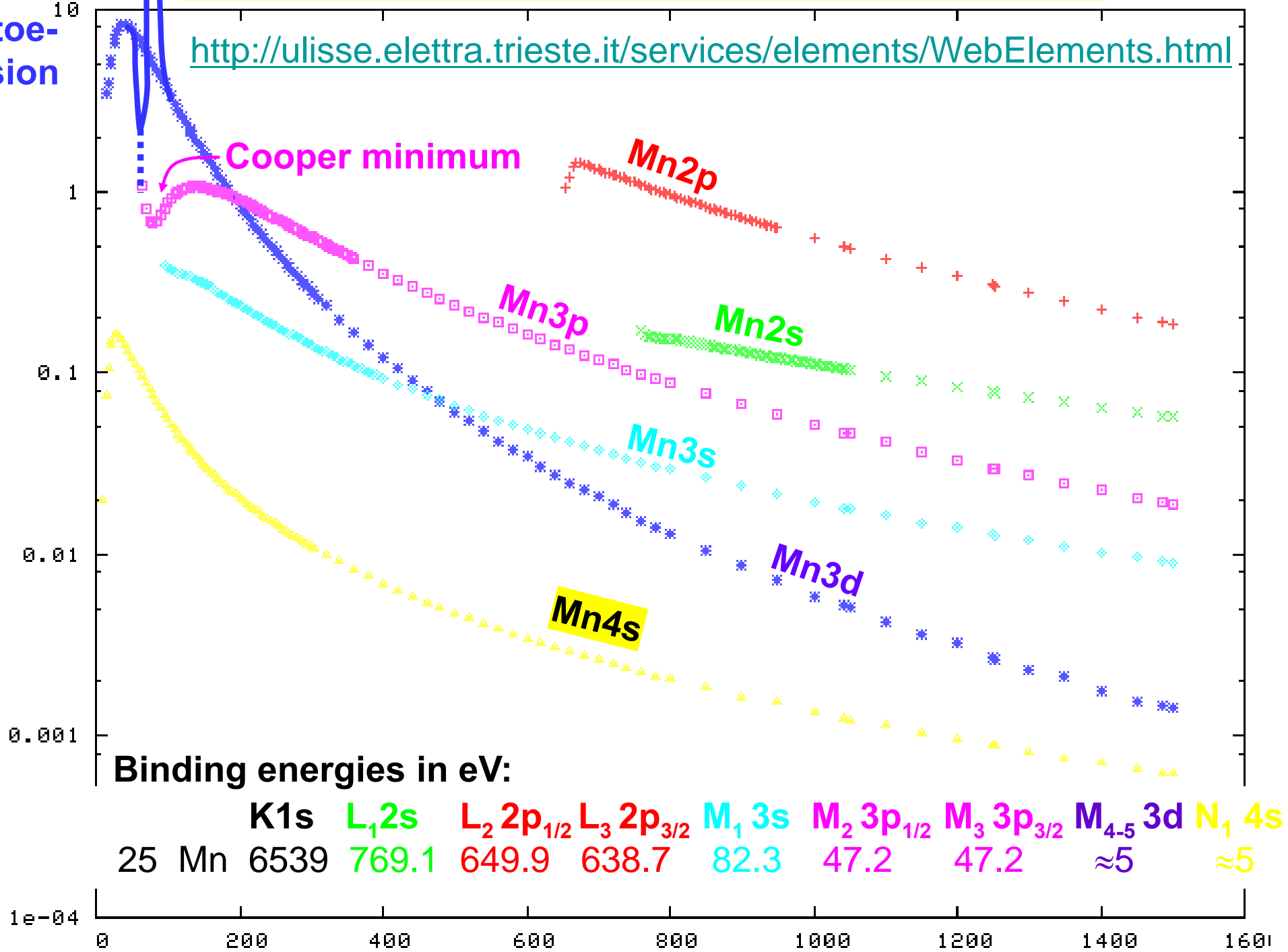
 $\text{INT.}_{UNP} = \text{INT.}_x + \text{INT.}_y$
 $= \text{INT.}_{LCP} + \text{INT.}_{RCP}$

PHOTOELECTRIC CROSS SECTIONS FOR Mn

<http://ulisse.elettra.trieste.it/services/elements/WebElements.html>

Resonant
Photoe-
mission

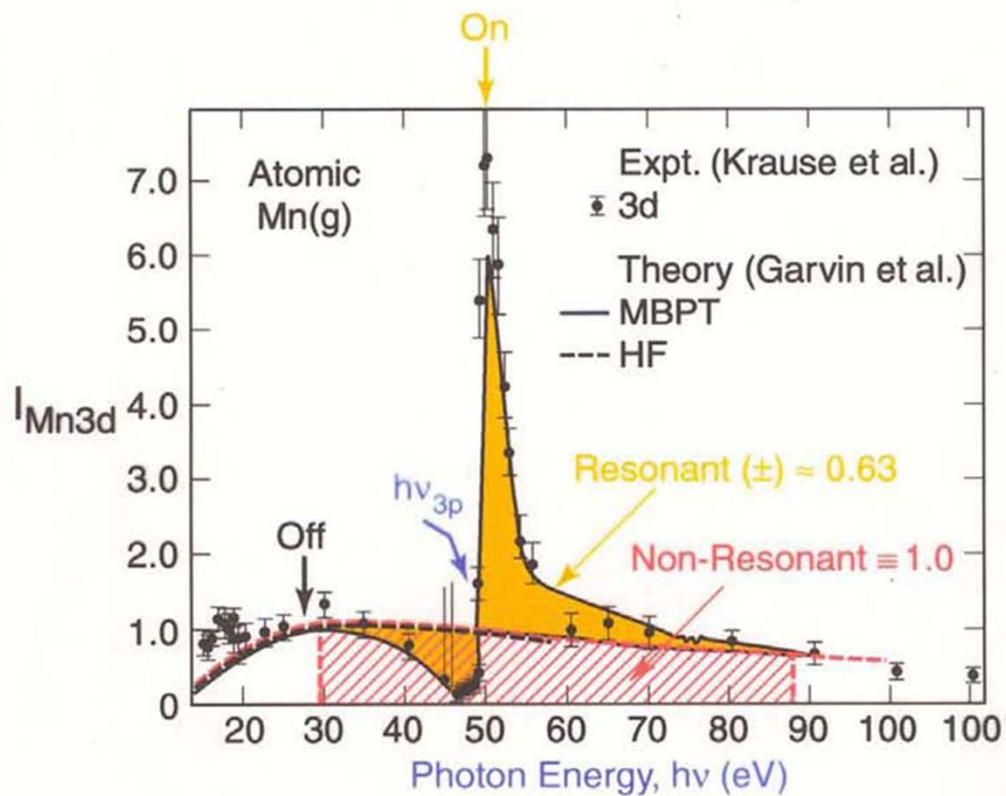
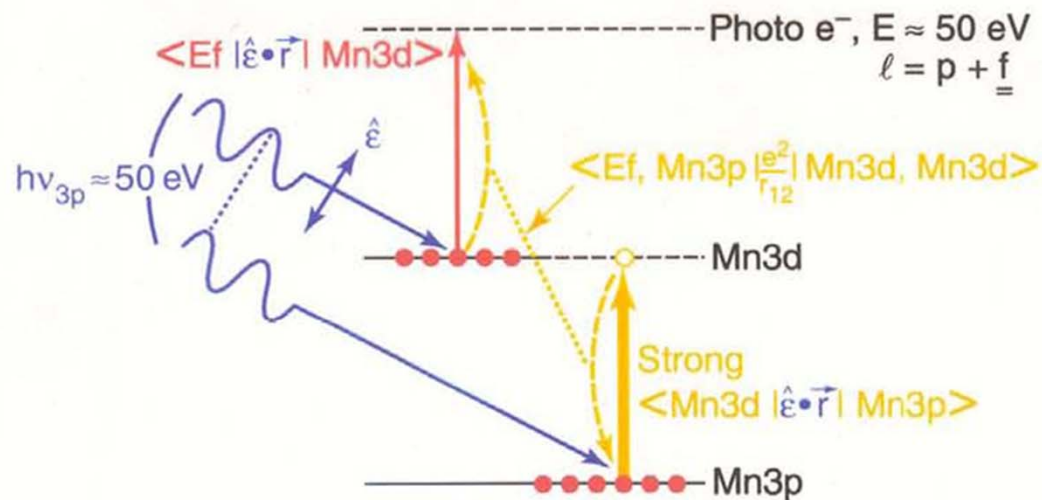
Cross section (Mbarns)



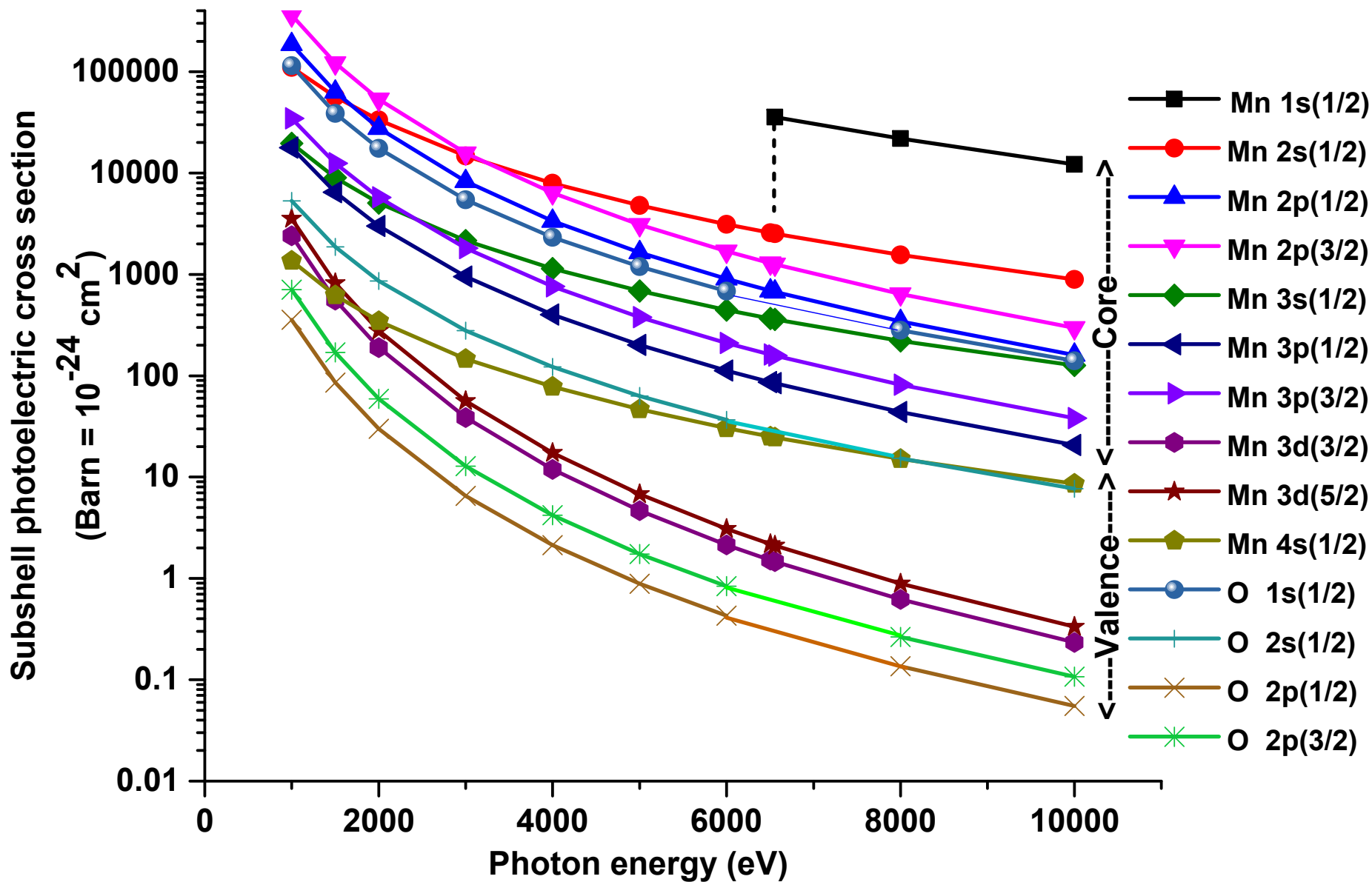
Photon Energy (eV)

Single-atom resonant photoemission:

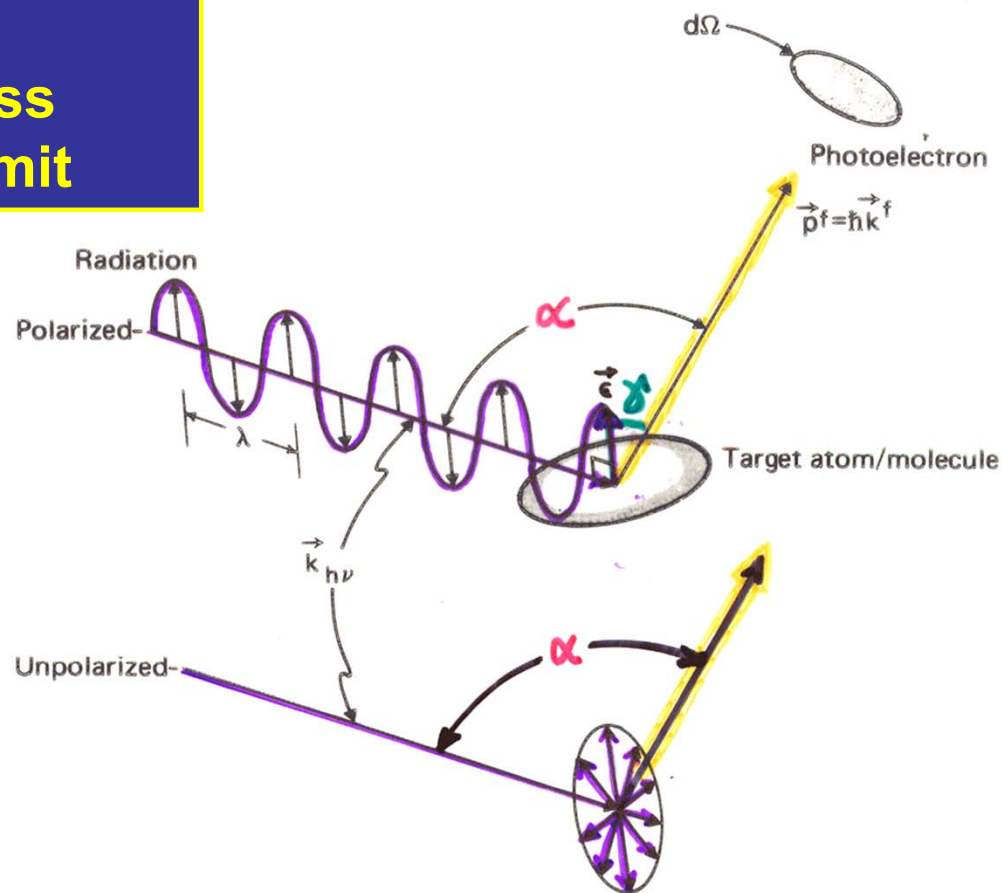
Ex. – Mn atom: Mn3d emission, resonance with Mn3p



Photoelectric cross sections for O and Mn (Scofield)



The differential photoelectric cross section—dipole limit



FOR ATOMIC-LIKE EMISSION:

LIN.

$$\text{POLARIZED: } \frac{d\sigma_{nl}(E_f)}{d\Omega} = \frac{\sigma_{nl}(E_f)}{4\pi} \left[1 + \beta_{nl}(E_f) \left(\frac{3}{2} \cos^2 \gamma - \frac{1}{2} \right) \right]$$

$$\text{UNPOLARIZED: } \frac{d\sigma_{nl}(E_f)}{d\Omega} = \frac{\sigma_{nl}(E_f)}{4\pi} \left[1 + \frac{1}{2} \beta_{nl}(E_f) \left(\frac{3}{2} \sin^2 \alpha - 1 \right) \right]$$

Figure 7 -- General geometry for defining the differential cross section $d\sigma/d\Omega$, showing both polarized and unpolarized incident radiation. The polarization vector \vec{e} is parallel to the electric field \vec{E} of the radiation. In order for the dipole approximation to be valid, the radiation wave length λ should be much larger than typical target dimensions (that is, the opposite of what is shown here).

WITH:

σ_{nl} = TOTAL CROSS SECTION

β_{nl} = ASYMMETRY PARAMETER

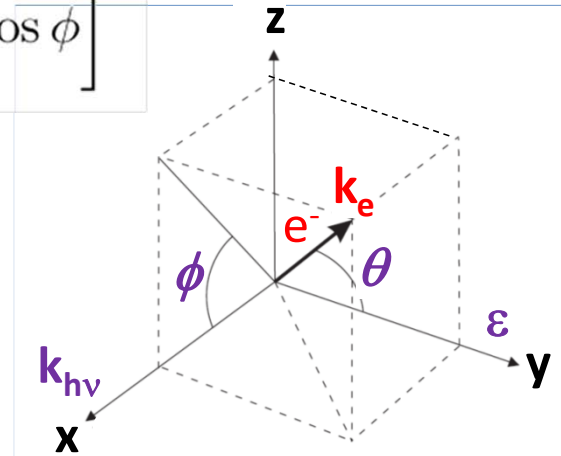
σ_{nl}, β_{nl} TABULATIONS IN: GOLDBERG ET AL., J. ELECT. SPECT. & YEH, LINDAU, AT. NUC. DATA 22, 1 ('85) \ 21, 285 ('81)

Differential photoelectric cross sections for filled $n\ell$ subshells, incl. non-dipole

$$\frac{d\sigma_{n\ell}(h\nu)}{d\Omega} = \frac{\sigma_{n\ell}(h\nu)}{4\pi} \left[1 + \frac{\beta_{n\ell}}{2}(3\cos^2\theta - 1) + (\delta_{n\ell} + \gamma_{n\ell}\cos^2\theta)\sin\theta\cos\phi \right]^*$$

$$\beta_{n\ell}(E^f) = \frac{\{l(l-1)R_{l-1}^2(E^f) + (l+1)(l+2)R_{l+1}^2(E^f) - 6l(l+1)R_{l+1}(E^f)R_{l-1}(E^f)\cos[\delta_{l+1}(E^f) - \delta_{l-1}(E^f)]\}}{(2l+1)[lR_{l-1}^2(E^f) + (l+1)R_{l+1}^2(E^f)]}$$

Dipole $d\sigma_{n\ell}/d\Omega$ calculated from R_{l-1} , R_{l+1} , δ_{l-1} , and δ_{l+1}



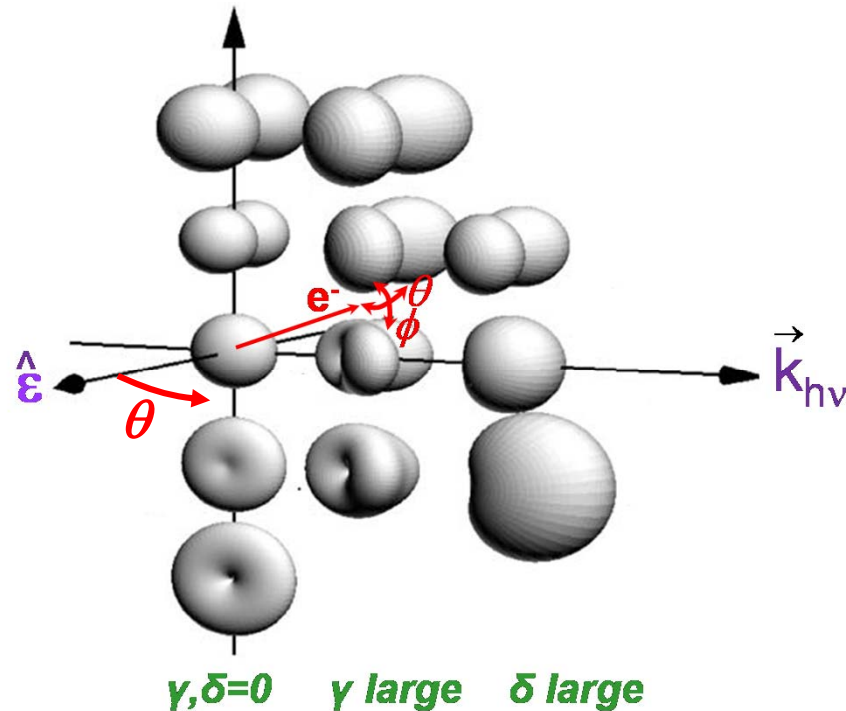
$$\beta_{n\ell} = 2$$

$$1$$

$$0$$

$$-0.5$$

$$-1$$



#At higher energies, valence cross sections are dominated by atomic-like part near the nucleus

*Guilleumin et al., Radiation Physics and Chemistry 75, 2258 (2006)

And for individual $d\sigma_{2p(x,y,z)}/d\Omega$ or $d\sigma_{3d(xy,yz,xz,z^2,x^2-y^2)}/d\Omega$?&

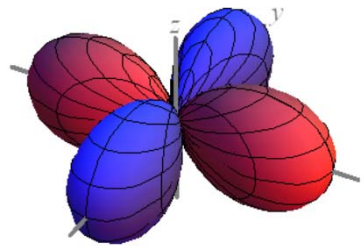
&Goldberg, Fadley, Kono, J. Electr. Spectr. 21, 285-363 (1985)

→Nemšák et al.

Gelius, in *Electron Spectroscopy*, D.A. Shirley, Ed. (North Holland, 1971) p. 311; Solterbeck et al., Phys. Rev. Lett. 79, 4681 (1997)

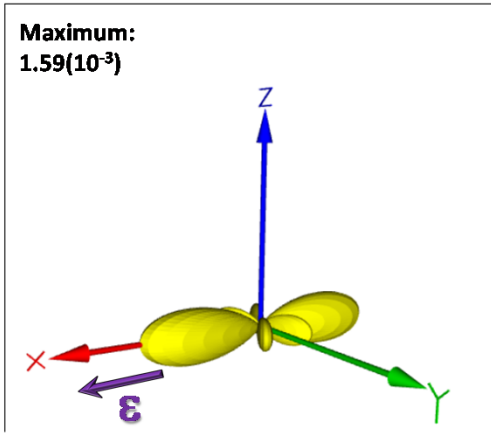


Energy and polarization dependence of orbital-specific differential cross sections: Cu $3d_{x^2-y^2}$ @ 800 and 5000 eV

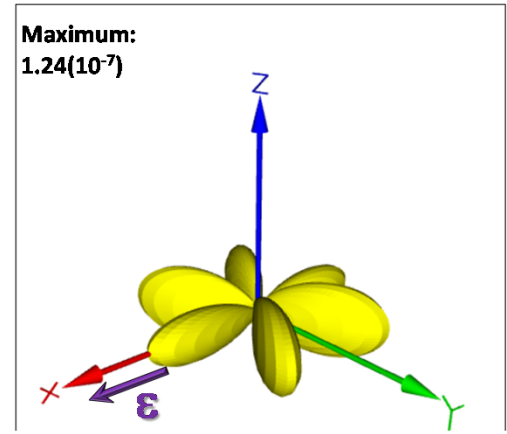


Cu $3d_{x^2-y^2}$

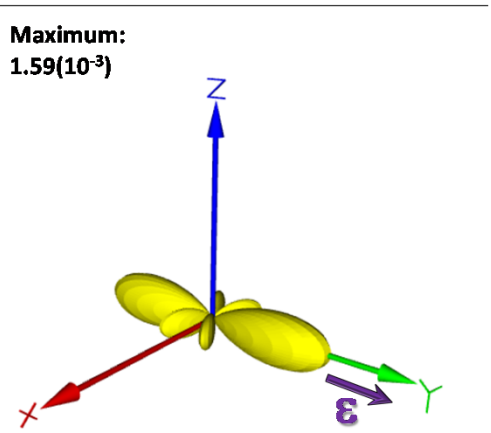
Nemšák et al., TBP; based on equations in Goldberg, Fadley, Kono, J. Electr. Spectr. 21, 285-363 (1985); CSF and S. Nemšák, J. Electron Spectr. 195, 409-422 (2014)



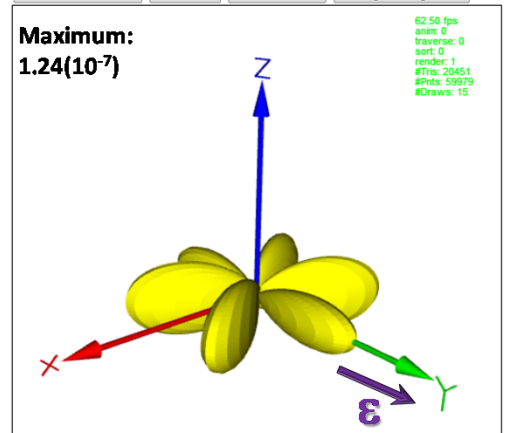
Cu $3d_{x^2-y^2}$ ($h\nu=800$ eV; $E \parallel [100]$)



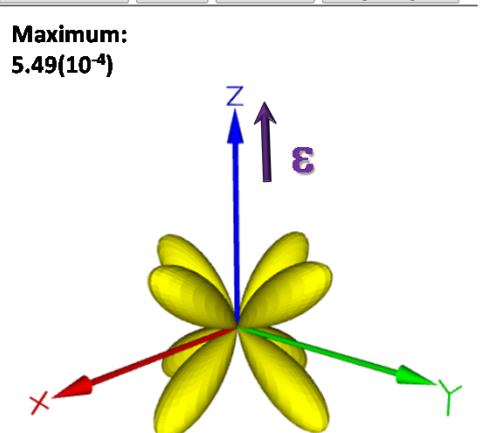
Cu $3d_{x^2-y^2}$ ($h\nu=5000$ eV; $E \parallel [100]$)



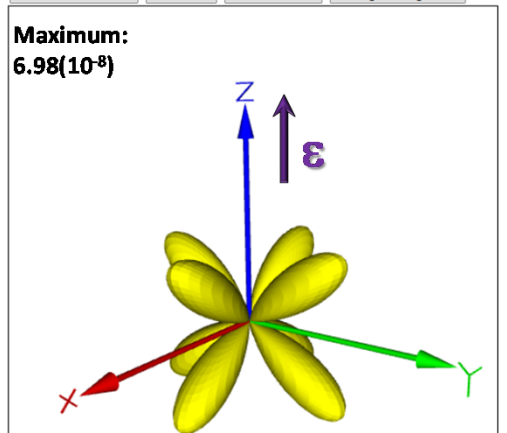
Cu $3d_{x^2-y^2}$ ($h\nu=800$ eV; $E \parallel [010]$)



Cu $3d_{x^2-y^2}$ ($h\nu=5000$ eV; $E \parallel [010]$)

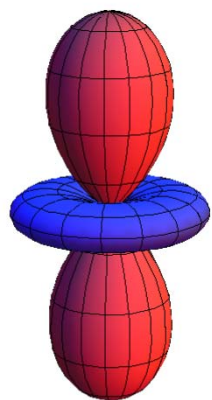


Cu $3d_{x^2-y^2}$ ($h\nu=800$ eV; $E \parallel [001]$)

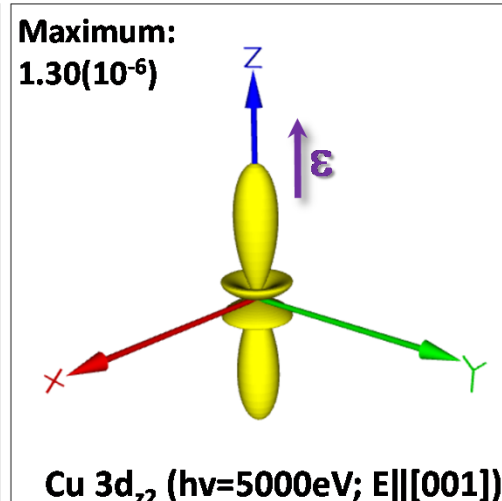
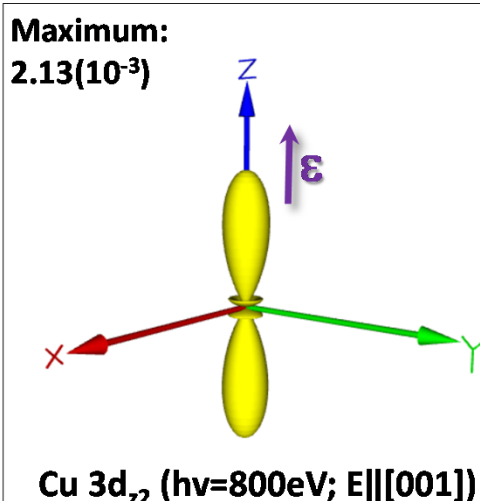
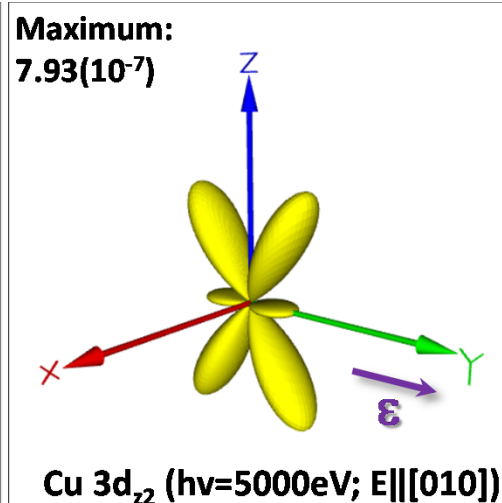
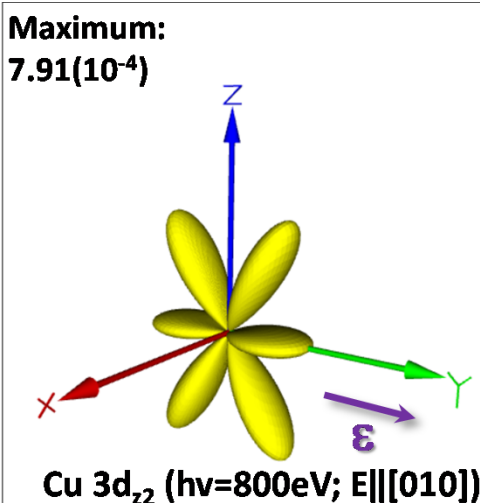
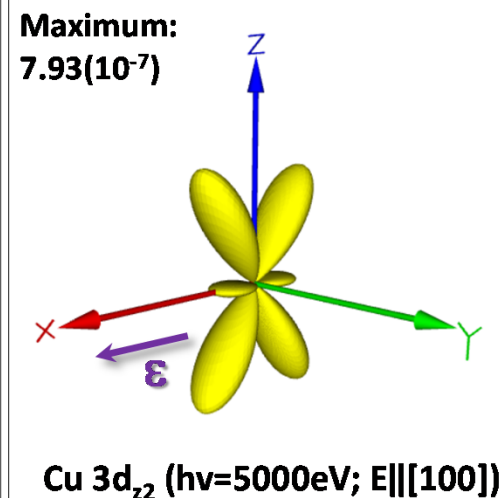
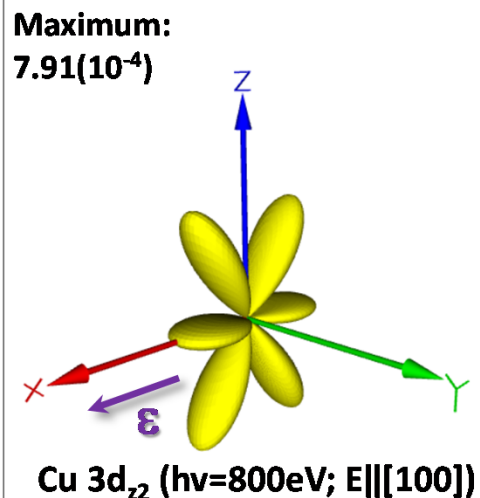


Cu $3d_{x^2-y^2}$ ($h\nu=5000$ eV; $E \parallel [001]$)

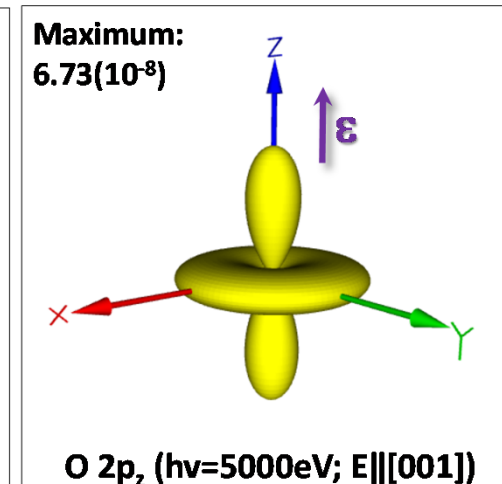
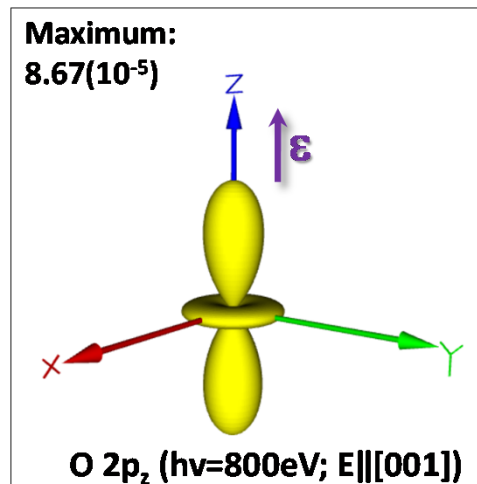
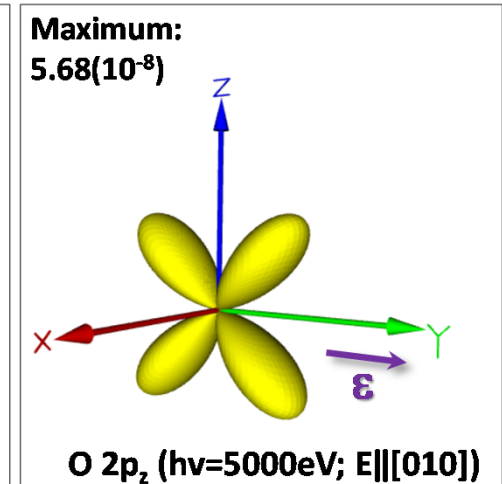
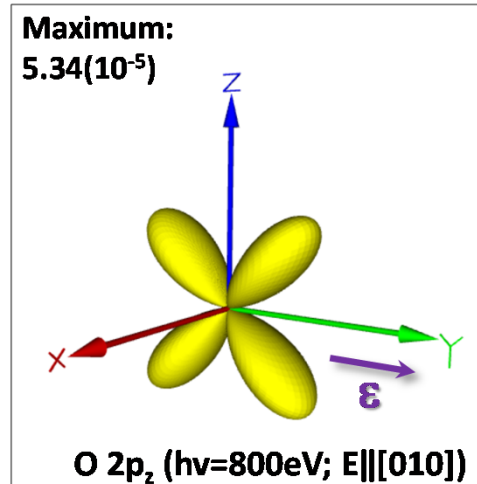
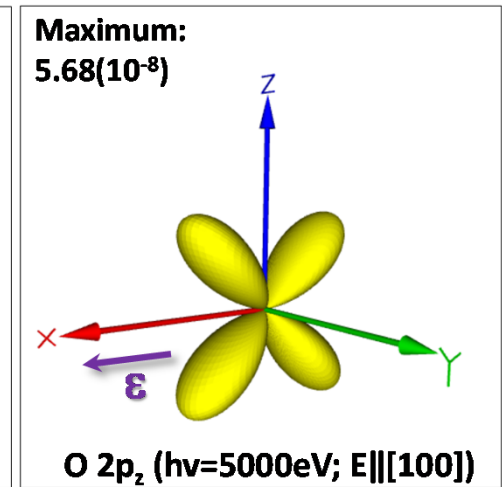
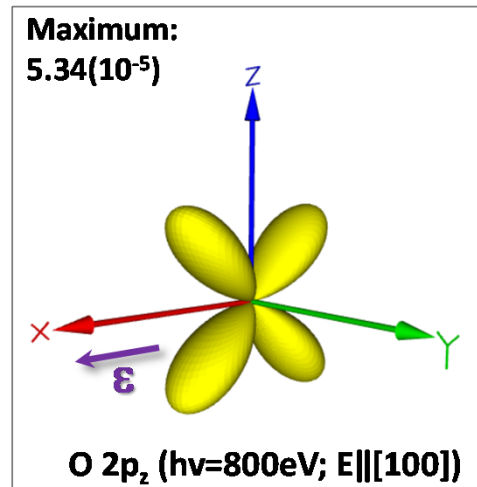
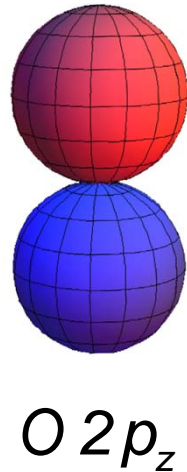
Energy and polarization dependence of orbital-specific differential cross sections: Cu $3d_{z^2}$ @ 800 and 5000 eV



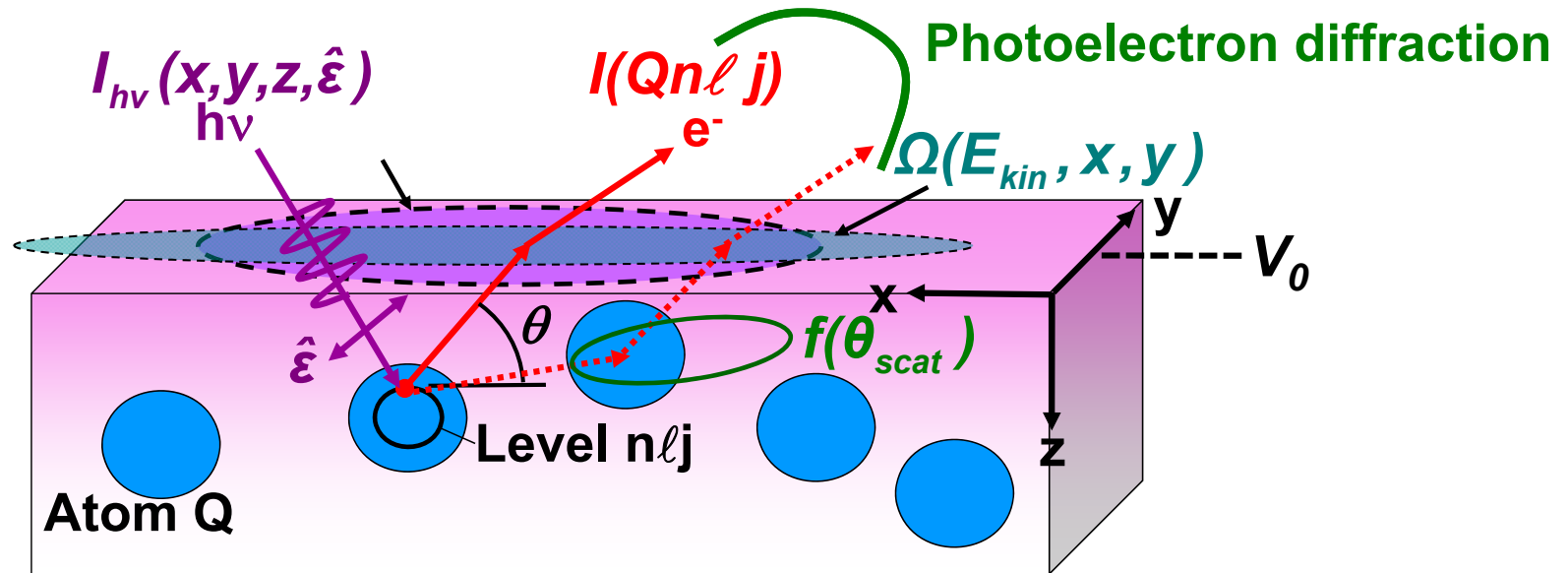
$Cu\ 3d_{z^2}$



Energy and polarization dependence of orbital-specific differential cross sections: O $2p_z$ @ 800 and 5000 eV



ATOMIC (CORE) PHOTOELECTRON INTENSITIES: THE THREE-STEP MODEL



$$I(Qn\ell j) =$$

$$C \int_0^{\infty} I_{hv}(x,y,z,\hat{\epsilon}) \rho_Q(x,y,z) \frac{d\sigma_{Qn\ell j}(hv,\hat{\epsilon})}{d\Omega} \exp\left[-\frac{z}{\Lambda_e(E_{kin}) \sin\theta}\right] \Omega(E_{kin},x,y) dx dy dz$$

$I_{hv}(x,y,z,\hat{\epsilon})$ = x-ray flux, $\hat{\epsilon}$ = polarization

$\rho_Q(x,y,z)$ = density of atoms Q → quantitative analysis

$\frac{d\sigma_{Qn\ell j}(hv,\hat{\epsilon})}{d\Omega}$ = **energy-dependent** differential photoelectric cross section for subshell Qnℓj

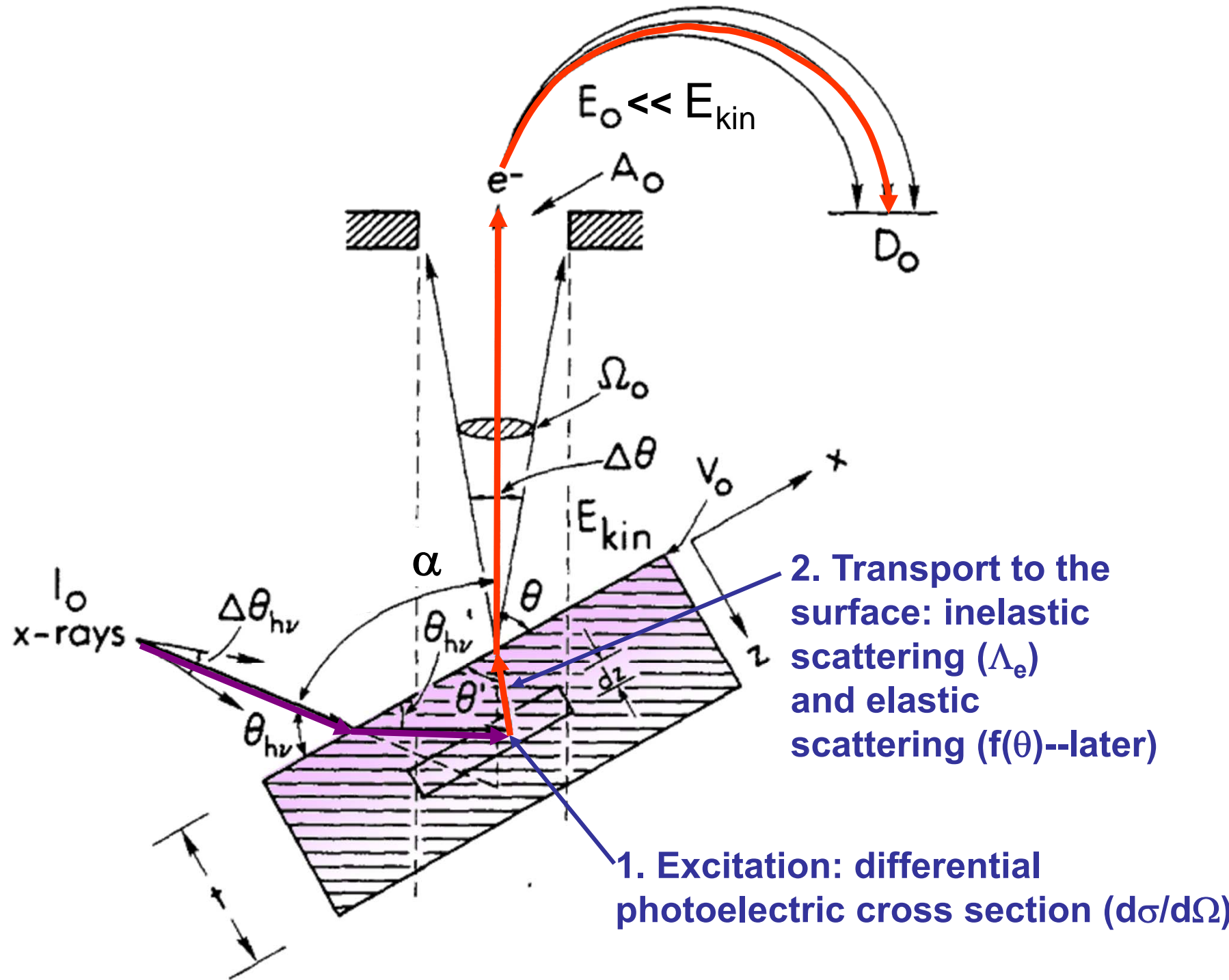
$\Lambda_e(E_{kin})$ = **energy-dependent** inelastic attenuation length + **elastic scattering**: $f(\theta_{scatt})$

→ Effective Attenuation Length (EAD) → Mean Emission Depth (MED)

$\Omega(E_{kin},x,y)$ = **energy-dependent** spectrometer acceptance solid angle = transmission function

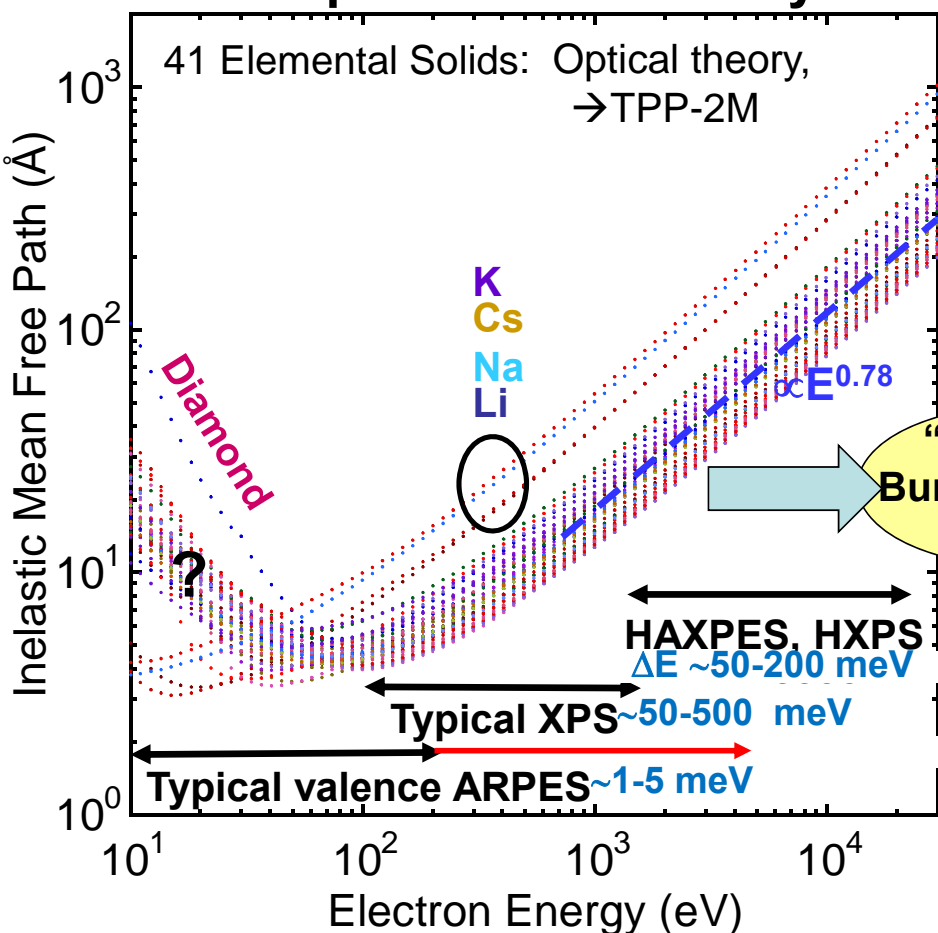
V_0 = inner potential

PHOTOELECTRON INTENSITIES—THE 3-STEP MODEL



More bulk sensitivity in photoemission by going to hard x-rays

Optical-based theory

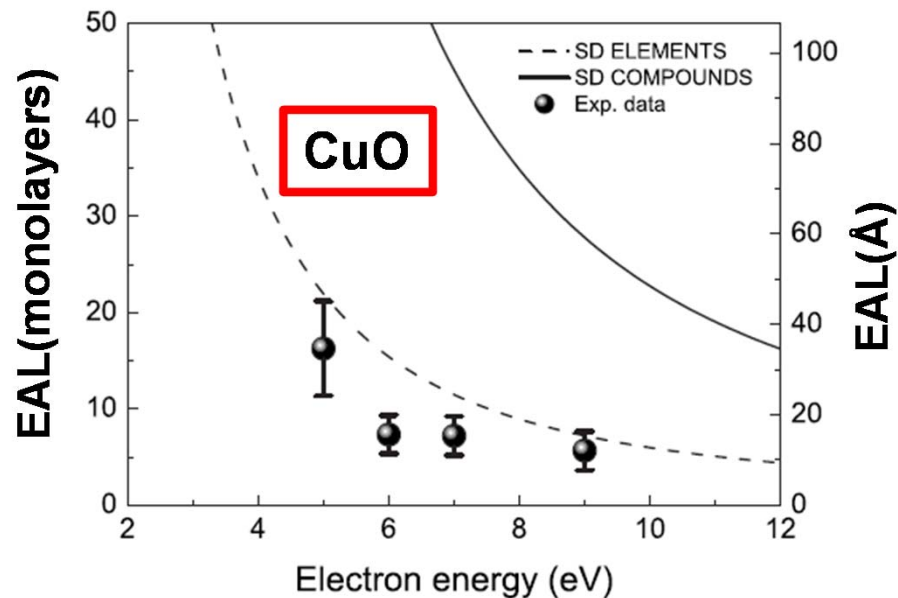


Tanuma, Powell, Penn, *Surf. and Interf. Anal.* **43**, 689 (2011)

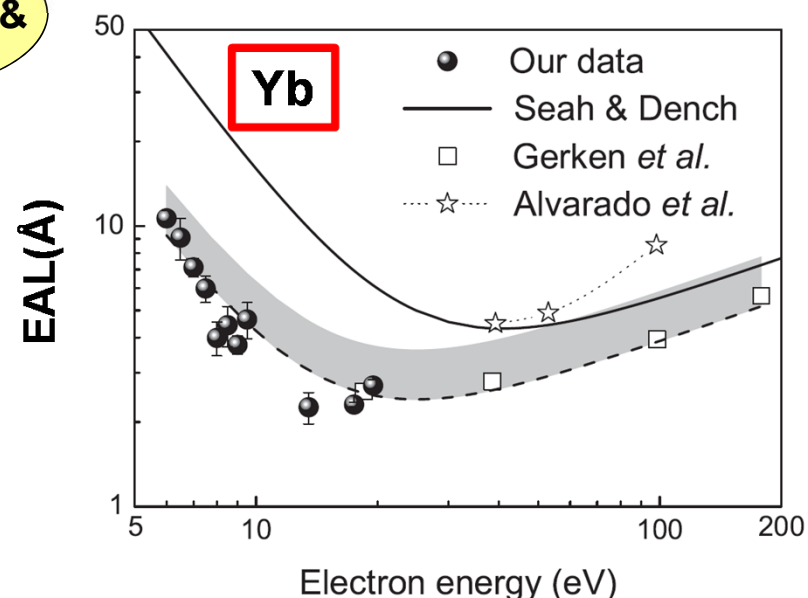
\rightarrow The only certain way to obtain more bulk sensitivity
And with competitive energy resolutions

“Bulklike”, Buried layers & interfaces

Experiment



Offi et al., *PRB* **77**, 201101R (2008)



Offi et al., *J. Phys.: Cond. Matt.* **22** (2010) 305002

Basic Concepts:

A Little Electronic Structure

The X-Ray-Based Experiments

X-Ray Sources, Synchrotron Radiation, Free Electron Lasers

Core-Level Photoemission



Intensities and Quantitative Analysis, the 3-Step Model

Varying Surface and Bulk Sensitivity

Chemical Shifts

Multiplet Splittings

Electron Screening and Satellite Structure

Magnetic and Non-Magnetic Dichroism

Resonant Photoemission

Photoelectron Diffraction and Holography

Valence-Level Photoemission

Band-Mapping in the Ultraviolet Photoemission Limit

Densities of States in the X-Ray Photoemission Limit

Some New Directions

Photoemission with Hard X-Rays (throughout lectures)

Photoemission with Standing Wave Excitation

Photoemission with: Higher Pressures → multi-Torr → Atmosphere?

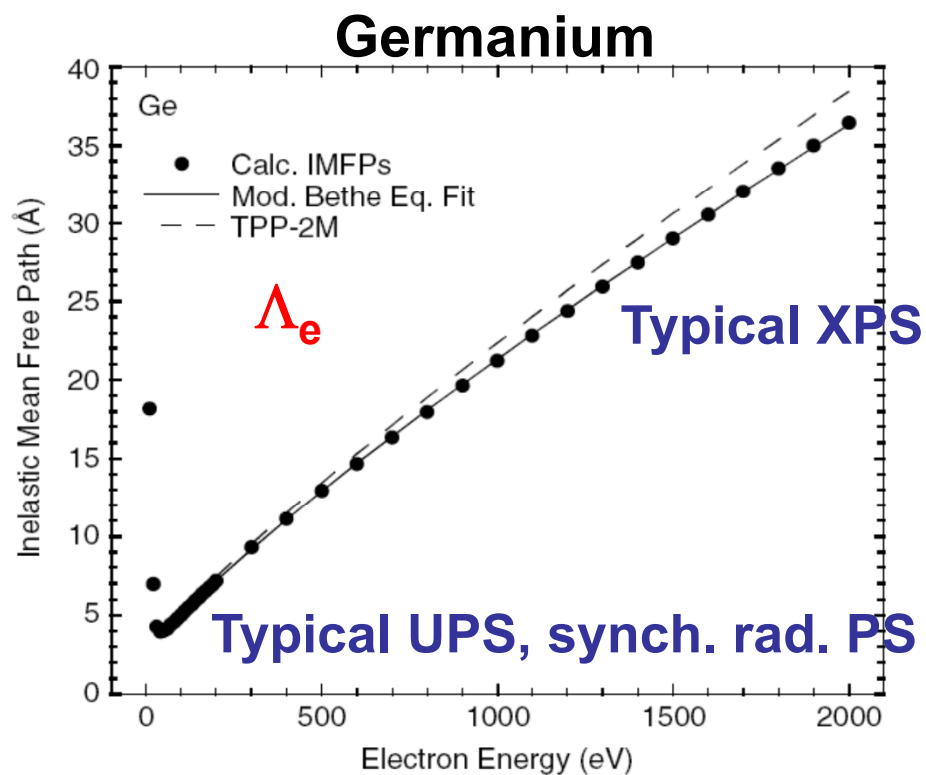
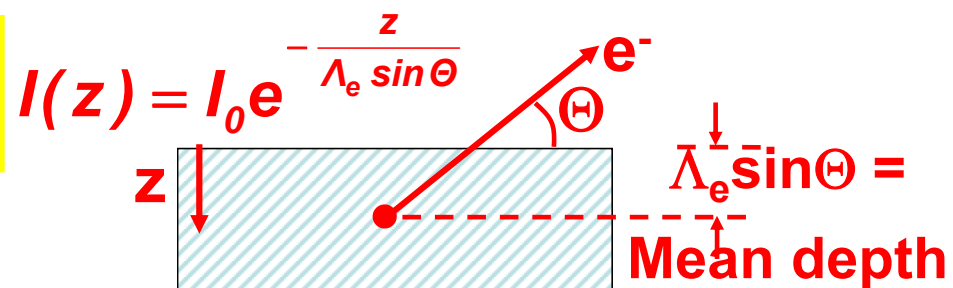
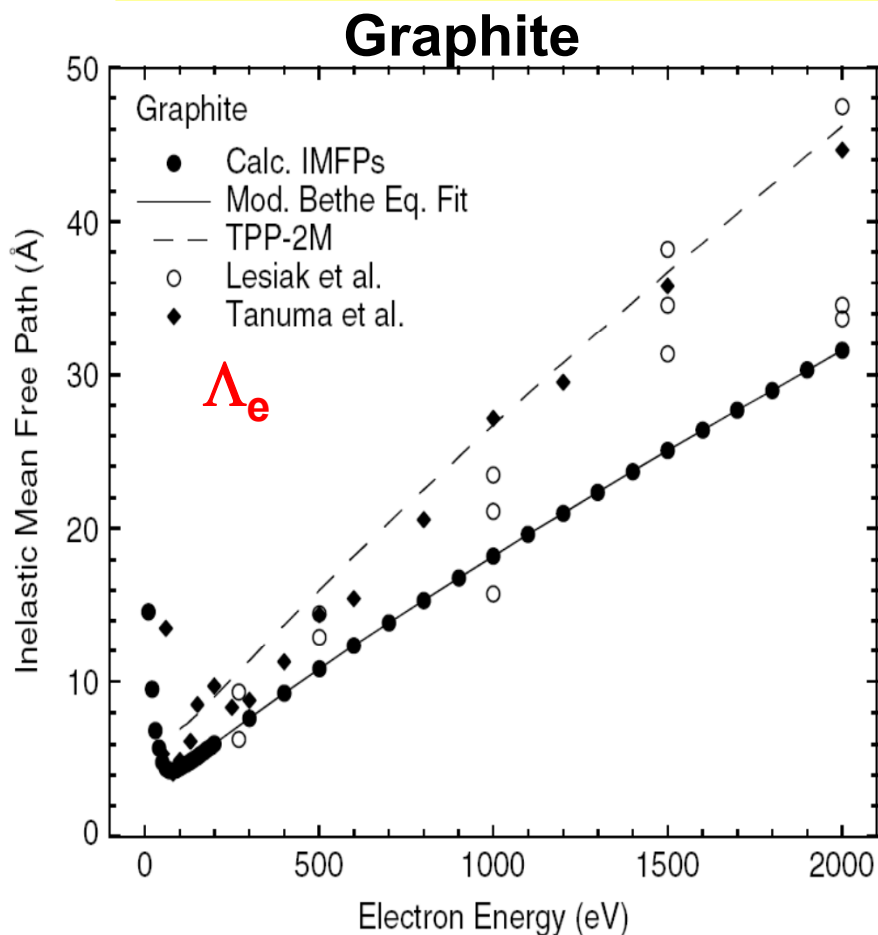
Spatial Resolution-Photoelectron Microscopy

Temporal Resolution

Electron inelastic attenuation length in solids—the “universal curve”

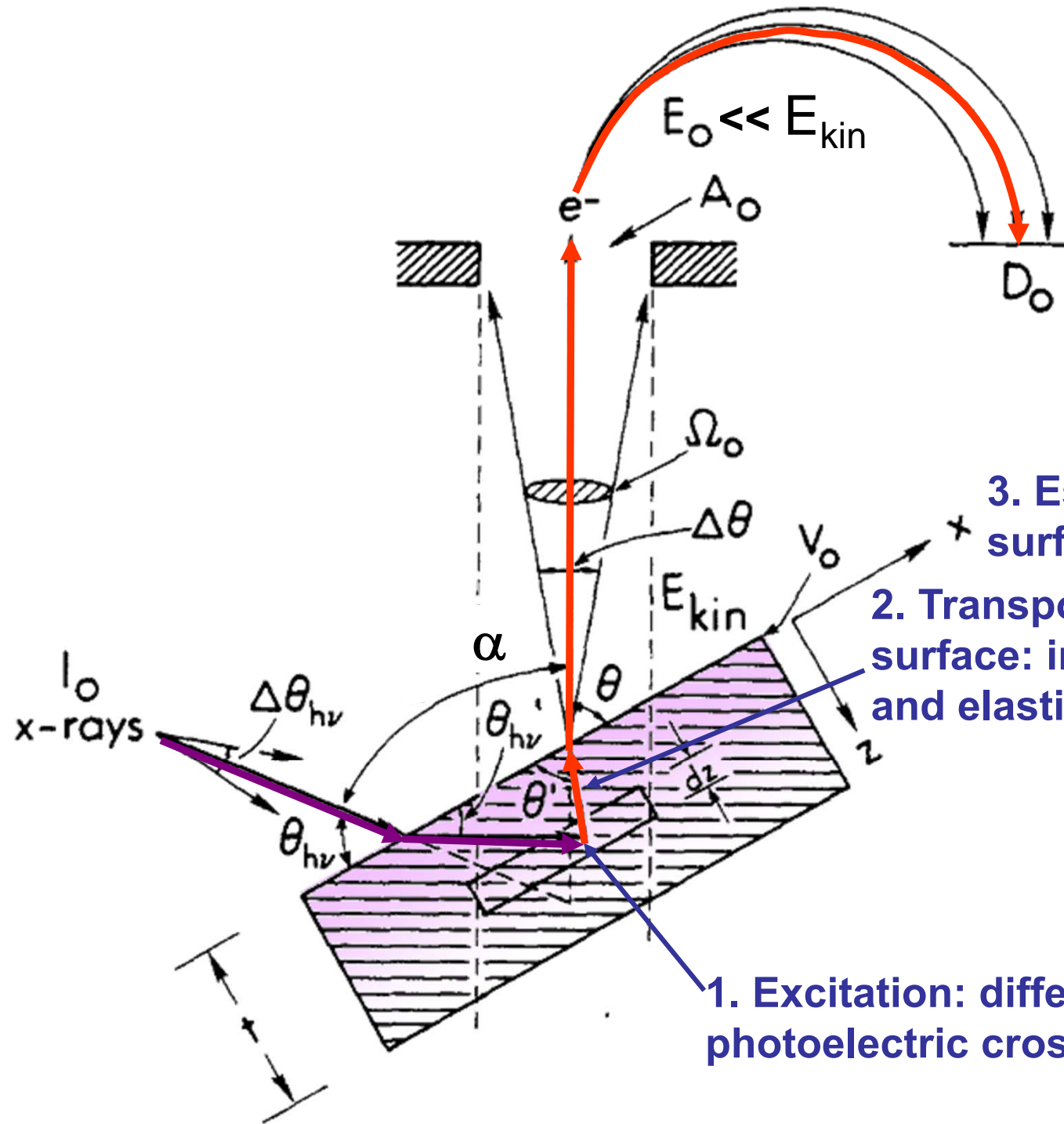
Photoemission is a surface sensitive experiment

Changing angle:
1st way to vary surface sensitivity



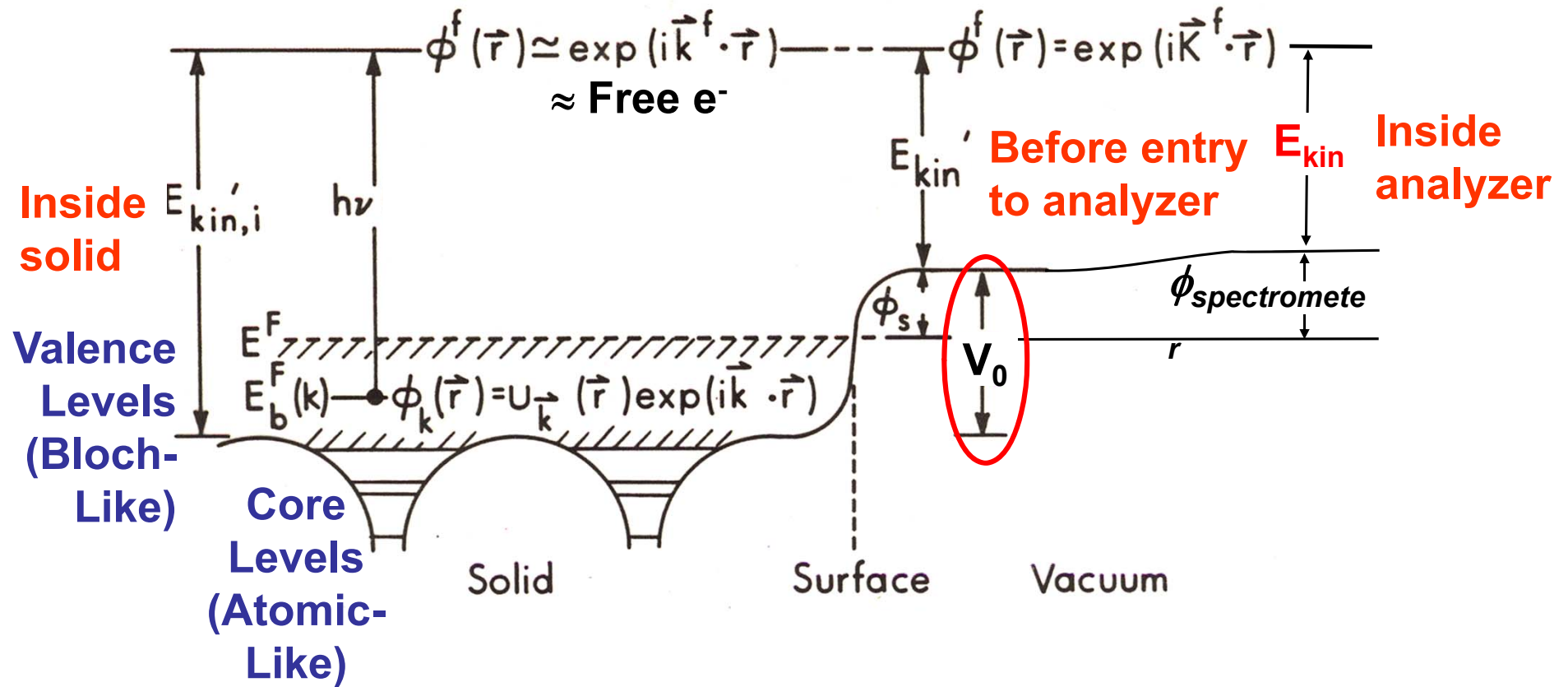
Changing photon energy:
2nd way to vary surface sensitivity

PHOTOELECTRON INTENSITIES—THE 3-STEP MODEL



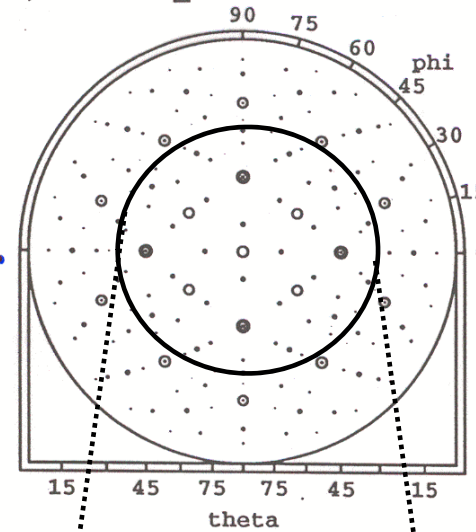
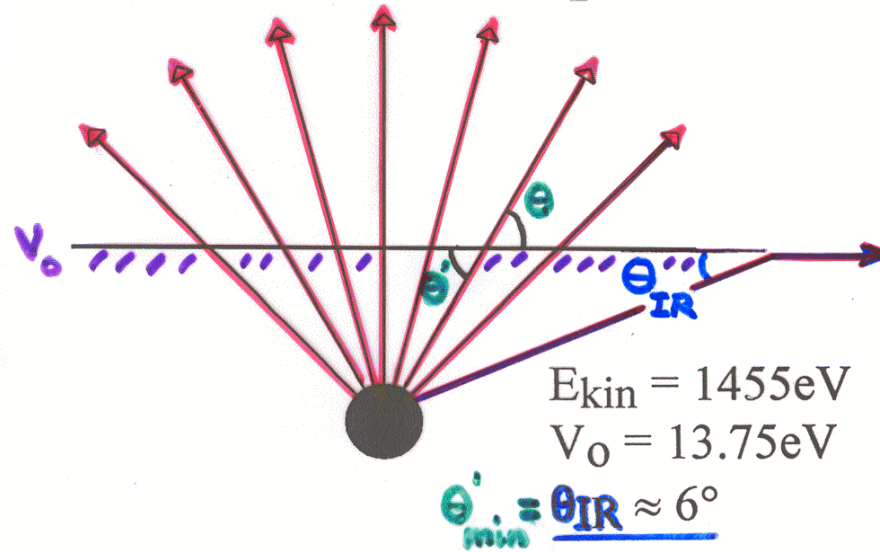
3. Escape across the surface barrier (V_0)
2. Transport to the surface: inelastic (Λ_e) and elastic ($f(\theta)$) scattering
1. Excitation: differential photoelectric cross section ($d\sigma/d\Omega$)

One-Electron Picture of Photoemission from a Surface

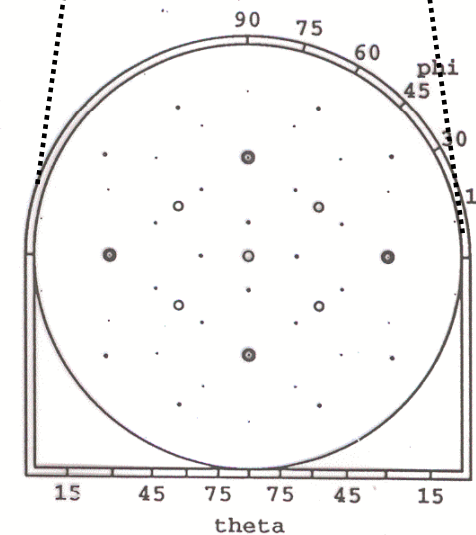
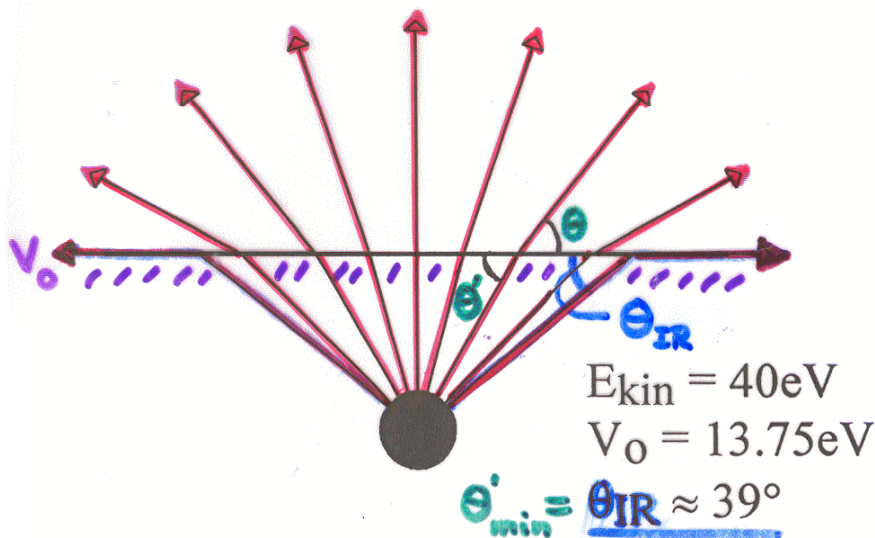


Electron Refraction at the Surface Due to the Inner Potential

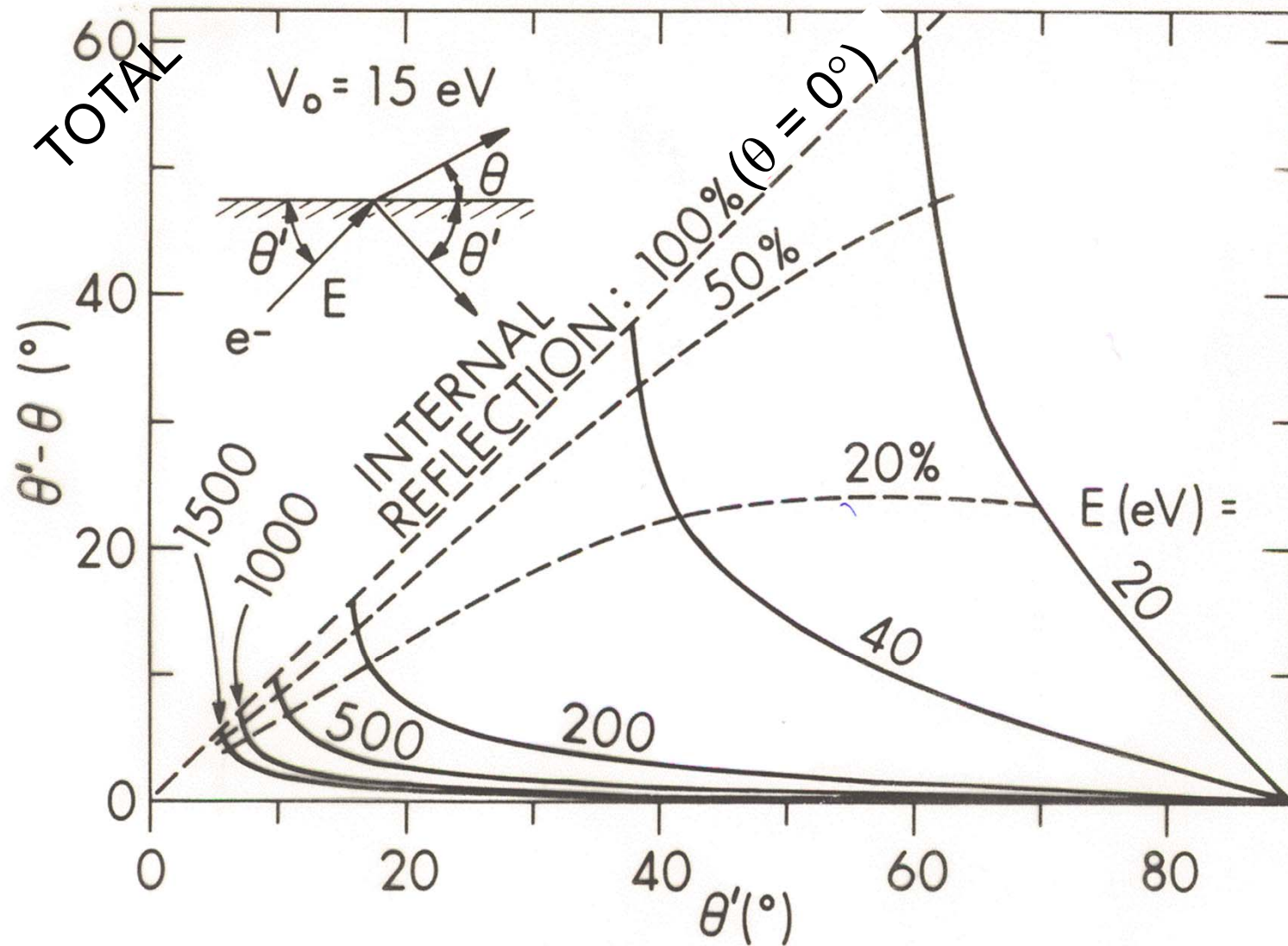
$$\theta = \tan^{-1} \left[\sqrt{\sin^2 \theta' - \frac{V_0}{E_{kin}}} / \cos \theta' \right], \theta_{IR} = \text{total internal reflection}$$



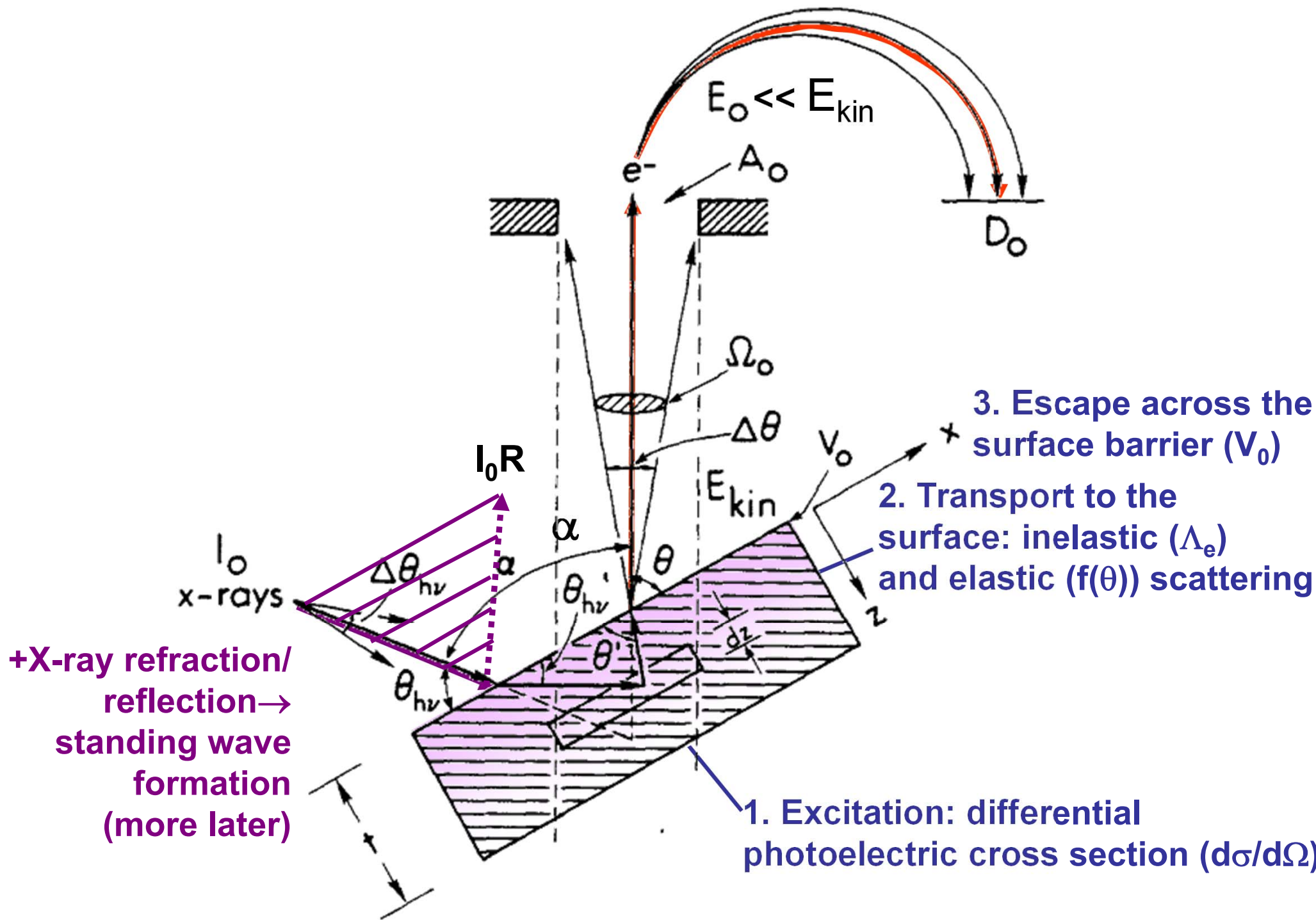
**Observed
Low-Index
Directions
Above
W(110)**



Electron Refraction at the Surface Due to the Inner Potential



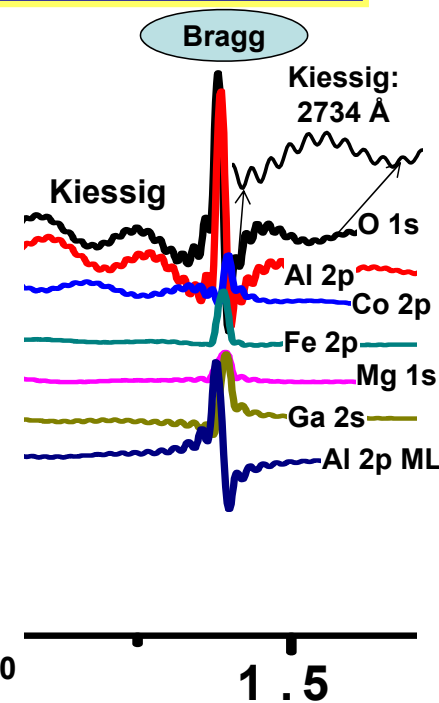
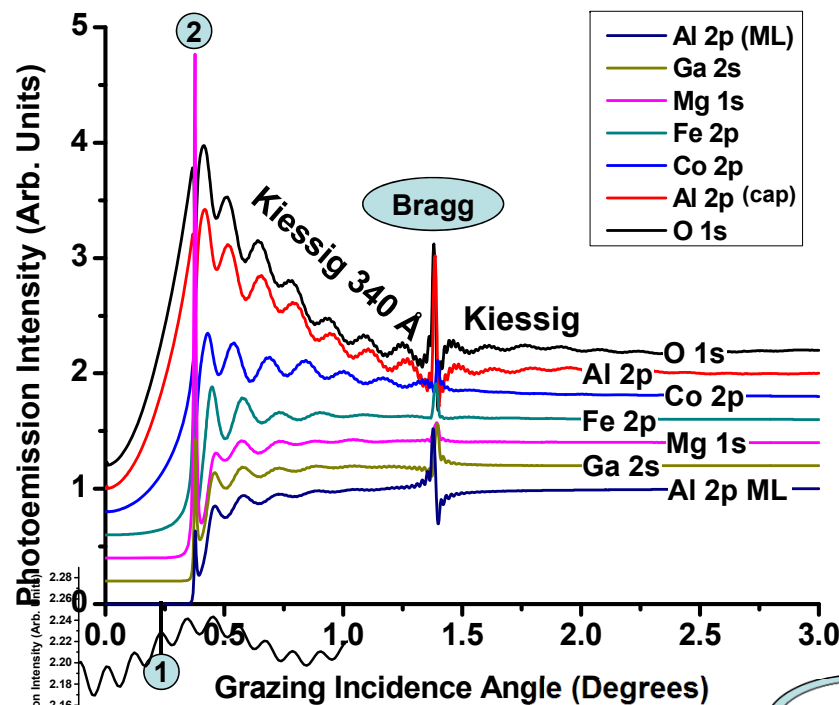
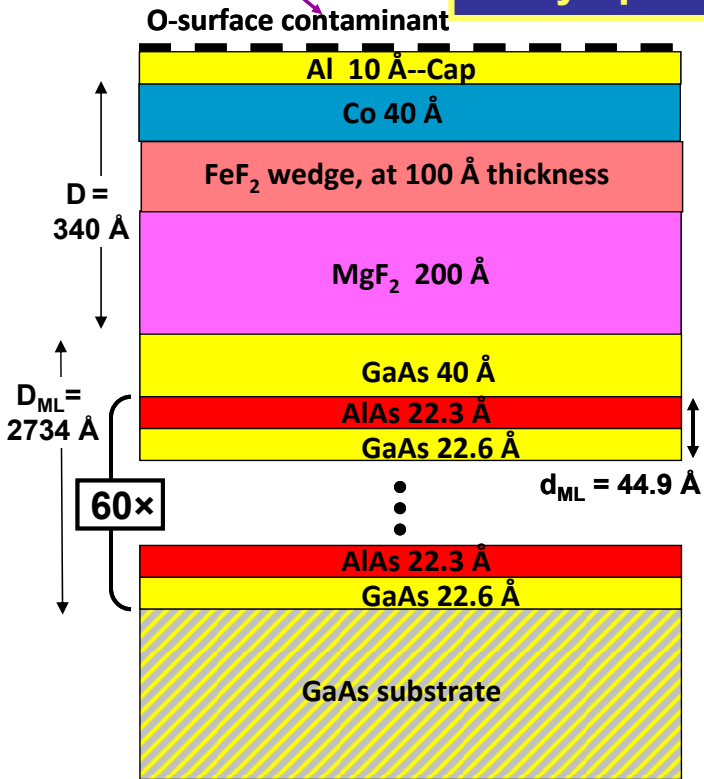
PHOTOELECTRON INTENSITIES—THE 3-STEP MODEL



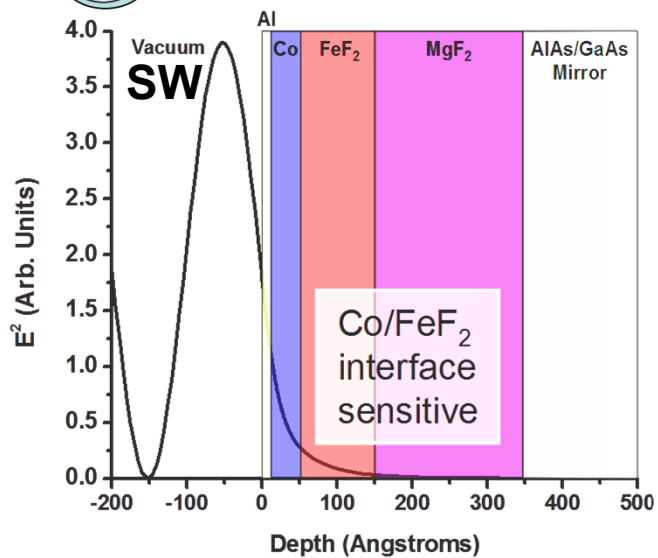
+X-ray refraction/
reflection →
standing wave
formation
(more later)

$h\nu = 5.9 \text{ keV}$

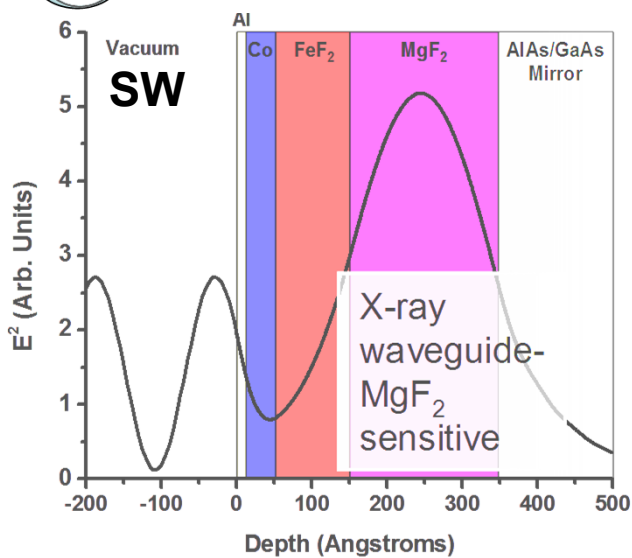
X-ray optical effects in hard x-ray reflectivity from a multilayer structure



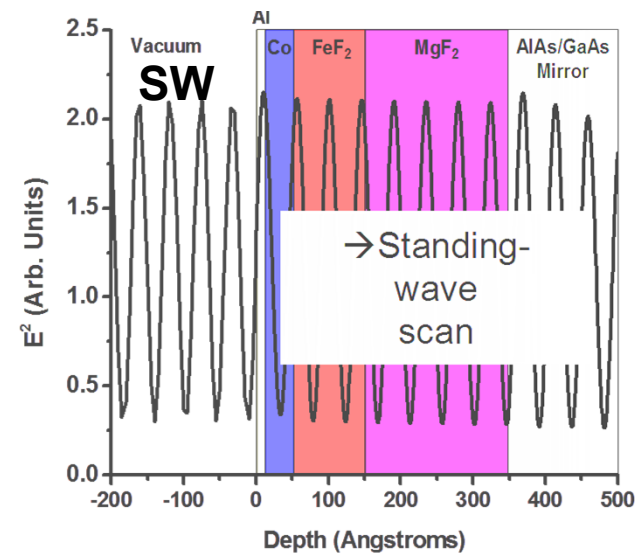
1 [Electric Field]² VS. Depth



2 [Electric Field]² VS. Depth



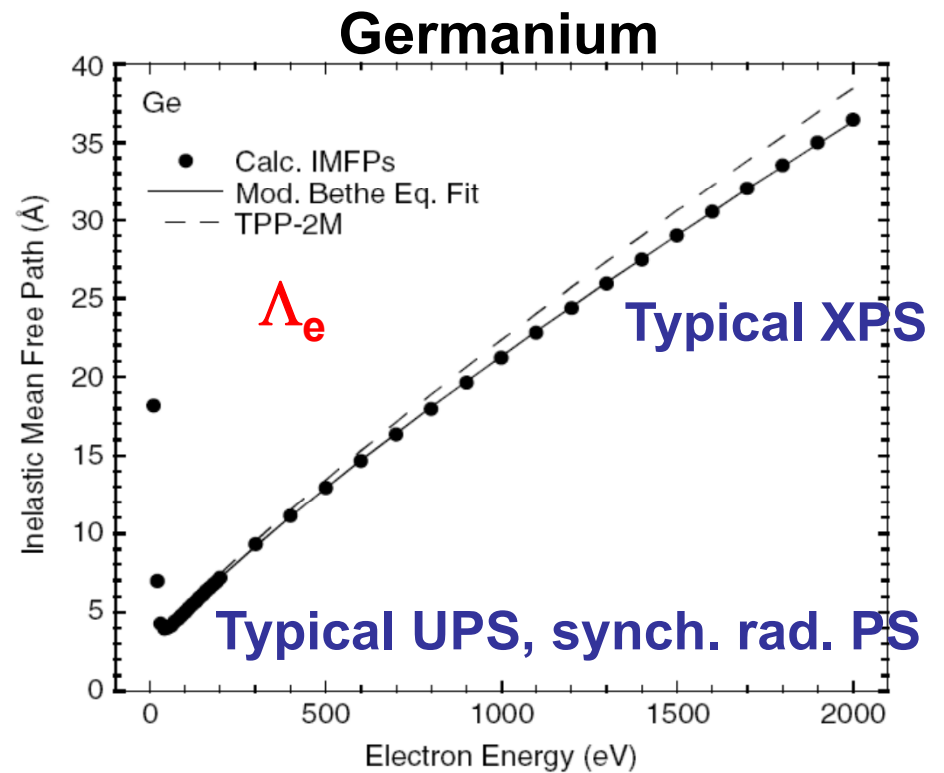
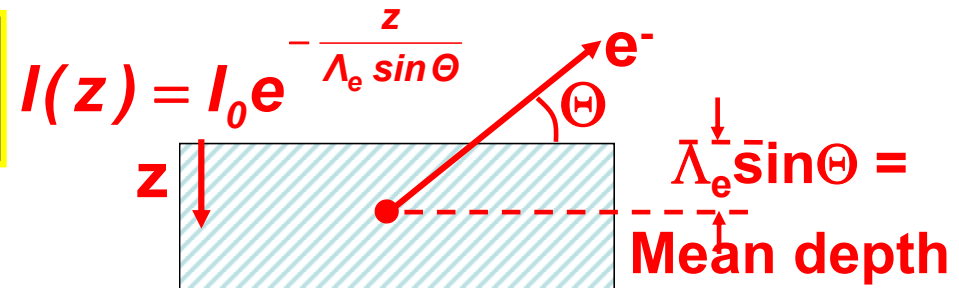
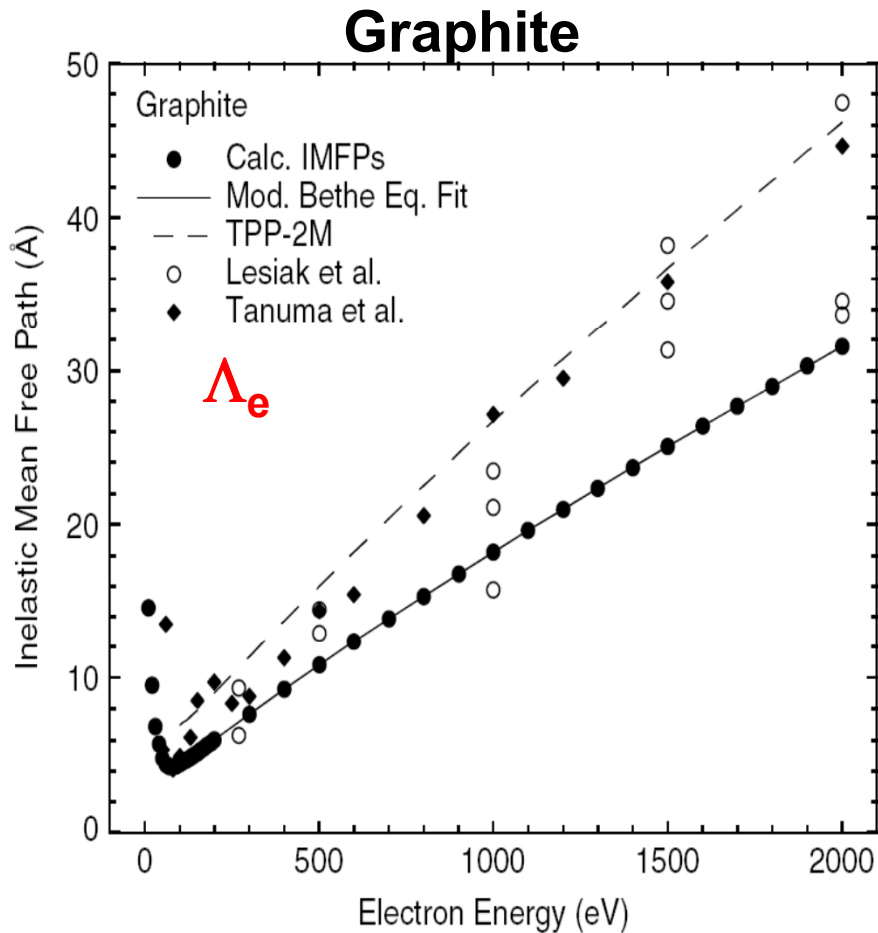
[Electric Field]² VS. Depth



Electron inelastic attenuation length in solids—the “universal curve”

Photoemission is a surface sensitive experiment

Changing angle:
1st way to vary surface sensitivity



Changing x-ray penetration/
standing wave/total reflection:
3rd way to vary surface sensitivity

Changing photon energy:
2nd way to vary surface sensitivity

SIMULATING XPS SPECTRA-WITH ELASTIC SCATTERING THE SESSA PROGRAM FROM NIST

www.nist.gov/srd/nist100.cfm

NIST Standard Reference Data

Products Services Publications NIST Organization

NIST Home > SRD > NIST Standard Reference Database 100

Select Language * SHARE

Powered by Google Translate

NIST Standard Reference Database 100

NIST Database for the Simulation of Electron Spectra for Surface Analysis (SESSA): Version 2.0

Price: \$900.00 **ONLINE PURCHASE**

Mac Version **ONLINE PURCHASE**

Linux Version **ONLINE PURCHASE**

Discounted prices apply to multiple purchases of SESSA by the same organization; for information click here.

Rate our Products and Services

If you are having problems with the Online Purchase or Fax/Mail Order Link.

Effective immediately, there will be a minimum \$30.00 shipping charge for all international shipments of databases via UPS International. Customer will be responsible for their own duties, tax, and VAT. Contact 301 975 2200 or data@nist.gov if you have questions.

Topic Areas

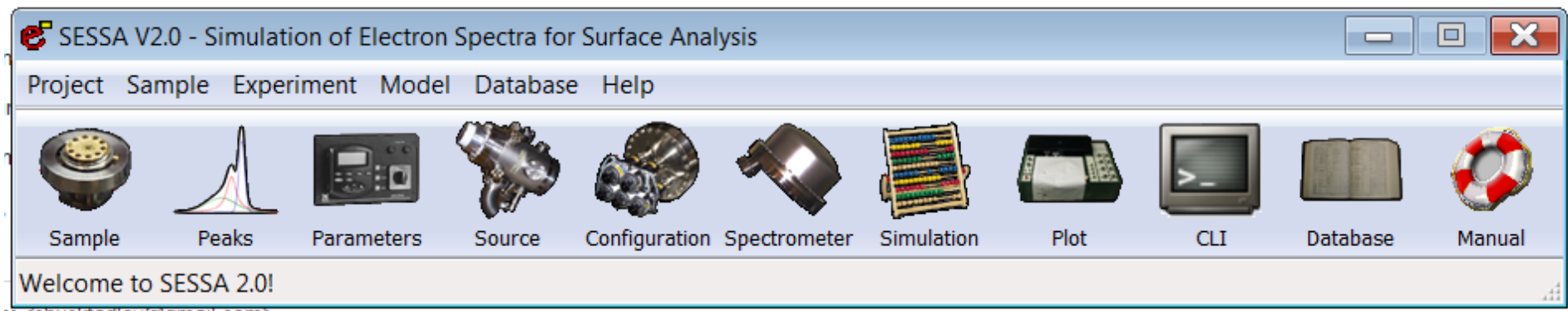
- Analytical Chemistry
- Atomic and Molecular Physics
- Biometrics
- Biotechnology
- Chemical and Crystal Structure
- Chemical Kinetics
- Chemistry
- Construction
- Environmental Data
- Fire
- Fluids
- International Trade
- Law Enforcement
- Materials Properties
- Mathematical Databases, Software and Tools
- Optical Character Recognition
- Personal Identity Verification

Includes:

- Cross sections
- Radiation polarization
- Inelastic mean free path
- Elastic scattering
- Exact experimental geometry
- Estimate of Auger intensities

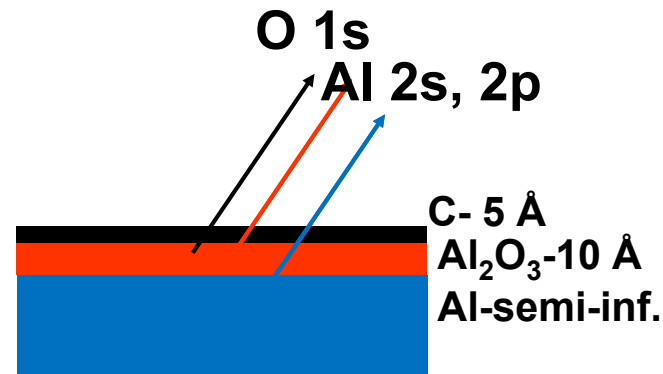
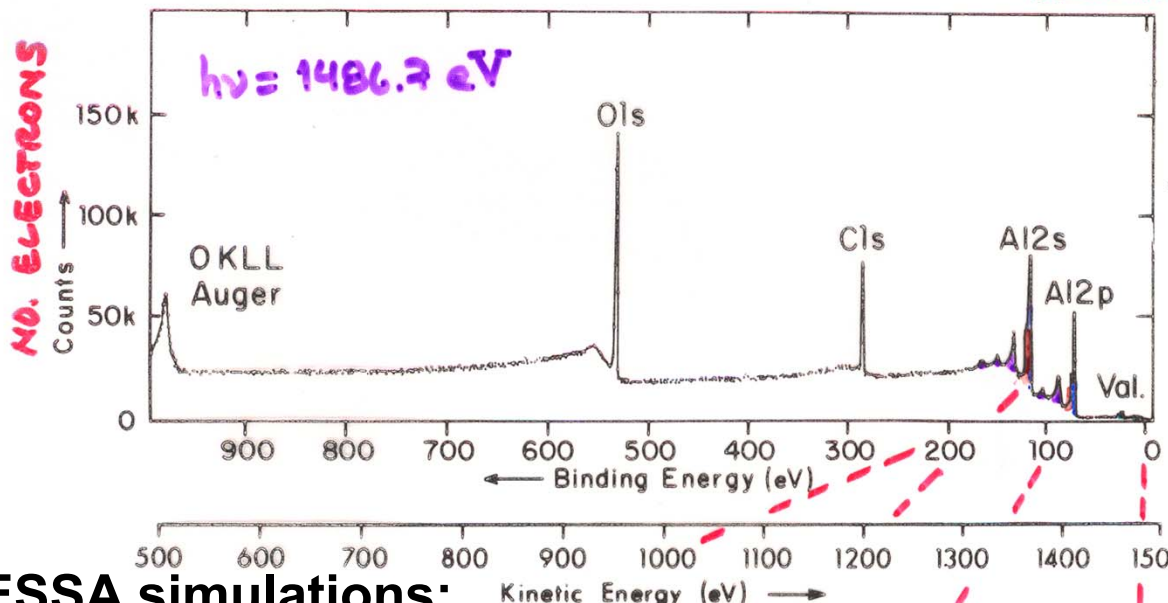
Does not include:

- Trajectory bending at the inner potential V_0
- Any x-ray optical effects (for that our YXRO program: **Yang et al., J. Appl. Phys. 113, 073513 (2013)**)

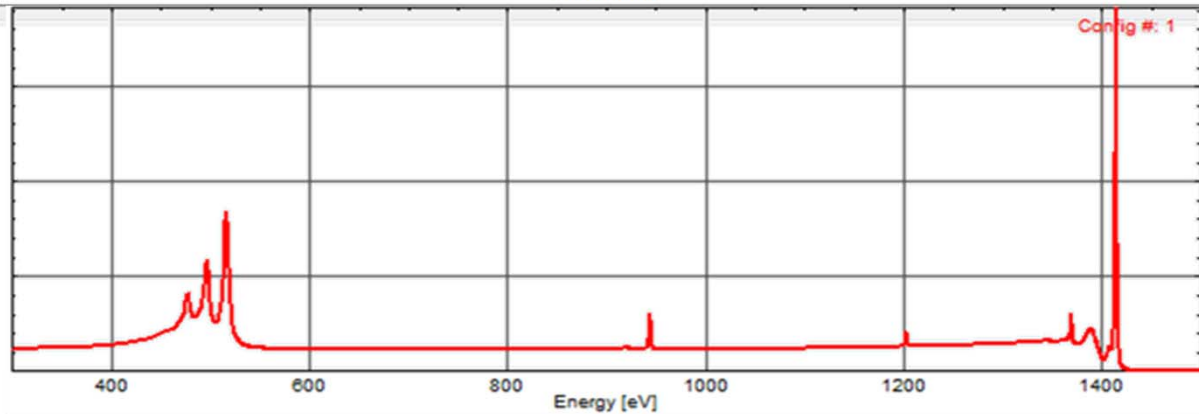
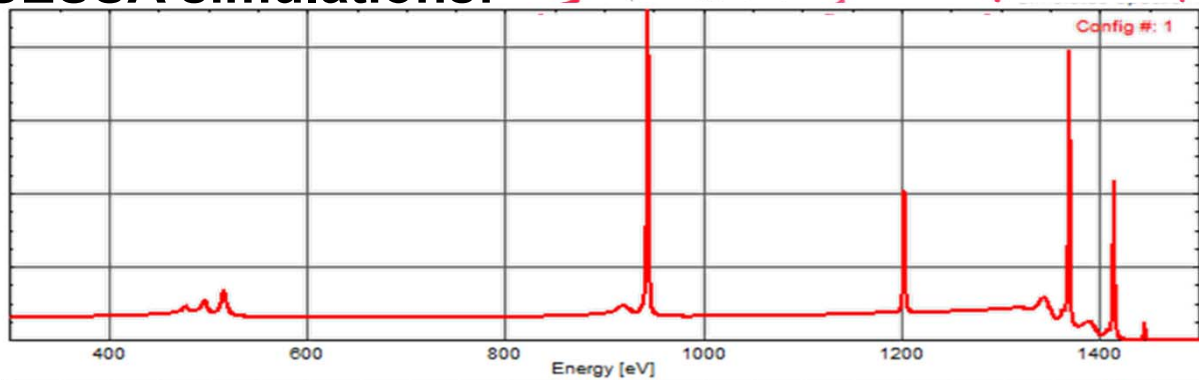


W. Smekal, W. S. M. Werner and C. J. Powell, Surf. Interface Anal. 3, 1059 (2005); W. S.M. Werner, W. Smekal, T. Hisch, J. Himmelsbach, C. J. Powell, J. Electron Spectrosc. 190, 137 (2013).

TYPICAL PHOTOELECTRON SPECTRA: OXIDIZED ALUMINUM



SESSA simulations:



Orientation of analyzer axis:

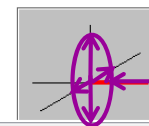
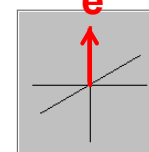
Phi [deg] 0.000

Theta [deg] 0.000

Orientation of source axis:

Phi [deg] 0.000

Theta [deg] 90.000



Unpolarized, with some components pointing into analyzer

Orientation of analyzer axis:

Phi [deg] 0.000

Theta [deg] 0.000

Orientation of source axis:

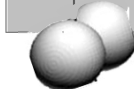
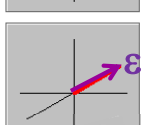
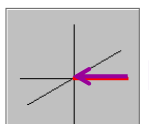
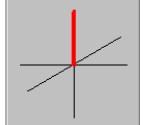
Phi [deg] 0.000

Theta [deg] 90.000

Orientation of polarization vector:

Phi [deg] 90.000

Theta [deg] 90.000



Polarized along axis perp. to plane of x-ray incidence and electron exit, and so yielding electron emission into the nodal line of any s-shell cross section

Basic Concepts:

A Little Electronic Structure

The X-Ray-Based Experiments

X-Ray Sources, Synchrotron Radiation, Free Electron Lasers

Core-Level Photoemission



Intensities and Quantitative Analysis, the 3-Step Model-Valence levels

Varying Surface and Bulk Sensitivity

Chemical Shifts

Multiplet Splittings

Electron Screening and Satellite Structure

Magnetic and Non-Magnetic Dichroism

Resonant Photoemission

Photoelectron Diffraction and Holography

Valence-Level Photoemission

Band-Mapping in the Ultraviolet Photoemission Limit

Densities of States in the X-Ray Photoemission Limit

Some New Directions

Photoemission with Hard X-Rays (throughout lectures)

Photoemission with Standing Wave Excitation

Photoemission with: Higher Pressures → multi-Torr → Atmosphere?

Spatial Resolution-Photoelectron Microscopy

Temporal Resolution